Science is organized knowledge.

Wisdom is organized life.

Immanuel Kant

Table of Contents

Chapter 1: General Introduction **7–25**

1. Four generations of Polymers 8
2. Conjugated Polymers: Semiconducting Materials 9
    - 2.1. Electronic Properties 9
    - 2.2. Optical Absorption Properties 11
    - 2.3. Applications 12
3. Poly(p-phenylene vinylene) (PPV) 15
    - 3.1. Synthetic Approaches 15
    - 3.2. Precursor Routes 16
4. Aim and Outline 18
5. References 20

Chapter 2: Exploring the Dithiocarbamate Precursor Route: Observation of a Base Induced regioregularity Excess in Poly[(2-methoxy-5-(3',7',-dimethyloctyloxy))-1,4-phenylene vinylene] **27–54**

1. Introduction 28
2. Experimental Section 30
    - 2.1. General Data 30
    - 2.2. Synthesis 31
3. Results and Discussion 33
    - 3.1. Monomer Synthesis 33
    - 3.2. Polymerization 33
    - 3.3. Thermal Conversion 36
    - 3.4. Regioregularity 39
    - 3.5. Quantitative ^{13}C NMR Study 42
4. Conclusions 50
5. Acknowledgment 50
6. Supporting Information 51
7. References and Notes 52

Chapter 3: An Efficient Acid-Induced Conversion of Dithiocarbamate Precursor Polymers into Conjugated Materials **57–83**

1. Introduction 58
2. Experimental Section 60
    - 2.1. General 60
    - 2.2. Synthesis 61
3. Results and Discussion 64
    - 3.1. Precursor Polymers 64
    - 3.2. In-Situ Thermal Conversion in Thin Film 65
    - 3.3. Thermal Conversion in Solution 70
    - 3.4. Acid-Induced Conversion 71
4. Conclusion 80
5. Acknowledgment 80
6. References and Notes 80

Chapter 4: Synthesis and Characterization of Water Soluble Poly(*p*-phenylene vinylene) Derivatives via the Dithiocarbamate Precursor Route **85–108**

1. Introduction 86
2. Experimental Section 88
    - 2.1. General 88
    - 2.2. Premonomer Synthesis 89
    - 2.3. Synthesis of Precursor Polymers 93
    - 2.4. Thermal Elimination of Precursor Polymer to Conjugated Polymer 94
3. Results and Discussion 96
    - 3.1. Premonomer Synthesis 96
    - 3.2. Polymerization 97
    - 3.3. Conversion 99
    - 3.4. Optical Characterization 100
    - 3.5. Electrical Characterization 102
4. Conclusions 105

5. Acknowledgments 105
6. References 106

Chapter 5: Tetra-alkoxy Substituted PPV Derivatives: A New Class of Highly Soluble Liquid Crystalline Conjugated Polymers **111−136**

1. Introduction 112
2. Experimental Section 113
    - 2.1. General 113
    - 2.2. Synthesis 114
    - 2.3. Device Preparation and Characterization 117
3. Results and Discussion 118
    - 3.1. Monomer and Polymer Synthesis 118
    - 3.2. Optical Characterization 121
    - 3.3. Thermal Stability 123
    - 3.4. Phase Behavior 124
    - 3.5. Device Characterization 126
4. Conclusions 128
5. Acknowledgments 129
6. Supporting Information 130
7. References 134

Chapter 6: Thermal Stability of Poly[2-methoxy-5-(2'-phenylethoxy))-1,4-phenylene vinylene] (MPE-PPV):Fullerene Bulk Heterojunction Solar Cells **139−166**

1. Introduction 140
2. Experimental Section 141
    - 2.1. General 141
    - 2.2. Synthesis 145
3. Results and Discussion 147
    - 3.1. Synthesis and Standard Characterization 147
    - 3.2. Thermal Analysis 149
    - 3.3. Device Characterization 152

4. Conclusions 161
5. Acknowledgments 162
6. Supporting Information 162
7. References and Notes 163

Chapter 7: A Quest for Controlling Molecular Weight 169–197
1. Introduction 170
2. Experimental Section 171
    2.1. General Data 171
    2.2. Synthesis 173
3. Results and Discussion 176
    3.1. Effect of Reaction Parameters 176
        3.1.1. Dithiocarbamate Route 176
        3.1.2. Sulfinyl Route 178
    3.2. Kinetic UV-vis Study 180
        3.2.1. Dithiocarbamate Route 181
        3.2.2. Sulfinyl Route 182
        3.2.3. Kinetic Modeling 183
    3.3. Effect of Chain Transfer Reagents on the Sulfinyl Route 184
    3.4. ESI-MS Analysis 188
        3.4.1. Dithiocarbamate Route 189
        3.4.2. Sulfinyl Route 190
4. Conclusions 193
5. Acknowledgments 193
6. References 194

Summary 199
Samenvatting 205
Publications & Conferences: Personal Contributions 213
Abbreviations & Symbols 219
Dankwoord 225

Chapter 1

General Introduction

ABSTRACT: In this first chapter, a general introduction on conjugated polymers and their use as semiconducting materials is given. The electronic and optical absorption properties of conjugated polymers are described, as well as the optoelectronic applications for which these materials are suitable candidates to be used. One major class of conjugated materials, the poly(*p*-phenylene vinylene)'s (PPV's) are discussed in more detail, since it is the main focus of this thesis. The various synthetic approaches towards PPV's are illuminated with an emphasis on the different *p*-quinodimethane based precursor routes. Finally, the aim and the outlook of the thesis are presented with a short overview of the different topics described in the following chapters.

1. Four Generations of Polymers

Polymer science as we know it, is a development of the last 80 years. In the 1920's, Hermann Staudinger was the first to develop the concept of a macromolecule: a very large molecule commonly created by some form of polymerization.[1] Polymers are synthesized from simple molecules called monomers. Staudinger's theories were confirmed by numerous experiments on polymerization reactions by Wallace Carothers in the 1930's.[2] Carothers also invented polyamide (nylon) fibers, which is an example of the first generation of polymeric materials.[3] Those polymers were introduced on the market before 1950 and consisted of simple plastics like polystyrene, poly(vinylchloride) (PVC), neoprene rubber and poly(acrylates).

In the 1950's, Karl Ziegler and Giullio Natta discovered the use of polymerization catalysts, which had a huge impact on the development of the modern plastics industry.[4,5] Furthermore, the theoretical and experimental studies of Paul Flory on macromolecules created major insights and understanding of macromolecular phenomena.[6] This knowledge leaded in the 1950's and 1960's to the development of the second generation polymers: High-density polyethylene (HDPE), isotactic polypropylene, polycarbonates and linear polyesters for fibers and films. The second generation materials have higher mechanical strength and can resist higher temperatures than the first generation polymers.

After 1965, a third generation of polymers was gradually developed: the so-called "specialty" polymers, such as for instance Kevlar® and Teflon®. Specialty polymers have very high chemical and thermal resistance, high mechanical strengths and usually consist of more complex chemical structures than the first and second generation polymers.

The materials developed so far were all insulators, and for a long time the general idea was that polymers would never be able to serve as electronic materials. However, in 1977 Alan Heeger, Alan MacDiarmid and Hideki Shirakawa discovered that polyacetylene could be made conductive upon doping.[7] In 2000, the three scientists received the Nobel Prize in Chemistry for their discovery and development of electrically conductive polymers. In

1991, Bengt Rånby designated this class of polymers as the fourth generation of polymeric materials.[3]

2. Conjugated Polymers: Semiconducting Materials

2.1. Electronic Properties

Since the discovery of Heeger, MacDiarmid and Shirakawa, numerous conductive polymers have been developed with the aim to be used in so-called "plastic electronics" (Figure 1). In these conjugated polymers, the polymer backbone consist of alternating single (σ bonds) and double bonds (π bonds). The π electrons are delocalized and polarizable, giving the polymer the possibility to transport charges along its backbone.

A second prerequisite to induce conductivity in a conjugated polymer, is the injection of charge carriers *i.e.* electrons and holes, into the polymer. This can, for instance, be executed via electrical stimulation, photo-excitation or chemical doping.[8] The positive or negative charges can travel along the conjugated polymer backbone (intrachain mobility) and can even move between backbones of different polymer chains (interchain "hopping").

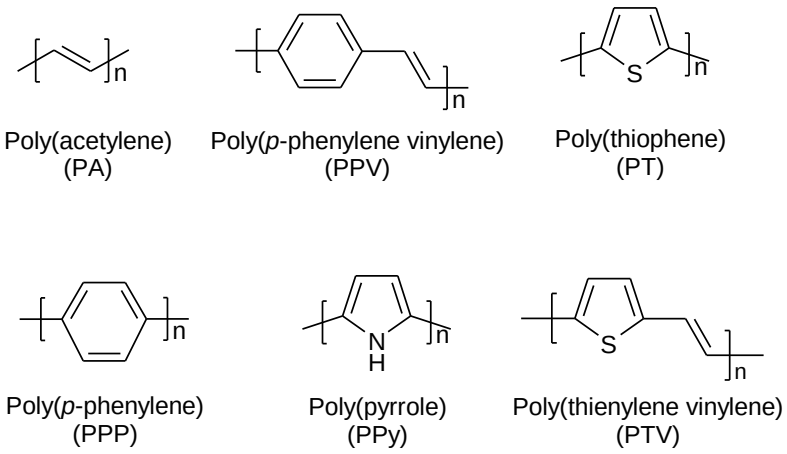

Figure 1. Some examples of conjugated polymers.

The electronic structure of a conjugated polymer, which determines the electrical properties, can be described by the molecular orbital theory.[9] Lower energy bonding (π) and higher energy anti-bonding (π^*) molecular orbitals are formed due to the overlap of adjacent atomic p_z-orbitals. Extended conjugated systems lead to further hybridization of the energy levels, yielding more and more bonding and anti-bonding molecular orbitals until a virtually continuous occupied valence band and an unoccupied conduction band, respectively, are generated. The highest occupied molecular orbital (HOMO) of the valence band and the lowest unoccupied molecular orbital (LUMO) of the conduction band are separated by an energy spacing, called the band gap (E_g). The electronic and optical properties of a conjugated polymer are determined by the size of the band gap, which should vary from 0.5 to 4 eV in order to have a semiconducting polymer.

The band gap of a conjugated polymer is dependent on the molecular structure of the repeating monomer unit. Synthetic modification of the monomers will vary the HOMO and/or LUMO levels, and therefore also the band gap, of the resulting conjugated polymer. Those modifications can consist of, for instance the introduction of certain side chains, inducing sterical hindrance or changing the effective conjugation length.

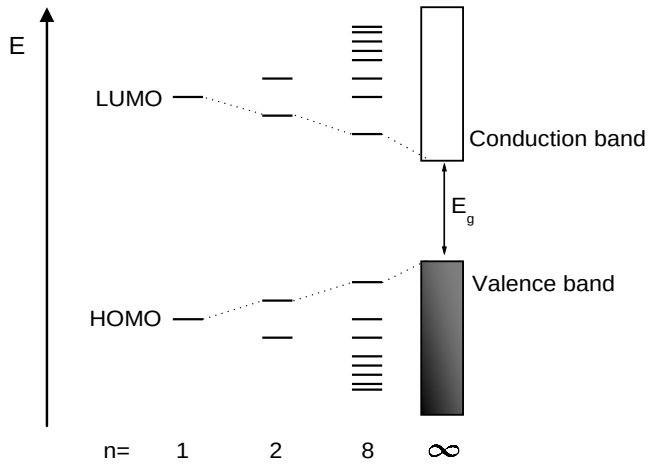

Figure 2. Band model for a semiconducting polymer. E_g is the bandgap.

2.2. Optical Absorption Properties

A material exhibits optical properties because of the interaction with electromagnetic radiation.[10] Because conjugated polymers have a band gap between 0.5 to 4 eV, they will interact with visible light. This is the reason why conjugated polymers are colored. When a photon has enough energy, it can be absorbed by the polymer, causing an electron to be excited from the HOMO level into the LUMO level, creating an exciton (electron-hole pair). The exciton can decay back to the ground state, either radiatively or non-radiatively. Photoluminescence is the radiative decay whereby a photon is generated with a wavelength longer than the initially absorbed photon.[11] The lowest energy (i.e. light with the highest wavelength) necessary to excite an electron, is equal to the band gap of the conjugated polymer. A polymer with a lower band gap will have a red shifted absorption in comparison to a polymer with a higher band gap. It is possible to determine the band gap of a conjugated polymer from its UV-vis absorption spectrum. By drawing the tangent on the higher wavelength side of the spectrum and taking the intersection of this tangent with the abscicca, a value for E_g can be determined.

To make the conversion from wavelength (nm) to energy (eV), the equation of Planck is used:

$$E = h\upsilon = \frac{hc}{\lambda}$$

In this equation, E is the energy (in J), h is the Planck constant ($6.626*10^{-34}$ Js), c is the speed of light ($3*10^{8}$ ms^{-1}), v is the frequency (in s^{-1} or Hz) and λ is the wavelength (in m). Since 1 eV equals $1.602*10^{-19}$ J, a simple conversion equation can be derived:

$$E(eV) = \frac{1240.8}{\lambda\,(nm)}$$

When the wavelength value at the intersection of tangent and abscissa is used in this formula, the optical band gap is derived.

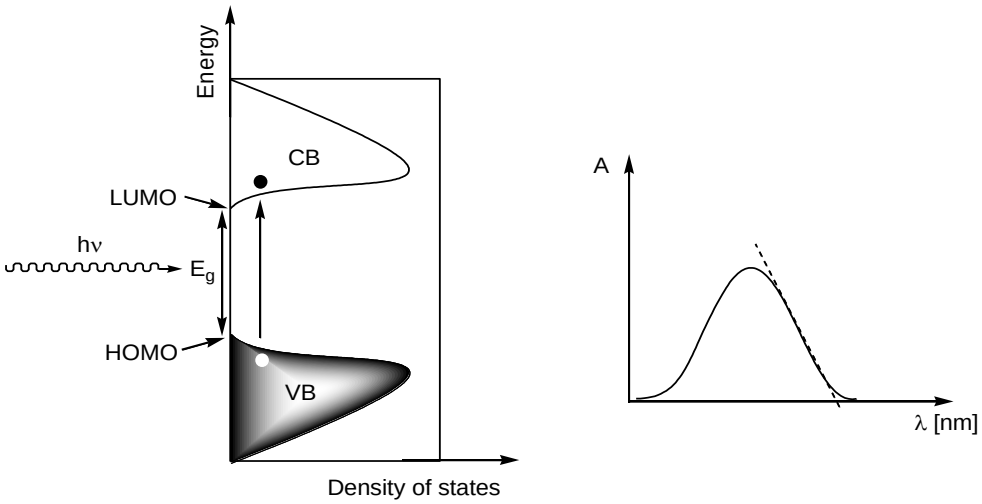

Figure 3. Density of states band structure (left); corresponding UV-vis absorption spectrum (right).

Another important optical property of conjugated polymers is the ability to generate light when electrical charges are injected into the polymer. This process is called electroluminescence.[11] When an electrical field is applied, electrons are injected into the polymers LUMO level by a cathode. At the same time electrons are extracted from the HOMO level by an anode, creating holes. The electrons will combine with the holes, generating excitons which can again decay non-radiatively or radiatively.

2.3. Applications

Conjugated polymers combine the mechanical properties and processing advantages of polymers with the electrical and optical properties of metals and semiconductors. They can be processed from solutions and easy deposition techniques such as spin-coating, spray-coating or inkjet printing can be used to make large area thin films in roll-to-roll processes.[12] Furthermore, conjugated polymers are lightweight and flexible materials, which are distinct advantages compared to their brittle and dense inorganic counterparts. Therefore, conjugated materials are extensively investigated for use in a wide range of optical and electronic applications such as organic

photovoltaic cells (OPV's),[13–16] organic light emitting diodes (OLED's),[11,17–22] organic field effect transistors (OFET's),[23–28] (bio)sensors[29–33] and a lot of other devices.[34–44]

Organic light emitting diodes (OLED's) can be used in LED lighting[45] and in displays.[46] To this end, the OLED's need to have sufficient operating lifetimes, stable electrical performance and should be available in red, green and blue emitting types. To address these requirements, new classes of light emitting polymers will have to be developed and LED devices with optimized structures will have to be fabricated. However, prototype OLED displays have already shown a lifetime of 10000 h, which is very reasonable for this type of applications.[47]

Because of the rather low field-effect mobility of semiconducting polymers compared to single crystalline silicon, organic field effect transistors (OFET's) can only be used in low-performance applications, for instance liquid crystal displays.[48] The electrical resistance and the operating speed of a transistor are determined by the field-effect mobility. For a conjugated polymer, the mobility is dependent on the molecular structure of the polymer as well as on the microstructure of this polymer in a thin film. Some semiconducting polymers have a field-effect mobility comparable to that of amorphous silicon, and could therefore be used in radio-frequency identification tags.[49]

Conjugated polymers can also be used to bridge the gap between electronics and biological systems. Via functionalization, one can alter the properties of a conjugated polymer to be biocompatible or biofunctional. As a result, these polymers can be used to sense biological systems or to modify biological functions.[29–33] The aim is to specifically control the interactions between conjugated polymers and biological species. In this area, still a significant amount of research has to be conducted before commercialization can take place.

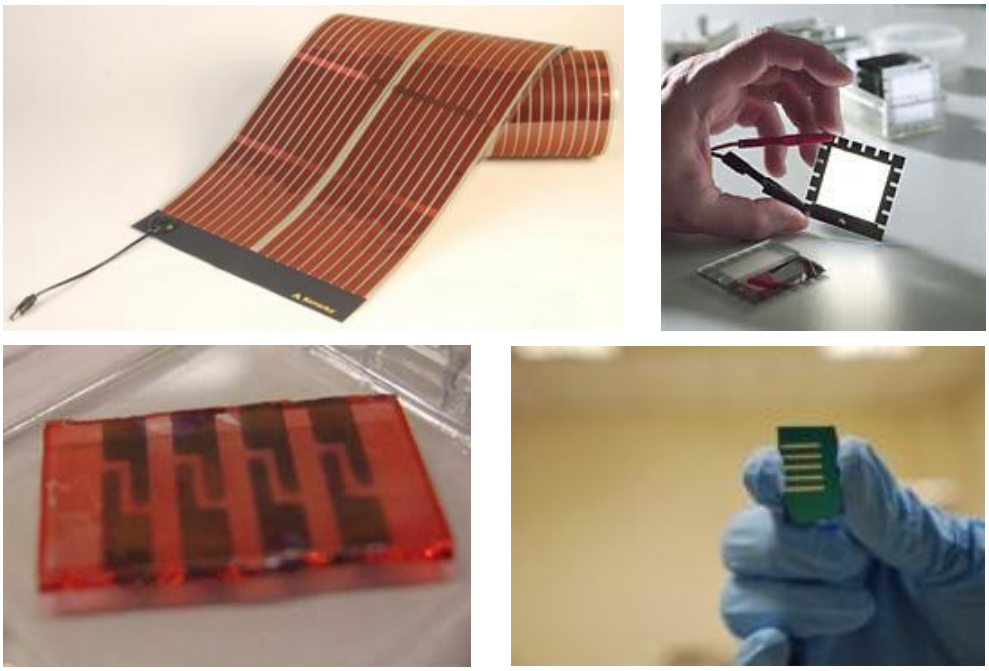

Figure 4. Various organic semiconductor applications: top left: a flexible organic solar panel (Konarka Power Plastic®); top right: an organic light emitting diode display; bottom left: a biosensor coated with MDMO-PPV; bottom right: an organic thin film transistor.

The continuously increasing demand of energy worldwide is mainly satisfied by either limited fossil fuels or by nuclear power. However, the use of these energy sources has a major impact on the environment. Therefore, a lot of effort has been put in research and development of renewable energy sources during the last decades. Solar energy is one of the most promising renewable resources since there is an unlimited supply of sunlight. The first photovoltaic cell was developed in 1954.[50] Since then, many different type of solar cells have been developed, usually using silicon as semiconductor material.[51] Today Si-based solar cells are used quite extensively in modern society.[52] However, the manufacturing costs for these type of solar cells are high and they are not that easy to process. Furthermore, there is an increasing demand for flexible solar cells, for instance to be incorporated

into clothing or to easily cover bended surfaces. Organic photovoltaic cells based on conjugated polymeric materials could provide an ideal solution to overcome these problems. The main issues for organic solar cells to be able to compete commercially with inorganic solar cells, is the device efficiency and the stability or lifetime. However, device fabrication is under constant optimization and new synthetic procedures are developed continuously, moving organic conjugated polymers closer to commercial use in photovoltaic systems.[53]

3. Poly(*p*-phenylene vinylene) (PPV)

Many different classes of conjugated polymers have been developed during the last decades. This thesis will focus on one class of polymers, namely poly(*para*-phenylene vinylene) (PPV) and on various functionalized PPV derivatives. The structure of PPV can be seen in Figure 1 and consists of phenylene rings which are connected in the *para* positions by vinylene bonds. It is a stable polymer which can be synthesized in high yields, high purity and high molecular weights.

By functionalizing the PPV backbone with side chains, properties such as the solubility and thermal behavior can be tuned towards the desired applications. The optical band gap of plain (un-substituted) PPV lies around 2.5 eV and the material is known for its bright yellow fluorescence,[11] making it useful in optoelectronic devices such as LED's and solar cells.[11,13–22] PPV derivatives are also used in biosensors and FET's.[23–33]

3.1. Synthetic Approaches

PPV's can be synthesized via two major different approaches, either direct routes or precursor routes. In the direct synthetic routes towards PPV, the vinylene bonds are formed *in-situ*. Some direct routes make use of step-growth polycondensation reactions, such as Wittig,[54,55] Horner,[56] McMurry[57,58] and Knoevenagel[59–61] polycondensations. More commonly used are the transition-metal catalyzed coupling reactions such as the Heck,[62,63] Stille[64,65] and Suzuki coupling,[66] which all make use of a palladium catalyst. The

electrochemical reaction of certain monomers can also lead to PPV's.[67,68] One of the disadvantages of these direct routes is that the achieved molecular weights are often significantly lower than those obtained by the precursor routes. Furthermore, for the direct routes the reaction is very sensitive towards the used conditions and is therefore not easy to control. Complex functionalized PPV derivatives cannot be synthesized via direct routes. Therefore, precursor routes are a more straightforward way to obtain desired soluble functionalized PPV structures.

3.2. Precursor Routes

The most common precursor routes make use of the polymerization behavior of *p*-quinodimethane systems. In literature, different precursor routes are well described, *i.e.* the Gilch route,[69] the Wessling-Zimmerman route,[70–73] the xanthate route[74–76] and the, in our group developed, dithiocarbamate[77–82] and sulfinyl routes.[83,84] All these routes differ by the identity of the polarizer (P) and leaving (L) functional group in the premonomer structure, the polymerization conditions, whether conversion to the conjugated structure occurs in situ or ex situ and to what extent the conversion is thermal induced or reagent induced. The general polymerization mechanism is depicted in Scheme 1. Via addition of a base, a proton is abstracted from the premonomer, followed by 1,6-elimination of the leaving group. This way, a *p*-quinodimethane system is formed, which is the actual monomer. Subsequently, this monomer can polymerize into the precursor polymer via a self-initiating radical mechanism.[85,86] In some cases a competition between this radical mechanism and an anionic mechanism[87,88] is observed, whereby typically the high molecular weight material is associated with the self-initiating radical mechanism and the rather low molecular weight material is produced via an anionic mechanism. In a last step, the precursor polymer is converted into a conjugated material via a thermal or reagent induced elimination reaction. The sulfinyl precursor route is the only route which has a premonomer with different leaving group and polarizer group. Due to the asymmetric premonomer, the polymerization reaction is fully controllable

and can be performed in common organic solvents such as alcohols.[83] However, the implementation of the non-symmetrical P and L groups into the premonomer is quite challenging.[89]

Scheme 1. Precursor Routes towards Poly(*p*-phenylene vinylene) Derivatives

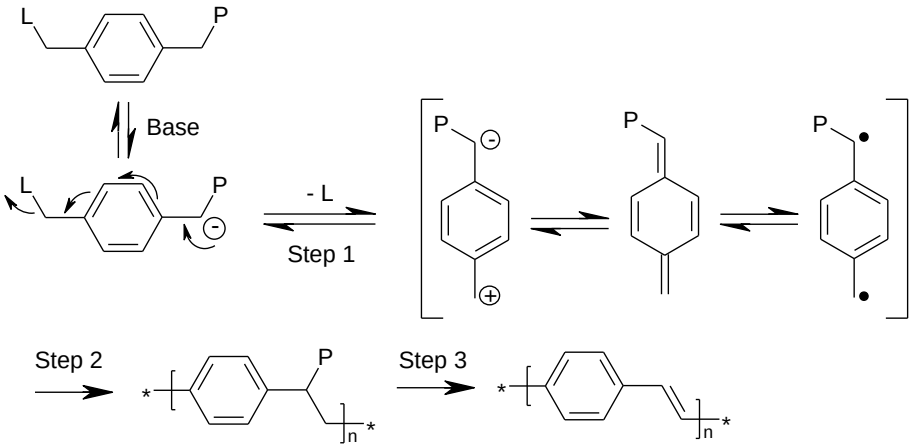

Gilch route:	L=P= Cl or Br
Sulfonium route:	L=P= R_2S-
Sulfinyl route:	L= Cl or Br ; P= RS(O)-
Xanthate route:	L=P= RO-C(S)-S-
Dithiocarbamate route:	L=P= R_2N-C(S)-S-

The characteristics of the obtained polymers vary along the different precursor routes. For instance, the xanthate precursor route yields typically broad polydispersities (PD) and shows structural defects in the final conjugated system. On the other hand the sulfinyl and the dithiocarbamate precursor routes lead to the formation of precursor polymers with low structural defect levels.[90,91] In this thesis, usually the dithiocarbamate precursor route has been used for the synthesis of various functionalized PPV derivatives.

4. Aim and Outline

The aim of the research presented in this thesis is the synthesis and characterization of novel functionalized PPV derivatives for a variety of optoelectronic devices. Different side chains have been built in onto the phenyl rings of the PPV premonomers and polymerizations usually have been carried out via the dithiocarbamate route. Whenever this precursor route could not be used (for instance due to steric hindrance of the side chains), polymers were prepared via the Gilch route.

The following chapters are written in manuscript style and are published or submitted to various peer-reviewed journals. Therefore, monomer and polymer structures are numbered again in each chapter. Furthermore, the references are formatted in different styles, depending on the requirements of the journal to which each chapter is submitted.

Chapter 2 describes the synthesis of MDMO-PPV via the dithiocarbamate precursor route, which combines a straightforward monomer synthesis with high quality resulting polymers. The optimal polymerization conditions are studied for two bases, lithium bis(trimethylsilyl)amide (LHMDS) and potassium *tert*-butoxide (K*t*BuO). The thermal conversion of the precursor polymer into the conjugated system is studied by in situ UV-vis and FT-IR spectroscopy. The microstructure of the resulting polymer is studied via NMR spectroscopy, to gain insight in the amount of defects and the degree of regioregularity.

In **Chapter 3** an acid induced conversion method for dithiocarbamate precursor poly(thienylene vinylene) (PTV) and poly(*p*-phenylene vinylene) (PPV) derivatives is presented, which can be executed at lower temperatures, comparing to the standard thermal conversion method. Two different acids, benzenesulfonic acid and trifluoroacetic acid, are used. The conjugation length of the resulting polymer chromophore structures is studied with UV-vis and FTIR spectroscopy. A tentative reaction mechanism for the acid induced conversion of PTV and PPV derivatives, is proposed.

Chapter 4 presents the synthesis and characterization of two hydrophilic branched oligo(ethylene glycol)-substituted PPV derivatives, poly(2,5-bis(1,3-

bis(triethoxymethoxy)propan-2-yloxy)-1,4-phenylene vinylene) (BTEMP-PPV) and poly(2-methoxy-5-(1,3-bis(triethoxymethoxy)propan-2-yloxy)-1,4-phenylene vinylene) (MTEMP-PPV), via the dithiocarbamate precursor route. The solubility of the polymers is studied with UV-vis spectroscopy. Since the polymers have nonionic polar side chains, they are soluble in a variety of solvents, including alcohols and even water. Therefore, these polymers are suitable candidates to be used in environment-friendly processed optoelectronic devices.

In **Chapter 5** two first examples of inherently regioregular tetra-alkoxy substituted PPV derivatives, poly(2,3,5,6-tetrahexyloxy-1,4-phenylene vinylene) (TH-PPV) and poly[2,3,5,6-tetra(2'-ethyl-hexyloxy)-1,4-phenylene vinylene] TEH-PPV, are presented. Because of large steric hindrance, the polymerizations are carried out via the Gilch route. The solubility in various solvents is tested and the conjugated structure is studied with UV-vis and fluorescence spectroscopy. Both polymers are studied with polarized light microscopy and differential scanning calorimetry to examine the thermal behavior and possible presence of ordering phenomena, such as liquid crystals. As a first demonstration of the charge transporting properties of TH-PPV, a simple solution processed electroluminescent device is prepared.

In order to improve the thermal stability of polymer:fullerene bulk heterojunction solar cells, a new polymer, poly[2-methoxy-5-(2'-phenylethoxy)-1,4-phenylene vinylene] (MPE-PPV), with a glass transition temperature (*Tg*) of 110 °C is presented in **Chapter 6**. Polymerizations are executed via the Gilch route. The phase behavior of MPE-PPV:[60]PCBM blends is investigated by means of (MT)DSC and RHC. Furthermore, MPE-PPV is used as an electron donor in polymer:[70]PCBM solar cells of which the thermal stability is compared with solar cells based on the reference material MDMO-PPV with a *Tg* of 45 °C. A systematic transmission electron microscope (TEM) study of the MPE-PPV:[60]PCBM active layer is executed. Finally, the MPE-PPV:fullerene devices are optimized for maximal photovoltaic performance.

Finally, **Chapter 7** describes a mechanistic and kinetic study of the dithiocarbamate and sulfinyl precursor routes. Since precursor routes usually yield very high molecular weight materials, the resulting PPV derivatives can show solubility problems. This may cause the failure of post-polymerization reactions, and any further functionalization of the PPV derivatives becomes troublesome. To gain more insight in the reaction mechanism and kinetics of both precursor routes, a kinetic UV-vis study is carried out to reveal the formation and subsequent polymerization of the *p*-quinodimethane system. Furthermore, the reaction conditions such as reaction time, temperature, and concentration are changed in order to see the effects on molecular weight and polymer yield. Chain transfer agents are added to the polymerization mixture to study the influence on reaction kinetics and on molecular weight. Finally, the polymerization reaction mixtures are analyzed by means of electron spray ionization - mass spectrometry (ESI-MS).
At the end of the thesis, a summary both in English and in Dutch is given and two appendices with a list of publications and a list of abbreviations. Last but not least, some words of thanks are addressed to all people who helped directly or indirectly to the realization of this PhD study and thesis.

5. References

(1) Staudinger, H. *Chem. Ber.* **1924**, *57*, 1203–1208.

(2) Mark, H.; Whitby, G. S. *Collected Papers of Wallace Hume Carothers on High Polymeric Substances,* Wiley-Interscience, New York, **1940**.

(3) Salaneck, W. R.; Lundstrom, I.; Rånby, B. *Conjugated Polymers and Related Materials : The Interconnection of Chemical and Electronic Structure,* Oxford University Press, Oxford, **2002**, 15–26.

(4) Ziegler, K.; Holzkamp, E.; Breil, H.; Martin, H. *Angew. Chem. Int. Ed.* **1955**, *67*, 541–547.

(5) Natta, G.; Pino, P.; Corradini, P.; Danusso, F.; Mantica, E.; Mazzanti, G.; Moraglio, G. *J. Am. Chem. Soc.* **1955**, *77*, 1708–1710.

(6) Flory, P. J. *Principles of Polymer Chemistry,* 2nd ed., Cornell University Press, Ithaca, N.Y., **1953**.

(7) Shirakawa, H.; Louis, E. J.; MacDiarmid, A. G.; Chiang, C. K.; Heeger, A. J. *J. Chem. Soc. Chem. Comm.* **1977**, 578–580.

(8) Heeger, A. J. *Synthetic Met.* **2001**, *125*, 23–42.

(9) Schriver, D. F.; Atkins, P. W.; Langford, C. H. *Inorganic Chemistry*, 2nd ed., Oxford University Press, Oxford, **1994**, 91.

(10) Rohatgi, M. *Fundamentals of Photochemistry*, Wiley Eastern Ltd., New Delhi, **1978**.

(11) Friend, R. H.; Gymer, R. W.; Holmes, A. B.; Burroughes, J. H.; Marks, R. N.; Taliani, C.; Bradley, D. D. C.; Dos Santos, D. A.; Brédas, J. L.; Lögdlund, M.; Salaneck, W. R. *Nature* **1999**, *397*, 121–128.

(12) Sheats, J. R. *J. Mater. Res.* **2004**, *19*, 1974–1989.

(13) Rostalski, J.; Meissner D. *Sol. Energ. Mat. Sol. C.* **2000**, *61*, 87–95.

(14) Brabec, J. C.; Sariciftci, N. S.; Hummelen, J. C. *Adv. Funct. Mater.* **2001**, *11*, 15–26.

(15) Hoppe, H.; Sariciftci, N. S. *J. Mater. Res.* **2004**, *19*, 1924–1945.

(16) Hoppe, H.; Niggeman, M.; Winder C.; Kraut, J.; Heisgen, R.; Hinsch, A.; Meissner, D.; Sariciftci, N. S. *Adv. Funct. Mater.* **2004**, *14*, 1005–1011.

(17) Braun, D.; Heeger, A. J. *Appl. Phys. Lett.* **1991**, *58*, 1982–1984.

(18) Burn, P. L.; Holmes, A. B.; Kraft, A.; Bradley, D. D. C.; Brown, A. R.; Friend, R. H.; Gymer, R. W. *Nature*, **1992**, *356*, 47–49.

(19) Bradley, D. D. C. *Synthetic. Met.* **1993**, *54*, 401–415.

(20) May, P. *Phys. World* **1995**, *8*, 52–57.

(21) Salbeck, J. *Ber. Bunsen. Phys. Chem.* **1996**, *100*, 1667–1677.

(22) Kraft, A.; Grimsdale, A. C.; Holmes, A. B. *Angew. Chem. Int. Ed.* **1998**, *37*, 402–428.

(23) Roth, S. *One-dimensional metals*, Weinheim VCH, **1995**, 209–231.

(24) Sirringhaus, H.; Tessler, N.; Friend, R. H. *Science* **1998**, *280*, 1741–1744.

(25) Horowitz, G. *Adv. Mater.* **1998**, *10*, 365–377.

(26) Bao, Z. *Adv. Mater.* **2000**, *12*, 227–230.

(27) Dimitrakopoulos, C. D.; Malenfant, R. L. *Adv. Mater.* **2002**, *14*, 99–117.

(28) Scheinert, S.; Paasch, G. *Phys. Status Solidi A* **2004**, *201*, 1263–1301.

(29) MacDiarmid, A. G.; Zhang, W. J.; Huang, Z.; Wang, P.-C.; Huang, F.; Xie, S. *Polym. Prepr.* **1997**, *11*, 333–334.

(30) Heeger, P. S.; Heeger, A. J. *Proc. Natl. Acad. Sci.* **1999**, *96*, 12219–12221.

(31) Chen, L.; McBranch, W.; Wang, H.; Helgeson, R.; Wudl, F.; Whitten, D. G. *Proc. Natl. Acad. Sci.* **1999**, *96*, 12287–12297.

(32) McQuade, D. T.; Pullen, A. E.; Swager, T. M. *Chem. Rev.* **2000**, *100*, 2537–2574.

(33) Gerard, M.; Chaubey, A.; Malhotra, B. D. *Biosens. Bioelectron.* **2002**, *17*, 345–359.

(34) Schwartz, B.; Diaz-Garcia, M.; Hide, F.; Andersson, M.; Pei, Q.; Heeger, A. *Polym. Prepr.* **1997**, *38*, 325.

(35) Tessler, N. *Adv. Mater.* **1999**, *11*, 363–370.

(36) McGehee, M.; Heeger, A. *Adv. Mater.* **2000**, *12*, 1655–1668.

(37) Nigrey, P.; MacInnes, D.; Nairns, D.; MacDiarmid, A.; Heeger, A. *J. Electrochem. Soc.* **1981**, *128*, 1651–1654.

(38) Wirsén, A. *Electroactive Polymer Materials*, Technomic publishing AG, Switzerland, **1987**.

(39) Kanatzidis, M. G. *Chem. Eng. News* **1990**, *68*, 36–50.

(40) Miller, J. *Adv. Mater.* **1993**, *5*, 671–676.

(41) Roth, S. *One-Dimensional Metals*, Weinheim VCH, **1995**, 209.

(42) Lu, W.; Fadeev, A. G.; Qi, B.; Smela, E.; Mattes, B. R.; Ding, J.; Spinks, G. M.; Mazurkiewicz, J.; Zhou, D.; Wallace, G. G.; MacFarlane, D. R.; Forsyth, S. A.; Forsyth, M. *Science*, **2002**, *297*, 983–987.

(43) Yu, G.; Wang, J.; McElvain, J.; Heeger, A. J. *Adv. Mater.* **1998**, *10*, 1431–1434.

(44) Miyazaki, S.; Itami, S.; Araki, T. *Rev. Sci. Instrum.* **1998**, *69*, 3751–3754.

(45) Schubert, E. F.; Kim, J. K. *Science* **2005**, *308*, 1274–1278.

(46) Geffroy, B.; Le Roy, P.; Prat, C. *Polym. Int.* **2006**, *55*, 572–582.

(47) Liu, M. S.; Niu, Y. H.; Luo, J. D. *Polym. Rev.* **2006**, *46*, 7–26.

(48) Chabinyc, M. L.; Salleo, A. *Chem. Mater.* **2004**, *16*, 4509–4521.

(49) Clemens, W.; Fix, I.; Ficker, J.; Knobloch, A.; Ullmann, A. *J. Mater. Res.* **2004**, 19, 1963–1973.

(50) Chapin, D. M.; Fuller, C. S.; Pearson, G. L. *J. Appl. Phys.* **1954**, *25*, 676–677.

(51) Miles, R. W.; Hynes, K. M.; Forbes, I. *Prog. Cryst. Growth Ch.* **2005**, *51*, 1–42.

(52) Goetzberger, A.; Hebling, C.; Schock, H. W. *Mat. Sci. Eng. R.* **2003**, *40*, 1–46.

(53) http://www.konarka.com

(54) McDonald, R. N.; Campbell, T. W. *J. Am. Chem. Soc.* **1960**, *82*, 4669–4671.

(55) Hörhold, H.-H.; Opfermann, J. *Makromol. Chem.* **1970**, *131*, 105–132.

(56) Pfeiffer, S.; Hörhold, H.-H. *Synthetic. Met.* **1999**, *101*, 109–110.

(57) Rehahn, M.; Schlüter, A.-D. *Makromol. Chem. Rapid Comm.* **1990**, *11*, 375–379.

(58) Stalmach, V.; Kolshorn, H.; Brehm, I.; Meier, M. *Liebigs Ann.* **1996**, 1449–1456.

(59) Lenz, R. W.; Handlovits, C. E. *J. Org. Chem.* **1960**, *25*, 813–817.

(60) Staring, E. G. J.; Demandt, R. C. J. E.; Braun, D.; Rikken, G. L. J.; Kessener, Y. A. R. R.; Venhuizen, A. H. J.; Knippenberg, M. M. F.; Bouwmans, M. *Synthetic Met.* **1995**, *71*, 2179–2180.

(61) Moratti, S. C.; Bradley, D. D. C.; Friend, R. H.; Greenham, N. C.; Holmes, A. B. *Polym. Prep.* **1994**, *35*, 214.

(62) Heck, R. F. *Org. Reactions* **1982**, *27*, 345–390.

(63) Greiner, A.; Heitz, W. *Makromol. Chem. Rapid Comm.* **1988**, *9*, 581–588.

(64) Babudri, F.; Cicco, S. R.; Farinola, G. M.; Naso, F.; Bolognesi, A.; Porzio, W. *Macromol. Rapid Comm.* **1996**, *17*, 905–911.

(65) Bao, Z.; Chan, W. K.; Yu, L. *J. Am. Chem. Soc.* **1995**, *117*, 12426–12435.

(66) Koch, F.; Heitz, W. *Macromol. Chem. Physic.* **1997**, *198*, 1531–1544.

(67) Chang, W. P.; Whang, W. T.; Lin, P. W. *Polymer* **1996**, *37*, 1513–1518.

(68) Nishihara, H.; Tateishi, M.; Aramaki, K.; Ohsawa, T.; Kimura, O. *Chem. Lett.* **1987**, 539–542.

(69) Gilch, H. G.; Wheelwright, W. L. *J. Polym. Sci.* **1966**, *4*, 1337–1349.

(70) Harper, K.; West, W. J. W. *Eur. Pat. Appl. No. 182548*, **1985**.

(71) Jen, K. Y.; Jow, R.; Eckhardt, H.; Elsenbaumer, R. L. *Polym. Mater. Sci. Eng.* **1987**, *56*, 49–53.

(72) Jen, K. Y.; Maxfield, M.; Shacklette, L. W.; Elsenbaumer, R. L. *J. Chem. Soc. Chem. Comm.* **1987**, 309–311.

(73) Wessling, R. A. *J. Polym. Sci. Pol. Sym.* **1985**, *72*, 55–66.

(74) Son, S.; Dodabalapur, A.; Lovinger, A. J.; Galvin, M. E. *Science* **1995**, *269*, 376–378.

(75) Kesters, E.; Gillissen, S.; Motmans, F.; Lutsen, L.; Vanderzande D. *Macromolecules* **2002**, *35*, 7902–7910.

(76) Mitchell, W. J.; Pena, C.; Burn, P. L. *J. Mater. Chem.* **2002**, *12*, 200–205.

(77) Henckens, A.; Lutsen, L.; Vanderzande, D.; Knipper, M.; Manca, J.; Aernouts, T.; Poortmans, J. *SPIE Proc.* **2004**, 52–59.

(78) Henckens, A.; Colladet, K.; Fourier, S.; Cleij, T. J.; Lutsen, L.; Gelan, J. *Macromolecules* **2005**, *38*, 19–26.

(79) Henckens, A.; Duyssens, I.; Lutsen, L.; Vanderzande, D.; Cleij, T. J. *Polymer* **2006**, *47*, 123–131.

(80) Banishoeib, F.; Fourier, S.; Cleij, T. J.; Lutsen, L.; Vanderzande, D. *Eur. Phys. J.-Appl. Phys.* **2007**, *37*, 237–240.

(81) Nguyen, L. H.; Günes, S.; Neugebauer, H.; Sariciftci, N. S.; Banishoeib, F.; Henckens, A.; Cleij, T. J.; Lutsen, L.; Vanderzande, D. *Sol. Energ. Mat. Sol. C.* **2006**, *90*, 2815–2828.

(82) Banishoeib, F.; Adriaensens, P.; Berson, S.; Guillerez, S.; Douheret, O.; Manca, J.; Fourier, S.; Cleij, T. J.; Lutsen, L.; Vanderzande, D. *Sol. Energ. Mat. Sol. C.* **2007**, *91*, 1026–1034.

(83) van Breemen, A. J. J. M.; Issaris, A. C. J.; de Kok, M. M.; Van Der Borght, M. J. A. N.; Adriaensens, P. J.; Gelan, J. M. J. V.; Vanderzande, D. J. M. *Macromolecules* **1999**, *32*, 5728–5735.

(84) Henckens, A.; Knipper, M.; Polec, I.; Manca, J.; Lutsen, L.; Vanderzande, D. *Thin solid films* **2004**, *451–452*, 572–579.

(85) Wiesecke, J.; Rehahn, M. *Angew. Chem., Int. Ed.* **2003**, *42*, 567–570.

(86) Schwalm, T. ; Wiesecke, J.; Immel, S.; Rehahn, M. *Macromolecules* **2007**, *40*, 8842–8854.

(87) Hontis, L.; Van Der Borght, M.; Vanderzande, D.; Gelan, J. *Polymer* **1999**, *40*, 6615–6617.

(88) Adriaensens, P.; Van der Borght, M.; Hontis, L.; Issaris, A.; van Breemen, A.; de Kok, M.; Vanderzande, D.; Gelan, J. *Polymer* **2000**, *41*, 7003–7009.

(89) van Breemen, A. J. J. M.; Vanderzande, D. J. M.; Adriaensens, P. J.; Gelan, J. M. J. V. *J. Org. Chem.* **1999**, *64*, 3106–3112.

(90) Roex, H.; Adriaensens, P.; Vanderzande, D.; Gelan, J. *Macromolecules* **2003**, *36,* 5613–5622.

(91) Vandenbergh, J.; Wouters, J.; Adriaensens, P. J.; Mens, R.; Cleij, T. J.; Lutsen, L.; Vanderzande, D. *Macromolecules* **2009**, *42*, 3661–3668.

Chapter 2

Exploring the Dithiocarbamate Precursor Route: Observation of a Base Induced Regioregularity Excess in Poly[(2-methoxy-5-(3',7',-dimethyloctyloxy))-1,4-phenylene vinylene] (MDMO-PPV)

ABSTRACT: The dithiocarbamate precursor route is a suitable way to synthesize poly(*p*-phenylene vinylene) derivatives in an efficient manner. It is demonstrated that this precursor route combines the straightforward monomer synthesis of the Gilch route with the superior polymer quality of the more complex sulfinyl route. To obtain the polymers, the bisdithiocarbamate MDMO-monomer has been polymerized using either lithium bis(trimethylsilyl)amide (LHMDS) or potassium *tert*-butoxide (K*t*BuO). The addition of either base results in the formation of high molecular weight precursor polymer. It is shown that the polymerization mechanism follows a radical pathway. Furthermore it is demonstrated that the molecular structure of the polymer shows a certain degree of regioregularity when LHMDS is used. The thermal conversion of the precursor polymer into the conjugated system is studied by in situ UV-vis and FT-IR spectroscopy. A NMR study on ^{13}C-labeled MDMO-PPV reveals the presence of only a minimal amount of structural defects in the microstructure of the polymer, further confirming the excellent characteristics of the dithiocarbamate precursor route.

---

*Vandenbergh, J.; Wouters, J.; Adriaensens, P. J.; Mens, R.; Cleij, T. J.; Lutsen, L.; Vanderzande, D. J. M. *Macromolecules* **2009**, *42*, 3661–3668.

1. Introduction

Nowadays, conjugated polymers find application in various optical and electronic devices such as light emitting diodes (LED),[1] field effect transistors (FET),[2] photovoltaic cells[3] and sensors.[4] Due to their interesting optoelectronic and electrical properties, a considerable amount of research has been performed on poly(*p*-phenylene vinylene) derivatives (PPV's).[1] PPV's can be synthesized via either direct routes or precursor routes. The most important direct routes make use of step-growth polycondensation reactions, such as Wittig[5] and Horner[6] polycondensations, or transition-metal catalyzed coupling reactions such as the Heck[7] coupling. One of the disadvantages of these direct routes is that the achieved molecular weights are often significantly lower than those obtained by the precursor routes which make use of the polymerization behavior of *p*-quinodimethane systems. Furthermore, for the direct routes the reaction is very sensitive towards the conditions used and is therefore not easy to control. Four different precursor routes are well described in literature, *i.e.* the Gilch route,[8] the Wessling-Zimmerman route,[9] the xanthate route[10] and the sulfinyl route.[11] The latter is superior because of its versatility, the fact that it can be performed at moderate temperatures in common organic solvents such as alcohols[12] and because it leads to the formation of precursor polymers with extremely low structural defect levels.[13] Each of these precursor routes makes use of a monomer bearing a polarizer and a leaving group. Via addition of a base, a quinodimethane system, which is the actual monomer, is formed (Scheme 1). Subsequently, this monomer can polymerize into the precursor polymer via a self-initiating radical mechanism.[14,15] In some cases a competition between this radical mechanism and a certain anionic mechanism[16,17] is observed, whereby typically the high molecular weight material is associated with the self-initiating radical mechanism and the rather low molecular weight material is produced via an anionic mechanism. In a last step, the precursor polymer is converted into a conjugated material via a thermal or base induced elimination reaction.

Scheme 1. Precursor Routes towards Poly(*p*-phenylene vinylene) Derivatives

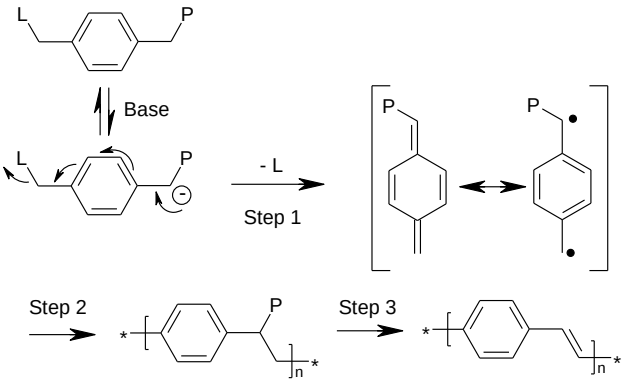

Gilch route:	L=P= Cl or Br
Sulfonium route:	L=P= R_2S-
Sulfinyl route:	L= Cl or Br ; P= RS(O)-
Xanthate route:	L=P= RO-C(S)-S-
Dithiocarbamate route:	L=P= R_2N-C(S)-S-

Recently our group introduced another precursor route, which also fits to this scheme, the so-called "dithiocarbamate route".[18] Some preliminary studies on the use of the dithiocarbamate precursor route towards the synthesis of poly(thienylene vinylene) (PTV)[19] and poly(*p*-phenylene vinylene) (PPV)[20] derivatives have already been reported. However, in both cases it became clear that the polymerization procedure used in this new precursor route still needed to be optimized. Initially lithium diisopropylamide (LDA) was used as the base in these polymerizations. This resulted quite often in the occurrence of side reactions and/or a strong competition between the radical and anionic polymerization mechanism, thus leading to a bimodal molecular weight distribution for the resulting precursor polymer.

This paper presents the use of lithium bis(trimethylsilyl)amide (LHMDS)[21] and potassium *tert*-butoxide (K*t*BuO) as bases in the dithiocarbamate route towards the synthesis of poly[(2-methoxy-5-(3',7',-dimethyloctyloxy))-1,4-phenylene vinylene] (MDMO-PPV). As will be demonstrated for both bases, precursor polymers are obtained with a monomodal molecular weight

distribution, high molecular weight and relative low polydispersities (PD) as compared to the typical PD values observed for the Gilch route.[22]

After synthesis and characterization of the precursor polymer, the conversion process towards the conjugated polymer is studied via in situ FT-IR and UV-vis spectroscopy. A NMR study on ^{13}C-labeled MDMO-PPV reveals that only a very small amount of defects is present and that the polymerization mainly occurs via head-to-tail additions. Furthermore, a regioregularity excess of 29% in the polymer structure could be calculated through the use of quantitative ^{1}H NMR. This phenomenon is explained by the sterical effects induced by the sterically demanding base LHMDS on deprotonation of the pre-monomer. For the less sterically hindered base K*t*BuO, no regioregular effect is observed.

2. Experimental Section

2.1. General Data

Unless otherwise stated, all reagents and chemicals were obtained from commercial sources (Acros and Aldrich) and used without further purification. Tetrahydrofuran (THF) was dried by distillation from sodium/benzophenone. NMR spectra were recorded with a Varian Inova 300 spectrometer at 300 MHz for ^{1}H NMR and at 75 MHz for ^{13}C NMR using a 5 mm probe. Gas chromatography/mass spectrometry (GC/MS) analyses were carried out with TSQ-70 and Voyager mass spectrometers (Thermoquest); the capillary column was a Chrompack Cpsil5CB or Cpsil8CB. Analytical size exclusion chromatography (SEC) was performed using a Spectra series P100 (Spectra Physics) pump equipped with two mixed-B columns (10 µm, 0.75 cm x 30 cm, Polymer Laboratories) and a refractive index detector (Shodex) at 40°C. THF was used as the eluent at a flow rate of 1.0 mL/min. Molecular weight distributions are given relative to polystyrene standards. FT-IR spectra were collected with a Perkin-Elmer Spectrum One FT-IR spectrometer (nominal resolution 4 cm-1, summation of 16 scans). UV-vis spectroscopy was performed on a VARIAN CARY 500 UV-vis-NIR spectrophotometer (scan rate: 600 nm/min). Samples for temperature-dependent thin-film FT-IR and UV-vis characterization were prepared by dropcasting the precursor polymer from a

$CHCl_3$ solution (10 mg/mL) onto NaCl disks or quartz disks. The disks were heated in a Harrick high-temperature cell (heating rate: 2 °C/min), which was positioned in the beam of either the FT-IR or the UV-vis spectrometer to allow in-situ measurements. Spectra were taken continuously under a continuous flow of N_2 during which the samples were in direct contact with the heating element.

2.2. Synthesis

*2,5-Bis(chloro-methyl)-1-(3,7-dimethyloctyloxy)-4-methoxybenzene (**1**).* Synthesis of 2,5-bis(chloro-methyl)-1-(3,7-dimethyloctyloxy)-4-methoxy benzene **1** was reported elsewhere.[23] All properties were in agreement with the previously reported materials.

*2,5-Bis(N,N-diethyldithiocarbamate-methyl)-1-(3,7-dimethyloctyloxy)-4-methoxybenzene (**2**).* To 50 mL of an ethanol solution of 2,5-bis(chloro-methyl)-1-(3,7-dimethyloctyloxy)-4-methoxybenzene **1** (1 g, 2.767 mmol), sodium diethyldithiocarbamate trihydrate (1.445 g, 6.365 mmol) was added as a solid. The mixture was stirred for 3 h at ambient temperature under a nitrogen atmosphere. Subsequently, 50 mL of water was added and the mixture was filtered over a Buchner to obtain white crystals which were washed with ethanol and water and used without further purification. Yield: 100% mp: 70.2−70.7 °C; ^{1}H NMR ($CDCl_3$): 6.99 (s, 2H), 4.52 (s, 2H), 4.48 (s, 2H), 3.95 (m, 4H+2H), 3.74 (s, 3H), 3.64 (m, 4H), 1.60−1.85 (m, 2H), 1.38−1.58 (m, 2H), 1.21 (t, 12H), 1.05−1.30 (m, 6H), 0.88 (d, 3H), 0.81 (d, 6H); ^{13}C NMR ($CDCl_3$): 196.11, 195.99, 151.27, 150.90, 125.08, 124.42, 114.75, 113.86, 67.13, 56.19, 49.41, 49.34, 46.61, 39.22, 37.32, 36.83, 36.30, 29.79, 27.95, 24.69, 22.69, 22.59, 19.62, 12.42, 11.59; MS (EI, *m*/*e*): 148 (M^+ SC(S) NEt_2), 116 (C(S)NEt_2); IR (NaCl, cm^{-1}): 2954, 2930, 2869, 1485, 1415, 1268, 1207.

*Polymerization of **2** (**3**).* In a typical procedure, 500 mg of monomer **2** was dissolved in 4.26 mL of dry THF giving a concentration of 0.2 M. The mixture was stirred at 35 °C under a continuous flow of nitrogen. 1.5 equiv of either a LHMDS solution (1 M in THF) or a K*t*BuO solution (0.87 M in THF) were added

in one go to the stirred monomer solution. The reaction proceeded for 1.5 h at 35 °C under a nitrogen atmosphere, and the mixture was subsequently quenched in 100 mL ice water. The excess of base was neutralized with HCl (1 M in H_2O). The aqueous phase was extracted with $CHCl_3$ (3 x 40 mL). After combination of the organic phases and evaporation of the solvent, the obtained crude polymer was again dissolved in 2 mL $CHCl_3$ and precipitated in 100 mL of stirred cold methanol. The mixture was filtered and the polymer was collected and dried *in vacuo*. The residual fractions contained only monomers and oligomers. Yields: 59%–67%; ^{1}H NMR ($CDCl_3$): 6.45–6.97 (br m, 2H), 5.50–5.87 (br s, 1H), 3.05–4.23 (br m, 11H), 1.02–1.95 (br m, 16H), 0.74–1.02 (m, 9H); ^{13}C NMR ($CDCl_3$): 195.76, 150.85, 127.68, 114.11, 113.09, 67.10, 56.39, 51.98, 49.08, 46.38, 39.27, 37.54, 36.60, 34.45, 29.91, 27.92, 24.67, 22.69, 22.58, 19.66, 12.47, 11.55; IR (NaCl, cm^{-1}): 2953, 2929, 1504, 1484, 1462, 1413, 1267, 1210, 1140, 1041.

*Thermal Elimination of Precursor Polymer **3** to Conjugated Polymer (**4**).* From a solution of **3** (160 mg) in dichlorobenzene (80 mL) oxygen was removed by purging for 1 h with nitrogen. Subsequently, the solution was heated to 180 °C and stirred for 3 h. After cooling to room temperature, the resulting dichlorobenzene was evaporated and the crude polymer mixture was dissolved in chloroform (2 mL). The solution was precipitated drop wise in cold methanol (100 mL). The polymer was filtered off, washed with cold methanol and dried at room temperature under reduced pressure. The conjugated MDMO-PPV **4** was obtained as a red polymer. The elimination procedure was performed a second time to ensure complete elimination. Yields were quantitative; ^{1}H NMR ($C_2D_2Cl_4$): 7.5 (br, 2H) 7.2 (br, 2H) 4.6–3.2 (br m, 5H) 2.1–0.6 (br m; 19H); ^{13}C NMR ($CDCl_3$): 151.4; 127.0; 123.3; 110.5; 108.8; 67.9; 56.4; 39.2; 37.4; 36.6; 30.2; 27.9; 24.6; 22.6; 19.8; IR (KBr, cm^{-1}): 2957, 2925, 2860, 1510, 1469, 1395, 1217, 1028, 872.

3. Results and Discussion

3.1. Monomer Synthesis

The MDMO bisdithiocarbamate monomer **2** is synthesized in one step from the corresponding Gilch bischloromethyl monomer (Scheme 2).[18] The synthetic route towards MDMO Gilch monomer was reported earlier.[23] The dichloride **1** is dissolved in ethanol and solid sodium diethyldithiocarbamate trihydrate is added to the mixture to obtain **2**. The resulting conversion is quantitative. Compared to the synthesis of the MDMO sulfinyl monomer, this one step synthesis is more straightforward.[11]

Scheme 2. Synthesis of MDMO-PPV via the Dithiocarbamate Route[a]

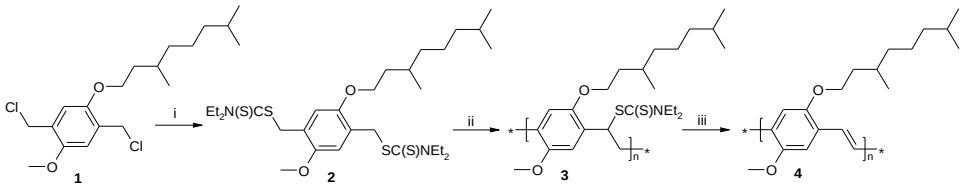

[a]Key: (i) $NaSC(S)NEt_2$ $.3H_2O$, EtOH; (ii) LHMDS or K*t*BuO, THF; (iii) Δ*T*, dichlorobenzene.

3.2. Polymerization

The polymerizations of the monomer are performed under nitrogen atmosphere. To this end, the bisdithiocarbamate MDMO monomer **2** is dissolved in dry THF (0.2 M) after which 1.5 equiv of either LHMDS or K*t*BuO is added as base. After polymerization, the reaction mixture is poured in ice-water, neutralized by hydrochloric acid and extracted with $CHCl_3$. The polymers are isolated via precipitation in cold methanol. Molecular weights (M_w) are determined by GPC relative to polystyrene (PS) standards with THF as the eluent.

In the first series of experiments, the polymerization of monomer **2** is performed with LHMDS as the base at three different temperatures. Increasing the polymerization temperature up to 65 °C leads to precursor polymers with higher polydispersities (PD), and is therefore not favorable.

The highest molecular weight is obtained for the precursor polymer synthesized at 35 °C (Table 1). Compared to previous polymerization results, obtained with LDA as base,[20] the use of LHMDS strongly suppresses the bimodal molecular weight distribution (Figure 1a). In view of the high molecular weights obtained, it seems that the radical polymerization mechanism[14,15] is dominating.

Table 1. Polymerization Results for LHMDS and K*t*BuO at Different Reaction Temperatures[a]

entry	base	temperature (°C)	yield (%)	M_w[b]	PD[b]
1	LHMDS	0	48	138 000	3.2
2	LHMDS	35	64	560 000	3.4
3	LHMDS	65	61	325 000	7.6
4	K*t*BuO	0	40	238 000	3.3
5	K*t*BuO	35	67	272 000	2.5
6	K*t*BuO	65	43	152 000	5.5

[a]Data represent average results of two experiments. [b]Determined by means of SEC in THF using polystyrene standards.

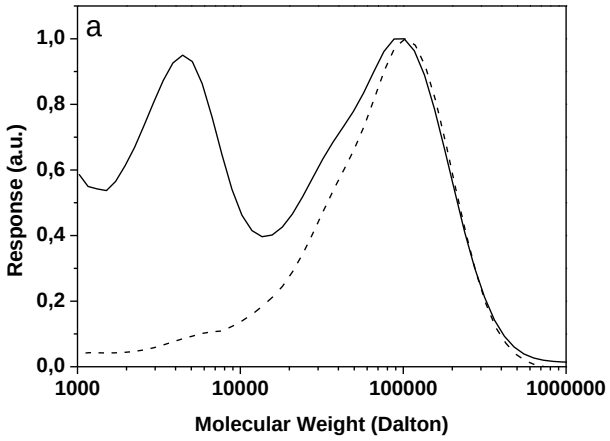

Figure 1a. Overlay of SEC chromatograms of precursor polymer **3** synthesized with LDA (solid line) or with LHMDS (dashed line).

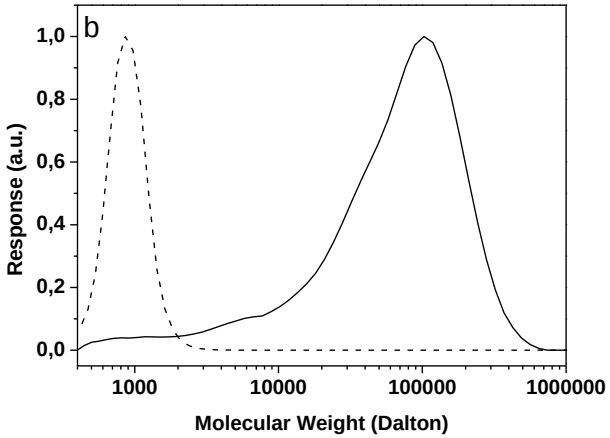

Figure 1b. Overlay of SEC chromatograms of precursor polymer **3** synthesized with TEMPO (dashed line) or without TEMPO (solid line).

To verify whether or not this polymerization reaction follows indeed a radical mechanism, 0.5 equiv of a radical inhibitor 2,2,6,6-tetramethylpiperidinoxyl (TEMPO) were added to a typical polymerization mixture (Table 2, Figure 1b). As expected, the addition of TEMPO decreases molecular weight and yield strongly, consistent with a radical polymerization mechanism. In a second experiment, the monomer was added dropwise to a solution of base (Table 2, Entry 3), which leads to favorable conditions for an anionic polymerization.[24] However, such reversed addition of monomer to base solution has no influence on yield, molecular weight and PD, further confirming the strong preference of this base for a radical polymerization mechanism.

Table 2. Polymerization Results for LHMDS and K*t*BuO at 35 °C under Different Conditions

entry	base	addition	yield (%)	M_w[a]	PD[a]
1	LHMDS	normal	59	216 000	2.4
2	LHMDS	TEMPO	/	1 000	1.1
3	LHMDS	reversed	59	234 000	2.4
4	K*t*BuO	normal	67	272 000	2.5
5	K*t*BuO	TEMPO	/	1 000	1.1
6	K*t*BuO	reversed	45	178 000	2.6

[a]Determined by means of SEC in THF using polystyrene standards.

When K*t*BuO is used as the base, the polymerization yields again high molecular weight polymer, with the highest value for the precursor polymer synthesized at 35 °C (Table 1). The use of K*t*BuO suppresses the bimodal molecular weight distribution in a similar way as was observed for the LHMDS polymerizations. The experiments with TEMPO and reversed addition also give similar results as was observed for LHMDS as the base (Table 2), indicating once again a preference for a radical polymerization mechanism.[14,15]

3.3. Thermal Conversion

The dithiocarbamate MDMO precursor polymer **3** can be converted into a conjugated material via thermal elimination. Upon heating, the dithiocarbamate groups of precursor polymer **3** are eliminated to form the corresponding conjugated MDMO-PPV **4**. The thermal elimination can be performed in film or in solution. In film, the process can be followed in situ with FT-IR and UV-vis spectroscopy. To perform the elimination in solution, the MDMO precursor polymer is dissolved in dichlorobenzene and heated at 180 °C for 3 h. This procedure is performed two times consecutively, to insure full conversion.[13] The polymer is isolated via precipitation in cold methanol.

For the study of the thermal elimination of MDMO precursor polymer **3** with in situ FT-IR and UV-vis spectroscopy, a thin film of precursor polymer **3** was heated at 2°C/min from ambient temperature to 200 °C under a continuous flow of nitrogen. Upon heating, a new absorption band appears in the UV-vis absorption spectra, associated with the conjugated system (Figure 2a). Concomitantly, the absorption band at 288 nm, associated with the precursor polymer, decreases. The absorption maximum (λ_{max}) of 460 nm at 134 °C is lower compared to λ_{max} of 490 nm at room temperature due to the thermochromic effect.[25] The elimination process can be more thoroughly analyzed using the absorbance profiles (Figure 2b). In these profiles between 95 °C and 130 °C, an increase in the absorbance at 460 nm can be noticed

under these heating conditions. In the same temperature range, a decrease in the absorbance at 288 nm takes place.

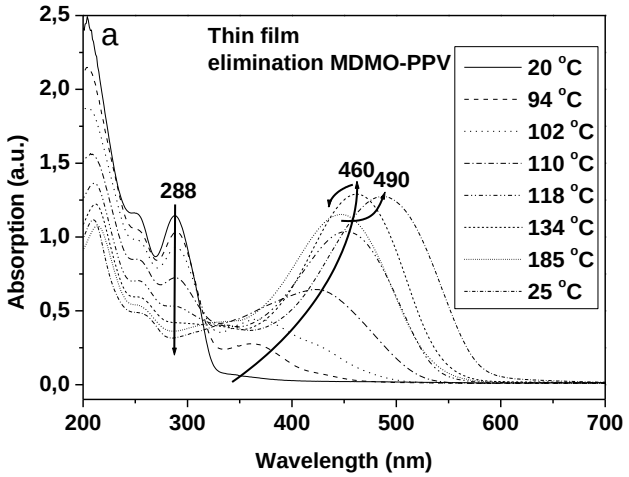

Figure 2a. Temperature-dependent UV-vis spectra of the thermal elimination of **3**.

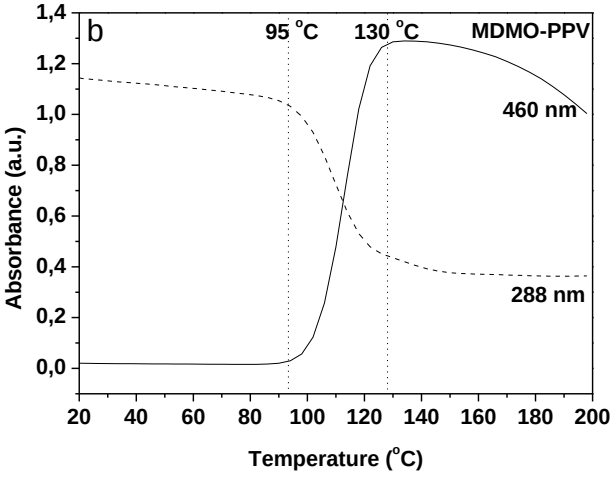

Figure 2b. UV-vis absorbance profiles at 288 nm and 460 nm as function of temperature during the thermal elimination of **3**.

This process can also be monitored using in situ FT-IR spectroscopy. Upon heating, a decrease is observed in the absorption bands at 1205, 1266, 1414

and 1486 cm^{-1}, which arise from vibrations of the dithiocarbamate group[26] (Figure 3a). At the same time, a new absorption band appears at 965 cm^{-1}, which originates from the *trans*-vinylene double bonds, formed during thermal elimination. From the FT-IR transmission profiles at 965 and 1266 cm^{-1}, it can be noticed that the elimination starts at 105 °C and is completed at 145 °C, under the heating conditions utilized (Figure 3b). These results are consistent with the UV-vis profiles.

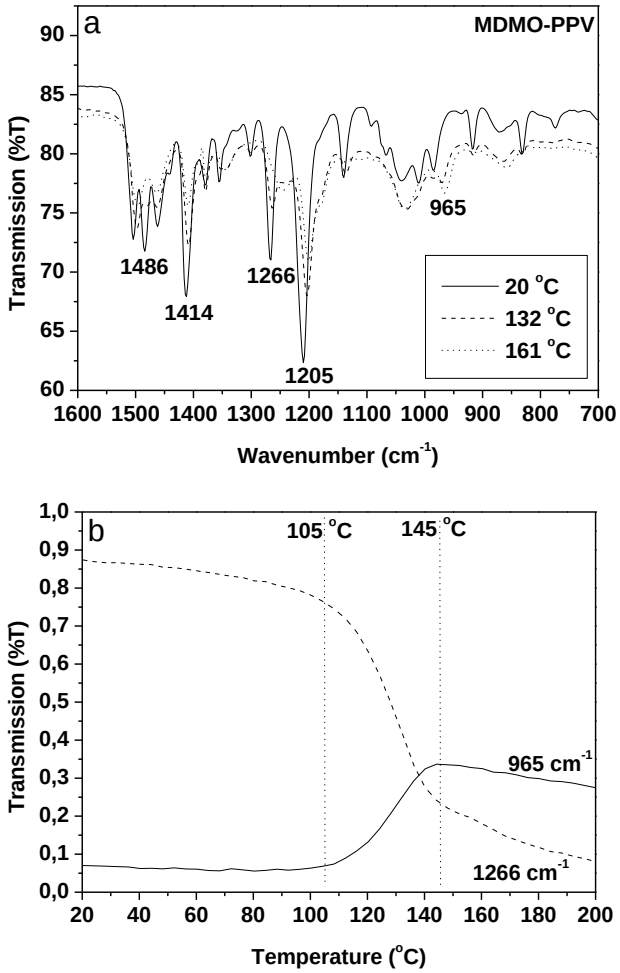

Figure 3. (a) Temperature-dependent FT-IR spectra of the thermal elimination of **3**. (b) IR absorption profiles at 965 cm^{-1} and 1266 cm^{-1} as function of temperature during the thermal elimination of **3**.

3.4. Regioregularity

As the MDMO monomer has a non-symmetrical structure relative to the position of the OCH_3 en $OC_{10}H_{21}$ substituents, upon polymerization typically a random incorporation of both possible quinodimethane systems (1:1) is found.[13] This has been observed for both the Gilch and the sulphinyl route. It has been previously shown that the degree of regioregularity in MDMO-PPV can be determined by quantitative ^{1}H NMR analysis using chlorobenzene-d_5 as solvent at 100 °C.[27] As the regioregularity may have a profound effect on the optoelectronic characteristics of these materials in devices,[28] the degree of regioregularity of the MDMO-PPV **4** obtained in our lab, was investigated using quantitative ^{1}H NMR spectroscopy.

Chart 1. Representation of Possible Environments for the Methoxy Group in Polymer 4

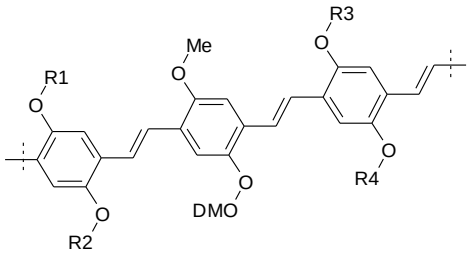

	R1	R2	R3	R4
A	Me	DMO	DMO	Me
B	DMO	Me	DMO	Me
C	Me	DMO	Me	DMO
D	DMO	Me	Me	DMO

In general, irrespectively of the precursor route used, the monomer units in MDMO-PPV can be coupled in 2 ways, creating four different types of environments for the methoxy-groups in the polymer side chain (Chart 1). In the ^{1}H NMR spectrum of polymer **4**, synthesized with K*t*BuO, 4 comparable peaks with chemical shifts of 3.98, 3.95, 3.88 and 3.85 ppm can be observed. All these peaks can be assigned to the methoxy-group, indicating a regiorandom MDMO-PPV (Figure 4a). The same peaks can be observed in the

^{1}H NMR spectrum of polymer **4**, synthesized with LHMDS (Figure 4b). However, for this ^{1}H NMR spectrum, a quantitative determination of the signal areas using deconvolution reveals that environment C is abundant for 47 %, while environments A, B and D are only abundant for respectively 20%, 17% and 16 % (Table 3).

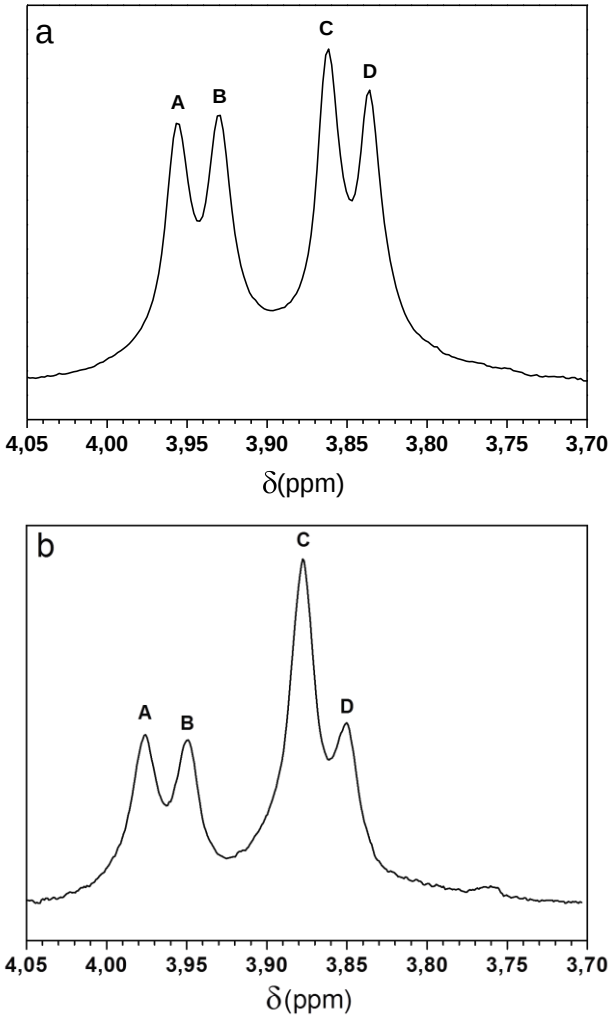

Figure 4. Methoxy region of ^{1}H NMR spectrum of **4**, measured in chlorobenzene-d_5 at 100 °C. (a) MDMO-PPV synthesized with K*t*BuO. (b) MDMO-PPV synthesized with LHMDS.

Tabel 3. Relative Abundance of Environments A−D in Polymer 4, Synthesized either with LHMDS or K*t*BuO

	abundance[a] (%)	
peak	LHMDS	K*t*BuO
A	20	22
B	17	25
C	47	27
D	16	26

[a] Error margin of 1%.

To calculate a degree of regioregularity out of these results, the following formula is used:

$$\%regioregularity = x - \left[(100 - x) \div 3\right]$$

In this equation, x stands for the % abundance of environment C. In this case, x = 47%, which indicates that the MDMO-PPV polymer prepared with LHMDS exhibits a regioregular excess of 29.3%.

Since the polymerization reaction mainly proceeds via head-to-tail additions, this degree in regioregularity can be explained by the reaction mechanism at the stage of the formation of quinodimethane systems.[29] The sterically hindered base LHMDS has a preference to extract a proton at the least sterically hindered position in the premonomer (Scheme 3). The more sterically hindered the base is, the higher this tendency will be. This way, a larger amount of quinodimethane systems is formed with the polarizer directed away from the long alkyl side chain. Due to head-to-tail additions during the propagation step of the polymerization, this results in a 29.3% regioregular MDMO-PPV. The degree of regioregularity in MDMO-PPV synthesized with the less sterically hindered K*t*BuO, is calculated to be only 2.7 %. By using K*t*BuO, the distribution of quinodimethane systems is reasonably balanced, leading to regiorandom MDMO-PPV.

Scheme 3. Formation of Quinodimethane Systems out of MDMO Premonomer, X= SC(S)NR$_2$

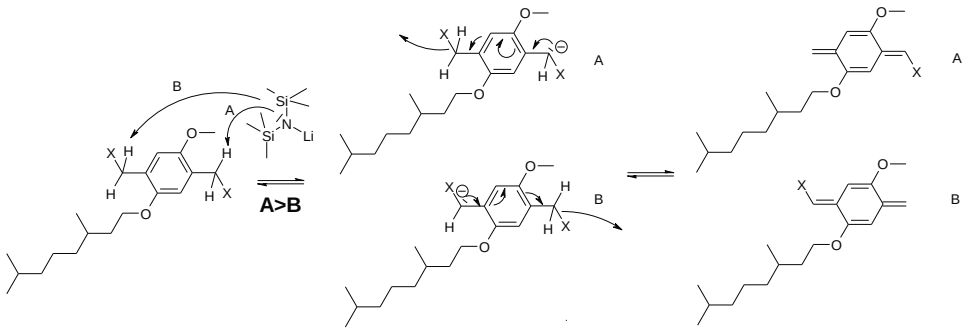

3.5. Quantitative ^{13}C NMR Study

As mentioned before, there are several distinct precursor routes available to synthesize PPV derivatives. The various precursor routes differ from each other in the identity of the functional group that is used as polarizer and leaving group. This chemical differentiation may have an influence on the polymer microstructure, which is a key parameter for the polymer performance in electronic devices.[30,31]

These differences in the microstructure of the PPV polymer can be identified as a consequence of structural defects.[32] By definition these defects are an integral part of the polymer microstructure and thus hard to remove or to avoid unless control at high level on the polymerization chemistry can be achieved. By introducing ^{13}C-labels into the polymer chain, the microstructure can be examined via ^{13}C NMR spectroscopy. The NMR study of isotopic labeled polymers is a very powerful technique to gain insight in polymerization mechanisms and resulting polymer structures.[13,23,33] The microstructure of Gilch-MDMO-PPV has been examined previously by others.[23] Although the concentration of defects in the polymer was very low, by using ^{13}C-labels, the intensity of the defect signals in a ^{13}C NMR spectrum could be increased with a factor 100, making them relatively easy to detect. As main structural defects they found the presence of single and triple bonds, the so called tolane-bisbenzyl (TBB) moieties (3–4.4%). Later studies[13] showed even

higher quantities of tolane-bisbenzyl defects in Gilch-MDMO-PPV (11.2%) and showed the presence of noneliminated locations (1.8%) as well as chlorovinyl bonds (*ca.* 1.4%), which are a product of tail-to-tail addition (Chart 2). In contrast, only a considerable amount of noneliminated groups was found in the conjugated sulfinyl polymers (6.8%), which could be reduced by a two-step elimination procedure to less than 0.5%. The sulfinyl polymer contained besides the noneliminated groups no other defects, except for aldehyde end groups and the bisbenzyl initiation defect.

Chart 2. Overview of Different Types of Structural Defects Present in MDMO-PPV Obtained via the Gilch Route

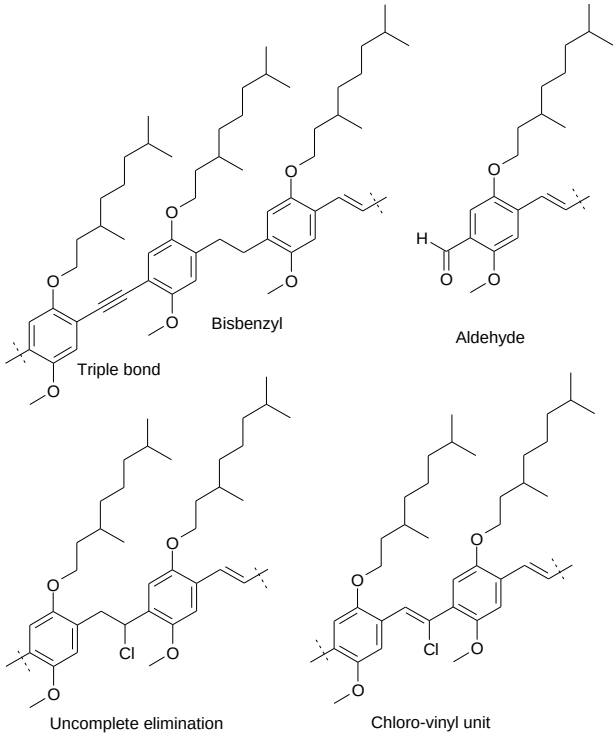

To obtain a profound insight in the microstructure of MDMO-PPV, synthesized via the dithiocarbamate route, a similar ^{13}C NMR study was initiated. As mentioned earlier, the dithiocarbamate route follows a free radical polymerization mechanism. The initiating moiety is a diradical (Scheme 4,

step 1), which can at both sides propagate independently via reaction with *p*-quinodimethane intermediates (Scheme 4, step 2). It is expected that this mainly happens via head-to-tail additions, creating a regular polymer chain. During the propagation step however, defects can be built in by head-to-head addition leading to a CH_2–CH_2 defect, while tail-to-tail addition causes the formation of a $CHSC(S)NR_2$–$CHSC(S)NR_2$ defect. For the termination reaction (Scheme 4, step 3), it is proposed that carbonyl formation by traces of oxygen can take place. As noted previously, after polymerization the precursor polymer chain is converted to the conjugated polymer by thermal elimination.

Scheme 4. Radical Precursor Polymerization Mechanism for MDMO-PPV[a]

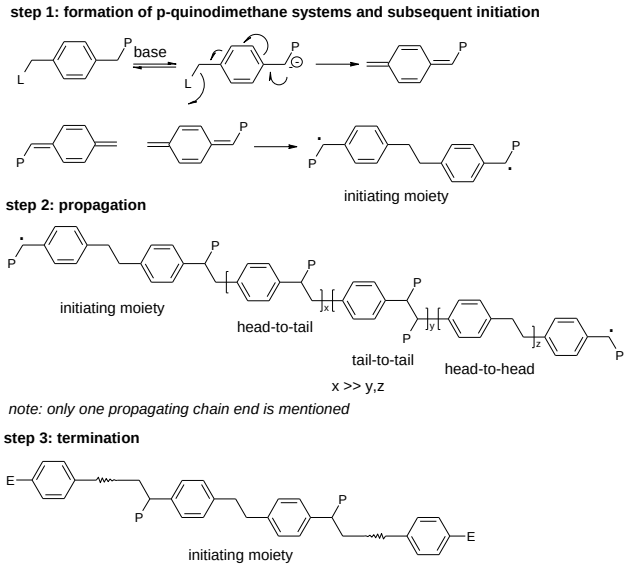

[a] L= $SC(S)NR_2$, P= $SC(S)NR_2$, and E= C(O)H or C(O)OH.

For this study the ^{13}C-labeled MDMO-PPV was synthesized using the dithiocarbamate route (Scheme 5). The ^{13}C-labeled bischloromethyl monomer was converted to the corresponding ^{13}C-bisdithiocarbamate monomer, which polymerized under the influence of LHMDS. The precursor polymer was then converted into the conjugated ^{13}C-labeled MDMO-PPV.

Scheme 5. Reaction Sequence for the Synthesis of ^{13}C-Labeled MDMO-PPV with the Dithiocarbamate Route

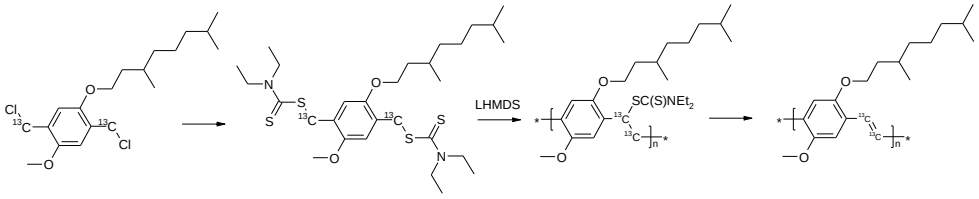

Quantitative ^{13}C NMR spectra are necessary to examine the nature and exact amount of structural defects in a polymers microstructure. To acquire quantitative ^{13}C NMR spectra, a preparation delay of five times the longest T1 relaxation decay time has to be respected between consecutive pulses, in order to let the magnetization return to equilibrium. The T1 decay times of all carbon resonances in MDMO-PPV have already been determined previously by means of the inversion recovery technique.[13] The influence of varying concentrations of the paramagnetic relaxation agent chromium(III) acetylacetonate on the T1 relaxation decay times was investigated. The longest T1 relaxation decay time in the presence of 25 mM of chromium(III) acetylacetonate was determined to be 1.0 s, allowing acquisition of quantitative data with a preparation delay of only 5.0 s.

By comparing the ^{13}C NMR spectra of the unlabeled (Figure 5) and labeled (Figure 6) conjugated MDMO-PPV obtained via the dithiocarbamate route, some additional resonances could be detected. These resonances were situated at 189.1 ppm and a downfield shoulder at 31 ppm. Because these resonances are not detected in the ^{13}C NMR spectrum of the unlabeled polymer, it is likely that they are present in amounts less than 10%. A summed integration of a selection of well-defined carbon signals (carbon atom 3, 6, 17 and 18) was taken as an internal reference, to which the other resonances were normalized. In this way, the amount of every type of structural defect could be quantified from the ^{13}C NMR spectra. The signal at 189.1 can be attributed to an aldehyde functionality (0.6%). This defect was also found with the Gilch (0.1%) and sulfinyl route (0.3%). Since OC_1C_{10}-PPV is stable up to about 175 °C,[34] this functionality can be assigned to the end

groups of the polymer. The intensity of the aldehyde signal did not change after performing a second elimination (Table 4). Furthermore, the aldehyde signal is also detected in the ^{13}C NMR spectrum of the labeled precursor polymer (Figure 7). This verifies that the origin of the aldehyde end groups lies not at the elimination step at relative high temperature, but rather at the termination reaction of traces of oxygen with the radical ends of the polymer chain during polymerization.

The only other defect visible can be found as a shoulder at 31 ppm, which can be attributed to a bisbenzyl unit (0.6%). Since no $CHSC(S)NR_2$–$CHSC(S)NR_2$ tail-to-tail defects and no triple bonds were observed, all bisbenzyl units originate from the initiating moieties and not from head-to-head couplings (Scheme 4). Furthermore, the absence of $CHSC(S)NR_2$–$CHSC(S)NR_2$ defects as well as triple bonds leads to the conclusion that recombination of two growing radical chain termini, as was proposed for the Gilch route,[35] is not observed for the dithiocarbamate route. Interestingly, the amount of both aldehyde and bisbenzyl initiation units are the same, indicating that all polymer end groups are aldehyde functionalities. Finally, no nonelimitated groups could be found at this detection level (< 0.1%) and no *cis*-vinylene bonds were observed with ^1H NMR (Supporting Information). Hence, we can conclude that also the dithiocarbamate route leads to polymers with very few microstructural defects.

Table 4. Amounts of Different Types of Structural Defects in MDMO-PPV after First and Second Elimination

defect	first elimination	second elimination
aldehyde	0.6%	0.6%
bisbenzyl-unit	0.6%	0.6%
noneliminated groups	< 0.1% (detection limit)	< 0.1% (detection limit)

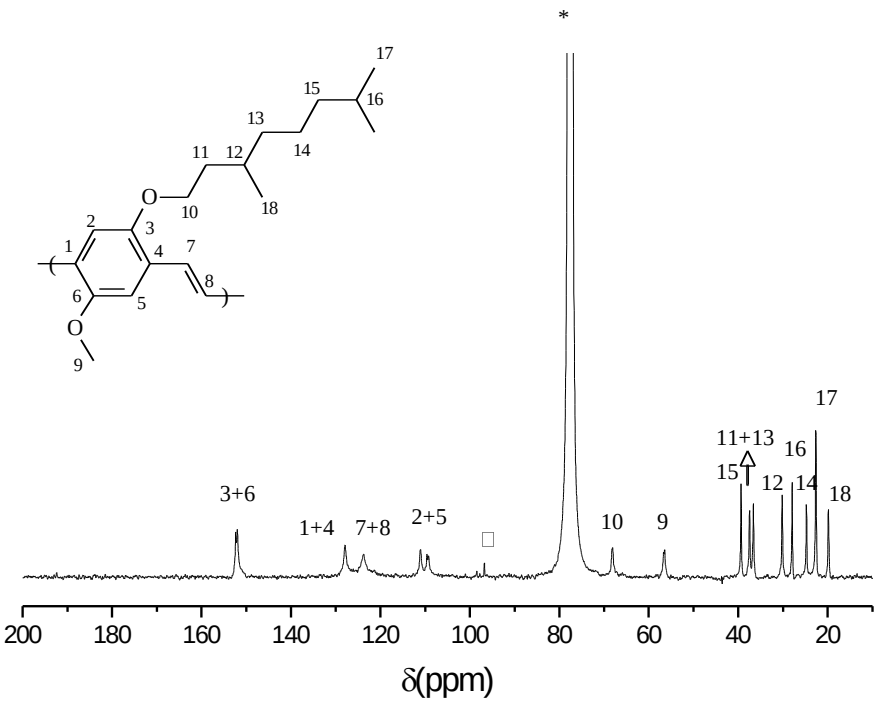

Figure 5. ^{13}C NMR spectrum of unlabeled MDMO-PPV at 40°C. The resonances marked with an asterisk and a square result from $CDCl_3$ and CCl_4 respectively. ^{13}C NMR (100 MHz, $CDCl_3$), δ = 151.4 (C_{3+6}, 2C); 127.0 (C_{1+4}, 2C), 123.3 (C_{7+8}, 2C); 110.5 (C_2, 1C); 108.8 (C_5, 1C); 67.9 (C_{10}, 1C); 56.4 (C_9, 1C); 39.2 (C_{15}, 1C); 37.4 (C_{13}, 1C); 36.6 (C_{11}, 1C); 30.2 (C_{12}, 1C); 27.9 (C_{16}, 1C); 24.6 (C_{14}, 1C); 22.6 (C_{17}, 2C); 19.8 (C_{18}, 1C).

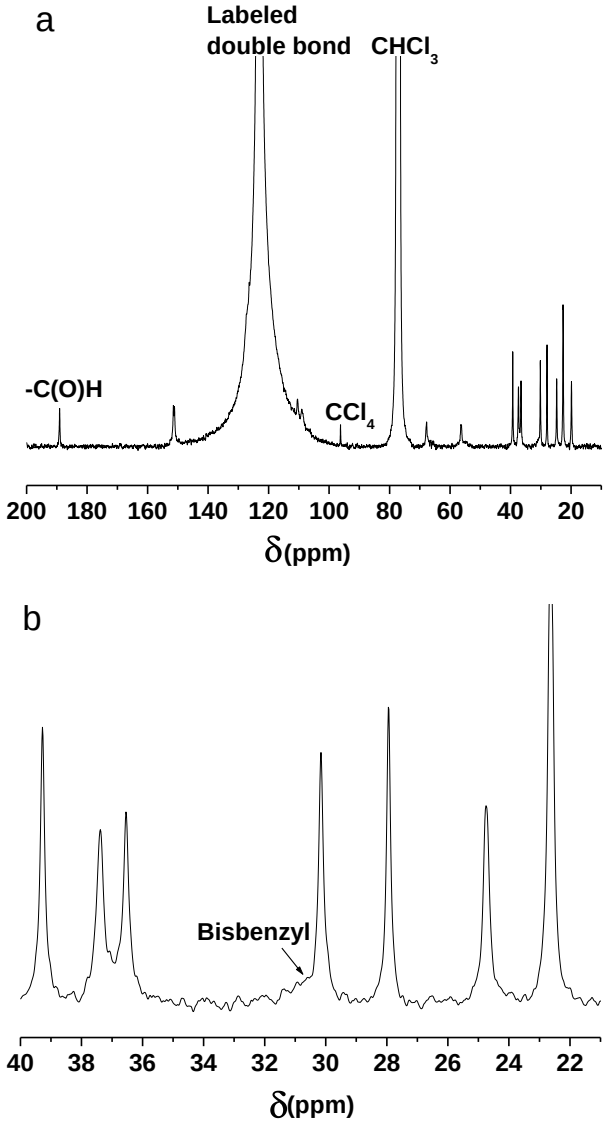

Figure 6. (a) ^{13}C NMR spectrum of labeled dithiocarbamate MDMO-PPV after second elimination. (b) Enlargement of labeled dithiocarbamate MDMO-PPV ^{13}C NMR spectrum between 21 and 40 ppm.

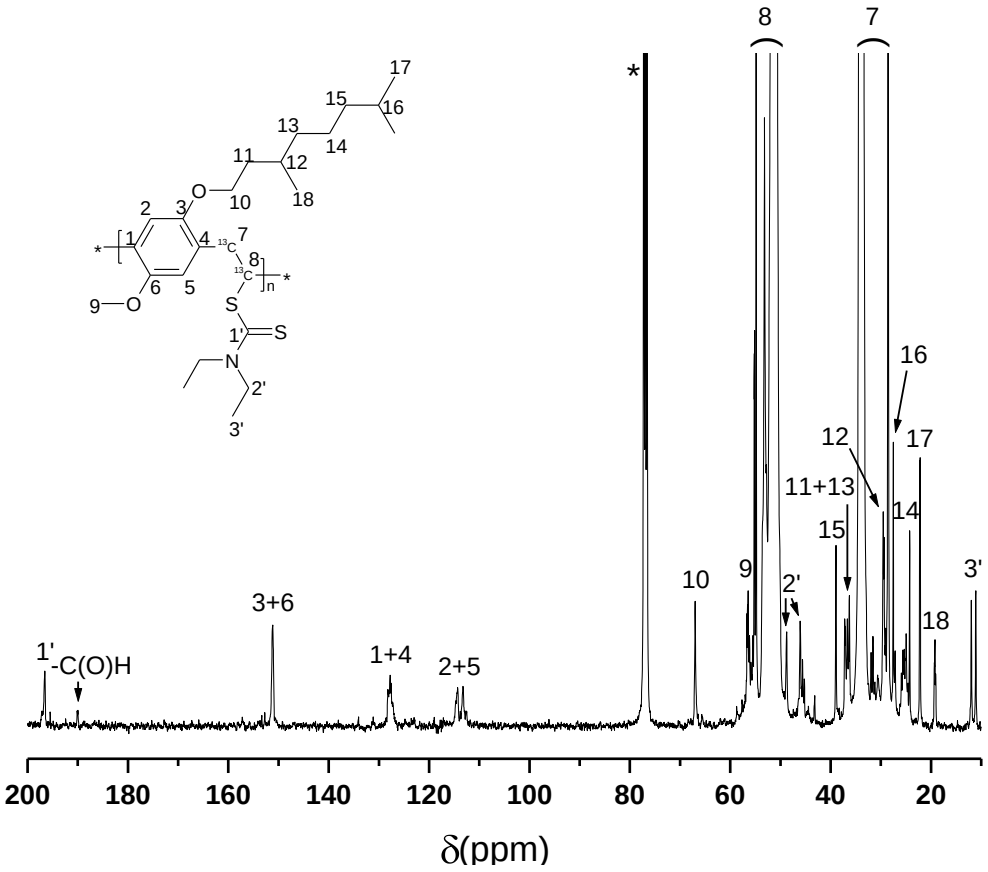

Figure 7. ^{13}C NMR spectrum of labeled precursor MDMO-PPV at 40 °C. The resonance marked with an asterisk results from $CDCl_3$ ^{13}C NMR (100 MHz, $CDCl_3$), δ = 197.5 ($C_{1'}$, 1C); 151.4 (C_{3+6}, 2C); 127.0 (C_{1+4}, 2C); 115.5 (C_{2+5}, 2C); 67.9 (C_{10}, 1C); 56.4 (C_9, 1C); 55.5–50.5 (C_8, 1C); 48.3 ($C_{2'}$, 2C); 39.2 (C_{15}, 1C); 37.0 (C_{13+11}, 2C); 35.7–29.3 (C_7, 1C); 30.2 (C_{12}, 1C); 27.9 (C_{16}, 1C); 24.6 (C_{14}, 1C); 22.6 (C_{17}, 2C); 19.8 (C_{18}, 1C); 11.6 ($C_{3'}$, 2C).

4. Conclusions

The synthesis of high quality MDMO-PPV with the dithiocarbamate route has been demonstrated. The use of LHMDS or K*t*BuO as a base, results in polymers with high molecular weight, low PD, and sufficient high λ_{max} values. Contrary to LDA-based dithiocarbamate polymerizations, no bimodal molecular weight distributions are obtained. Furthermore, the dithiocarbamate monomer is more readily synthesized than the sulfinyl monomer. Unlike the Gilch route, ^{13}C NMR studies have shown that polymerization of bisdithiocarbamate monomers mainly proceeds via head-to-tail additions and only very small amounts of defects are present in the resulting microstructure. These results prove that the dithiocarbamate route is an optimal balance between the straightforwardness of the Gilch route and the excellent material qualities of the sulfinyl route. Furthermore, MDMO-PPV synthesized with LHMDS shows a 29.3% regioregularity excess, as revealed by ^{1}H NMR. By using even more sterically hindered bases, there is potential to synthesize PPV's with even higher degrees of regioregularity.

5. Acknowledgment

The authors thank H. Penxten for the in situ UV-vis and FT-IR measurements. The authors gratefully acknowledge The Fund for Scientific Research-Flanders (FWO) and the BELSPO in the frame of network IAP P6/27, for the financial support. We also thank the IWT (Institute for the Promotion of Innovation by Science and Technology in Flanders) for the financial support via the SBO project "Polyspec".

6. Supporting Information

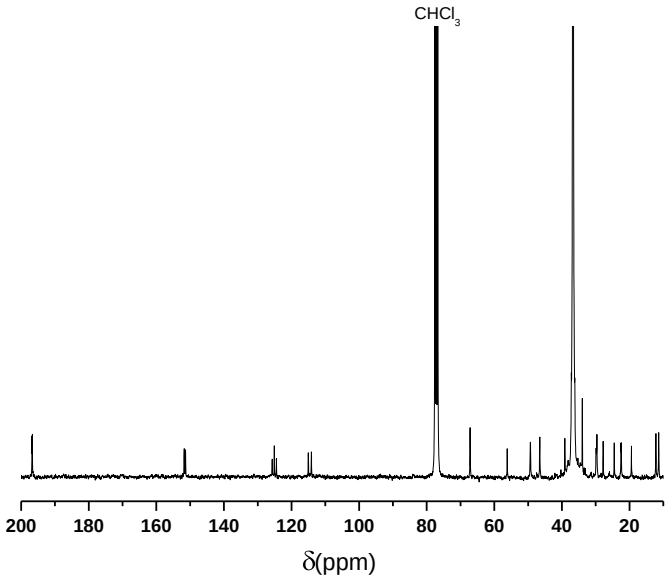

Figure 8. Raw ^{13}C NMR spectrum of ^{13}C-labeled dithiocarbamate monomer 2.

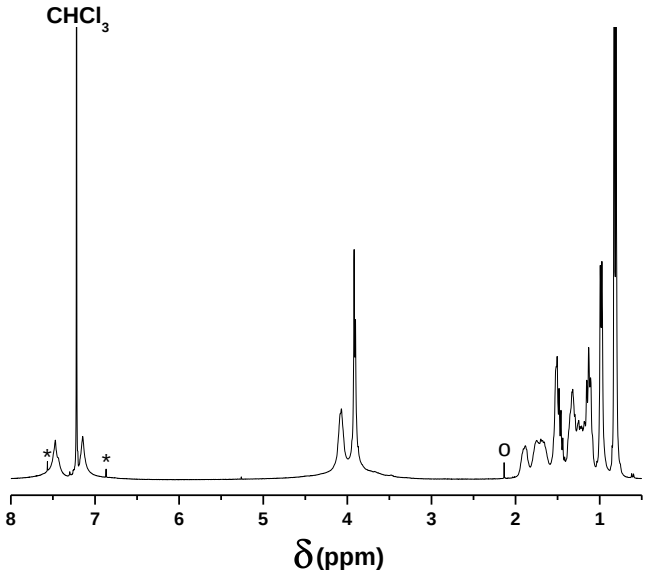

Figure 9. Raw ^{1}H NMR spectrum of unlabeled MDMO-PPV 4. The resonances marked with an asterisk result from $CDCl_3$ ^{13}C- satellites and the resonance marked with a circle results from aceton residual solvent.

7. References and Notes

(1) Kraft, A.; Grimsdale, A. C.; Holmes, A. B. *Angew. Chem., Int. Ed.* **1998**, *37*, 403–428.

(2) Dimitrakopoulos, C. D.; Mascaro, D. J. *IBM J. Res. Dev.* **2001**, *45*, 11–27.

(3) Nunzi, J.-M. *C. R. Physique* **2002**, *3*, 523–542.

(4) MacDiarmid, A. G.; Zhang, W. J.; Huang, Z.; Wang, P. C.; Huang, F.; Xie, S. *Polym. Prepr.* **1997**, *38*, 333–334.

(5) Hörhold, H.-H.; Opfermann, J. *Macromol. Chem* **1970**, *131*, 105–132.

(6) Pfeiffer, S.; Hörhold, H.-H. *Synth. Met.* **1999**, *101*, 109–110.

(7) Heitz, W.; Brügging, W.; Freund, L.; Gailberger, M.; Greiner, A.; Jung, H.; Kampschulte, U.; Nießner, N.; Osan, F.; Schmidt, H.-W.; Wicker, M. *Macromol. Chem.* **1988**, *189*, 119–127.

(8) Gilch, H. G.; Wheelwright, W. L. *J. Polym. Sci.* **1966**, *4*, 1337–1349.

(9) Wessling, R. A. *J. Polym. Sci., Polym. Symp.* **1985**, *72*, 55–66.

(10) Son, S.; Dodabalapur, A.; Lovinger, A. J.; Galvin, M. E. *Science* **1995**, *269*, 376–378.

(11) Louwet, F.; Vanderzande, D.; Gelan, J. *Synth. Met.* **1995**, *69*, 509–510.

(12) Van Breemen, A. J. J. M.; Issaris, A. C. J.; de Kok, M. M.; Van Der Borght, M. J. A. N.; Adriaensens, P. J.; Gelan, J. M. J. V.; Vanderzande, D. J. M. *Macromolecules* **1999**, *32*, 5728–5735.

(13) Roex, H.; Adriaensens, P.; Vanderzande, D.; Gelan, J. *Macromolecules* **2003**, *36*, 5613–5612.

(14) Wiesecke, J.; Rehahn, M. *Angew. Chem., Int. Ed.* **2003**, *42*, 567–570.

(15) Schwalm, T. ; Wiesecke, J.; Immel, S.; Rehahn, M. *Macromolecules* **2007**, *40*, 8842–8854.

(16) Hontis, L.; Van Der Borght, M.; Vanderzande, D.; Gelan, J. *Polymer* **1999**, *40*, 6615–6617.

(17) Adriaensens, P.; Van der Borght, M.; Hontis, L.; Issaris, A.; van Breemen, A.; de Kok, M.; Vanderzande, D.; Gelan, J. *Polymer* **2000**, *41*, 7003–7009.

(18) Henckens, A.; Lutsen, L.; Vanderzande, D.; Knipper, M.; Manca, J.; Aernouts, T.; Poortmans, J. *SPIE Proc.* **2004**, 52–59.

(19) Henckens, A.; Colladet, K.; Fourier, S.; Cleij, T. J.; Lutsen, L.; Gelan, J. *Macromolecules* **2005**, *38*,19–26.

(20) Henckens, A.; Duyssens, I.; Lutsen, L.; Vanderzande, D.; Cleij, T. J. *Polymer* **2006**, *47*, 123–131.

(21) Banishoeib, F.; Adriaensens, P.; Berson, S.; Guillerez, S.; Douheret, O.; Manca, J.; Fourier, S.; Cleij, T. J.; Lutsen, L.; Vanderzande, D. *Solar Energy Materials & Solar Cells* **2007**, *91*, 1026–1034.

(22) Hontis, L.; Vrindts, V.; Vanderzande, D.; Lutsen, L. *Macromolecules* **2003**, *36*, 3035–3044.

(23) Becker, H.; Spreitzer, H.; Ibrom, K.; Kreuder, W. *Macromolecules* **1999**, *32*, 4925–4932.

(24) Neef, C. J.; Ferraris, J. P. *Macromolecules* **2000**, *33*, 2311–2314.

(25) Kesters, E.; Vanderzande, D.; Lutsen, L.; Penxten, H.; Carleer, R. *Macromolecules* **2005**, *38*,1141–1147.

(26) Chambon, S.; Rivaton, A.; Gardette, J.-L.; Firon, M.; Lutsen, L. *J. Polym. Sci : Part A : Polym. Chem.* **2007**, *45*, 317–331.

(27) Suzuki, Y.; Hashimoto, K.; Tajima, K. *Macromolecules* **2007**, *40*, 6521–6528.

(28) Mozer, A. J.; Denk, P.; Scharber, M. C.; Neugebauer, H.; Sariciftci, N. S.; Wagner, P.; Lutsen, L.; Vanderzande, D.; Kadashchuk, A.; Staneva, R.; Resel, R. *Synth. Met.* **2005**, *153*, 81–84.

(29) Wiesecke, J.; Rehahn, M. *Macromol. Rapid. Commun.* 2007, *28*, 188–193.

(30) Lutsen, L.; Adriaensens, P.; Becker, H.; Van Breemen, A. J.; Vanderzande, D.; Gelan, J. *Macromolecules* **1999**, *32*, 6517–6525.

(31) Munters, T.; Martens, T.; Goris, L.; Vrindts, V.; Manca, J.; Lutsen, L.; De Ceuninck, W.; Vanderzande, D.; De Schepper, L.; Gelan, J.; Sariciftci, N. S.; Brabec, C. J. *Thin Solid Films* **2002**, *403–404*, 247–251.

(32) Schoo, H. F. M.; Demandth, R. J. C. E. *Philips J. Res.* 1998, *51*, 527–533.

(33) Bjerring, M.; Nielsen, J. S.; Nielsen, N. C.; Krebs, F. C. *Macromolecules* **2007**, *40*, 6012–6013.

(34) Kesters, E.; Lutsen, L.; Vanderzande, D.; Gelan, J.; Nguyen, T. P.; Molinie, P. *Thin Solid Films* **2002**, *403–404*, 120–125.

(35) Schwalm, T.; Rehahn, M. *Macromol. Rapid Commun.* **2008**, *29*, 207–213.

Chapter 3

An Efficient Acid-Induced Conversion of Dithiocarbamate Precursor Polymers into Conjugated Materials

ABSTRACT: An acid-induced conversion method for dithiocarbamate precursor poly(thienylene vinylene) (PTV) and poly(phenylene vinylene) (PPV) derivatives is presented, which has the advantage that it can be executed at moderate temperatures. The lower conversion temperature avoids possible thermal degradation of the polymer chromophore structure and therefore conjugated polymers with a higher effective conjugation length can be obtained. This process was studied using UV-vis and FTIR spectroscopy. The obtained results indicate that trifluoroacetic acid yields a more defect free structure as compared to benzenesulfonic acid which induces degradation after prolonged reaction times. A tentative mechanism is proposed in which the formation of an intermediate carbenium ion is part of the rate limiting step. It also implicates a competition between elimination and substitution reactions depending on specific reaction conditions.

*Diliën, H.; Vandenbergh, J.; Banishoeb, F.; Adriaensens, P.; Cleij, T. J.; Lutsen, L.; Vanderzande, D. J. M. *Macromolecules* **2011**, *44*, 711−718.

1. Introduction

Nowadays, conjugated polymers find application in various optical and electronic devices such as light emitting diodes (LED),[1] field effect transistors (FET),[2] photovoltaic cells[3] and sensors.[4] Due to their interesting optoelectronic and electrical properties, a considerable amount of research has been performed on poly(arylene vinylene) derivatives.[5,6] These polymers have been typically synthesized via precursor routes in which a *p*-quinodimethane system acts as the actual monomer. This monomer will polymerize into the precursor polymer via a self-initiating radical chain mechanism.[7–11] In a second step, the obtained precursor polymers can be transformed into the conjugated form in situ or ex situ. The major advantage of such precursor routes is the ease by which high molecular weight materials are obtained. Over the last 50 years several different precursor routes have been developed such as: the sulfonium route,[12–15] the Gilch route,[16] the xanthate route,[17–19] and the, in our research group developed, sulfinyl[20,21] and dithiocarbamate route.[22–27] All these routes differ by the identity of the polarizer (P) and leaving (L) functional group in the premonomer structure, the polymerization conditions, whether conversion to the conjugated structure occurs in situ or ex situ and to what extent the conversion is thermal induced or reagent induced (Scheme 1).

Furthermore, the characteristics of the obtained polymers can vary along the different precursor routes. For instance, the xanthate precursor route yields typically broad polydispersities (PD) and shows structural defects in the final conjugated system. On the other hand the sulfinyl and the, in this study discussed, dithiocarbamate precursor route lead to the formation of precursor polymers with low structural defect levels.[28,29] Furthermore, in case of the sulfinyl route the conversion from the precursor polymer toward the conjugated polymer already starts at 65 °C.[30] However the implementation of the non-symmetrical P and L groups into the premonomer is quite challenging.[31] For the dithiocarbamate precursor route the opposite situation occurs: here the monomer synthesis is rather simple and results into highly stable monomers. However, higher conversion temperatures (180 °C) are

necessary to reach fully conjugated polymers and therefore degradation of the polymer chromophore structure is a realistic threat.[32] In a serendipitous way, we discovered that the dithiocarbamate functional group in the precursor is eliminated, inducing the formation of the conjugated system, in the presence of acid. Typically, a temperature of 70 °C can be used, but also at ambient temperature conversion occurs. Such low conversion temperatures may avoid the degradation of the polymeric chromophore and therefore guarantee the formation of conjugated structures with optimal electronic properties.

Scheme 1. Precursor Routes toward Poly(*p*-phenylene vinylene) Derivatives

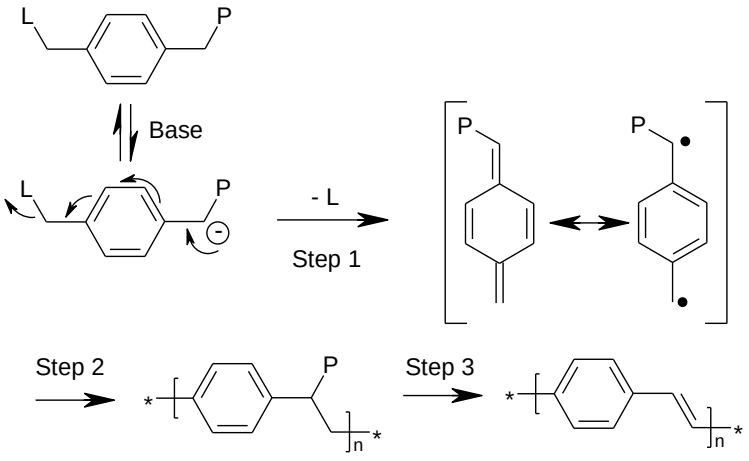

Gilch route:	L=P= Cl or Br
Sulfonium route:	L=P= R_2S-
Sulfinyl route:	L= Cl or Br ; P= RS(O)-
Xanthate route:	L=P= RO-C(S)-S-
Dithiocarbamate route:	L=P= R_2N-C(S)-S-

Specifically in this study, poly(3-octyl-2,5-thienylene vinylene) (O-PTV) and poly[(2-methoxy-5-(3',7'-dimethyloctyloxy))-1,4-phenylene vinylene] (MDMO-PPV) have been synthesized using the dithiocarbamate precursor route.[28] Furthermore, to combine the advantages of both the sulfinyl and dithiocarbamate routes, e.g. low conversion temperatures and easy monomer

synthesis, a new conversion process for dithiocarbamate precursor polymers has been developed. After synthesis and characterization of the precursor polymer, the thermal conversion as well as the acid-induced conversion process toward O-PTV and MDMO-PPV is studied via FT-IR and UV-vis spectroscopy. Finally, a tentative reaction mechanism is proposed and preliminary results are presented concerning the specific characteristics of the acid-induced elimination reaction of dithiocarbamate groups.

2. Experimental Section

2.1. General

Unless otherwise stated, all reagents and chemicals were obtained from commercial sources (Acros and Aldrich) and used without further purification. A xanthate precursor toward plane PTV was synthesized according to a literature procedure.[19] Tetrahydrofuran (THF) was dried by distillation from sodium/benzophenone. NMR spectra were recorded with a Varian Inova 300 spectrometer at 300 MHz for ^{1}H NMR and at 75 MHz for ^{13}C NMR using a 5 mm probe. Gas chromatography/mass spectrometry (GC/MS) analyses were carried out with TSQ-70 and Voyager mass spectrometers (Thermoquest); the capillary column was a Chrompack Cpsil5CB or Cpsil8CB. Analytical size exclusion chromatography (SEC) was performed using a Spectra series P100 (Spectra Physics) pump equipped with two mixed-B columns (10 µm, 0.75 cm x 30 cm, Polymer Labs) and a refractive index detector (Shodex) at 40°C. THF was used as the eluent at a flow rate of 1.0 mL/min. Molecular weight distributions are given relative to polystyrene standards. FT-IR spectra were collected with a Perkin-Elmer Spectrum One FT-IR spectrometer (nominal resolution 4 cm-1, summation of 16 scans). UV-vis spectroscopy was performed on a VARIAN CARY 500 UV-vis-NIR spectrophotometer (scan rate: 600 nm/min). Samples for temperature-dependent thin-film FT-IR and UV-vis characterization were prepared by dropcasting the precursor polymer from a $CHCl_3$ solution (10 mg/mL) onto NaCl disks or quartz disks. The disks were heated in a Harrick high-temperature cell (heating rate: 2 °C/min), which was positioned in the beam of either the FT-IR or the UV-vis spectrometer to

allow in-situ measurements. Spectra were taken continuously under a continuous flow of N_2 during which the samples were in direct contact with the heating element. "Timebase software" supplied by Perkin-Elmer and "Scanning Kinetics software" supplied by Varian, respectively, were used to investigate regions of interest.

2.2. Synthesis

Monomer Synthesis. The synthetic routes toward the MDMO-PPV bisdithiocarbamate premonomer **1** and the O-PTV bisdithiocarbamate premonomer **4** have been reported earlier.[22,33,34]

*Synthesis of MDMO Precursor PPV **2***. Premonomer **1** (500 mg, 0.851 mmol) was dissolved in dry THF (4.2 mL) giving a concentration of 0.2 M. The mixture was stirred at 35 °C under a continuous flow of nitrogen. 1,5 equiv of a LHMDS solution (1 M in THF) were added in one go to the stirred monomer solution. The reaction proceeded for 1.5 h at 35 °C under a nitrogen atmosphere, and the mixture was subsequently quenched in ice water (100 mL). The excess of base was neutralized with HCl (1 M). The aqueous phase was extracted with $CHCl_3$ (3 × 40 mL). After combination of the organic phases and evaporation of the solvent, the obtained crude polymer was again dissolved in $CHCl_3$ (2 mL) and precipitated in stirred cold methanol (100 mL). The mixture was filtered and the polymer was collected and dried in vacuo. The residual fractions contained only premonomer and oligomers (yield 64%, 239 mg). ^{1}H NMR ($CDCl_3$): 6.97–6.45 (br m, 2H), 5.87–5.50 (br s, 1H), 4.23–3.05 (br m, 11H), 1.95–1.02 (br m, 16H), 1.02–0.74 (m, 9H); ^{13}C NMR ($CDCl_3$): 195.76, 150.85, 127.68, 114.11, 113.09, 67.10, 56.39, 51.98, 49.08, 46.38, 39.27, 37.54, 36.60, 34.45, 29.91, 27.92, 24.67, 22.69, 22.58, 19.66, 12.47, 11.55; IR (NaCl, cm^{-1}): 2953, 2929, 1504, 1484, 1462, 1413, 1267, 1210, 1140, 1041. SEC: $M_w = 220 \times 10^3$; PD = 2.3.

*Thermal Conversion of Precursor Polymer to Conjugated MDMO-PPV **3a***. From a solution of **2** (50 mg, 0.114 mmol) in *o*-dichlorobenzene (25 mL) oxygen was removed by purging for 1 h with nitrogen. Subsequently, the solution was heated to 180 °C and stirred for 3 h. After cooling to room temperature, the

o-dichlorobenzene was evaporated and the crude polymer mixture was dissolved in chloroform (2 mL). The solution was precipitated drop wise in cold methanol (50 mL). The polymer was filtered off, washed with cold methanol and dried at room temperature under reduced pressure. The conjugated MDMO-PPV **3a** was obtained as a red polymer. The elimination procedure was performed a second time to ensure complete elimination (yield: 97%, 32 mg). ^{1}H NMR ($C_2D_2Cl_4$): 7.5 (br, 2H) 7.2 (br, 2H) 4.6–3.2 (br m, 5H) 2.1–0.6 (br m; 19H); ^{13}C NMR ($CDCl_3$): 151.4; 127.0, 123.3; 110.5; 108.8; 67.9; 56.4; 39.2; 37.4; 36.6; 30.2; 27.9; 24.6; 22.6; 19.8; IR (KBr, cm^{-1}): 2957, 2925, 2860, 1510, 1469, 1395, 1217, 1028, 872. UV-vis: λ_{max} (thin film) = 530 nm. SEC: $M_w = 351 \times 10^3$; PD = 3.0.

*Benzenesulfonic Acid-Induced Conversion of Precursor Polymer to Conjugated MDMO-PPV **3b***. From a solution of **2** (50 mg, 0.114 mmol) in chlorobenzene (25 mL) oxygen was removed by purging for 1 h with nitrogen. Subsequently, the solution was heated to 70 °C and 1.5 equiv (based on the amount of dithiocarbamate moieties in the precursor polymer) of a benzenesulfonic acid solution (0.342M in chlorobenzene) were added. After stirring for 30 min, the excess of acid was neutralized with $NaHCO_3$ and the mixture was extracted with $CHCl_3$. The solvent was evaporated and the crude polymer mixture was redissolved in chloroform (2 mL). The solution was precipitated drop wise in cold methanol (50 mL). The polymer was filtered off, washed with cold methanol and dried at room temperature under reduced pressure. The conjugated MDMO-PPV **3b** was obtained as a red polymer (yield: 97%, 32 mg). UV-VIS: λ_{max} (thin film) = 534 nm. SEC: $M_w = 284 \times 10^3$; PD = 4.1.

*Trifluoroacetic Acid-Induced Conversion of Precursor Polymer to Conjugated MDMO-PPV **3b***. From a solution of **2** (200 mg, 0.456 mmol) in chlorobenzene (100 mL) oxygen was removed by purging for 1 h with nitrogen. Subsequently, the solution was heated to 70 °C and 1.5 equiv (based on the amount of dithiocarbamate moieties in the precursor polymer) of trifluoroacetic were added. After stirring for 8 h, the excess of acid was neutralized with $NaHCO_3$ and the mixture was extracted with $CHCl_3$. The solvent was evaporated and the crude polymer mixture was redissolved in chloroform (8 mL). The solution

was precipitated drop wise in cold methanol (200 mL). The polymer was filtered off, washed with cold methanol and dried at room temperature under reduced pressure. The conjugated MDMO-PPV **3b** was obtained as a red polymer (yield: 98%, 130 mg). UV-VIS: λ_{max} (thin film) = 538 nm. SEC: M_w = 385 × 10^3; PD = 2.8.

*Synthesis of the Octyl Precursor PTV **5***. The premonomer **4** (2.8 g, 5.4 mmol) was previously freeze dried. A solution, with a premonomer concentration of 0.4 M, in dry THF (13.5 mL) was degassed by passing through a continuous nitrogen flow. The solution was cooled to 0 °C. Sodium bis(trimethylsilyl)amide (NaHMDS) (11 mL of a 1 M solution in THF) was added in one go to the stirred monomer solution. The resulting mixture was stirred for 90 min under continuous nitrogen flow at 0 °C. The polymer was precipitated in ice water and the water layer was neutralized with diluted HCl before extraction with chloroform. The solvent of the combined organic layers was evaporated under reduced pressure and a second precipitation was performed in pure cold methanol. The precursor polymer **5** was collected and dried in vacuo (yield 56 %, 1.1 g). ^{1}H NMR ($CDCl_3$): 6.57 (br, 1H), 5.46 (br, 1H), 3.96 (br, 2H), 3.66 (br, 4H), 2.27 (br, 2H), 1.21 (br, 18H), 0.85 (br, 3H); ^{13}C NMR ($CDCl_3$): 193.96, 139.5, 138.8, 133.8, 127.6, 52.7, 48.9, 46.6, 31.8, 30.7, 29.5, 29.3, 28.2, 22.6, 14.0, 12.5, 11.5; UV-vis: λ_{max} = 261 nm (in film); IR: 2931, 2846, 1486, 1415, 1268, 1206 cm^{-1}; SEC: M_w = 86 × 10^3; PD = 3.1.

*Thermal Conversion of the Octyl Precursor PTV **5** toward Octyl-PTV **6a***. The precursor polymer **5** (51 mg, 0.14 mmol) was dissolved in *o*-dichlorobenzene (2.8 mL) and refluxed for 4.5 h. After being cooled, the obtained slurry was precipitated in methanol. The precipitate was filtered off, washed several times with methanol and dried in vacuo. A purple/black solid has been obtained (yield 92 %, 28 mg). ^{1}H NMR ($CDCl_3$): 6.97 (s, 1H), 5.00 (s, 1H), 2.26 (br, 2H), 1.24 (br, 12H), 0.85 (br, 3H); ^{13}C NMR ($CDCl_3$): 140.2, 139.3, 134.4, 128.4, 121.1, 53.3, 37.2, 32.7, 31.6, 30.4, 30.1, 29.0, 23.4, 14.9; UV-vis: λ_{max} = 548 nm (in solution); IR (cm^{-1}): 2931, 2846, 1460, 1250, 1016, 926; SEC: M_w = 47 × 10^3; PD = 3.3.

*Benzenesulfonic Acid-Induced Conversion of the Octyl Precursor PTV **5** toward Octyl-PTV **6b***. The precursor polymer **5** (30 mg, 0.1 mmol) was dissolved in chlorobenzene (5 mL) and heated till 70 °C before benzenesulfonic acid (0.019 g, 0.12 mmol) was added. The solution was stirred for 10 min at 70 °C. After being cooled, the solution was poured into H_2O and extracted with diethyl ether. The solvent was evaporated under reduced pressure and the obtained slurry was precipitated in MeOH, filtered off and dried in vacuo. A purple/black solid was obtained (17 mg, yield 93 %). UV-vis: λ_{max} = 580 nm; SEC: $M_w = 72 \times 10^3$; PD = 3.7.

*Trifluoroacetic Acid-Induced Conversion of the Octyl Precursor PTV **5** toward Octyl-PTV **6b***. The precursor polymer **5** (36 mg, 0.1 mmol) was dissolved in chlorobenzene (5 mL) and heated till 70 °C before trifluoroacetic acid (0.011 mL, 0.15 mmol) was added. The solution was stirred for 10 min at 70 °C. After being cooled, the solution was poured into H_2O and extracted with diethyl ether. The solvent was evaporated under reduced pressure and the obtained slurry was precipitated in MeOH, filtered off and dried in vacuo. A purple/black solid was obtained (21 mg, yield 95 %). UV-vis: λ_{max} = 583 nm (shoulder: 628 nm); SEC: $M_w = 57 \times 10^3$; PD = 3.4.

3. Results and Discussion

3.1. Precursor Polymers

The synthetic routes toward the MDMO-PPV bisdithiocarbamate premonomer **1** and the O-PTV bisdithiocarbamate premonomer **4** have been reported earlier.[22,33,34] The polymerizations are performed under nitrogen atmosphere. To this end, the monomers are dissolved in dry THF (0.2 M for MDMO-PPV premonomer and 0.4 M for the O-PTV premonomer) and the base is added (Scheme 2). In case of the MDMO-PPV premonomer an amount of 1.5 equiv of lithium hexamethyldisilazide (LHMDS), for the O-PTV monomer 2.0 equiv of sodium hexamethyldizilazide (NaHMDS) have been used. After polymerization both reaction mixtures are poured into ice water, neutralized by hydrochloric

acid (1 M) and extracted with $CHCl_3$. The precursor polymers **2** and **5** are isolated by precipitation in cold methanol.

Scheme 2. Synthesis of MDMO-PPV and O-PTV via the Dithiocarbamate Precursor Route, Followed by the Thermal or Acid-Induced Elimination

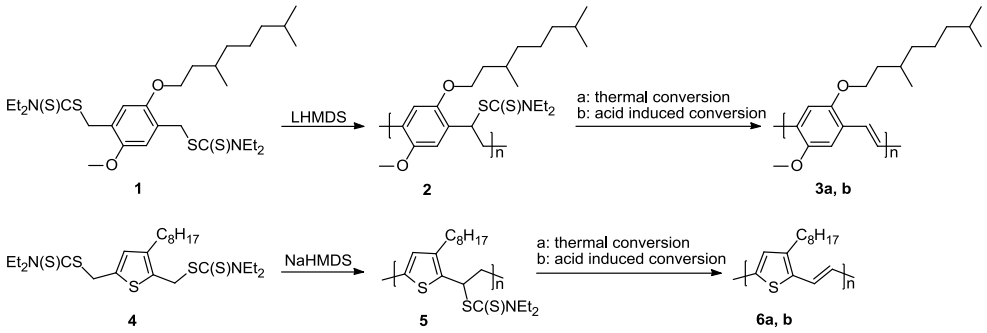

3.2. In-Situ Thermal Conversion in Thin Film

To examine the conversion conditions for dithiocarbamate precursor polymers the thermal elimination was studied in thin films by in situ UV-vis and FT-IR spectroscopy. Thin films were obtained by dropcoating a solution of the precursor polymers in $CHCl_3$ on quartz or NaCl disks, these films have been placed into a Harrick high-temperature cell under a continuous nitrogen flow, which was positioned in the beam of either the UV-vis or the FT-IR spectrometer, respectively. The thin precursor polymer films were heated at 2 °C/min from ambient temperature to 200 °C and spectra were collected at different temperatures.

Upon heating, a new absorption band appears in the UV-vis absorption spectra, associated with the formation of the conjugated system. Concomitantly, the absorption band associated with the precursor polymer decreases. For MDMO-PPV the precursor band is situated at 288 nm (Figure 1a). The absorption maximum (λ_{max} 460 nm) at 134 °C is lower as compared to this observed (λ_{max} 490 nm) after cooling to room temperature due to the thermochromic effect.[26] The elimination process can be more thoroughly analyzed by plotting the absorption profiles at 460 and 288 nm as a function

of temperature (Figure 1, b). In these profiles an increase of the absorbance at 460 nm can be noticed between 95 °C and 130 °C under these heating conditions (2 °C/min). In the same temperature range, a decrease in the absorbance at 288 nm takes place.

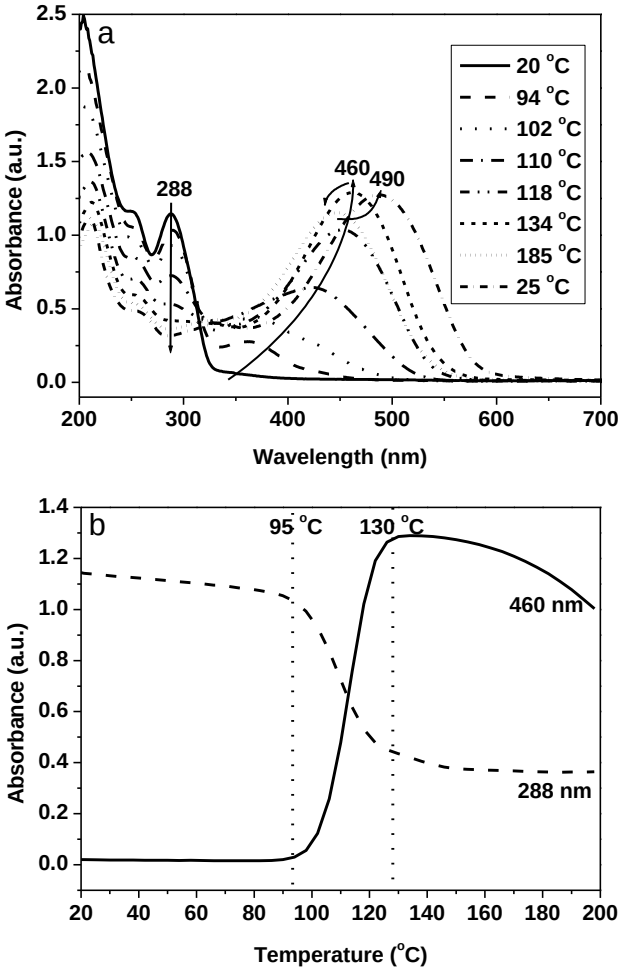

Figure 1. (a) UV-vis spectra of precursor polymer **2** at different temperatures. (b) UV-vis absorbance profiles at 288 and 460 nm at different temperatures for **2**.

For the O-PTV a similar behaviour is observed. The absorption at 275 nm, corresponding to the precursor polymer, decreases during the reaction.

Simultaneously the absorption consistent with the conjugated system appears around 560 nm. From the absorbance profiles, it can be concluded that under these heating conditions (2 °C/min) the formation of the conjugated system starts above 100 °C.

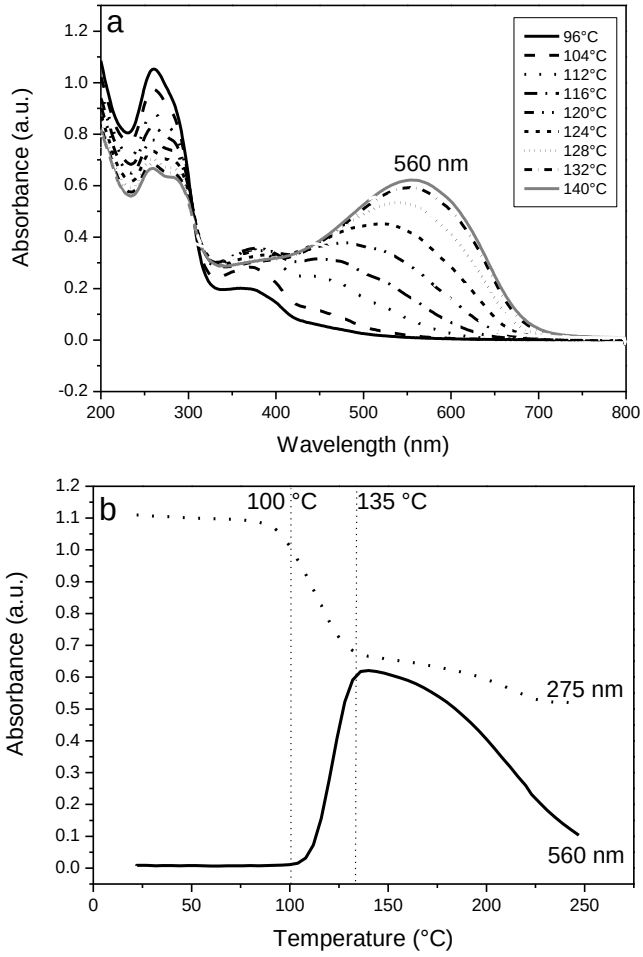

Figure 2. UV-vis spectra of **5** at different temperatures. (b) UV-vis absorbance profiles at 275 and 560 nm at different temperatures for **5**.

These processes can also be monitored using in situ FT-IR spectroscopy. Using this technique, upon heating a decrease is observed of the absorption bands at 1205, 1266, 1414 and 1486 cm^{-1}, which can be assigned to vibrations of the

dithiocarbamate functional group. At the same time, a new absorption band appears (at 965 cm^{-1}, for MDMO-PPV)[35] which originates from the *trans*-vinylene double bonds formed during thermal elimination. Concerning MDMO-PPV it can be noticed from the FT-IR transmission profiles at 965 and 1266 cm^{-1}, that the elimination starts at 105 °C and is completed at 145 °C, under the heating conditions used. These results are consistent with the UV-vis profiles.

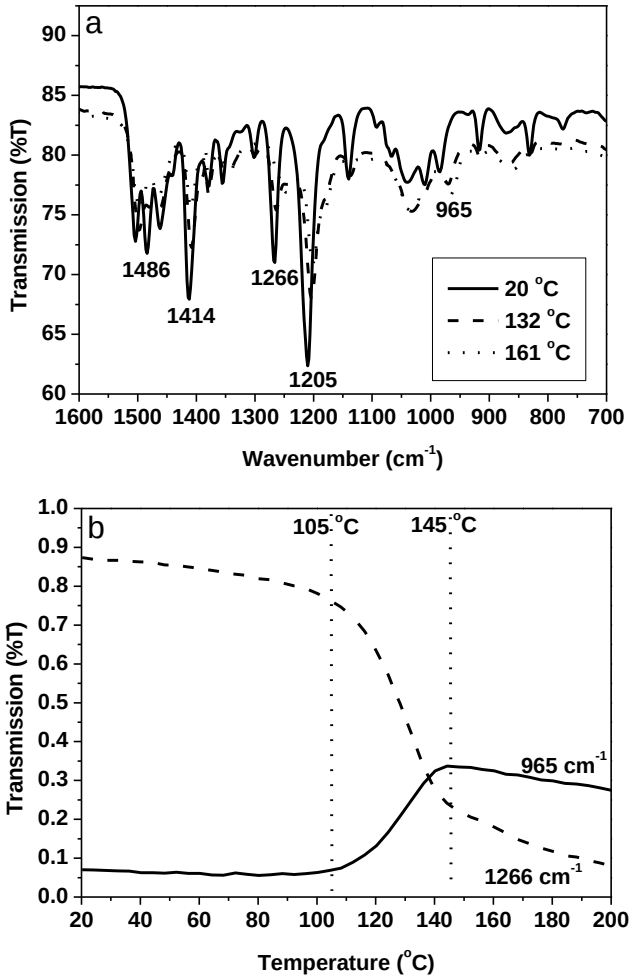

Figure 3. (a) FT-IR spectra of **2** at different temperatures. (b) IR absorption profiles at 965 and 1266 cm^{-1} at different temperatures for **2**.

Also for O-PTV the disappearance of the dithiocarbamate functional group and the formation of the trans-vinylene double bond (at 926 cm^{-1}) can be observed (Figure 4a) using FT-IR spectroscopy. From the absorption profiles, results are obtained totally consistent with the UV-vis profiles (Figure 4b).

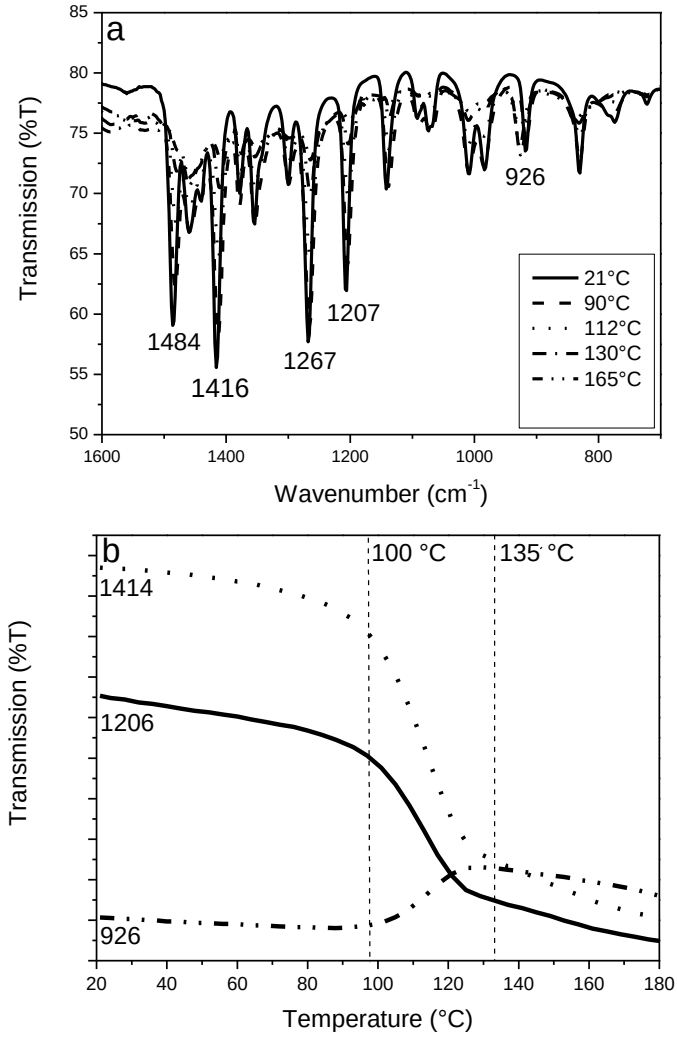

Figure 4. (a) FT-IR spectra of **5** at different temperatures. (b) IR absorption profiles at 926, 1206, and 1414 cm^{-1} at different temperatures for **5**.

3.3. Thermal Conversion in Solution

The dithiocarbamate precursor polymers can also be converted into their conjugated form by means of a thermal conversion in solution, which is typically done at a temperature of 180 °C. To determine the time period necessary for a complete conversion in solution, the polymers are dissolved in *o*-dichlorobenzene (*o*-DCB) and heated at 180 °C. Samples were taken with regular intervals and studied with UV-vis spectroscopy (Figure 5, a and b). From these spectra it can be concluded that the MDMO-PPV precursor polymer is fully converted under these heating conditions within 60 min.

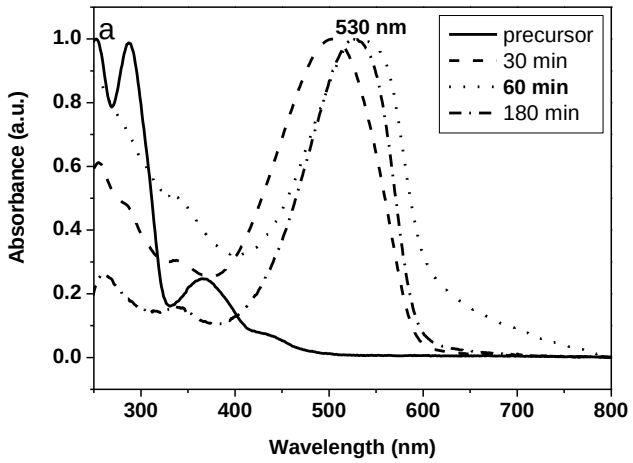

Figure 5a. UV-vis absorption spectra for the thermal conversion (180 °C, *o*-DCB) in solution of MDMO precursor PPV.

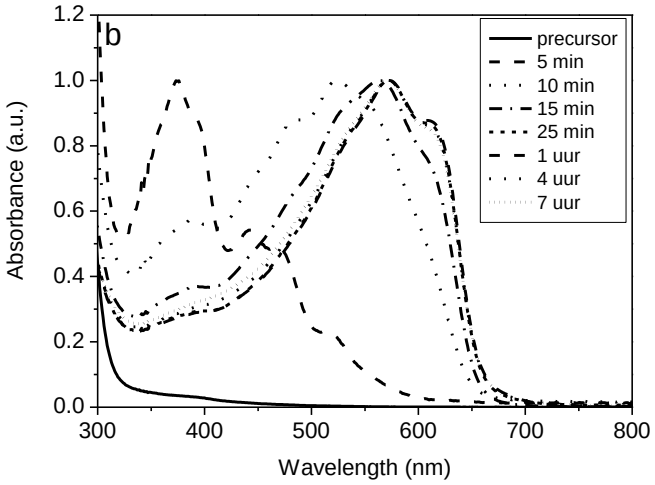

Figure 5b. UV-vis absorption spectra for the thermal conversion (180 °C, *o*-DCB) in solution of octyl precursor PTV.

In case of the O-PTV precursor, the conversion proceeds faster. Already after 25 min, the maximum wavelength (573 nm) has been reached (Figure 5b). However, elimination at 180 °C may lead to degradation of the polymer chromophore structure (conjugated system).[32] Prolonged heating (> 4 h) of the O-PTV leads to a blue shift in the UV-vis spectra, which is indicative for a thermal degradation of the conjugated system. This underlines the necessity to find alternative conversion processes to avoid detrimental degradation of the conjugated system.

3.4. Acid-Induced Conversion

Recently a haphazard observation in our research group showed that dithiocarbamate precursor polymers have the tendency to change color in "acid" solvents, e.g. chloroform.[36] As this might refer to a partial conversion of the precursor polymer to the conjugated form, a study of the influence of acids on the conversion of dithiocarbamate precursor polymers was started.

The acid-induced elimination is studied in solution using UV-vis spectroscopy. Hereto, the precursor polymers are dissolved in chlorobenzene (CB) and heated at 70 °C in the presence of 1,5 equiv of either benzenesulfonic acid

or trifluoroacetic acid and the reaction is followed by taking samples at regular time intervals. When no further changes in the UV-vis spectra are observed, the reaction mixture is neutralized and extracted with $CHCl_3$. If possible (sufficient quantity) the polymers are isolated by precipitation in cold methanol.

When the MDMO-PPV precursor is treated with benzenesulfonic acid, the conversion seems to be very fast. It takes only 30 min to convert the precursor polymer and reach the maximum absorption wavelength (Figure 6a). This is not the case for the conversion with trifluoroacetic acid. Here it takes about 7 h before the conversion is complete (Figure 6b). The distinction between these two experiments can simply be explained by the acid strength, e.g. benzenesulfonic acid has a pKa value of -6.5 (at 25 °C). Trifluoroacetic acid is a much weaker acid with a pKa value of 0.5 (at 25°C). The obtained absorption maxima (λ_{max}) are similar (534 and 538 nm) to those obtained after thermal elimination (530 nm).

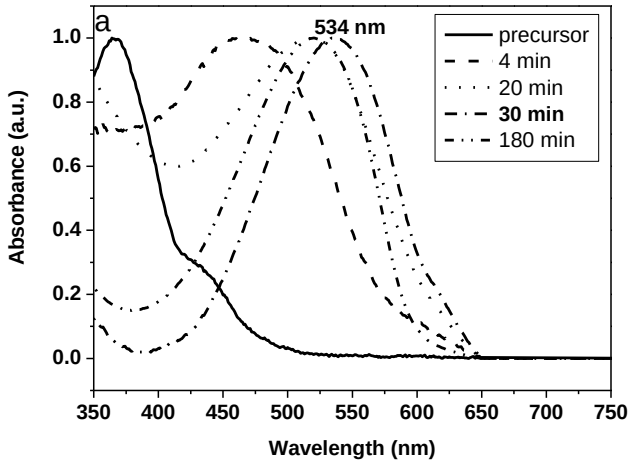

Figure 6a. UV-vis absorption spectra for the acid-induced conversion (70 °C in CB) of MDMO precursor PPV with benzenesulfonic acid.

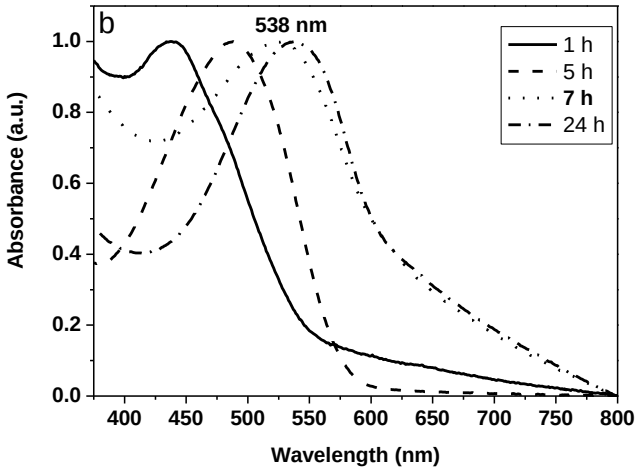

Figure 6b. UV-vis absorption spectra for the acid-induced conversion (70 °C in CB) of MDMO precursor PPV with trifluoroacetic acid.

In case of precursor O-PTV, the acid-induced conversion with benzenesulfonic acid is extremely fast, the new absorption maximum is reached almost instantaneously, already after 10 min the maximum value of 580 nm has been reached (Figure 7a). If the weaker trifluoroacetic acid is used the reaction is still very fast (Figure 7b). Upon addition of the acid, an instant color change (from orange to purple) occurs. Already the first sample (after 10 min) shows a fully conjugated polymer.

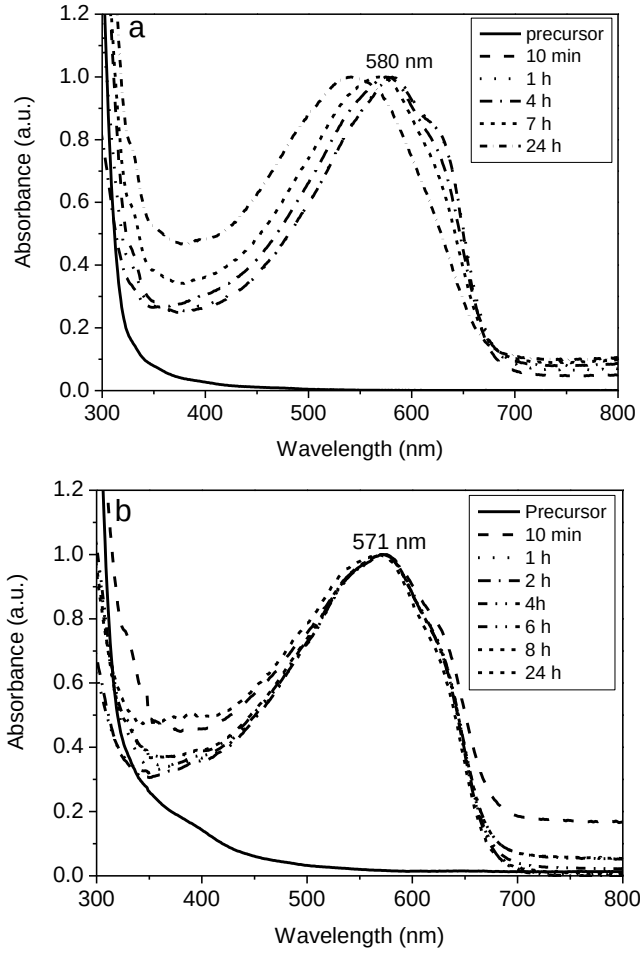

Figure 7. UV-vis absorption spectra for the acid-induced conversion (70 °C in CB) of octyl precursor PTV with (a) benzene sulfonic acid and (b) trifluoroacetic acid.

For longer reaction times however, a clear difference between the two acids can be observed. With benzenesulfonic acid as reagent, it can be stated that the absorption maximum after 7 h and especially after 24 h (Figure 7a) shows a clear hypsochromic shift, which is probably due to partial degradation of the polymer. A similar effect is observed for MDMO-PPV when benzenesulfonic acid is used (Figure 6a, spectrum at 180 min). So, in the case of benzenesulfonic acid, it is very important to avoid long exposure to acid to

avoid degradation of the conjugated system. In the case of trifluoroacetic acid the degradation process is much slower and is not observed within a time frame of 24 h (Figures 6b and 7b). Seemingly because of the lower acidity, the kinetic separation between the elimination process and the degradation process is large enough to limit the reaction to the first process.
Next, the conversion process of precursor O-PTV is studied at room temperature for which the conversion with benzenesulfonic acid was still quit fast. The maximal absorption wavelength reached is however about 50 nm lower than the one at 70 °C (Figure 8). Longer exposure to acid only leads to degradation. A very similar result was obtained when using trifluoroacetic acid at room temperature. Seemingly at room temperature a side reaction limits the extent to which the conjugation in the O-PTV system develops.

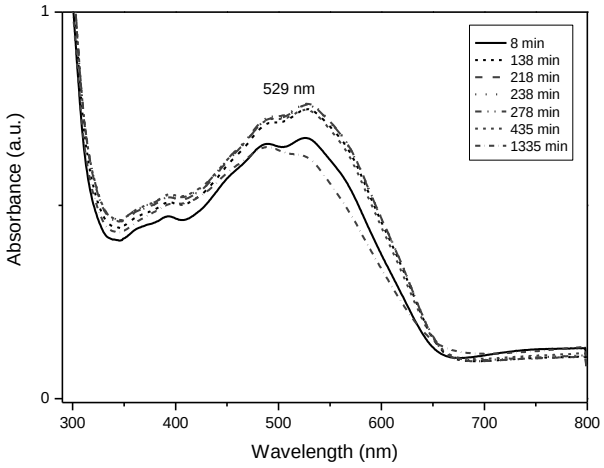

Figure 8. UV-vis spectra for the acid-induced conversion of octyl precursor PTV with benzenesulfonic acid at room temperature.

To achieve a deeper understanding of the acid-induced elimination of the dithiocarbamate functional group in the corresponding precursor polymers a mechanistic scheme is proposed as presented in Scheme 3. This mechanism assumes as a first step the protonation of the dithiocarbamate group converting it to a better leaving group. Next the dithiocarbamate group is expelled and decomposes in carbon disulphide and a secondary amine. At the

same time a carbenium ion is formed in the precursor polymer structure. This opens a path for two competitive reactions, e.g. an elimination reaction (A) forming a double bond and a substitution reaction (B) with the conjugated base of the acid used, onto the carbenium ion site. In the former reaction the secondary amine will trap the proton liberated during the elimination reaction. This implies that the acid does not act as a catalyst but is effectively consumed. Given this mechanism it should be expected that higher temperatures favour elimination, lower temperature or added nucleophiles would make the substitution reaction more competitive.[37]

Scheme 3. Proposed Mechanism for the Acid-Induced Conversion Reaction of DTC Precursor Polymers.

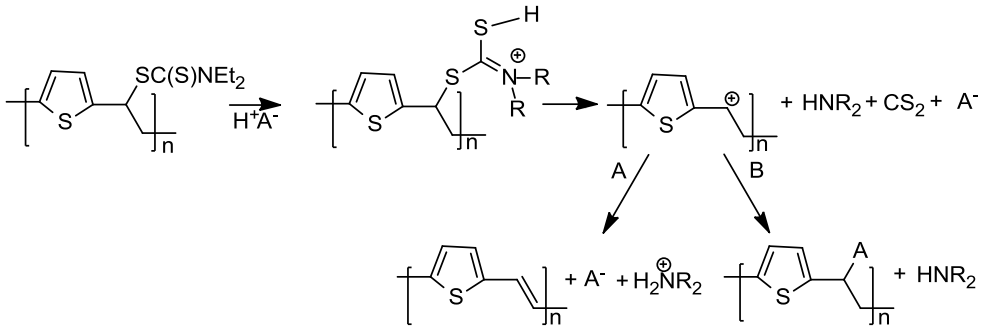

To test the latter effect a nucleophile reagent, i.e. 1 equiv of octanethiol, has been added at room temperature to the reaction mixture with trifluoroacetic acid (Figure 9). Here, it can be observed that the conjugated system did not develop fully, even if the mixture was allowed to react for 24 h. It may be assumed that the addition of octanethiol favours a nucleophilic substitution and creates a collection of oligomeric conjugated fragments.

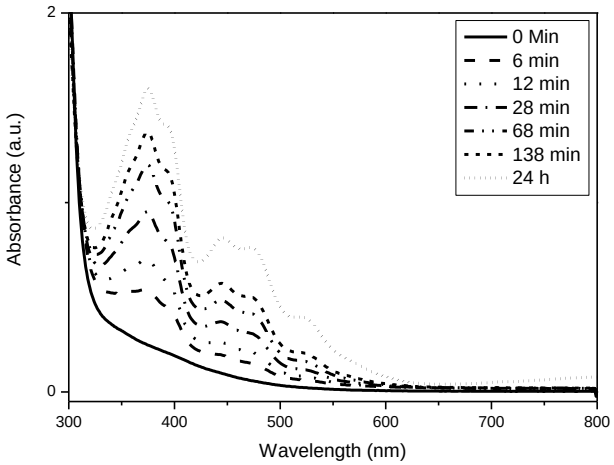

Figure 9. UV-vis spectra of the trifluoroacetic acid-induced conversion of octyl precursor PTV at room temperature in the presence of octanethiol.

Another experiment evaluates the influence of the acid concentration. On addition of only 0.3 equiv of trifluoroacetic acid instead of 1.5 (Figure 10), it is observed that the conjugation length is limited again to oligomeric fragments of the conjugated system.[38] This demonstrates that the acid is effectively consumed during the conversion and does not act as a catalyst.

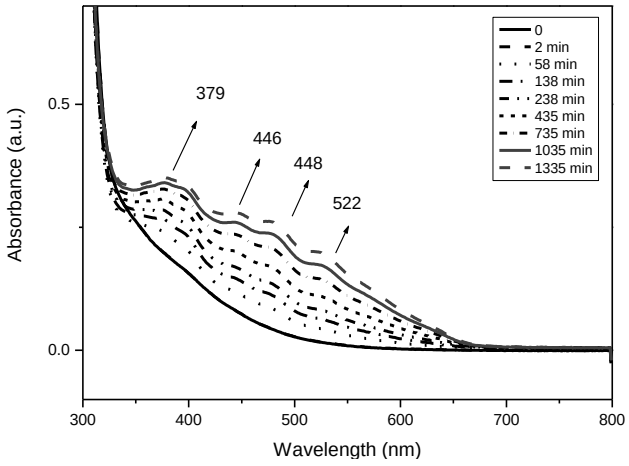

Figure 10. UV-vis spectra of the acid-induced conversion of octyl precursor PTV with 0.3 equiv of trifluoroacetic acid.

Consistent with the proposed reaction mechanism in Scheme 3 the acid-induced conversion of the PTV precursor polymer is much faster than for the PPV precursor polymer. If it is assumed that the reaction proceeds via an intermediate carbenium ion, this carbenium ion will be stabilized by the aromatic core next to it. In the case of PTV, the aromatic core is a thiophene unit which is much more electron rich than the core of the PPV precursor polymer. Therefore, the thiophene ring gives raise to a better stabilization of the intermediate and so a faster reaction.

To explore the unique character of this conversion method for dithiocarbamate precursor polymers, a comparison with another precursor route has been performed. A xanthate precursor toward plain PTV[19] has been converted in the presence of 1,5 equiv benzenesulfonic acid at room temperature in CB and the reaction is monitored by UV-vis spectroscopy in solution (Scheme 4). The spectra (Figure 11a) only show the absorption band of the precursor polymer and there is no indication for the formation of the conjugated system. For comparison, the results from in situ UV-Vis spectroscopy for a thermal elimination of a thin film of the xanthate precursor polymer are shown in Figure 11b. A film of the precursor polymer has been heated with a ramping temperature of 2 °C/ min from room temperature up to 350 °C. Clearly said behavior, i.e. acid-induced elimination, is only displayed for the dithiocarbamate precursor polymers and is unprecedented in literature for this class of functional groups. Future work is in progress in which we focus on a detailed NMR study using ^{13}C labeled PTVs to unravel details of the defect structures present in thermal and acid-induced converted PTV precursors. Furthermore a study has been started to gain a deeper insight in the chemistry of dithiocarbamate functional groups using model compounds. This work will be reported in due time.

Scheme 4. Acid-Induced and Thermal Conversion of a Xanthate Precursor Polymer

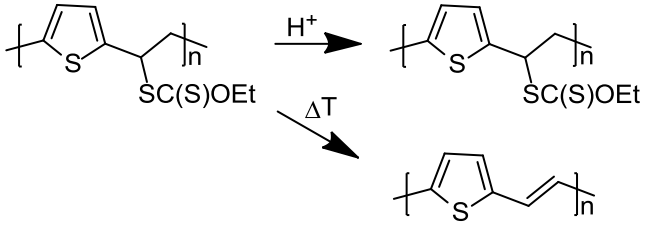

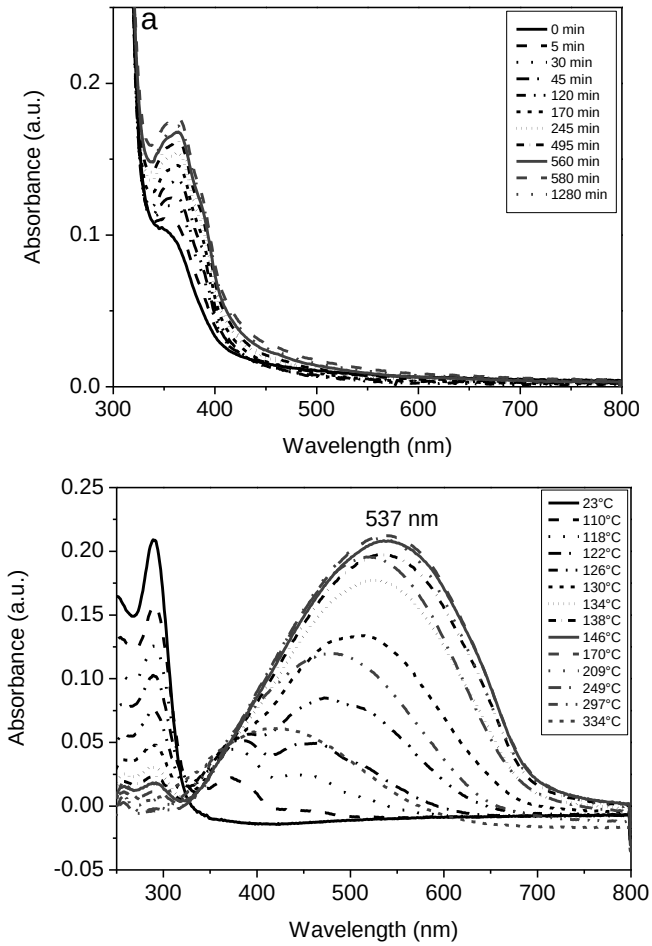

Figure 11. (a) UV-vis spectra of the benzenesulfonic acid-induced conversion of the xanthate precursor polymers, at room temperature in CB. (b) In-situ UV-vis experiment of the thermal conversion of xanthate precursor polymer.

4. Conclusion

Two conversion processes for dithiocarbamate precursor polymers have been studied and compared, the thermal conversion and the acid-induced conversion. The acid-induced conversion allows lowering the conversion temperature from 180 °C to 70 °C. The concentration and the nature (strength) of the acid are of importance to avoid degradation and therefore defects. By tuning the reaction conditions, the competition between an elimination and a substitution reaction can be controlled in favor of elimination. Finally a mechanistic framework is presented to explain the main features observed for the acid-induced elimination.

5. Acknowledgment

The authors would like to thank H. Penxten for the in situ UV-vis and FT-IR measurements. The authors gratefully acknowledge the Fund for Scientific Research-Flanders (FWO) and Belspo in the frame of network IAP P6/27, initiated by the Belgian State Prime Minister's Office, for financial support. We also want to thank the IWT (Institute for the Promotion of Innovation by Science and Technology in Flanders) for the financial support via the IWT-SBO project 060843 "Polyspec".

6. References and Notes

(1) Kraft, A.; Grimsdale, A. C.; Holmes, A. B. *Angew. Chem., Int. Ed.* **1998**, *37*, 403–428.

(2) Dimitrakopoulos, C. D.; Mascaro, D. J. *IBM J. Res. Dev.* **2001**, *45*, 11–27.

(3) Helgesen, M. ; Sondergaard, R.; Krebs, F. C. *J. Mater. Chem.* **2010**, *20*, 36–60.

(4) 4. MacDiarmid, W.; Zhang, W.; Huang, Z.; Wang, P. C.; Huang, F.; Xie, S. *Polym. Prepr.* **1997**, *11*, 333–334.

(5) Li, A.-K.; Janarthanan, N.; Hsu, C.-S. *Polym. Bull.* **2000**, *45*, 129–135.

(6) Cacialli, F.; Daik, R.; Feast, W. J.; Friend, R. H.; Lartigau, C. *Opt. Mater.* **1999**, *12*, 7.

(7) Denton, F. R.; Lathi P. M.; Karasz F. E. *J. Polym. Sci., Part A : Polym. Chem.* **1992**, *30*, 2223–2231.

(8) Issaris, A.; Vanderzande, D.; Gelan J. *Polymer* **1997**, *38*, 2571–2574.

(9) Hontis, L.; Vrindts, V.; Lutsen, L.; Vanderzande, D.; Gelan J. *Polymer* **2001**, *42*, 5793–5796.

(10) Wiesecke, J.; Rehahn, M. *Angew. Chem., Int. Ed.* **2003**, *42*, 567–570.

(11) Schwalm, T.; Wiesecke, J.; Immel, S.; Rehahn, M. *Macromolecules* **2007**, *40*, 8842–8854.

(12) Harper, K.; West, W. J. W. Eur. Pat. Appl. No. 182548, 1985.

(13) Jen, K. Y.; Jow, R.; Eckhardt, H.; Elsenbaumer, R. L. *Polym. Mater. Sci. Eng.* **1987**, *56*, 49–53.

(14) Jen, K. Y.; Maxfield, M.; Shacklette, L. W.; Elsenbaumer, R. L. *J. Chem. Soc., Chem. Commun.* **1987**, 309–311.

(15) Wessling, R. A. *J. Polym. Sci., Polym. Symp.* **1985**, *72*, 55–66.

(16) Gilch, H. G.; Wheelwright, W. L. *J. Polym. Sci.* **1966**, *4*, 1337–1349.

(17) Son, S.; Dodabalapur, A.; Lovinger, A. J.; Galvin, M. E. *Science* **1995**, *269*, 376–378.

(18) Kesters, E.; Gillissen, S.; Motmans, F.; Lutsen, L.; Vanderzande D. *Macromolecules* **2002**, *35*, 7902–7910.

(19) Mitchell, W. J.; Pena, C.; Burn, P. L. *J. Mater. Chem.* **2002**, *12*, 200–205.

(20) van Breemen, A. J. J. M.; Issaris, A. C. J.; de Kok, M. M.; Van Der Borght, M. J. A. N.; Adriaensens, P. J.; Gelan, J. M. J. V.; Vanderzande, D. J. M. *Macromolecules* **1999**, *32*, 5728–5735.

(21) Henckens, A.; Knipper, M.; Polec, I.; Manca, J.; Lutsen, L.; Vanderzande, D. *Thin Solid Films* **2004**, *451–452*, 572–579.

(22) Henckens, A.; Lutsen, L.; Vanderzande, D.; Knipper, M.; Manca, J.; Aernouts, T.; Poortmans, J. *SPIE Proc.* **2004**, 52–59.

(23) Henckens, A.; Colladet, K.; Fourier, S.; Cleij, T. J.; Lutsen, L.; Gelan, J. *Macromolecules* **2005**, *38*, 19–26.

(24) Henckens, A.; Duyssens, I.; Lutsen, L.; Vanderzande, D.; Cleij, T. J. *Polymer* **2006**, *47*, 123–131.

(25) Banishoeib, F.; Fourier, S.; Cleij, T. J.; Lutsen, L.; Vanderzande, D. *Eur. Phys. J.: Appl. Phys.* **2007**, *37*, 237–240.

(26) Nguyen, L. H.; Günes, S.; Neugebauer, H.; Sariciftci, N. S.; Banishoeib, F.; Henckens, A.; Cleij, T. J.; Lutsen, L.; Vanderzande, D. *Sol. Energ. Mat. Sol. C.* **2006**, *90*, 2815–2828.

(27) Banishoeib, F.; Adriaensens, P.; Berson, S.; Guillerez, S.; Douheret, O.; Manca, J.; Fourier, S.; Cleij, T. J.; Lutsen, L.; Vanderzande, D. *Sol. Energ. Mat. Sol. C.* **2007**, *91*, 1026–1034.

(28) Roex, H.; Adriaensens, P.; Vanderzande, D.; Gelan, J. *Macromolecules* **2003**, *36,* 5613–5622.

(29) Vandenbergh, J.; Wouters, J.; Adriaensens, P. J.; Mens, R.; Cleij, T. J.; Lutsen, L.; Vanderzande, D. *Macromolecules* **2009**, *42*, 3661–3668.

(30) Kesters, E.; Vanderzande, D.; Lutsen, L.; Penxten, H.; Carleer, R. *Macromolecules* **2005,** *38*, 1141–1147.

(31) van Breemen, A. J. J. M.; Vanderzande, D. J. M.; Adriaensens, P. J.; Gelan, J. M. J. V. *J. Org. Chem.* **1999**, *64*, 3106–3112.

(32) Breban, L.; Lutsen, L.; Vanhoyland, G.; D'Haen, J.; Manca, J.; Vanderzande, D. *Thin Solid Films* **2006,** *511–512*, 695–700.

(33) Becker, H.; Spreitzer, H.; Ibrom, K.; Kreuder, W. *Macromolecules* **1999**, *32*, 4925–4932.

(34) Diliën, H.; Palmaerts, A.; Lenes, M.; de Boer, B.; Blom, P.; Cleij, T.J.; Lutsen, L.; Vanderzande, D. *Macromolecules* **2010**, *43*, 10231–10240.

(35) Chambon, S.; Rivaton, A.; Gardette, J. -L.; Firon, M.; Lutsen, L. *J. Polym. Sci., Part A: Polym. Chem.* **2007**, *45*, 317–331.

(36) Stability of $CHCl_3$: Stable under ordinary conditions of use and storage. pH decreases on prolonged exposure to light and air due to formation of HCl. Chloroform; MSDS No. c2915; Mallinckrodt Baker: Phillipsburg, NJ, 07/02/09

http://www.jtbaker.com/msds/englishhtml/c2915.htm (accessed 01/04/11).

(37) McMurry, J. *Organic Chemistry*, 6th ed., Thomson: London, 2004.

(38) Jestin, I.; Frère, P.; Blanchard, P.; Roncali, J. *Angew. Chem., Int. Ed.* **1998**, *37*, 942–945.

Chapter 4

Synthesis and Characterization of Water-Soluble Poly(*p*-phenylene vinylene) Derivatives via the Dithiocarbamate Precursor Route

ABSTRACT: Two hydrophilic branched oligo(ethylene glycol)-substituted PPV derivatives, poly(2,5-bis(1,3-bis(triethoxymethoxy)propan-2-yloxy)-1,4-phenylene vinylene) (BTEMP-PPV) and poly(2-methoxy-5-(1,3-bis(triethoxy methoxy)propan-2-yloxy)-1,4-phenylene vinylene) (MTEMP-PPV), are presented. Polymerizations have been performed via the dithiocarbamate precursor route, using lithium hexamethyldisilazide (LHMDS) as a base, to obtain high molecular weight precursor polymers. After thermal conversion of the precursor polymers into the fully conjugated systems, the solubility of the polymers has been examined. The polar nonionic side chains of MTEMP-PPV and BTEMP-PPV render the PPV backbone soluble in a variety of solvents, including alcohols and even water, making these polymers suitable candidates to be used in optoelectronic devices that can be processed from environmentally friendly solvent systems.

*Vandenbergh, J.; Dergent, J.; Conings, B.; Gopala Krishna, T. V. V.; Maes, W.; Cleij, T. J.; Lutsen, L.; Manca, J.; Vanderzande, D. J. M. *European Polymer Journal*, **2011**, submitted.

1. Introduction

During the last decade, water-soluble conjugated polymers (WSCPs) have been thoroughly studied as active materials in highly sensitive biological [1−3] or chemical sensors [4] and all kinds of optoelectronic devices [5] such as (multilayer) organic light-emitting diodes (OLEDs) [6−12], polymer light-emitting electrochemical cells (PLECs) [13−15] and organic photovoltaics (OPVs) [16,17]. Since conventional conjugated polymers are only soluble in toxic organic solvents, e.g. chlorobenzene or toluene, the biggest advantage of WSCPs is that harmless and environmentally friendly solvents, e.g. water or alcohols, can be used during device processing. Furthermore, WSCPs can induce major improvements in the development of hybrid organic/inorganic solar cells. Conventional conjugated polymers are hydrophobic, while the inorganic metal-oxide or other nanocrystal compounds used in hybrid solar cells are hydrophilic. This can cause compatibility problems at the donor-acceptor interface, resulting in decreased overall power conversion efficiencies. Since WSCPs are hydrophilic in nature, the above mentioned compatibility issues can be avoided to a large extent and improved interface areas can be obtained [18,19].

WSCPs can be synthesized by attaching hydrophilic side chains to the conjugated polymer backbone. This approach has been used for various conjugated structures such as poly(*p*-phenylene vinylene) [20], poly(*p*-phenylene) [21], poly(*p*-phenylene ethylene) [22], polyfluorene [23] and polythiophene [24] based polymers. The hydrophilic side chains often consists of charged groups such as phosphonates, sulfonates, carboxylates or ammonium salts [25−28]. With ionic WSCPs multilayered films can be fabricated using the electrostatic-driven layer-by-layer self-assembly technique, with the aim to construct fluorescence based devices [29]. On the other hand, also neutral groups such as hydroxyl and ethylene glycol moieties can be used to afford water-soluble polymers [30,31]. By using these charged or neutral groups, water-solubility is generated by several non-covalent binding forces such as ion pairing interactions, ion-dipole interactions, dipole-dipole interactions and hydrogen bonds [32]. When water is used as

solvent, ionic side groups result in stronger binding forces than when neutral side chains are used. Because water forms a hydration shell around each salt ion group, it can be problematic to obtain a totally water-free layer when such an ionic WSCP is spincoated from water onto a substrate. This might induce major problems when these polymers are to be used in organic photovoltaic cells. The water molecules present in the active layer would act as energy traps for the generated charge carriers, thereby substantially decreasing the device performance. Furthermore, also the ionic functionality itself could possibly act as a charge trap. To avoid these problems, in this study, polar poly(*p*-phenylene vinylene) (PPV) derivatives bearing nonprotic, nonionic, branched tri(ethylene glycol) side chains have been synthesized. Besides the lower binding forces towards water molecules, these side chains have low reactivity and therefore interference with other functionalities is minimized. The aim was to study the solubility of these ethylene oxide substituted PPVs in environment-friendly solvents and how well these polymers would operate in optoelectronic devices. To this end, two polar PPV derivatives, poly(2,5-bis(1,3-bis(triethoxymethoxy) propan-2-yloxy)-1,4-phenylene vinylene) (BTEMP-PPV) and poly(2-methoxy-5-(1,3-bis(triethoxy methoxy)propan-2-yloxy)-1,4-phenylene vinylene) (MTEMP-PPV), were synthesized using the dithiocarbamate precursor route [33−35], which typically leads to high molecular weight polymers with extremely low structural defect levels [36]. In a subsequent step the precursor polymers were converted into conjugated materials via a thermal induced elimination reaction.

After the synthesis and characterization of the MTEMP-PPV and BTEMP-PPV derivatives, the solubility of the polymers in a broad variety of solvents was tested and the UV-vis absorption characteristics were determined. Furthermore, some electronic properties such as the relative permittivity (ε_r) and the hole-mobility (μ_h) of the polymers were investigated with impedance spectroscopy and space charge limited current (SCLC) measurements, respectively. Finally, a proof-of-concept solar cell device was processed from an environmentally friendly solvent.

2. Experimental Section

2.1. General

Unless otherwise stated, all reagents and chemicals were obtained from commercial sources (Acros and Aldrich) and used without further purification. Tetrahydrofuran (THF) was dried by distillation from Na/benzophenone. NMR spectra were recorded with a Varian Inova 300 spectrometer at 300 MHz for ^{1}H NMR and at 75 MHz for ^{13}C NMR using a 5 mm probe. Gas chromatography/mass spectrometry (GC/MS) analyses were carried out with TSQ-70 and Voyager mass spectrometers (Thermoquest); the capillary column was a Chrompack Cpsil5CB or Cpsil8CB. Analytical size exclusion chromatography (SEC) was performed using a Spectra series P100 (Spectra Physics) pump equipped with two mixed-B columns (10 µm, 0.75 cm x 30 cm, Polymer Labs) and a refractive index detector (Shodex) at 40 °C. THF was used as the eluent at a flow rate of 1.0 mL/min. Molecular weight distributions are given relative to polystyrene standards. FT-IR spectra were collected with a Perkin-Elmer Spectrum One FT-IR spectrometer (nominal resolution 4 cm^{-1}, summation of 16 scans). UV-vis spectroscopy was performed on a VARIAN CARY 500 UV-vis-NIR spectrophotometer (scan rate: 600 nm/min). Thin film morphologies were investigated via a Zeiss Axiovert 40 MAT optical microscope.

To determine the relative permittivity ε_r of the polymers, spectral impedance measurements were carried out on ITO/polymer/Al sandwich structures. Polymers were dissolved in chlorobenzene (3 wt%) and spincoated on patterned ITO coated substrates (15 Ω/sq, Kintec) with different spincoat speeds to obtain different thicknesses. A 60 nm Al top electrode was evaporated through a shadow mask at a pressure of $1x10^{-6}$ mbar. Capacitors of different size were defined by the intersections of the Al electrodes and the ITO coated parts of the substrate. The complex impedance was measured with a HP4284 LCR-meter by applying a DC voltage of 0.8 V and AC voltage of 25 mV over frequencies ranging from 20 Hz to 10 MHz. The impedance spectrum was fitted assuming a Randles circuit. ε_r was then calculated from

the fitted value of the capacitance C, and the formula $C = \varepsilon_0 x \varepsilon_r A/d$, with A and d the area and thickness of the devices, respectively [37]. The device thickness was measured with a Dektak ST3 profilometer.

For the hole mobility μ_h, hole-only devices were made by sandwiching the polymer in a ITO/PEDOT-PSS/polymer/Au sandwich structure, where the work function of PEDOT-PSS (H.C. Starck, Clevios P VP AI 4083) and Au approximately coincides with the HOMO level of the polymer. The PEDOT-PSS layer was spincoated to form a layer of 40 nm. 200−600 nm thick layers of polymer were spincoated from a 3 wt% chlorobenzene solution. An Au contact of 60 nm was evaporated at a pressure of $1x10^{-6}$ mbar. Current-voltage characteristics were measured with a Keithley 2400 source meter. The resulting curves were fitted with a field dependent space charge limited current equation to extract the hole mobility [38].

The bilayer solar cell devices were made by sandwiching the polymer in a ITO/PEDOT-PSS/polymer/C_{60}/Al sandwich structure. The PEDOT-PSS layer was spincoated to form a layer of 30 nm. A 620 nm thick layer of MTEMP-PPV was spincoated from a 3 wt% acetone solution. A 90 nm thick C_{60} acceptor layer was evaporated at a pressure of $9.4x10^{-7}$ mbar. An Al contact of 50 nm was evaporated on top at a pressure of $1.2x10^{-6}$ mbar. The devices were annealed at 150 °C on a hotplate for 10 min inside a N_2 glovebox. Current-voltage characteristics were measured in nitrogen atmosphere under AM1.5 illumination of 100mW/cm^2 (1 sun) with an Oriel/Newport class B solar simulator, using an Oriel Si detector and a Keithley 2400 source meter.

2.2. Premonomer Synthesis

1,3-Bis(2-(2-(2-methoxyethoxy)ethoxy)ethoxy)propan-2-ol ***(1)***

Tri(ethylene glycol) monomethyl ether (200 g, 1.22 mol, 3.05 equiv.) was stirred at 100 °C under N_2 atmosphere and sodium (9.6 g, 0.42 mol, 1.05 equiv.) was added in small portions. After all sodium had reacted, the reaction mixture was cooled down to 80 °C. Subsequently, epichlorohydrine (37 g, 0.40 mol, 1 equiv.) was added drop wise and the mixture was stirred for 12 h at 100 °C under N_2 atmosphere. After cooling to room temperature,

the reaction mixture was filtered and purified by Kugelrohr distillation. The second fraction (p = $5x10^{-3}$ mbar, T = 205 °C) contained **1** as a pure clear oil (83.3 g, 54%). ^{1}H NMR ($CDCl_3$): δ = 3.87–3.80 (m, 1H, OCH), 3.56–3.50 (m, 20H, OCH_2), 3.46–3.38 (m, 8H, OCH_2), 3.26 (s, 6H, OCH_3); ^{13}C NMR ($CDCl_3$): δ = 74.3, 71.5, 70.5, 69.5, 58.5; MS (CI, m/z): 385 $[M+1]^+$.

1,3-Bis(2-(2-(2-methoxyethoxy)ethoxy)ethoxy)propan-2-yl-toluenesulfonate ***(2)***

In a three-necked flask **1** (83.3 g, 0.22 mol, 1 equiv.) and *p*-toluenesulfonyl chloride (42.6 g, 0.22 mol, 1.03 equiv.) were dissolved in CH_2Cl_2 (225 mL) and stirred under N_2 atmosphere. The mixture was cooled to -5 °C with a $CHCl_3$/liquid N_2 bath. KOH (48.6 g, 0.87 mol, 4 equiv.) was added to the mixture in small portions, maintaining the reaction temperature below 5 °C (exothermic reaction). The mixture was stirred for 3 h at 0 °C after which CH_2Cl_2 (225 mL) and ice water (300 mL) were added. After extraction, the organic phase was dried ($MgSO_4$) and concentrated under reduced pressure. The product was isolated as a clear brown oil (109 g, 93%) and used without further purification. ^{1}H NMR ($CDCl_3$): δ = 7.77 (d, 2H, ArH), 7.28 (d, 2H, ArH), 4.63–4.52 (m, 1H, OCH), 3.60–3.40 (m, 28H, OCH_2), 3.26 (s, 6H, OCH_3), 2.35 (s, 3H, CH_3); ^{13}C NMR ($CDCl_3$): δ = 144.2, 133.5, 129.2, 127.5, 79.3, 71.5, 70.5, 69.5, 58.5, 21.5; MS (CI, m/z): 539 $[M+1]^+$.

1-Methoxy-4-(1,3-bis(2-(2-(2-methoxyethoxy)ethoxy)ethoxy)propan-2-yloxy)benzene ***(3)***

4-Methoxyphenol (5.3 g, 0.04 mol, 1 equiv.) was dissolved in EtOH (100 mL). Subsequently, Na*t*BuO (4.5 g, 0.05 mol, 1.1 equiv.) was added. The mixture was stirred at room temperature for 1 h under N_2 atmosphere. Afterwards, **2** (25 g, 0.05 mol, 1.1 equiv.) was added drop wise. The reaction mixture was stirred for 48 h at reflux temperature. After partial evaporation of the solvent, H_2O was added and the mixture was extracted with CH_2Cl_2. The organic extracts were washed with 10% NaOH-solution, dried over anhydrous $MgSO_4$ and the solvent was evaporated to afford the crude product. After

column chromatography (SiO_2, eluent diethyl ether/methanol 9/1), a yellow oil of **3** (19 g, 92%) was obtained. ^{1}H NMR ($CDCl_3$): δ = 6.90 (d, 2H, ArH), 6.75 (d, 2H, ArH), 4.40–4.30 (m, 1H, OCH), 3.70 (s, 3H, OCH_3), 3.68–3.54 (m, 24H, OCH_2), 3.52–3.48 (m, 4H, OCH_2), 3.35 (s, 6H, OCH_3); ^{13}C NMR ($CDCl_3$): δ = 152.5, 150.5, 119.0, 113.0, 79.3, 71.5, 70.5, 58.5, 55.5; MS (CI, m/z): 491 $[M+1]^+$.

2,5-Bis(chloromethyl)-1-methoxy-4-(1,3-bis(2-(2-(2-methoxyethoxy)ethoxy)ethoxy)propan-2-yloxy)benzene ***(4)***

To a stirred mixture of **3** (19 g, 0.04 mol, 1 equiv.) and *p*-formaldehyde (3.2 g, 0.11 mol, 2.75 equiv.), concentrated HCl (21 mL, 0.26 mol, 6.6 equiv.) was added drop wise under N_2 atmosphere at 0 °C. Subsequently, acetic anhydride (36.7 mL, 0.39 mol, 10 equiv.) was added at such a rate that the temperature of the mixture did not exceed 70 °C. The mixture was stirred at 75 °C for 4 h after which it was cooled down and poured into water. The product was extracted with $CHCl_3$. The organic phase was washed with $NaHCO_3$ (10%), dried ($MgSO_4$) and concentrated under reduced pressure. The crude product was purified by column chromatography (SiO_2, eluent diethyl ether/methanol 9/1) after which the pure product was obtained as a clear yellow oil (14.7 g, 64%). ^{1}H NMR ($CDCl_3$): δ = 7.10 (s, 1H, ArH), 6.85 (s, 1H, ArH), 4.62 (s, 2H, CH_2Cl), 4.57 (s, 2H, CH_2Cl), 4.42–4.38 (m, 1H, OCH), 3.80 (s, 3H, OCH_3), 3.70–3.52 (m, 24H, OCH_2), 3.50–3.45 (m, 4H, OCH_2), 3.35 (s, 6H, OCH_3); ^{13}C NMR ($CDCl_3$): δ = 151.5, 149.5, 128.5, 126.5, 118.0, 112.0, 79.3, 71.5, 70.5, 58.5, 55.5, 41.0; MS (CI, m/z): 587 $[M+1]^+$.

2,5-Bis(N,N-diethyldithiocarbamate-methyl)-1-methoxy-4-(1,3-bis(2-(2-(2-methoxyethoxy)ethoxy)ethoxy)propan-2-yloxy)benzene ***(5)***

Precursor **4** (6.1 g, 0.01 mol, 1 equiv.) was dissolved in EtOH (300 mL) under N_2 atmosphere. Subsequently, sodium diethyldithiocarbamate trihydrate salt (5.4 g, 0.02 mol, 2.3 equiv.) was added. The mixture was stirred for 3 h at ambient temperature after which H_2O was added. The product was extracted with $CHCl_3$. The organic phase was dried over anhydrous $MgSO_4$ and the

solvent was evaporated. The crude product was purified by column chromatography (SiO_2, eluent diethyl ether/methanol 9/1) to obtain pure product **5** as a clear yellow oil (2.7 g, 32%). ^{1}H NMR ($CDCl_3$): δ = 7.10 (s, 1H, ArH), 6.95 (s, 1H, ArH), 4.55 (s, 2H, CH_2S), 4.45 (s, 2H, CH_2S), 4.42−4.38 (m, 1H, OCH), 4.02−3.92 (m, 4H, CH_2N), 3.75 (s, 3H, OCH_3), 3.70−3.52 (m, 28H, OCH_2 and CH_2N), 3.50−3.45 (m, 4H, OCH_2), 3.30 (s, 6H, OCH_3), 1.20 (t, 12H, CH_3); ^{13}C NMR ($CDCl_3$): δ = 195.5, 152.0, 149.5, 126.5, 124.5, 118.0, 113.0, 79.3, 71.5, 70.5, 58.5, 55.5, 49.0, 46.0, 36.5, 12.5, 11.0; MS (CI, m/z): 813 $[M+1]^+$.

*1,4-Bis(1,3-bis(2-(2-(2-methoxyethoxy)ethoxy)ethoxy)propan-2-yloxy)benzene **(6)***

Hydroquinone (2.3 g, 0.02 mol, 1 equiv.) was dissolved in EtOH (100 mL). Subsequently, Na*t*BuO (4.5 g, 0.05 mol, 2.2 equiv.) was added. The mixture was stirred at room temperature for 1 h under N_2 atmosphere. Afterwards, **2** (25 g, 0.05 mol, 2.2 equiv.) was added drop wise. The reaction mixture was stirred for 48 h at reflux temperature. After partial evaporation of the solvent, H_2O was added and the mixture was extracted with CH_2Cl_2. The organic extracts were washed with 10% NaOH solution, dried over anhydrous $MgSO_4$ and the solvent was evaporated to afford the crude product. After column chromatography (SiO_2, eluent diethyl ether/methanol 9/1) a yellow product oil (12.9 g, 73%) was obtained. ^{1}H NMR ($CDCl_3$): δ = 6.85 (s, 4H, ArH), 4.40−4.30 (m, 2H, OCH), 3.70−3.52 (m, 48H, OCH_2), 3.50−3.45 (m, 8H, OCH_2), 3.34 (s, 12H, OCH_3); ^{13}C NMR ($CDCl_3$): δ = 152.3, 119.4, 78.9, 71.6, 70.5, 58.8; MS (CI, m/z): 843 $[M+1]^+$.

*2,5-Bis-chloromethyl-1,4-bis(1,3-bis(2-(2-(2-methoxyethoxy)ethoxy)ethoxy)propan-2-yloxy)benzene **(7)***

To a stirred mixture of **6** (12.9 g, 0.02 mol, 1 equiv.) and *p*-formaldehyde (1.3 g, 0.04 mol, 2.75 equiv.), concentrated HCl (8.3 mL, 0.10 mol, 6.6 equiv.) was added drop wise under N_2 atmosphere at 0 °C. Subsequently, acetic anhydride (14.4 mL, 0.15 mol, 10 equiv.) was added at such a rate

that the temperature of the mixture did not exceed 70 °C. The mixture was stirred at 75 °C for 4 h after which it was cooled down and poured into water. The product was extracted with $CHCl_3$. The organic phase was washed with $NaHCO_3$ (10%), dried ($MgSO_4$) and concentrated under reduced pressure. The crude product was purified by column chromatography (SiO_2, eluent diethyl ether/methanol 9/1) after which the pure product was obtained as a clear yellow oil (8 g, 56%). ^{1}H NMR ($CDCl_3$): δ = 7.04 (s, 2H, ArH) 4.59 (s, 4H, CH_2Cl), 4.45–4.35 (m, 2H, OCH), 3.70–3.52 (m, 48H, OCH_2), 3.50–3.45 (m, 8H, OCH_2), 3.35 (s, 12H, OCH_3); ^{13}C NMR ($CDCl_3$): δ = 150.3, 128.5, 117.4, 78.9, 71.6, 70.5, 58.8, 40.9; MS (CI, m/z): 940 $[M+1]^+$.

*2,5-Bis(N,N-diethyldithiocarbamate-methyl)-1,4-bis(1,3-bis(2-(2-(2-methoxyethoxy)ethoxy)ethoxy)propan-2-yloxy)benzene **(8)***

Precursor **7** (8.0 g, 0.01 mol, 1 equiv.) was dissolved in EtOH (400 mL) under N_2 atmosphere. Subsequently, sodium diethyldithiocarbamate trihydrate salt (4.4 g, 0.02 mol, 2.3 equiv.) was added. The mixture was stirred for 3 h at ambient temperature after which H_2O was added. The product was extracted with $CHCl_3$. The organic phase was dried over anhydrous $MgSO_4$ and the solvent was evaporated. The crude product was purified by column chromatography (SiO_2, eluent diethyl ether/methanol 9/1) to obtain the pure product **8** as a clear yellow oil (5.0 g, 51%). ^{1}H NMR ($CDCl_3$): δ = 7.10 (s, 2H, ArH), 4.47 (s, 4H, CH_2S), 4.42–4.36 (m, 2H, OCH), 4.02–3.92 (m, 4H, CH_2N), 3.70–3.52 (m, 52H, OCH_2 and CH_2N), 3.50–3.45 (m, 8H, OCH_2), 3.32 (s, 12H, OCH_3), 1.20 (t, 12H, CH_3); ^{13}C NMR ($CDCl_3$): δ = 195.5, 150.0, 126.0, 117.2, 78.9, 71.6, 70.5, 58.8, 49.5, 46.5, 36.5, 12.5, 11.0; MS (CI, m/z): 1166 $[M+1]^+$.

2.3. Synthesis of Precursor Polymers

*MTEMP precursor polymer **(9)***

Premonomer **5** (250 mg, 0.31 mmol, 1 equiv.) was dissolved in dry THF (15.3 mL, 0.02 M). The mixture was stirred at 35 °C under a continuous flow of N_2. Subsequently, a LHMDS solution (0.5 mL, 1 M in THF, 1.5 equiv.) was added in

one go to the stirred monomer solution. The reaction proceeded for 1.5 h at 35 °C under a nitrogen atmosphere, and the mixture was subsequently quenched in ice water (50 mL). The excess of base was neutralized with HCl (1 M). The aqueous phase was extracted with $CHCl_3$ (3 x 20 mL). After combination of the organic phases and evaporation of the solvent, the crude polymer was obtained. Since this mixture still contained monomers and oligomers, no NMR or mass analysis was performed at this stage. Purification was executed after thermal conversion to the conjugated polymer only.

*BTEMP precursor polymer **(11)***

Premonomer **8** (250 mg, 0.22 mol, 1 equiv.) was dissolved in dry THF (10.8 mL, 0.02 M). The mixture was stirred at 35 °C under a continuous flow of N_2. Subsequently, a LHMDS solution (0.3 ml, 1 M in THF, 1.5 equiv.) was added in one go to the stirred monomer solution. The reaction proceeded for 1.5 h at 35 °C under a nitrogen atmosphere, and the mixture was subsequently quenched in ice water (50 mL). The excess of base was neutralized with HCl (1 M). The aqueous phase was extracted with $CHCl_3$ (3 x 20 mL). After combination of the organic phases and evaporation of the solvent, the crude polymer was obtained. Since this mixture still contained monomers and oligomers, no NMR or mass analysis was performed at this stage. Purification was executed after thermal conversion to the conjugated polymer only.

2.4. Thermal Elimination of Precursor Polymer to Conjugated Polymer

*Poly(2-methoxy-5-(1,3-bis(2-(2-(2-methoxyethoxy)ethoxy)ethoxy)propan-2-yloxy)-1,4-phenylene vinylene) (MTEMP-PPV) **(10)***

A solution of precursor polymer **9** (204 mg) in 1,2-dichlorobenzene (100 mL) was degassed for 1 h by passing through a continuous stream of nitrogen. The solution was heated to 180 °C and stirred for 3 h in a dark environment. After cooling to room temperature, the resulting 1,2-dichlorobenzene was evaporated and the crude polymer mixture was dissolved in $CHCl_3$ (2 mL). The solution was precipitated drop wise in cold cyclohexane (100 mL). The

polymer was filtered off, washed with cold cyclohexane and dried at room temperature under reduced pressure. The conjugated polymer MTEMP-PPV **10** was obtained as a red polymer. The elimination procedure was performed a second time to ensure complete elimination. Yield (combined polymerization and conversion): 50%. ^{1}H NMR ($CDCl_3$): δ = 7.50–7.30 (br d, 2H, CHCH) 7.20–7.00 (br s, 2H, ArH) 4.60–4.40 (br m, 1H, OCH), 4.00–3.85 (br s, 3H, OCH_3), 3.80–3.40 (br m; 28H, OCH_2), 3.40–3.20 (br s, 6H, OCH_3); ^{13}C NMR ($CDCl_3$): δ = 153.2, 151.0, 129.8, 127.8, 125.0, 116.5, 109.6, 80.1, 72.2, 71.2, 59.8, 56.5; IR (NaCl, cm^{-1}): 3059, 2923, 2871, 1503, 1467, 1411, 1352, 1256, 1201, 1109, 1031, 976, 858, 799; UV-vis ($CHCl_3$): λ_{max} = 487 nm; SEC (THF): M_w = 248 ×10^3 g/mol (PD = 3.8).

Poly(2,5-bis(1,3-bis(2-(2-(2-methoxyethoxy)ethoxy)ethoxy)propan-2-yloxy)-1,4-phenylene vinylene) (BTEMP-PPV) ***(12)***

A solution of precursor polymer **11** (120 mg) in 1,2-dichlorobenzene (60 mL) was degassed for 1 h by passing through a continuous stream of nitrogen. The solution was heated to 180 °C and stirred for 3 h in a dark environment. After cooling to room temperature, the resulting 1,2-dichlorobenzene was evaporated and the crude polymer mixture was dissolved in $CHCl_3$ (2 mL). The solution was precipitated drop wise in cold cyclohexane (100 mL). In some cases, the precipitate only formed after evaporation of $CHCl_3$. The polymer was filtered off, washed with cold cyclohexane and dried at room temperature under reduced pressure. The conjugated polymer BTEMP-PPV **12** was obtained as an orange polymer. The elimination procedure was performed a second time to ensure complete elimination. The polymer distribution was narrowed by size exclusion chromatography on Bio-Beads® (S-X1) with toluene as the solvent. Yield (combined polymerization and conversion): 50%. ^{1}H NMR ($CDCl_3$): δ = 7.40–7.30 (br d, 2H, CHCH) 7.20–7.00 (br s, 2H, ArH) 4.60–4.40 (br m, 2H, OCH), 3.80–3.40 (br m; 56H, OCH_2), 3.40–3.20 (br s, 12H, OCH_3); ^{13}C NMR ($CDCl_3$): δ = 151.0, 129.0, 124.0, 114.2, 78.9, 71.6, 70.5, 58.8; IR (NaCl, cm^{-1}): 3059, 2959, 2922, 2871, 1503, 1455,

1415, 1352, 1260, 1197, 1105, 1028, 972, 850, 799; UV-vis ($CHCl_3$): λ_{max} = 463 nm; SEC (THF): M_w = 113 $\times 10^3$ g/mol (PD = 5.5).

3. Results and Discussion

3.1. Premonomer Synthesis

The synthetic route towards the MTEMP and BTEMP bisdithiocarbamate premonomers is outlined in Scheme 1. In a first step, the branched side chain 1,3-bis(triethoxymethoxy)propan-2-ol **1** was prepared starting from tri(ethylene glycol) monomethyl ether and epichlorohydrine. Subsequently, the hydroxyl group of **1** was converted to the corresponding tosylate derivative **2**, which was then coupled to 4-methoxyphenol or to hydroquinone using a Williamson etherification reaction, affording the mono- and bis-substituted derivatives **3** and **6**, respectively. The functionalized benzene moiety of derivatives **3** and **6** was chloromethylated using concentrated HCl and formaldehyde in acetic anhydride yielding precursors **4** and **7**. In a final step, derivatives **4** and **7** were dissolved in ethanol and solid sodium diethyldithiocarbamate trihydrate was added to obtain the bisdithiocarbamate MTEMP premonomer **5** and BTEMP premonomer **8**.

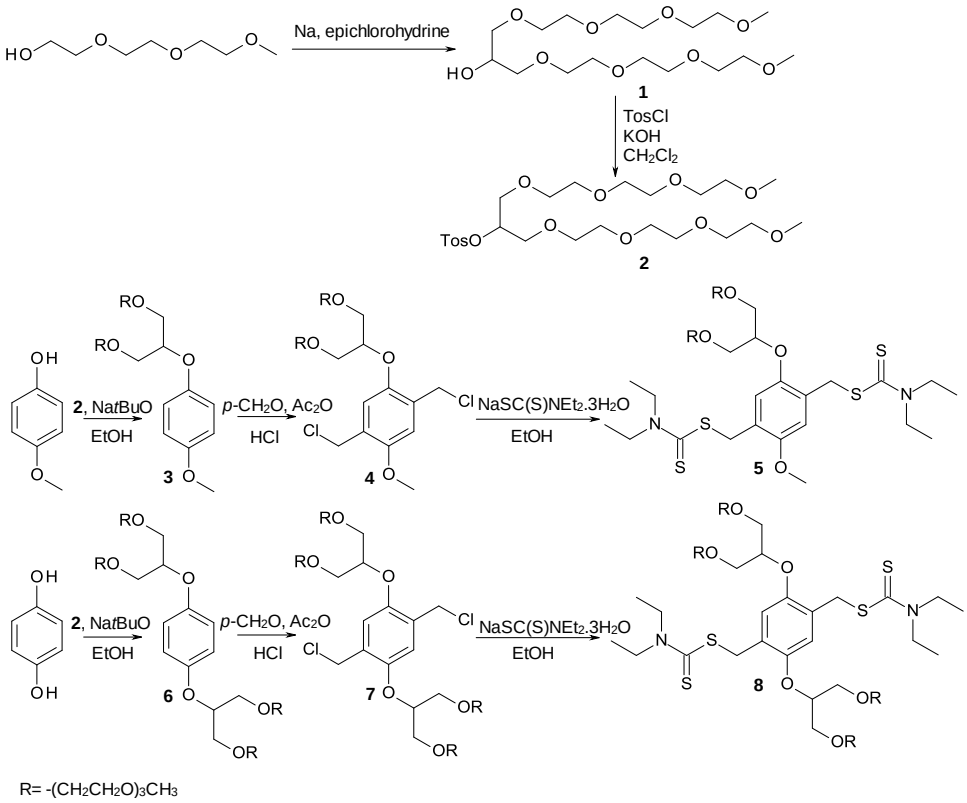

Scheme 1. Synthesis of MTEMP (**5**) and BTEMP (**8**) premonomers.

3.2. Polymerization

The dithiocarbamate precursor route is based upon the polymerization behavior of *p*-quinodimethane systems (Scheme 2). A premonomer bearing a polarizer and a leaving group is converted into the real monomer, a *p*-quinodimethane system, via addition of a proper base. In this study, the bisdithiocarbamate MTEMP and BTEMP premonomers **5** and **8** were both dissolved in dry THF and lithium hexamethyldisilazide (LHMDS) was added as a base (Scheme 3). The real monomers then polymerized via a self-initiating radical pathway into the MTEMP and BTEMP precursor polymers [39–43]. After work-up, the crude precursor polymers **9** and **11** could be converted into their corresponding conjugated equivalents.

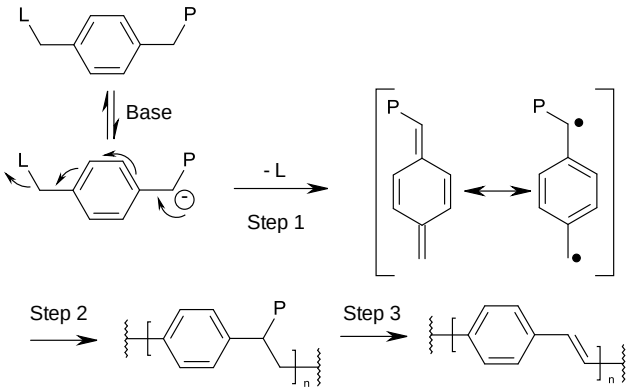

Scheme 2. Dithiocarbamate precursor route towards poly(*p*-phenylene vinylene) derivatives.

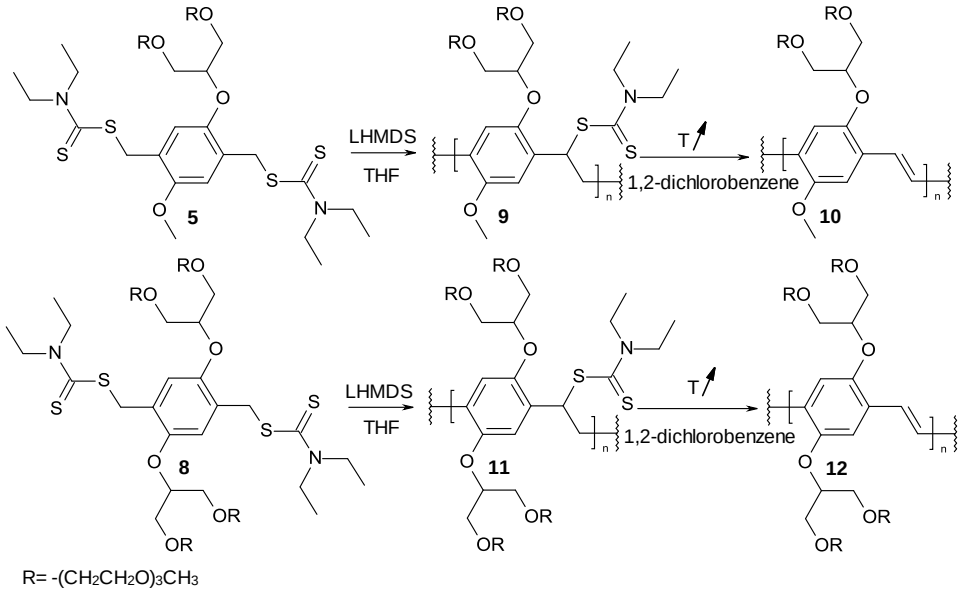

Scheme 3. Synthesis of MTEMP-PPV (**10**) and BTEMP-PPV (**12**) via the dithiocarbamate precursor route.

3.3. Conversion

The dithiocarbamate MTEMP and BTEMP precursor polymers were converted into conjugated materials via thermal elimination. Upon heating, the dithiocarbamate groups of precursor polymers **9** and **11** were eliminated to form the corresponding conjugated polymers MTEMP-PPV **10** and BTEMP-PPV **12**. To perform the elimination reaction, the MTEMP and BTEMP precursor polymers were dissolved in 1,2-dichlorobenzene and subjected to 180 °C for 3 h. The polymers were isolated via precipitation in cold cyclohexane. Molecular weights were determined by analytical size exclusion chromatography (SEC) (MTEMP-PPV: M_w = 248 x10^3 g/mol, PD = 3.8 and BTEMP-PPV: M_w = 113 x10^3 g/mol, PD = 5.5) (Fig. 1). Initially, for BTEMP-PPV a very high polydispersity (PD = 16) was observed, indicating the presence of an oligomeric fraction. To separate the polymer from the oligomeric fraction, size exclusion chromatography on Bio-Beads® (S-X1) was performed with toluene as the solvent. In this way the polydispersity could be reduced to a value of 5.5.

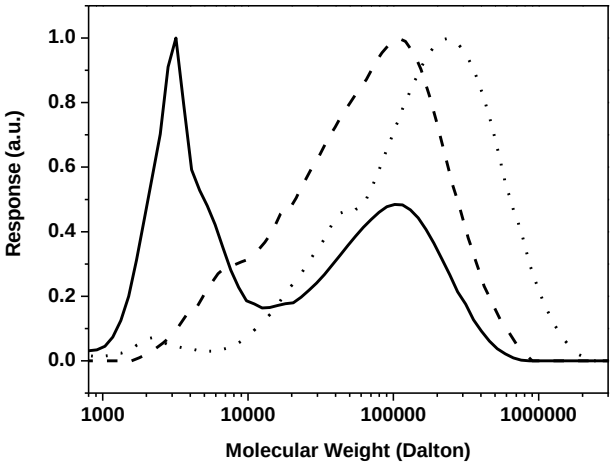

Fig. 1. Overlay of SEC chromatograms of BTEMP-PPV initially (solid line), BTEMP-PPV after separation on Bio-Beads® (S-X1) (dashed line) and MTEMP-PPV (dotted line).

3.4. Optical Characterization

To study the solubility and UV-vis absorption characteristics of MTEMP-PPV and BTEMP-PPV, both polymers were dissolved in a range of solvents with varying polarities [44]. For the UV-vis measurements, solutions with a diluted concentration of 5×10^{-5} M were prepared in order to avoid saturation of the UV-vis detector. The solution absorption maxima (λ_{max}) for both polymers were compared to the values obtained for MDMO-PPV, which acted as a reference material. From Table 1 it can be concluded that BTEMP-PPV is completely soluble in almost any solvent, except for the very apolar hexane. MTEMP-PPV is insoluble in highly polar solvents. However, solutions could still easily be obtained in moderately polar solvents such as DMSO. The solution absorption maxima for BTEMP-PPV range from 463 to 473 nm, while for MTEMP-PPV λ_{max} varies from 485 to 500 nm (Fig. 2). These values are somewhat lower than the λ_{max} values for MDMO-PPV (505 to 512 nm), indicating that the bulky oligo(ethylene glycol) side chains likely induce a twist in the polymer backbone, thereby decreasing the effective conjugation length. This effect is more pronounced for BTEMP-PPV than for MTEMP-PPV. The solubility study shows that for both polymers solutions of 30 mg/mL or more could easily be prepared in environment-friendly solvents such as DMSO and acetone. The symmetrically substituted BTEMP-PPV is even soluble in alcohols and water (≥ 30mg/mL). These observations open new perspectives for ecological processing and “green” device fabrication.

Table 1

Overview of UV-vis absorption maxima of BTEMP-PPV, MTEMP-PPV and MDMO-PPV in different solvents.

Solvent[a]	Polarity (E_T^N)	BTEMP-PPV λ_{max} (nm)	MTEMP-PPV λ_{max} (nm)	MDMO-PPV λ_{max} (nm)
water	1	464	/	/
methanol	0.762	465	/	/
ethanol	0.654	466	/	/
acetic acid	0.648	464	485	/
2-propanol	0.546	466	/	/
acetonitrile	0.460	464	491	/
DMSO	0.444	473	500	/
acetic anhydride	0.407	466	493	/
DMF	0.404	469	488	/
acetone	0.355	468	495	/
dichloromethane	0.309	464	488	505
chloroform	0.259	463	487	505
ethyl acetate	0.228	465	495	/
THF	0.207	466	488	506
chlorobenzene	0.188	467	488	512
1,4-dioxane	0.164	466	485	512
diethyl ether	0.117	463	/	/
toluene	0.099	466	489	509
hexane	0.009	/	/	/

[a] Solvents in bold are determined as environmentally friendly solvents, according to the United States Environmental Protection Agency (EPA).

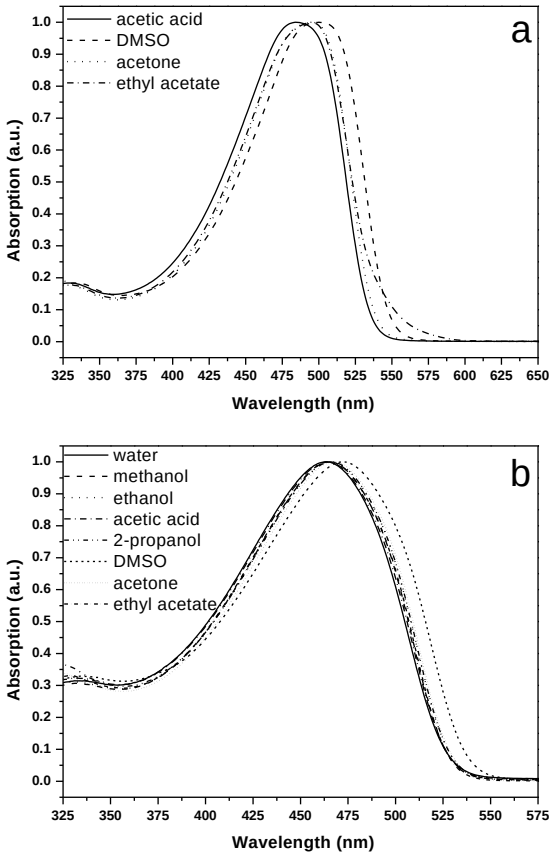

Fig. 2. Normalized UV-vis absorption spectra of a) MTEMP-PPV and b) BTEMP-PPV in environmentally friendly solvents.

3.5. Electrical Characterization

To gain more insight in the effect of the side chains on the electrical properties of the materials, an attempt to determine the relative permittivity (ε_r) and hole mobility (μ_h) with impedance spectroscopy and space charge limited current (SCLC) measurements was executed. Unfortunately no meaningful results could be obtained for BTEMP-PPV due to the extremely high film roughness and the presence of large local thickness variations in the obtained thin films, which were spincoated from chlorobenzene (Fig. 3). Poor film quality might also be the reason for the low hole mobility of MTEMP-PPV (μ_h= $2x10^{-13}$ m^2/Vs) compared to MDMO-PPV (μ_h=

$1x10^{-10}$ m^2/Vs), despite the fact that their identical backbones suggest a comparable value. Previous studies on oligo(ethylene oxide) substituted PPV derivatives yielded comparable hole mobilities for the PEO-PPV as for MDMO-PPV [45,46]. This indicates that after optimization of the active layer in hole-only devices, also for BTEMP-PPV and MTEMP-PPV similar hole mobilities, as compared to MDMO-PPV, should be obtained.

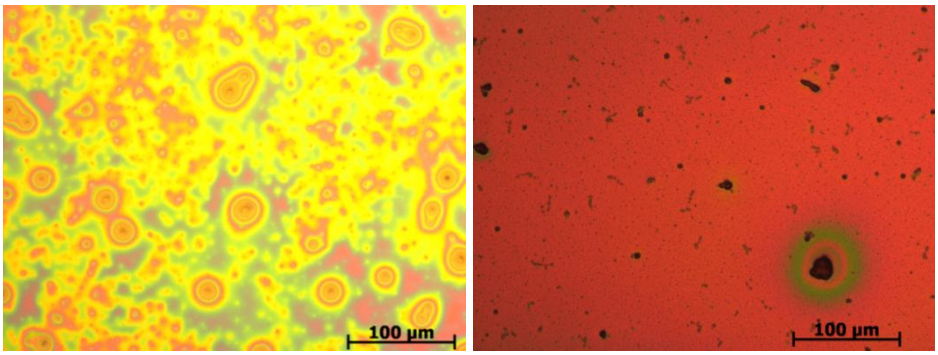

Fig. 3. Optical microscopy images of a thin film layer of BTEMP-PPV (left) and MTEMP-PPV (right), spincoated at 500 rpm from a 3 wt% solution in chlorobenzene onto a ITO coated glass substrate. Film thickness: 200 nm (±50 nm). Magnification: 20x.

In a recent paper of Xu et al, the effects of the solvent polarity on the chain conformation of a similar PEO substituted PPV derivative and the effects on the resulting film morphology have been thoroughly studied [47]. It was shown that, depending on the polarity of the solvent, the ethylene glycol substituted PPV adopted different chain conformations: an extended chain conformation in chloroform, a coiled chain conformation in methanol and a collapsed chain conformation in water. When these solutions were transferred into thin films, the polymer chains aggregated and formed closely packed structures, without changing their conformation. This resulted in different film morphologies with different roughness and domain sizes. Therefore, in order to optimize the film morphology of BTEMP-PPV and MTEMP-PPV, elaborate studies on the effects of the different solvents on the

thin film properties will have to be executed. This is subject of further research.

Despite the fact of an inferior film morphology, still some very promising results could be obtained for MTEMP-PPV. The side chains have a large influence on the relative permittivity, which is doubled for MTEMP-PPV (ε_r= 6.4) compared to MDMO-PPV (ε_r= 3.1). This indicates that MTEMP-PPV is a promising material to implement in optoelectronic devices since ε_r has a major influence on the dissociation characteristics of electron-hole pairs in organic solar cells [48]. In a previous study it was already shown that, even with a lower hole mobility as compared to MDMO-PPV, the charge dissociation in blends with fullerenes was increased by using a high permittivity PPV [45]. Furthermore, also the separation distance and the decay rate were improved.

To this end, a first environment-friendly photovoltaic bilayer device was prepared for which MTEMP-PPV was spincoated from acetone. Vacuum deposited C_{60} was used as the acceptor layer. To create a larger contact area between the donor and acceptor layer, the devices were annealed for 10 min at 150 °C [49]. The device was not optimized for a maximal photovoltaic efficiency. The I-V characteristics are plotted in Fig. 4.

A clear photovoltaic effect was observed, with an overall solar-energy-conversion efficiency of 0.04%. Although the achieved efficiency is low, it is clearly demonstrated that environment-friendly processed solar cells can be fabricated, whereby the donor polymer can be spincoated from harmless solvents such as acetone. Further optimization of the film formation properties of both MTEMP-PPV and BTEMP-PPV, as well as the development of suitable polar fullerene derivatives [50], can possibly lead to fully water based bulk heterojunction solar cells and a substantial increase in solar power conversion efficiencies.

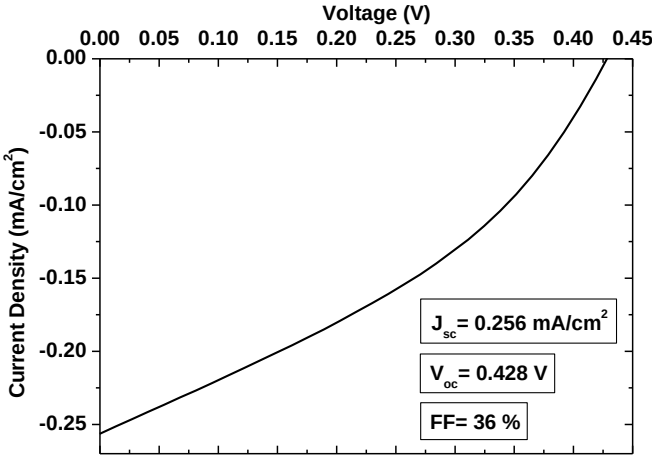

Fig. 4. Current-voltage characteristics obtained for an environment-friendly processed bilayer MTEMP-PPV:C_{60} solar cell under AM 1.5 illumination.

4. Conclusions

The synthesis of highly polar BTEMP-PPV and MTEMP-PPV via the dithiocarbamate route has been demonstrated. Solubility tests have shown that these polymers are soluble in a broad variety of "green" solvents, such as alcohols and water. Impedance spectroscopy revealed a higher relative permittivity for MTEMP-PPV as compared to MDMO-PPV. On the other hand, SCLC measurements showed a reduced hole mobility due to the roughness and heterogeneity of the obtained thin films. As a proof-of-concept, a solar cell device with MTEMP-PPV as donor material has been processed from acetone. Although film formation optimization is still required and will be subject of further studies, these materials clearly show potential in the development of sustainable optoelectronic devices.

5. Acknowledgments

The authors gratefully acknowledge the Fund for Scientific Research-Flanders (FWO) and the Belgian Science Policy (BELSPO) in the frame of network IAP P6/27, initiated by the Belgian State Prime Minister's Office, for the financial support. We also thank the Institute for the Promotion of Innovation through

Science and Technology in Flanders (IWT) for financial support via the IWT-SBO project 060843 “Polyspec”.

6. References

(1) Gaylord BS, Heeger AJ, Bazan GC. J Am Chem Soc 2003;125:896–900.

(2) Liu B, Bazan GC. J Am Chem Soc 2004;126:1942–1943.

(3) Nilsson KPR, Herland A, Hammarstrom P, Inganas O. Biochemistry 2005;44:3718–3724.

(4) McQuade DT, Pullen AE, Swager TM. Chem Rev 2000;100:2537–2574.

(5) Hoven CV, Garcia A, Bazan GC, Nguyen TQ. Adv Mater 2008;20:3793–3810.

(6) Huang F, Wu HB, Wang D, Yang W, Cao Y. Chem Mater 2004;16:708–716.

(7) Mikroyannidis JA, Barberis VP, Cimrova VJ. Polym Sci, Part A: Polym Chem 2007;45:1016–1027.

(8) Wu HB, Huang F, Mo YQ, Yang W, Wang DL, Peng JB, Cao Y. Adv Mater 2004;16:1826–1830.

(9) Ma WL, Iyer PK, Gong X, Liu B, Moses D, Bazan GC, Heeger AJ. Adv Mater 2005;17:274–277.

(10) Yang RQ, Wu HB, Cao Y, Bazan GC. J Am Chem Soc 2006;128:14422–14423.

(11) Garcia A, Yang R, Jin Y, Walker B, Nguyen TQ. Appl Phys Lett 2007;91:153502.

(12) Hoven C, Yang R, Garcia A, Heeger AJ, Nguyen TQ, Bazan GC. J Am Chem Soc 2007;129:10976–10977.

(13) Cimrova V, Schmidt W, Rulkens R, Schulze M, Meyer W, Neher D. Adv Mater 1996;8:585–588.

(14) Edman L, Pauchard M, Liu B, Bazan G, Moses D, Heeger AJ. Appl Phys Lett 2003;82:3961–3963.

(15) Cheng CHW, Boettcher SW, Johnston DH, Lonergan MC. J Am Chem Soc 2004;126:8666–8667.

(16) Kawai T, Yamaue T, Onoda M, Yoshino K. Synth Met 1999;102:971–972.

(17) Yang JH, Garcia A, Nguyen TQ. Appl Phys Lett 2007;90:103514.

(18) Lee W, Mane RS, Min SK, Yoon TH, Han SH, Lee SH. Appl Phys Lett 2007;90:263503.

(19) Holder E, Tessler N, Rogach A. J Mater Chem 2008;18:1064–1078.

(20) Peng Z, Xu B, Zhang J, Pan Y. Chem Commun 1999;1855–1856.

(21) Balanda PB, Ramey MB, Reynolds JR. Macromolecules 1999;32:3970–3978.

(22) Levitsky IA, Kim J, Swager TM. J Am Chem Soc 1999;121:1466–1472.

(23) Liu B, Yu WL, Lai YH, Huang W. Chem Commun 2000;551–552.

(24) Patil AO, Ikenoue Y, Wudl F, Heeger AJ. J Am Chem Soc 1987;109:1858–1859.

(25) Tan CY, Pinto MR, Kose ME, Ghiviriga I, Schanze KS. Adv Mater 2004;16:1208–1212.

(26) Shi S, Wudl F. Macromolecules 1990;23:2119–2124.

(27) Fujii A, Sonoda T, Fujisawa T, Ootake R, Yoshino K. Synth Met 2001;119:189–190.

(28) Cheng F, Zhang GW, Lu XM, Huang YQ, Chen Y, Zhou Y, Fan QL, Huang W. Macromol Rapid Comm 2006;27:799–803.

(29) Zhang B, Lin H, Tang J, Liu JS. Chinese Sci Bull 2009;54:3515–3520.

(30) Khan A, Müller S, Hecht S. Chem Commun 2005;584–586.

(31) Kim KN, Kwon YW, Choi DH, Jin JI. Macromol Chem Physic 2009;210:1372–1378.

(32) Anslyn EV, Dougherty DA. Modern Physical Organic Chemistry. University Science Books, Sausalito, California, 2006, p.163–180.

(33) Henckens A, Lutsen L, Vanderzande D, Knipper M, Manca J, Aernouts T, Poortmans J. SPIE Proc 2004;52–59.

(34) Henckens A, Colladet K, Fourier S, Cleij TJ, Lutsen L, Gelan J. Macromolecules 2005;38:19–26.

(35) Henckens A, Duyssens I, Lutsen L, Vanderzande D, Cleij TJ. Polymer 2006;47:123–131.

(36) Vandenbergh J, Wouters J, Adriaensens PJ, Mens R, Cleij TJ, Lutsen L, Vanderzande DJM. Macromolecules 2009;42:3661–3668.

(37) Breselge M, Van Severen I, Lutsen L, Adriaensens P, Manca J, Vanderzande D, Cleij T. Thin Solid Films 2006;511–512:328–332.

(38) Blom PWM, Tanase C, de Leeuw DM, Coehoorn R. Appl Phys Lett 2005;86:092105.

(39) Issaris A, Vanderzande D, Gelan J. Polymer 1997;38:2571–2574.

(40) Hontis L, Vrindts V, Lutsen L, Vanderzande D, Gelan J. Polymer 2001;42:5793–5796.

(41) Hontis L, Vrindts V, Vanderzande D, Lutsen L. Macromolecules 2003;36:3035–3044.

(42) Wiesecke J, Rehahn M. Angew Chem, Int Ed 2003;42:567–570.

(43) Schwalm T, Wiesecke J, Immel S, Rehahn M. Macromolecules 2007;40:8842–8854.

(44) Reichardt C. Solvents and Solvent Effects in Organic Chemistry, 2nd ed. Weinheim: VCH, 1990, pp. 408–410.

(45) Lenes M, Kooistra FB, Hummelen JC, Van Severen I, Lutsen L, Vanderzande D, Cleij TJ, Blom PWM. J Appl Phys 2008;104:114517.

(46) Van Severen I, Breselge M, Fourier S, Adriaensens P, Manca J, Lutsen L, Cleij TJ, Vanderzande D. Macromol Chem Physic 2007;208:196–206.

(47) Xu Z, Tsai H, Wang H-L, Cotlet M. J Phys Chem B 2010;114:11746–11752.

(48) Michailetchi VD, Koster LJA, Blom PWM, Melzer C, de Boer B, van Duren JKJ, Janssen RAJ. Adv Funct Mat 2005;15:795–801.

(49) Drees M, Premaratne K, Graupner W, Heflin JR, Davis RM, Marciu D, Miller M. Appl Phys Lett 2002;81:4607–4609.

(50) Lu FS, Li YL, Liu HB, Zhuang JP, Gan LB, Zhu DB. Synth Met 2005;153:317–320.

Chapter 5

Tetra-alkoxy Substituted PPV Derivatives: A New Class of Highly Soluble Liquid Crystalline Conjugated Polymers

ABSTRACT: Two first examples of highly soluble tetra-alkoxy substituted PPV derivatives, poly(2,3,5,6-tetrahexyloxy-1,4-phenylene vinylene) (TH-PPV) and poly[2,3,5,6-tetra(2'-ethyl-hexyloxy)-1,4-phenylene vinylene] TEH-PPV, are presented. Both polymers have been fully characterized and the solubility and UV-vis absorption characteristics have been studied in various organic solvents. Due to the symmetric nature of the repeating unit, TH-PPV and TEH-PPV have an inherently regioregular nature, which is unusual for PPV-type polymers. Observations from polarized light microscopy and differential scanning calorimetry indicate that TH-PPV exhibits thermally induced order resulting in a liquid crystalline mesophase. In contrast, due to steric hindrance of the branched alkyl side chains, TEH-PPV is rather disordered. As a first demonstration of the charge transporting properties of TH-PPV, a simple solution processed electroluminescent device has been prepared. The electroluminescence spectrum shows a detailed structure similar to that observed from the solid-state photoluminescence spectrum and shows one of the highest energy emission observed for PPVs. It is speculated that the enhanced order in TH-PPV will benefit the usage of this new class of polymers in optoelectronic applications, in which improved charge carrier mobility is desirable.

*Vandenbergh, J.; Van Severen, I.; Lutsen, L.; Adriaensens, P.; Bolink, H. J.; Cleij, T. J.; Vanderzande, D. *Polymer Chemistry*, **2011**, *2*, DOI:10.1039/C1PY00027F.

1. Introduction

Poly(*p*-phenylene vinylene) (PPV) and related polymers exhibit numerous attractive optical and electronic properties, which make them interesting candidates for applications such as organic light emitting diodes (OLEDs), organic field effect transistors (OFETs), (bio)sensors and photovoltaic cells.[1–5] For the successful integration of PPV-type polymers in devices, it is often of considerable importance to obtain a well defined, ordered morphology of the active layer.[6–8] Potentially, this can be achieved by using polymeric materials, which exhibit ordering phenomena. However, the 2,5-substituted structure of commonly used PPV derivatives, *i.e.* OC_1C_{10}-PPV and MEH-PPV, has been originally designed to minimize aggregation phenomena, which usually result in a lowering of the luminescent quantum yields in thin films. For example, while successfully optimizing the electroluminescence, only moderate charge carrier mobilities have been reported for these polymers.[7] Hence, considerable interest exists in the development of novel PPV-type polymers, which display enhanced stacking and ordering phenomena. To this end, various approaches have been presented in the literature. Examples include the introduction of linear side chains,[7–9] the introduction of regioregularity[6,10] as well as the introduction of chiral substituents.[11,12] Although indeed notable improvements have been observed for most of these modified PPV derivatives, the quest for even further improved PPV derivatives continues. Especially novel PPV derivatives, which combine ordering phenomena and straightforward accessibility, are of considerable interest.

Remarkably, all of the previously mentioned approaches towards novel PPV-type materials focus on 2,5-dialkoxy substituted PPV derivatives. This is a result of the synthetic accessibility of this class of materials for the past decades.[13] In contrast, thus far interest in the synthesis and optoelectronic properties of tetra-alkoxy substituted PPV derivatives has been rather limited. This is surprising, since they have an inherently regioregular nature and potentially have a favorable geometry for intra- and intermolecular ordering phenomena. Whereas soluble trialkoxyalkyl substituted PPV

derivatives have been reported,[14] tetra-alkoxy PPV derivatives remain mostly elusive. Hitherto, only one tetra-alkoxy PPV derivative has been reported in the literature, *i.e.* poly(2,3,5,6-tetramethoxy-1,4-phenylene vinylene) (TM-PPV).[15–17] This polymer contains the readily accessible tetramethoxybenzene structure. Furthermore, a number of copolymers containing this structural unit have been prepared.[15,18,19] Both TM-PPV and the copolymers were found to have unusual optical and electronic properties. However, the obtained conjugated polymers were in all cases completely insoluble, which impedes not only a full characterization, but also hampers their purification and processability towards applications. Hence, our attention focused on the development of a novel and versatile route towards soluble tetra-alkoxy substituted PPV derivatives.

Here we present such a route as well as the synthesis and full characterization of the first two examples of highly soluble tetra-alkoxy substituted PPV derivatives, *i.e.* poly(2,3,5,6-tetrahexyloxy-1,4-phenylene vinylene) (TH-PPV) and poly[2,3,5,6-tetra(2'-ethyl-hexyloxy)-1,4-phenylene vinylene] (TEH-PPV). In addition, the solubility and UV-vis absorption characteristics of TH-PPV and TEH-PPV in various solvents with different polarities have been studied. Observations from polarized light microscopy (PLM) and differential scanning calorimetry (DSC) indicate that TH-PPV exhibits thermally induced order, resulting in an ordered liquid crystalline mesophase. This confirms our assumption that the tetra-alkoxy substitution pattern indeed can give rise to desirable ordering phenomena. However, due to steric hindrance of the branched alkyl side chains, the second polymer, *i.e.* TEH-PPV, has a comparatively lower molecular weight and remains rather disordered. Finally, the first data on the application and optoelectronic characterization of TH-PPV in a P-LED device will be presented.

2. Experimental Section

2.1. General

NMR spectra were recorded with a Varian Inova Spectrometer (^{1}H-NMR 300 MHz, ^{13}C-NMR 75 MHz). Analytical Size Exclusion Chromatography (SEC)

(eluent THF, flow rate 1.0 mL/min) was performed using a Spectra series P100 pump equipped with a pre-column and two mixed-B columns (Polymer Labs) and a Refractive Index (RI) detector (Shodex) at 40 °C. Molecular weight distributions are given relative to polystyrene standards. GC-MS data were obtained with a Varian TSQ 3400 Gas Chromatograph and a TSQ 700 Finnigan Mat mass spectrometer. Direct insertion probe pyrolysis mass spectrometry (DIP-MS) analysis was carried out on a Finnigan TSQ 70 (EI; mass range 35-500; heating rate 10 °C/min; electron energy 70 eV). TGA analysis was carried out on a TA Instruments 951 (heating rate 20 °C/min, Ar atmosphere). FT-IR spectra were collected with a Perkin Elmer Spectrum One spectrometer. Fluorescence spectra were collected on a Perkin Elmer LS-5B luminescence spectrometer. UV-vis measurements were performed on a Cary 500 UV-vis-NIR spectrophotometer (scan rate 600 nm/min). Elemental analysis was performed with a Flash EA 1112 Series CHNS-O analyzer. DSC measurements were carried out on a DSC 910-2000 analyzer (temperature program -100 °C to 200 °C; heating rate 10 °C/min, N_2 atmosphere). The second heating curves were evaluated. Polarized Light Microscopy (PLM) observations were made with a Nikon 144040 polarization microscope equipped with a Linkam temperature-controlled stage. Thin films were drop-casted from $CHCl_3$ solutions on glass substrates, made apolar by treatment with trimethylsilyl chloride. The thin-film quantum yield measurements were performed in a nitrogen environment and determined on a thin film (100 nm) using the quantum yield measurement system from Hamamatsu, model C9920-01, equipped with an integrated sphere.

2.2. Synthesis

All chemicals were purchased from Aldrich or Acros and used without further purification. 1,4-Dioxane was distilled from sodium/benzophenone.

1,2,4,5-Tetrahexyloxybenzene (1) (Scheme 1).

1,2,4,5-tetrahydroxybenzene was generated quantitatively by in situ hydrogenation of 2,5-dihydroxy-1,4-benzoquinone (5.2 g, 37 mmol) in dry

DMF (1220 mL) at atmospheric pressure (p_{H2}= 1 atm.) with PtO_2 (40 mg) as a catalyst according to an adapted literature procedure.[20,21] Subsequently 1-bromohexane (27.0 g, 163.0 mmol) and cesium carbonate (72.4 g, 222.3 mmol) were added. The reaction mixture was stirred for 6 days at 65 °C. After cooling to room temperature DMF was removed under reduced pressure and CH_2Cl_2 (600 mL) was added. The reaction mixture was washed with H_2O (3 x 100 mL), after which the organic extracts were dried over $MgSO_4$ and concentrated under reduced pressure to yield crude **1** as a brown solid, which was recrystallized twice from MeOH giving 13.9 g (78% yield) white crystalline **1**.

^{1}H NMR (300 MHz, $CDCl_3$, δ): 6.55 (s, 2H, Ar H), 3.91 (t, J= 5.7 Hz, 8H, OCH_2), 1.74 (m, 8H, CH_2), 1.43 (m, 8H, CH_2), 1.30 (m, 16H, CH_2), 0.89 (t, J= 7.1 Hz, 12H, CH_3); ^{13}C NMR (75 MHz, $CDCl_3$, δ):143.4, 105.4, 70.4, 31.5, 29.4, 25.6, 22.5, 13.9; EIMS (*m*/*z* (%)): 478 [M^+], 394, 309, 225, 141.

1,2,4,5-Tetra(2'-ethyl-hexyloxy)benzene (2).

Using a similar procedure as described for **1**, first 1,2,4,5-tetrahydroxybenzene was generated quantitatively by the *in situ* hydrogenation of 2,5-dihydroxy-1,4-benzoquinone (5.2 g, 37 mmol). Subsequently 1-bromo-2-ethylhexane (31.5 g, 163 mmol) and cesium carbonate (72.4 g, 222.3 mmol) were added, giving after reaction workup and column chromatography (SiO_2, eluent hexane/ethyl acetate 9/1) 12 g (55% yield) clear yellow oil **2**.

^{1}H NMR (300 MHz, $CDCl_3$, δ): 6.55 (s, 2H, Ar H), 3.80 (d, J= 5.7 Hz, 8H, OCH_2), 1.70 (m, 4H, CH), 1.43 (m, 16H, CH_2), 1.30 (m, 16H, CH_2), 0.91 (t, J= 7.3 Hz, 24H, CH_3); ^{13}C NMR (75 MHz, $CDCl_3$, δ): 143.5, 107.5, 53.5, 40.3, 30.5, 29.5, 24.0, 23.5, 14.5, 11.5; EIMS (*m*/*z* (%)):590 [M^+], 477, 363, 250, 141.

1,4-Bis-chloromethyl-2,3,5,6-tetrahexyloxybenzene (3).

To a stirred mixture of **1** (5.0 g, 10.4 mmol) and *p*-formaldehyde (3.1 g, 104 mmol) at 0 °C, concentrated HCl (9.6 mL, 114.8 mmol) was added dropwise under N_2 atmosphere. Subsequently, acetic anhydride (19.6 mL, 208.8 mmol)

was added. After addition was complete, the resulting solution was stirred at 95 °C for 6 days after which it was cooled down and poured into water (100 mL). The reaction mixture was extracted with CH_2Cl_2 (3 x 100 mL) and dried over $MgSO_4$. Evaporation of the solvent gave the crude product. The pure product was obtained by column chromatography (SiO_2, eluent hexane/ethyl acetate 95/5) as a white solid (4.1 g, 68 % yield).

^{1}H NMR (300 MHz, $CDCl_3$, δ): 4.65 (s, 4H, CH_2Cl), 4.02 (t, J= 6.6 Hz, 8H, OCH_2), 1.78 (m, 8H, CH_2), 1.48 (m, 8H, CH_2), 1.30 (m, 16H, CH_2), 0.89 (t, J= 7.1 Hz, 12H, CH_3); ^{13}C NMR (75 MHz, $CDCl_3$, δ): 147.0, 126.9, 73.8, 35.6, 31.5, 30.1, 25.5, 22.5, 13.9; EIMS (*m*/*z* (%)): 574 [M^+], 539 [M^+ - Cl], 492 [M^+ - 2 Cl-CH_2], 456, 370.

1,4-Bis-chloromethyl-2,3,5,6-tetra(2'-ethyl-hexyloxy)benzene (4).

Using a similar procedure as described for **3**, compound **4** was prepared from **2** (12 g, 20.3 mmol), *p*-formaldehyde (6.1 g, 203 mmol), concentrated HCl (18.3 mL, 223 mmol) and acetic anhydride (38.4 mL, 406 mmol). After column chromatography (SiO_2, eluent hexane/ethyl acetate 99/1), **4** was obtained as a clear colorless oil (4.6 g, 33 % yield).

^{1}H NMR (300 MHz, $CDCl_3$, δ): 4.65 (s, 4H, CH_2Cl), 3.90 (d, J= 6.6 Hz, 8H, OCH_2), 1.80 (m, 4H, CH), 1.50 (m, 8H, CH_2), 1.42 (m, 8H, CH_2), 1.30 (m, 16H, CH_2), 0.89 (t, J= 7.3 Hz, 24H, CH_3); ^{13}C NMR (75 MHz, $CDCl_3$, δ): 147.5, 127.5, 53.5, 40.3, 36.0, 30.5, 29.5, 24.0, 23.5, 14.5, 11.5; EIMS (*m*/*z* (%)): 687 [M^+], 574, 462, 350, 238, 202.

Poly(2,3,5,6-tetrahexyloxy-1,4-phenylenevinylene) (TH-PPV).

1.5 g (3.1 mmol) of **2** was dissolved in dry 1,4-dioxane (200 mL) under N_2 atmosphere. After heating to 96 °C, a solution of K*t*BuO (0.91 g, 8.1 mmol) in dry 1,4-dioxane (9 mL) was added dropwise while stirring. During this addition, the solution turned from colorless to white. After 5 min, a second solution of K*t*BuO (0.70 g, 6.2 mmol) in dry 1,4-dioxane (7 mL) was added at which the solution turned yellow. The polymerization was allowed to proceed for 3 h at 98 °C after which the total volume was reduced to 20 mL by

evaporation and the solution was precipitated dropwise in cold MeOH (200 mL). The resulting polymer was filtered off, washed with MeOH and dried under reduced pressure at room temperature giving TH-PPV as a yellow solid (702 mg, 55% yield).

^{1}H NMR (300 MHz, $CDCl_3$, δ): 7.8 (br d, 2H, CHCH), 3.9 (br t, 8H, OCH_2), 1.7 (br m, 8H, CH_2), 1.4 (br m, 8H, CH_2), 1.3 (br m, 16H, CH_2), 0.8 (br t, 12H, CH_3); ^{13}C NMR (75 MHz, $CDCl_3$, δ): 147.3, 126.2, 125.4, 73.3, 31.7, 30.3, 25.7, 22.5, 13.9; FT-IR (NaCl): 2955, 2859, 1445, 1378, 1301, 1266, 1121, 726 cm^{-1}; UV-Vis ($CHCl_3$) λ_{max} = 430 nm and (thin film) λ_{max}= 442 nm; SEC (THF) M_w = 4×10^5 g/mol (PD = M_w/M_n = 3.1) (73.4%) + 5×10^3 g/mol (PD = M_w/M_n = 1.3) (26.6%); Anal. calcd for $(C_{32}H_{54}O_4)_n$: C 76.5, H 10.8, O 12.7; found C 76.7, H 11.4, O 11.9.

Poly[2,3,5,6-tetra(2'-ethyl-hexyloxy)-1,4-phenylene vinylene] (TEH-PPV). Using a similar procedure as described for TH-PPV, TEH-PPV was prepared from 0.5 g (0.73 mmol) of **4** and K*t*BuO in two batches (total amount 0.382 g, 3.34 mmol). After polymerization and purification TEH-PPV was isolated as a yellow sticky oil (260 mg, 58% yield).

^{1}H NMR (300 MHz, $CDCl_3$, δ): 7.8 (br d, 2H, CHCH), 3.7 (br d, 8H, OCH_2), 1.7 (br m, 4H, CH), 1.4 (br m, 16H, CH_2), 1.3 (br m, 16H, CH_2), 0.8 (br t, 24H, CH_3); ^{13}C NMR (75 MHz, $CDCl_3$, δ): 147.3, 127.2, 125.4, 53.5, 40.2, 30.7, 29.3, 23.7, 13.9, 11.1; FT-IR (NaCl): 2960, 2929, 2873, 2858, 1445, 1378, 1295, 1260, 1117, 1046, 730 cm^{-1}; UV-Vis ($CHCl_3$): λ_{max}= 370 nm and (thin film) λ_{max}= 372 nm; SEC (THF) M_w = 2.2×10^4 g/mol (PD = M_w/M_n = 2.5) (64.9%) + 1×10^3 g/mol (PD = M_w/M_n = 1.1) (35.1%); Anal. calcd for $(C_{40}H_{70}O_4)_n$: C 78.1, H 11.5, O 10.4; found C 77.2, H 11.7, O 11.1.

2.3. Device Preparation and Characterization

Poly(3,4-ethylenedioxythiophene): polystyrenesulfonate (PEDOT:PSS) was purchased from HC-Starck and solvents used were obtained from Aldrich. Indium tin oxide (ITO)-coated glass plates obtained from Naranjo substrates were patterned using conventional photolithography. The substrates were

extensively cleaned using sonification in subsequently water-soap, water and 2-propanol baths. After drying, the substrates were placed in a UV-ozone cleaner for 20 min. The electroluminescent devices were prepared as follows. Transparent thin films of TH-PPV were obtained by spinning from toluene solutions using concentrations of 20 mg/mL at 2000 rpm for 40 seconds, resulting in a 110 nm thick film. Prior to the deposition of the emitting layer a 100 nm layer of PEDOT:PSS was deposited to increase the device preparation yield. The thickness of the films was determined using an Ambios XP1 profilometer. After spinning the organic layers, the samples were transferred to an inert atmosphere glovebox (< 0.1 ppm O_2 and H_2O, MBraun) and dried on a hot plate at 80 °C for 1 h. Barium and silver metal electrodes (5 and 80 nm, respectively) were thermally evaporated using a shadow mask under a vacuum (< 1×10^{-6} mbar) using an Edwards Auto500 evaporator integrated into an inert atmosphere glovebox. Current density and luminance *versus* voltage were measured using a Keithley 2400 source meter and a photodiode coupled to a Keithley 6485 pico-amperometer using a Minolta LS100 to calibrate the photocurrent. External quantum efficiencies (EQE) were determined using an integrated sphere coupled to an UDT instruments S370 Optometer.

3. Results and Discussion

3.1. Monomer and Polymer Synthesis

Key to the preparation of tetra-alkoxy substituted PPV-type polymers is a straightforward method to obtain the corresponding benzene derivatives in good yield. Previously, for the studies on TM-PPV the corresponding benzene derivative was prepared from benzoquinone in three steps.[22] However, this procedure gave unsatisfactory yields when attempted with larger alkoxy substituents. Fortunately, an elegant method has been presented in the literature to prepare benzenes with a 2,3,5,6-substitution patterns.[20,21] Using this method, the synthesis of 1,2,4,5-tetrahexyloxybenzene **1** and 1,2,4,5-tetra(2'-ethyl-hexyloxy)benzene **2** has been accomplished in a satisfactory

yield (78 % and 55 %, respectively) *via* a Williamson ether synthesis of 1,2,4,5-tetrahydroxybenzene obtained *in situ* by hydrogenation of 2,5-dihydroxybenzene-1,4-benzoquinone (Scheme 1). Subsequently, **1** and **2** have been chloromethylated according to an adapted literature procedure[23] using concentrated HCl and formaldehyde in acetic anhydride to give **3** and **4**. Whereas for 2,5-subsituted benzenes this reaction usually proceeds within h at *circa* 60 °C, the preparation of **3** and **4** requires more elevated temperatures (95 °C) and extended reaction times (6 days) to achieve a reasonable yield (68 % and 33 %, respectively). At lower temperatures and shorter reaction times only mono-chloromethylated compounds could be identified. The reduced reaction rates presumably are a result of steric hindrance of the neighboring alkyl chains. It should be noted that the yields of **2** and **4** are significantly lower than the yields observed for **1** and **3**. This difference is a result of of a difference in steric hindrance between the linear alkyl substituents present in **1** and **3** and the more sterically demanding branched alkyl substituents present in **2** and **4**.

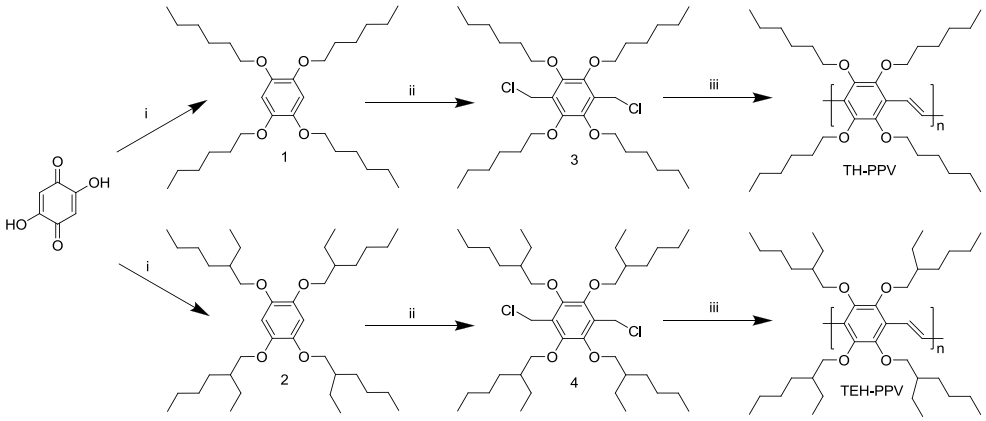

Scheme 1. Synthesis of **1**, **2, 3, 4,** TH-PPV and TEH-PPV. (i: PtO_2, $H_{2(g)}$ followed by Cs_2CO_3, C_6H_{13}-Br or $CH_3(CH_2)_3CH(C_2H_5)CH_2Br$; ii: *p*-$CH_2O$, Ac_2O, HCl; iii: K*t*BuO, 1,4-dioxane).

Monomers **3** and **4** have been polymerized according to the Gilch procedure (dehydrohalogenation polymerization), which is one of the common methods

to prepare PPV-type polymers.[24,25] TH-PPV has been obtained in a yield of 55 % as a yellow solid. In contrast, TEH-PPV was obtained as a yellow oil, albeit in a similar yield (58%). Both TH-PPV and TEH-PPV have been fully characterized using different analytical techniques. NMR-spectroscopy confirms that, as expected, these tetra-substituted PPV derivatives have an inherently regioregular nature. Analytical SEC measurements of TH-PPV display a bimodal character, with both high molecular weight (M_w = 4×10^5 g/mol) (73.4%) and low molecular weight polymers (M_w = 5×10^3 g/mol) (26.6%) being presented in the mixture. The same observation can be made for TEH-PPV, although the observed molecular weights are significantly lower, *i.e.* the high molecular weight M_w = 2.2×10^4 g/mol (64.9%) and the low molecular weight fraction M_w = 1×10^3 g/mol (35.1%). To our knowledge, this is the first time that such a bimodal character of the molecular weight distribution is observed for a Gilch polymerization. Previously reported mechanistic studies have demonstrated that the main propagation mechanism for the Gilch route is a self-initiating radical polymerization, usually leading to very high molecular weight material.[26–32] However, the simultaneous occurrence of an anionic mechanism cannot be fully excluded. In other precursor routes, a competition between a radical and an anionic mechanism has already been observed.[33–35] This competiton leads to a bimodal molecular weight distribution in which typically the high molecular weight material is associated with the self-initiating radical mechanism and the low molecular weight material is produced *via* an anionic mechanism. Hence, the low molecular weight material formed during the Gilch polymerization of TH-PPV and TEH-PPV may well originate from an anionic polymerization mechanism. Apparently, tetra-substitution and thus increased steric hindrance results in an increased competition between the normal radical mechanism and the anionic mechanism. In view of this, it can be expected that the molecular weight distributions can be improved by further optimization of the polymerization conditions.

3.2. Optical Characterization

The solubility and UV-vis absorption characteristics of TH-PPV en TEH-PPV in various solvents with different polarities have been studied. The polymers are readily soluble in a variety of solvents ranging from apolar solvents, such as *n*-hexane and toluene, to solvents of medium polarity, such as chloroform and dichloromethane. It is noteworthy that TH-PPV and TEH-PPV are even soluble in cyclohexane, a very apolar solvent in which most other available PPV derivatives are insoluble. The UV-vis absorption spectrum of TH-PPV and TEH-PPV exhibit typical absorption bands associated with the π-π^* transition, both in thin film and solution (Fig. 1). To study the influence of the bimodal weight distribution on the optical properties, the high and low molecular weight fractions of the TH-PPV were separated using preparative size exclusion chromatography on Bio-Beads® (S-X1) with toluene as the solvent. Subsequently, the optical characterization of TH-PPV was executed both before and after separation and identical results were obtained. The solution UV-vis absorption maximum λ_{max} of TH-PPV is virtually independent of the solvent used and is positioned at 429 nm. The λ_{max} of TH-PPV in a thin film is slightly red-shifted and positioned at 442 nm. Both values are somewhat red-shifted in comparison to the previously reported TM-PPV derivatives.[17,18] This is probably a result of the enhanced purity of TH-PPV due to its improved solubility, which allows for a careful purification of all intermediates as well as the conjugated polymer itself. In contrast, for TEH-PPV, both in solution and in a thin film, a broad absorption band is found between 300 and 400 nm, which is composed of several overlapping smaller bands. Apparently, the backbone of TEH-PPV is considerably distorted as compared to TH-PPV, which results in a distribution of polymer segments with a strongly reduced effective conjugated length. This is not surprising since all observed λ_{max} values for all tetra-substituted polymers are significantly blue shifted as compared to OC_1C_{10}-PPV, which exhibits a λ_{max} in the 480-520 nm range, with the exact position being dependent on the preparation procedure.[36–38]

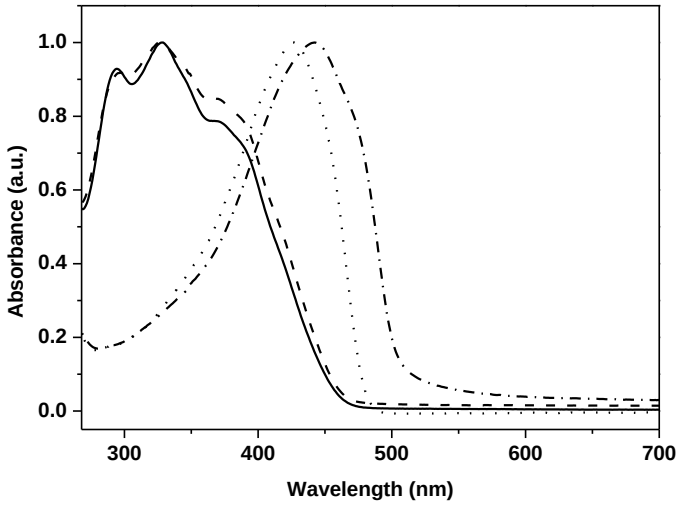

Fig. 1. UV-vis absorption spectra of TH-PPV (solution dotted; thin film dash-dot) and TEH-PPV (solution solid; thin film dashed).

The blue shifts of the absorption maxima can be attributed to the steric hindrance between the side chains of both TH-PPV and TEH-PPV. This causes a more "twisted" conformation of the polymer backbone, which would directly affect the bandgap and thus the λ_{max}. The presence of this effect was previously predicted in a quantum-chemical investigation on the conformations and electronic properties of a variety of methoxy-substituted PPV derivatives.[39] According to these studies, strong steric repulsions between adjacent sites in the phenylene ring leads to rotation of the substituents around the C(sp^2)-O bonds and consequently the overlap between the π-type p-orbital of oxygen and the π molecular orbital of the polymer decreases. This effect leads to a wider bandgap for tetra-methoxy substituted PPV derivatives, as compared to their dialkoxy-substituted counterparts. However, it should be noted that by using other precursor routes, a different λ_{max} may be found for these polymers, since it is well know that the λ_{max} of PPV-type polymers is dependent on the polymerization route utilized.[38,40] TH-PPV and TEH-PPV have also been studied using fluorescence spectroscopy (Fig. 2). In a thin film, TH-PPV exhibits a distinct fluorescence emission at λ_{em} = 495 nm with a shoulder around 530 nm

(excitation wavelength λ_{exc} = 442 nm). In dilute solution, a similar λ_{em} = 488 nm and shoulder around 519 nm are found (λ_{exc} = 430 nm). Whereas the shape is similar to OC_1C_{10}-PPV, also in this case the maximums are significantly blue shifted, as was observed for the absorption characteristics. This corroborates the hypothesis of a wider bandgap due to stronger distortion of the effective conjugation length in the polymer chain. For TEH-PPV, in thin film the fluorescence emission maximum is positioned at λ_{em} = 462 nm with a shoulder around 490 nm (excitation wavelength λ_{exc} = 370 nm). In dilute solution, a similar λ_{em} = 460 nm is found (λ_{exc} = 370 nm). This confirms the reduced conjugation length of TEH-PPV as compared to TH-PPV. In view of this observation, further characterization and analysis, as described in the following sections, have focused on TH-PPV.

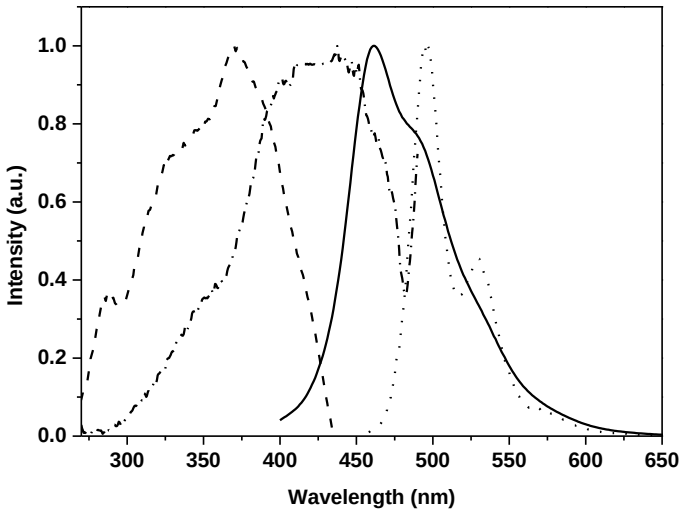

Fig. 2. Photoluminescence excitation and emission spectra of thin films of TH-PPV (PLE λ_{em} = 495 nm dash-dot; PL λ_{ex} = 442 nm dotted) and TEH-PPV (PLE λ_{em} = 462 nm dashed; PL λ_{ex} = 370 nm solid).

3.3. Thermal Stability

The impact of tetra-substitution on the thermal stability of the PPV derivative is of considerable interest for application of this type of materials

in optoelectronics. Thermogravimetric analysis (TGA) indicates that for TH-PPV polymer degradation commences above 250 °C, with the derivative of weight loss to the temperature exhibiting one maximum at 378 °C. A similar observation has been made with direct insertion probe pyrolysis mass spectrometry (DIP-MS). The total reconstructed ion chromatogram shows an increasing current starting around 250 °C with a peak at 293 °C related to polymer degradation. It should be noted that both TGA and DIP-MS give information on the thermal stability of the polymer, but do not monitor the actual degradation of the conjugated system itself. Therefore, the thermal stability of specifically the conjugated system has been specifically probed using a third technique, *i.e. in situ* UV-vis spectroscopy. Heating the TH-PPV to temperatures up to 220 °C results in a significant thermochromic shift. Upon cooling, the room temperature UV-vis spectrum is fully recovered, confirming the reversibility of this process. However, heating at temperatures of 240 °C and higher results in an irreversible blue-shift of λ_{max}, indicating that the degradation of the conjugated system starts between 220 °C and 240 °C. This thermal stability is in a similar order of magnitude as was observed for OC_1C_{10}-PPV and indicates that the thermal stability of our novel tetra-substituted material is sufficient for optoelectronic applications.[38]

3.4. Phase Behavior

The behavior of TH-PPV upon thermal treatment has been studied in more detail with DSC and PLM. For the PLM studies, TH-PPV has been drop-casted from a $CHCl_3$ solution onto a trimethylsilyl chloride treated glass substrate. The obtained film is only weakly birefringent under cross-polarization. However, upon heating to temperatures above 100 °C, followed by cooling, nematic-like optical textures become more apparent (Fig. 3). A similar observation has been previously made for 2,5-subsituted PPV derivatives with linear alkoxy side chains.[9] During the subsequent thermal cycling between room temperature and 200 °C at a heating/cooling rate of 10 °C/min, little variation in texture is observed. The birefringence weakens above 200 °C, due to isotropization, but is fully recovered upon subsequent cooling. Above

220 °C degradation phenomena are observed, which are in line with the observations on the thermal stability of the conjugated system (*vide supra*).

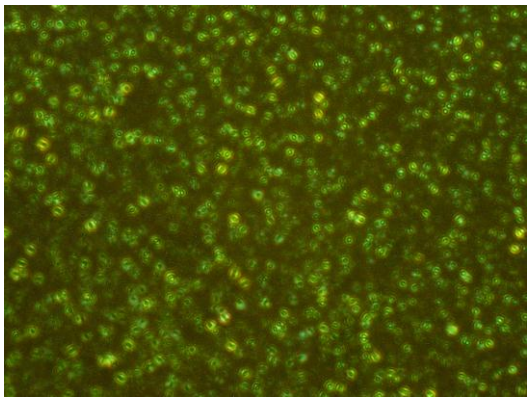

Fig. 3. PLM of a thin film of TH-PPV at RT after thermal treatment (Magnification: 60P, cross-polarization).

Mesophase formation is further evident from DSC measurements (Fig. 4). The lower curve corresponds to a heating process and shows double "melting endotherms" (T_m = 51 °C and 89 °C). These endotherms are associated with order-disorder transitions of the side chains. The subsequent cooling process displays a distinct "crystallization" peak at T_c = 72 °C. In contrast, DSC measurements on TEH-PPV do not indicate the presence of any thermal transitions at temperatures as high as 200 °C. Apparently, the branched side chains hamper the formation of an organized phase. Because the monomer of TH-PPV does not display liquid crystalline behavior, it can be assumed that the observed mesophase originates from the rodlike nature of the main chain of TH-PPV. The formation of a mesophase in TH-PPV is a direct indication for the enhanced structural order of this material. Such an enhanced structural order is a desirable property, since often concomitantly an increase in charge carrier mobility is observed. Furthermore, it can be anticipated that by altering the length of the alkoxy side chains, the mesogenic properties of the polymer (layer spacing, packing of the side chains) and as a result, the optoelectronic properties, can be controlled and tuned.

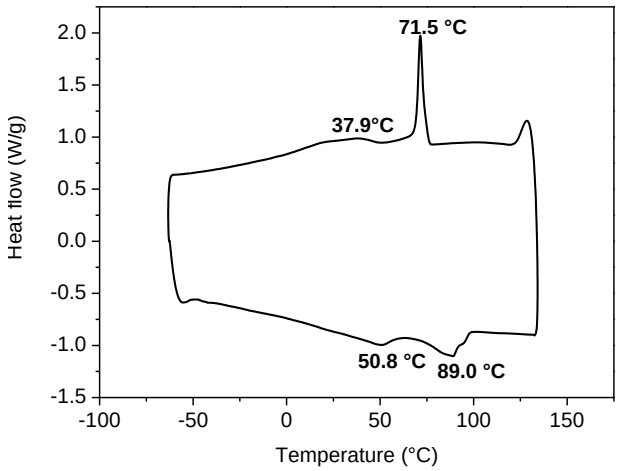

Fig. 4. DSC curve of the heating (bottom) and cooling (top) of TH-PPV between -60 and 135 °C. The second heating/cooling cycle is shown.

3.5. Device Characterization

Many PPV-type polymers have been studied on their performance in organic light-emitting diodes (OLEDs) due to their very good PL efficiencies and ambipolar charge transport. With TH-PPV now being readily available as a tetra-substituted representative with a high purity, this compound was chosen for further device studies. To verify the performance of the TH-PPV in an OLED, a simple two layer solution processed OLED was prepared (*cf.* experimental section for details). Due to the soft character of the TH-PPV, the determination of the active layer could not be directly obtained with a profilometer. As an alternative, first a 50 nm small molecular layer of (1,3,5-tris(2-N-phenylbenzimidazolyl) benzene (TPBI) was evaporated on top of the TH-PPV layer and the total thickness of the double layer was determined. Subsequently, by substracting the layer thickness of the TPBI layer, the thickness of the TH-PPV layer was obtained. The layer thickness of the TH-PPV layer (110 nm) was slightly more than optimal, but was needed to obtain working devices. It can be assumed that the low T_g of the TH-PPV allows for some penetration of the metal cathode into the active layer, which results in

the formation of weak spots that eventually lead to the formation of shorts circuits.

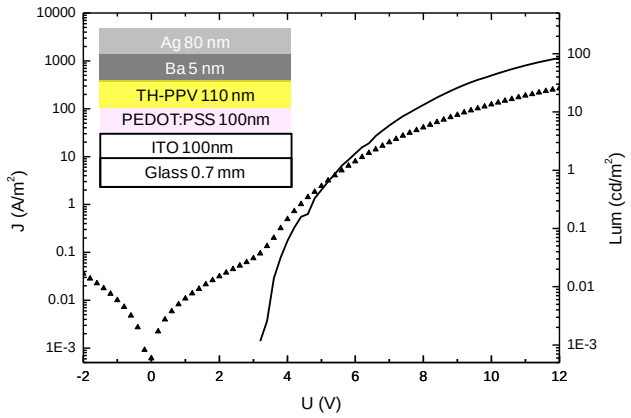

Fig. 5. Current density (triangles) and luminance (solid) for a ITO/PEDOT:PSS/TH-PPV/Ba/Ag device.

The current density and the luminance *versus* applied voltage are depicted in Fig. 5. The current density rises at voltages slightly higher than what would be expected for conventional PPV based OLEDs. Part of this is due to the thicker films. Upon injection, diode behavior is clearly observed as the current density rises rapidly. It rises continuously with increasing voltage levels. The luminance turns on at similar voltages indicating that the charge injection is balanced. The luminance, however, does level off at moderate values around 100 cd/m^2. This indicates that there is a dominant charge carrier being transported through the TH-PPV as the current density appears to be space charge limited. Further analysis is required to determine the nature of the majority carrier and how its mobility compares with other PPVs. This is of interest since on the one hand the TH-PPV is regioregular, which should increase the solid state ordering and hence increase the carrier mobility. However, on the other hand the conjugation is limited by the out of plane distortion due to steric hindrance, which is expected to decrease the carrier mobility.[41] The electroluminescence (EL) observed from the above described device is almost identical to the luminance spectrum obtained by

photo-excitation (PL) (Fig. 6). Both are very similar to the photoluminescence spectra obtained from the TH-PPV in solution. The EL spectrum starts at slightly lower wavelength when compared to the PL spectrum, which may be due to the slightly increased self-absorption for the photo-excitation spectrum.

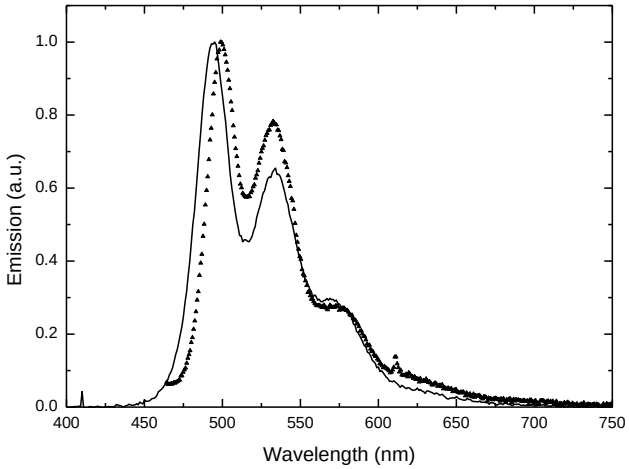

Fig. 6. Photoluminescence (triangles) and electroluminescence (solid) spectra obtained from a ITO/PEDOT:PSS/TH-PPV/Ba/Ag device by photo-excitation at 400 nm or electro-excitation at 7 volts, respectively.

4. Conclusions

The synthesis and full characterization of the first two soluble tetra-alkoxy substituted PPV derivatives, poly(2,3,5,6-tetrahexyloxy-1,4-phenylene vinylene) TH-PPV and poly[2,3,5,6-tetra(2'-ethyl-hexyloxy)-1,4-phenylene vinylene] TEH-PPV, is reported. The monomer synthesis is straightforward and feasible in high yields. The polymerization is accomplished using the well-known dehydrohalogenation route. The resulting polymers are highly soluble in various organic solvents ranging from solvents at the apolar side of the polarity scale, such as cyclohexane, to the more common organic solvents, such as dichloromethane. Furthermore, the conjugated structure has a thermal stability until well above 200 °C. TH-PPV exhibits desirable

ordering phenomena as well as a liquid crystalline mesophase. In contrast, due to steric hindrance of the branched alkyl side chains, TEH-PPV is rather disordered. As a first demonstration of the charge transporting properties of TH-PPV, a simple solution processed electroluminescent device has been prepared, which functions well. With the described route, soluble tetra-alkoxy substituted PPV derivatives are now readily available for further study and application.

5. Acknowledgments

The authors thank H. Penxten for the PL and PLE measurements and Sonsoles Garcia Santamaria for the careful device preparation. The authors gratefully acknowledge the Fund for Scientific Research (FWO) for granting a PhD fellowship (I.V.S. and J.V.) and for the funding of the project G.0091.07, the Institute for the promotion of Innovation by Science and Technology in Flanders (IWT, SBO-project "Polyspec" IWT-060843), the Spanish Ministry of Science and Innovation (MICINN) and CSD2007-00010) and the Generalitat Valenciana. Furthermore, this work is part of the European Science Foundation EUROCORES Program SONS II (CRP nr. 05-SONS-FP-021 "SOHYDs")that is supported by funds from the FWO (G.068506), and by MICINN (MAT2006-28185-E) and the EC Sixth Framework Program, under Contract N. ERAS-CT-2003-980409'.

6. Supporting Information

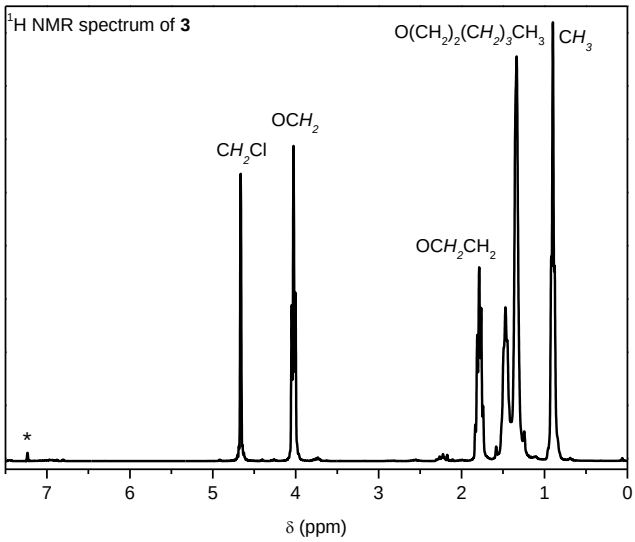

Fig. 7. ^{1}H NMR spectrum of monomer **3**, recorded in $CDCl_3$ at RT. The resonance marked with an asterisk result from the solvent residual peak of $CDCl_3$.

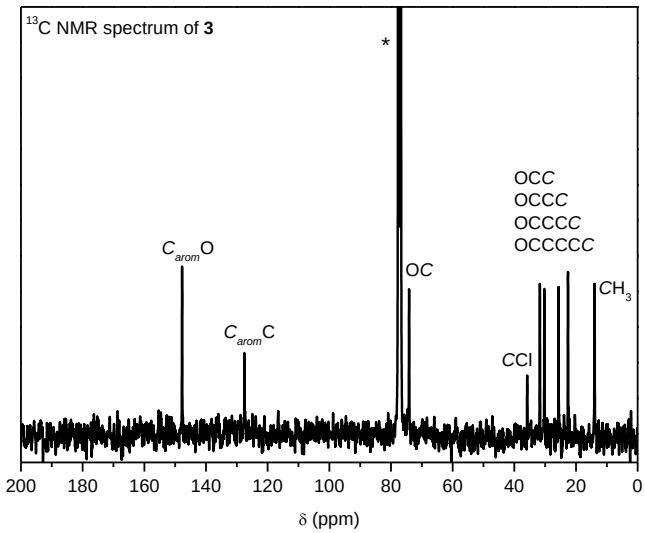

Fig. 8. ^{1}C NMR spectrum of monomer **3**, recorded in $CDCl_3$ at RT. The resonance marked with an asterisk result from the solvent residual peak of $CDCl_3$.

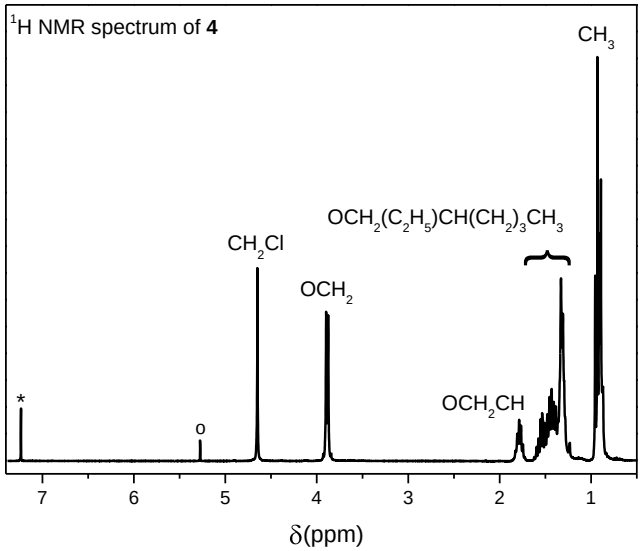

Fig. 9. ^{1}H NMR spectrum of monomer **4**, recorded in $CDCl_3$ at RT. The resonance marked with an asterisk result from the solvent residual peak of $CDCl_3$.

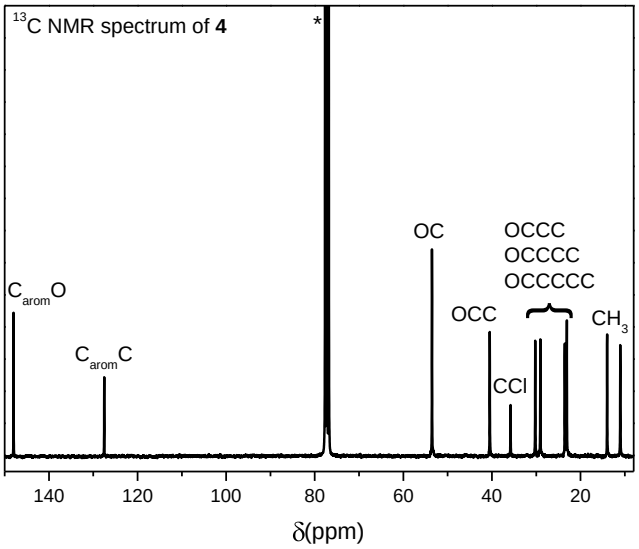

Fig. 10. ^{1}C NMR spectrum of monomer **4**, recorded in $CDCl_3$ at RT. The resonance marked with an asterisk result from the solvent residual peak of $CDCl_3$.

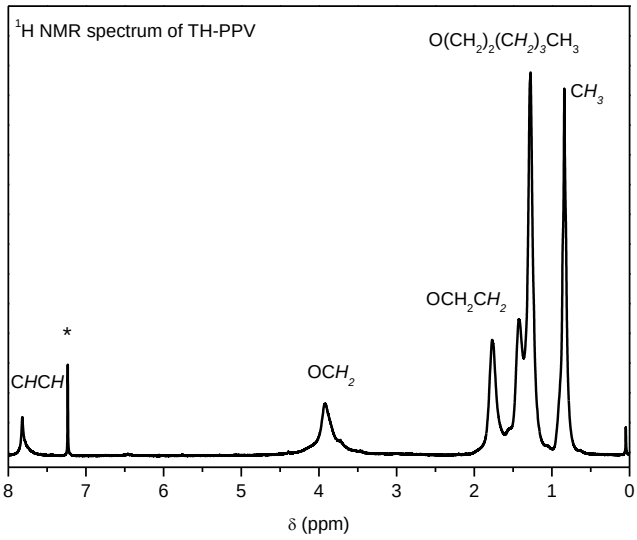

Fig. 11. ^{1}H NMR spectra of polymer TH-PPV, recorded in $CDCl_3$ at RT. The resonance marked with an asterisk result from the solvent residual peak of $CDCl_3$.

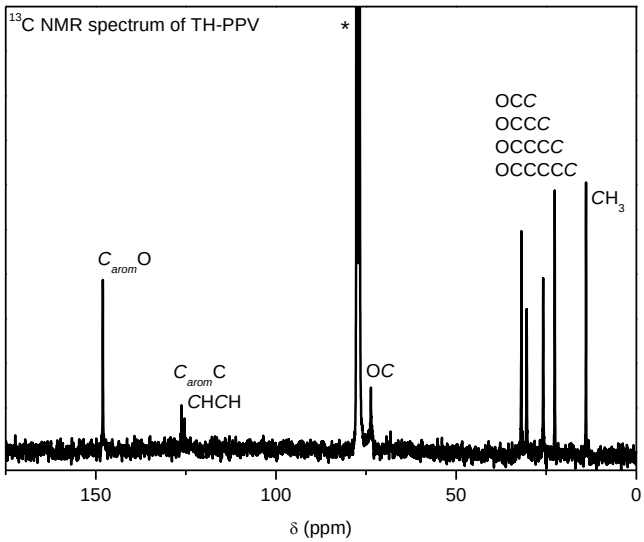

Fig. 12. ^{1}C NMR spectra of polymer TH-PPV, recorded in $CDCl_3$ at RT. The resonance marked with an asterisk result from the solvent residual peak of $CDCl_3$.

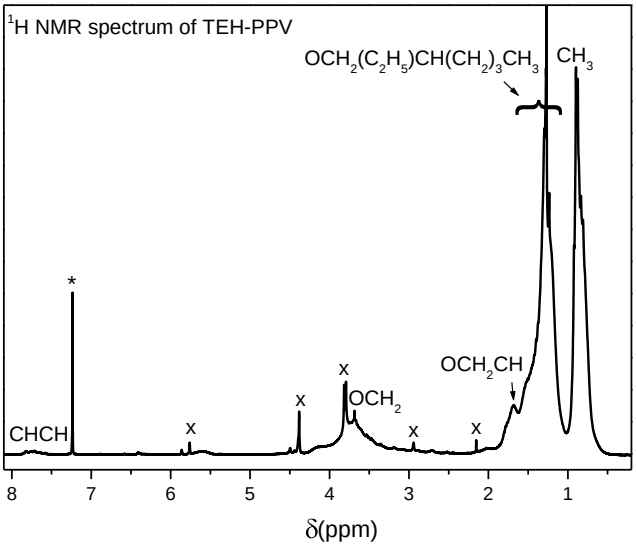

Fig. 13. ^{1}H NMR spectra of polymer TEH-PPV, recorded in $CDCl_3$ at RT. The resonance marked with an asterisk result from the solvent residual peak of $CDCl_3$ and the resonances marked with an x result from impurities unable to remove from the oily TEH-PPV.

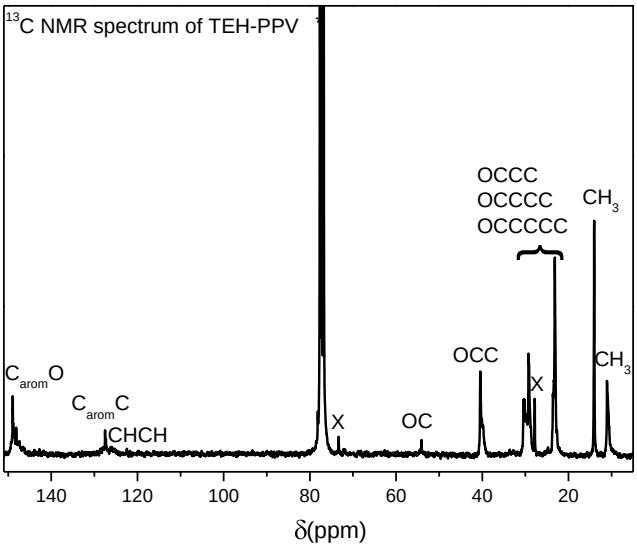

Fig. 14. ^{1}C NMR spectra of polymer TEH-PPV, recorded in $CDCl_3$ at RT. The resonance marked with an asterisk result from the solvent residual peak of $CDCl_3$.

7. References

(1) J. H. Burroughes, D. D. C. Bradley, A. R. Brown, R. N. Marks, K. Mackay, R. H. Friend, P. L. Burns, A. B. Holmes, *Nature* **1990**, *347*, 539.

(2) R. H. Friend, R. W. Gymer, A. B. Holmes, J. H. Burroughes, R. N. Marks, C. Taliani, D. D. C. Bradley, D. A. Dos Santos, J. L. Brédas, M. Lögdlund and W. R. Salaneck, *Nature* **1999**, *397*, 121.

(3) S. Scheinert and G. Paasch, *Phys. Status Solidi A* **2004**, *201*, 1263.

(4) D. Tyler McQuade, A. E. Pullen and T. M. Swager, *Chem. Rev.* **2000**, *100*, 2537.

(5) H. Hoppe, M. Niggemann, C. Winder, J. Kraut, R. Hiesgen, A. Hinsch, D. Meissner and N. S. Sariciftci, *Adv. Funct. Mat.* **2004**, *14*, 1005.

(6) A. J. Mozer, P. Denk, M. C. Scharber, H. Neugebauer, N. S. Sariciftci, P. Wagner, L. Lutsen and D. Vanderzande, *J. Phys. Chem. B.* **2004**, *108*, 5235.

(7) A. J. J. M. van Breemen, P. T. Herwig, C. H. T. Chlon, J. Sweelssen, H. F. M. Schoo, E. M. Benito, D. M. de Leeuw, C. Tanase, J. Wildeman and P. W. M. Blom, *Adv. Funct. Mat.* **2005**, 872.

(8) L. Breban, L. Lutsen, G. Vanhoyland, J. D'Haen, J. Manca and D. Vanderzande, *Thin Solid Films* **2006**, *511–512*, 695.

(9) S. H. Chen, A. C. Su, S. R. Han, S. A. Chen and Y. Z. Lee, *Macromolecules* **2004**, *37*, 181.

(10) K. Tajima, Y. Suzuki and K. Hashimoto, *J. Phys. Chem. C.* **2008**, *112*, 8507.

(11) E. Peeters, A. Delmotte, R. A. J. Janssen and E. W. Meijer, *Adv. Mater.* **1997**, *9*, 493.

(12) M. Kemerink, J. K. J. van Duren, P. Jonkheijm, W. F. Pasveer, P. M. Koenraad, R. A. J. Janssen, H. W. M. Salemink and J. H. Wolters, *Nano Lett.* **2003**, *3*, 1191.

(13) N. S. Sariciftci, L. Smilowitz, A. J. Heeger and F. Wudl, *Science* **1992**, *258*, 1474.

(14) J-H. Lee and D-H. Hwang, *Synth. Met.* **2008**, *158*, 273.

(15) J-I. Jin, C-K. Park and H-K. Shim, *Macromolecules* **1993**, *26*, 1799.

(16) O. Levi, G. Perepelitsa, D. Davidov, S. Shalom, I. Benjamin, R. Neumann, A. J. Agranat and Y. Avny, *J. Appl. Phys.* **2000**, *88*, 1236.

(17) A. Donval, D. Josse, G. Kranzelbinder, R. Hierle, E. Toussaere, J. Zyss, G. Perpelitsa, O. Levi, D. Davidov, I. Bar-Nahum and R. Nemann, *Synth Met.* **2001**, *124*, 59.

(18) J-I. Jin, H-J. Kang and H-K. Shim, *Bull. Korean Chem. Soc.* **1990**, *11*, 415.

(19) S-J. Chung, D. W. Lee, D-K. Oh, C. E. Lee and J-I. Jin, *Acta Polym.* **1999**, *50*, 298.

(20) E. M. D. Keegstra, B-H. Huisman, E. M. Paardekooper, F. J. Hoogesteger, J. W. Zwikker, L. W. Jenneskens, H. Kooijman, A. Schouten, N. Veldman and A. L. Spek, *J. Chem. Soc., Perkin Trans. 2* **1996**, 229.

(21) J. J. H. Schlotter, I. J. A. Mertens, A. M. A. van Wageningen, F. P. J. Mulders, J. W. Zwikker, H-J. Buschmann and L. W. Jenneskens, *Tetrahedron Lett.* **1994**, *35*, 7255.

(22) F. Benington, R. D. Morin and L. C. Clark, *J. Org. Chem.* **1955**, *20*, 102.

(23) I. Van Severen, F. Motmans, L. Lutsen, T. J. Cleij and D. Vanderzande, *Polymer* **2005**, *46*, 5466.

(24) H. G. Gilch and W. L. Wheelwright, *J. Polym. Sci. Part A* **1966**, *4*, 1337.

(25) H. Becker, H. Spreitzer, K. Ibrom and W. Kreuder, *Macromolecules* **1999**, *32*, 4925.

(26) T. Schwalm, J. Wiesecke, S. Immel, M. Rehahn, *Macromolecules* **2007**, *40*, 8842.

(27) J. Wiesecke, M. Rehahn, *Angew. Chem. Int. Ed.* **2003**, *42*, 567.

(28) J. Wiesecke, M. Rehahn, *Macromol. Rapid Commun.* **2007**, *28*, 78.

(29) J. Wiesecke, M. Rehahn, *Macromol. Rapid Commun.* **2007**, *28*, 188.

(30) T. Schwalm, M. Rehahn, *Macromolecules* **2007**, *40*, 33921.

(31) L. Hontis, V. Vrindts, L. Lutsen, D. Vanderzande, J. Gelan, *Polymer* **2001**, *42*, 5793.

(32) L. Hontis, V. Vrindts, D. Vanderzande, L. Lutsen, *Macromolecules* **2003**, *36*, 3035.

(33) L. Hontis, M. Van Der Borght, D. Vanderzande, J. Gelan, *Polymer* **1999**, *40*, 6615.

(34) P. Adriaensens, M. Van Der Borght, L. Hontis, A. Issaris, A. van Breemen, M. de Kok, D. Vanderzande, J Gelan, *Polymer* **2000**, *41*, 7003.

(35) D. J. M. Vanderzande, L. Hontis, A. Palmaerts, D. Van Den Berghe, J. Wouters, L. Lutsen and T. Cleij, *Proc. SPIE* **2005**, *5937*, 116.

(36) L. Lutsen, P. Adriaensens, H. Becker, A. J. Van Breemen, D. Vanderzande and J. Gelan, *Macromolecules* **1999**, *32*, 6517.

(37) E. Kesters, D. Vanderzande, L. Lutsen, H. Penxten and R. Carleer, *Macromolecules* **2005**, *38*, 1141.

(38) A. Henckens, I. Duyssens, L. Lutsen, D. Vanderzande and T. J. Cleij, *Polymer* **2006**, *47*, 123.

(39) S. Y. Hong, *Bull. Korean Chem. Soc.* **1999**, *20*, 42.

(40) H. Roex, P. Adriaensens, D. Vanderzande and J. Gelan, *Macromolecules* **2003**, *36*, 5613.

(41) P. W. M. Blom and M. C. J. M. Vissenberg, *Mat. Sci. Eng.* **2000**, *27*, 53.

Chapter 6

Thermal Stability of Poly[2-methoxy-5-(2'-phenylethoxy)-1,4-phenylene vinylene] (MPE-PPV):Fullerene Bulk Heterojunction Solar Cells

ABSTRACT: In order to improve the thermal stability of polymer:fullerene bulk heterojunction solar cells, a new polymer, poly[2-methoxy-5-(2'-phenylethoxy)-1,4-phenylene vinylene] (MPE-PPV), has been designed and synthesized, which shows an increased glass transition temperature (T_g) of 111 °C. The thermal characteristics and phase behavior of MPE-PPV:[6,6]-phenyl C_{61}-butyric acid methyl ester ([60]PCBM) blends was investigated by means of modulated temperature differential scanning calorimetry and rapid heating-cooling calorimetry. The thermal stability of MPE-PPV:[60]PCBM solar cells was compared with similar devices based on the reference MDMO-PPV material with a T_g of 45 °C. Monitoring of the photocurrent–voltage characteristics at elevated temperatures revealed that the use of high T_g MPE-PPV resulted in a substantial improvement of the thermal stability of the solar cells. Furthermore, a systematic transmission electron microscope study of the active polymer:fullerene layer at elevated temperatures likewise demonstrated a more stable morphology for the MPE-PPV:[60]PCBM blend. Both observations indicate that the use of high T_g MPE-PPV as donor material leads to a reduced free movement of the fullerene molecules within the active layer of the photovoltaic device. Finally, optimization of the PPV:fullerene solar cells revealed that for both types of devices the use of [6,6]-phenyl C_{71}-butyric acid methyl ester ([70]PCBM) resulted in a substantial

---

*Vandenbergh, J.; Conings, B.; Bertho, S.; Kesters, J.; Spoltore, D.; Piersimoni, F.; Esiner, S.; D' Haen, J.; Zhao, J.; Van Assche, G.; Wienk, M. M.; Maes, W.; Cleij, T. J.; Lutsen, L.; Van Mele, B.; Janssen, R. A. J.; Manca, J.; Vanderzande, D. J. M. *in preparation*.

increase of current density and power conversion efficiency, up to 3.0% for MDMO-PPV:[70]PCBM and 2.3% for MPE-PPV:[70]PCBM.

1. Introduction

In polymer:fullerene bulk heterojunction solar cells, the nanoscale morphology of the active layer influences the electronic properties of the devices to a great extent.[1–4] Via proper sample preparation, such as annealing conditions and the choice of solvents, the (nano)morphology of the donor-acceptor blend can be optimized, leading to improved exciton dissociation and charge transport.[3–6] It was already demonstrated, however, that this initial optimized morphology deteriorates rather fast (during storage at elevated temperatures).[7–17] Long term annealing treatments induce severe phase separation between the donor polymer and the fullerene acceptor material, leading to a decreased interfacial area and less efficient exciton dissociation.[18–20] To stabilize the initial (nano)morphology of a bulk heterojunction layer, several pathways can be followed. A first approach is to use donor-acceptor diblock copolymers to covalently fixate the morphology via the scale of the block lengths.[13,14] A second way to obtain a stable network is to build in a certain amount of functional groups in the donor polymer which can crosslink and freeze in the ultimate morphology after a thermal or UV light treatment.[21] In this paper, a third approach is applied based on the use of a donor polymer with a high glass transition temperature (T_g).[22–26] It is well-known that the *Tg* of a polymer is dependent on its chemical structure. By changing the side chain substituents of a polymer, the *Tg* will be altered. Poly[(2-methoxy-5-(3',7'-dimethyloctyloxy))-1,4-phenylene vinylene] (MDMO-PPV) has a quite low *Tg* of around 45 °C due to the long flexible alkoxy side chains, which cause a plasticizing effect on the PPV backbone.[22] To reduce the side chain flexibility, a novel poly(*p*-phenylene vinylene) derivative, poly[2-methoxy-5-(2'-phenylethoxy)-1,4-phenylene vinylene] (MPE-PPV), has been designed and synthesized. The bulky and rigid phenyl side chains decrease the rotational freedom of the polymer chains, thereby increasing the T_g at which the amorphous polymer

transfers from a rigid glass into soft flexible material. The T_g of the polymer as well as the phase behavior in blends with [6,6]-phenyl C_{61}-butyric acid methyl ester ([60]PCBM) was determined by means of advanced thermal analysis techniques, i.e. modulated temperature differential scanning calorimetry (MTDSC) and rapid heating-cooling calorimetry (RHC). The effect of elevated temperatures on the bulk morphology of MPE-PPV:[60]PCBM blends as well as on the photovoltaic performance of the resulting devices has been studied via the use of transmission electron microscopy (TEM) and via in situ monitoring of the photovoltaic output (i.e. the short circuit current, open circuit voltage, fill factor, and efficiency). The results were compared with reference MDMO-PPV:[60]PCBM solar cells. Finally, the MPE-PPV:fullerene and MDMO-PPV:fullerene devices were optimized for maximal photovoltaic output. Different spincoating solvents were applied and both [60]PCBM as well as [6,6]-phenyl C_{71}-butyric acid methyl ester ([70]PCBM) fullerene derivatives were used as acceptor materials.

2. Experimental Section

2.1. General

Unless stated otherwise, all reagents and chemicals were obtained from commercial sources (Acros and Aldrich) and used without further purification. 1,4-Dioxane was dried by distillation from Na/benzophenone. NMR spectra were recorded with a Varian Inova 300 spectrometer using a 5 mm probe. Gas chromatography/mass spectrometry (GC/MS) analyses were carried out with TSQ-70 and Voyager mass spectrometers (Thermoquest); the capillary column was a Chrompack Cpsil5CB or Cpsil8CB. Analytical size exclusion chromatography (SEC) was performed using a Spectra series P100 (Spectra Physics) pump equipped with two mixed-B columns (10 µm, 0.75 cm × 30 cm, Polymer Labs) and a refractive index detector (Shodex) at 40 °C. THF was used as the eluent at a flow rate of 1.0 mL/min. Molecular weight distributions are given relative to polystyrene standards. FT-IR spectra were collected with a Perkin-Elmer Spectrum One FT-IR spectrometer (nominal resolution 4 cm^{-1}, summation of 16 scans). UV-vis spectroscopy was

performed on a VARIAN CARY 500 UV-vis-NIR spectrophotometer (scan rate 600 nm/min). Samples for thin-film FT-IR and UV-vis characterization were prepared by dropcasting the precursor polymer from a $CHCl_3$ solution (10 mg/mL) onto NaCl or quartz disks.

The DSC and MTDSC measurements were performed on a TA Instruments Q2000 DSC (Tzero DSC technique) with the MDSC option, equipped with an RCS cooling accessory and purged with nitrogen (50 mL min^{-1}). Baseline, heat capacity, and temperature were calibrated with sapphire and indium. About 5 mg samples were sealed in aluminum crucibles (Tzero, 40 μL). For the DSC measurements, the scan rate was 10.0 K min^{-1}. The isothermal hold time at the lower limit temperature of -90.0 °C was 10 min, while the isothermal hold time at the upper limit temperature of 300.0 °C was 1 min. Three heating-cooling cycles were run to check the reproducibility. The first heating curve was different from the subsequent two heating curves due to the complex thermal history of the as-prepared samples and their poor contact with the crucibles in the first heating, while all three cooling curves coincide very well. The second and third heating curves also coincide very well. To reduce the sample preparation effects, the first cooling and the second heating were used for discussion. Actually, such a methodology can to a certain extent avoid the effects of casting solvents[19,20] and annealing conditions.[6,21] The melting and crystallization peaks were characterized by their peak temperatures. For the MTDSC measurements, the modulation amplitude was 0.5 K with a period of 60 s. First, the samples were kept at 300.0 °C for 1 min. Subsequently, they were quenched in the DSC cell at about 100 K min^{-1} to -90.0 °C and then reheated to 300.0 °C at 2.5 K min^{-1}. The RHC measurements were performed on a TA Instruments RHC B1 (Tzero DSC technique) equipped with a LNCS cooling accessory and purged with neon (10 mL min^{-1}). Baseline, heat capacity, and temperature were calibrated with sapphire and indium. About 0.5 mg samples were sealed in aluminum RHC crucibles with a weight of less than 2 mg. First, the samples were kept at 350.0 °C for 0.1 min. Subsequently, they were quenched in the RHC cell at

about 2000 K min^{-1} to -150.0 °C and then reheated to 350.0 °C at 500.0 K min^{-1}.

Non-optimized bulk heterojunction solar cells, combining one out of two different conjugated polymers, poly[(2-methoxy-5-(3',7'-dimethyloctyloxy))-1,4-phenylene vinylene] (MDMO-PPV) with T_g ≈ 45 °C (Covion, Mw = 716 kg/mol, PD = 6.5), or poly[(2-methoxy-5-(2'-phenylethoxy))-1,4-phenylene vinylene] (MPE-PPV) with T_g ≈ 111 °C (M_w = 123 kg/mol, PD = 2.3), as electron donor materials with [60]PCBM (Solenne-BV) as acceptor material were made according to the following preparation guidelines. The devices had an ITO/PEDOT-PSS/polymer:[60]PCBM/Ca/Al structure. Each device had an active area of 25.0 mm^2. Indium tin oxide (ITO, 100 nm) coated glass plates were successively cleaned in a soap solution, demineralized water and acetone, each for 10 min in an ultrasonic bath. This was followed by an additional cleaning step in boiling isopropanol for 10 min and an UV/O_3 treatment of 30 min. A 60 nm thick poly(3,4-ethylenedioxythiophene-polystyrenesulfonate (PEDOT-PSS (HC Starck, Clevios P VP AI 4083)) layer was spincoated on the clean glass/ITO substrates. The substrates were dried for 20 min on a hotplate at 120 °C. The active layer, with thickness of 80 nm, consisting of a blend of the respective PPV polymer and [60]PCBM in chlorobenzene, was spincoated on top of the PEDOT-PSS layer. The polymer:[60]PCBM ratio for MDMO-PPV and MPE-PPV was 1:4 (this ratio was chosen because it resulted in the best solar cell performance). The concentrations of the polymer solutions were 0.5 wt% (weight percentage of polymer in chlorobenzene solvent). To obtain complete dissolution, the polymer:[60]PCBM solutions were stirred overnight at 50 °C. The solar cells were completed by subsequently evaporating 20 nm of Ca on top of the active layer, followed by 60 nm of Al. The current–voltage (IV) characteristics were measured with a Newport class A solar simulator (model 91195A) calibrated with a silicon solar cell to give an AM1.5 spectrum. The influence of thermal annealing on the photovoltaic performance was measured in a set-up that measures IV characteristics at regular time intervals (illumination with a White LED LZ4-00CW10 (LedEngin)) while the samples were kept under

continuous annealing in a nitrogen atmosphere. In between of the measurements, the samples were kept in the dark. The active layer morphology was studied with a transmission electron microscope (Philips CM12-STEM), operated at 80 kV. To prepare TEM specimens, the flotation technique was used to remove the films from the glass surface, via treatment with HF (40%). The films floating on the surface of deionized water were subsequently picked up by a 400 mesh copper grid.

Optimized bulk heterojunction solar cells with either MDMO-PPV or MPE-PPV as electron donor materials and either [60]PCBM or [70]PCBM (Solenne-BV) as acceptor material were made according to the following preparation guidelines. The devices had an ITO/PEDOT-PSS/polymer:fullerene/LiF/Al structure. The devices had active areas of either 9 mm^2 or 16 mm^2. Indium tin oxide (ITO, 100 nm) coated glass plates were successively cleaned and rubbed in aceton, ethanol, soap solution, demineralized water and isopropanol, each for 15 min in an ultrasonic bath, followed by an UV/O_3 treatment of 30 min. A 60 nm thick poly(3,4-ethylenedioxythiophene-polystyrenesulfonate (PEDOT-PSS (HC Starck, Clevios P VP AI 4083)) layer was spincoated on the clean glass/ITO substrates. Subsequently, polymer:fullerene (1:4) active layers with different thicknesses were spincoated from different solvents on top of the PEDOT-PSS layer. The concentrations of the solutions were 0.5 wt% (weight percentage of polymer in solvent) for both polymers. To obtain complete dissolution, the polymer:fullerene solutions were stirred overnight at 60 °C. The toluene solutions were stirred subsequently at 90 °C for 1 h. The solar cells were completed by subsequently evaporating 1 nm of LiF on top of the active layer, followed by 100 nm of Al. The current–voltage (IV) characteristics were measured with a Keithley 2400 SMU, under white light illumination with UV(GG 385) and infrared (KG1) filtered light from a tungsten halogen lamp with a maximum estimated light output of 1000 W/m^2. The solar simulator was calibrated with a silicon solar reference cell. The currents reported were corrected for spectral mismatch.[8]

2.2. Synthesis

1-Methoxy-4-(2'-phenylethoxy)benzene (**1**)

In a three-necked round-bottom flask, 4-methoxyphenol (32.0 g, 0.256 mol) and Na*t*BuO (29.8 g, 0.310 mol) were dissolved in ethanol (260 mL). The mixture was stirred for 1 h at ambient temperature under a nitrogen atmosphere. Subsequently, 2-bromoethylbenzene (52.1 g, 0.280 mol) was added dropwise to the mixture and NaI (1.0 g, 0.007 mol) was additionally added in one go. The mixture was heated at reflux for 16 h under nitrogen atmosphere. Water (200 mL) was added, ethanol was evaporated and the mixture was extracted with $CHCl_3$ (3 × 50 mL). The organic phase was washed with 10% NaOH and subsequently dried over $MgSO_4$. After evaporation of the solvent, the crude product was obtained as a clear brown solid. The product was purified by column chromatography (SiO_2, eluent hexane/chloroform 1/1) to afford white crystals. Yield: 39% (23.0 g). ^{1}H NMR ($CDCl_3$): 7.35−7.18 (m, 5H, ArH), 6.82 (s, 4H, ArH), 4.10 (t, 2H, OCH_2, *J* = 6.1 Hz), 3.75 (s, 3H, OCH_3), 3.07 (t, 2H, CH_2-Ar, *J* = 5.9 Hz); ^{13}C NMR ($CDCl_3$): 151.7, 150.8, 138.1, 129.3, 128.5, 115.0, 114.1, 69.2, 56.0, 35.7; MS (EI, *m*/*z*): 228 [M^+]; IR (NaCl, cm^{-1}): 2956, 2924, 2850, 1591, 1500, 1462, 1412, 1380, 1315, 1261, 1206, 1040, 867.

2,5-Bis(chloromethyl)-1-methoxy-4-(2'-phenylethoxy)benzene (**2**)

1-Methoxy-4-(2'-phenylethoxy)benzene (**1**) (3.2 g, 0.014 mol) and *p*-formaldehyde (1.2 g, 0.038 mol) were added to a three-necked round-bottom flask, which was placed in an ice bath and under nitrogen atmosphere. After addition of HCl (37%) (9.0 g, 0.092 mol), acetic anhydride (14.2 g, 0.140 mol) was added dropwise at such a rate that the temperature of the mixture did not exceed 70 °C. Subsequently, the mixture was stirred for 6 h at 70 °C under nitrogen atmosphere. Afterwards, the mixture was cooled down to room temperature and decanted into water (100 mL) to form a white precipitate. After filtration of the mixture, the crude product was purified via recrystallization in $CHCl_3$ to obtain white crystals. Yield: 88% (4.0 g). ^{1}H NMR ($CDCl_3$): 7.38−7.18 (m, 5H, ArH), 6.88 (s, 2H, ArH), 4.60 (s, 2H, CH_2Cl), 4.58 (s, 2H, CH_2Cl), 4.20 (t, 2H, OCH_2, *J* = 6.6 Hz), 3.82 (s, 3H, OCH_3), 3.10

(t, 2H, CH_2-Ar, *J* = 6.4 Hz); ^{13}C NMR ($CDCl_3$): 151.2, 150.3, 138.0, 129.3, 128.5, 127.5, 127.0, 126.5, 114.5, 113.0, 69.5, 56.2, 41.0, 35.8; MS (EI, *m*/*z*): 324 [M^+]; IR (NaCl, cm^{-1}): 2956, 2924, 2850, 1591, 1500, 1462, 1412, 1380, 1315, 1261, 1206, 1040, 867, 736, 704, 681.

Synthesis of poly[(2-methoxy-5-(2'-phenylethoxy))-1,4-phenylene vinylene] (MPE-PPV) (**3**)

In a typical Gilch procedure, 2,5-bis(chloromethyl)-1-methoxy-4-(2'-phenylethoxy)benzene (**2**) (0.5 g, 1.540 mmol) was dissolved in dry 1,4-dioxane (152 mL) giving a concentration of 0.01 M. The mixture was stirred at 25 °C under a continuous flow of nitrogen. A K*t*BuO solution (1.5 equiv, 0.87 M in 1,4-dioxane) was added dropwise over a time period of 15 min to the stirred monomer solution. The reaction was kept for 2 h at 25 °C under a nitrogen atmosphere, and the mixture was subsequently quenched in ice water (100 mL). The excess of base was neutralized with HCl (1 M in H_2O). The aqueous phase was extracted with $CHCl_3$ (3 × 40 mL). After combination of the organic phases, the solvent was evaporated and the polymer was redissolved in 1,4-dioxane (100 mL). The mixture was refluxed for 16 h under nitrogen atmosphere to ensure complete formation of the conjugated system. Subsequently, the mixture was cooled down to room temperature and the polymer was precipitated via addition of cold methanol (100 mL). The mixture was filtered and the red fibrous polymer was collected and dried *in vacuo*. The residual fractions contained only monomers and oligomers. Yield: 60% (218.0 mg). ^1H NMR ($CDCl_3$): 7.6–7.0 (br, 9H, ArH, CH=CH), 4.4–4.2 (br, 2H, OCH_2), 4.0–3.8 (br, 3H, OCH_3), 3.25–2.95 (br, 2H, CH_2-Ar); ^{13}C NMR ($CDCl_3$): 151.5, 150.8, 138.2, 129.0, 128.5, 127.4, 127.0, 126.5, 123.5, 110.5, 109.1, 70.0, 56.1, 35.7; IR (NaCl, cm^{-1}): 2956, 2924, 2850, 1591, 1500, 1462, 1412, 1351, 1261, 1206, 1040, 965, 867; UV-vis (thin film): λ_{max} = 506 nm; SEC (THF): M_w = 123 ×10^3 g/mol (PD = 2.5).

3. Results and Discussion

3.1. Synthesis and Standard Characterization

PPV derivatives are usually prepared via precursor routes, of which the Gilch procedure (dehydrohalogenation polymerization) is the most straightforward method.[27] The desired MPE-PPV polymer was prepared through a convenient three-step sequence (Scheme 1). First, 1-methoxy-4-(2'-phenylethoxy)benzene (**1**) was synthesized using a Williamson ether reaction combining 4-methoxyphenol and 2-bromoethylbenzene. In a second step, the MPE Gilch precursor monomer, bischloromethyl derivative **2**, was prepared via chloromethylation with *p*-formaldehyde and HCl in acetic anhydride. Premonomer **2** was efficiently purified via recrystallization in chloroform.

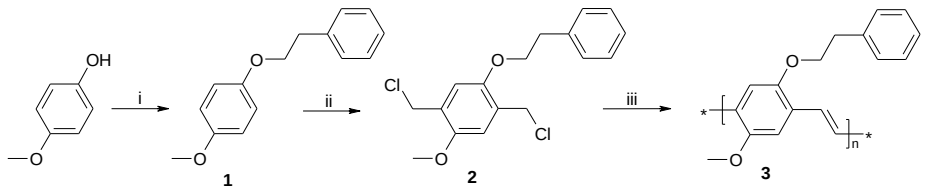

Scheme 1. Synthesis of MPE-PPV via the Gilch precursor route: (i) 2-bromoethylbenzene, Na*t*BuO, NaI, EtOH (39% yield); (ii) *p*-CH_2O, Ac_2O, HCl (88% yield); (iii) K*t*BuO, 1,4-dioxane, ΔT (56% yield).

Polymerization was performed under nitrogen atmosphere. To this end, bis(chloromethyl) premonomer **2** was dissolved in dry 1,4-dioxane (0.01 M) after which 1.5 equiv of K*t*BuO base were added. After work-up, the orange sticky precursor polymer was isolated via precipitation in cold methanol. The precursor polymer was already partially conjugated at this stage due to the small excess of base applied during polymerization. UV-vis spectroscopy of the precursor polymer revealed an absorption maximum of 468 nm (Figure 1a). The material was converted further into a fully conjugated polymer via a thermal elimination at 100 °C in 1,4-dioxane. Upon heating, the chlorine groups were eliminated to form fully conjugated MPE-PPV **3**. In the UV-vis spectrum, the absorption band at 468 nm shifted to 506 nm and increased in

absorptivity, indicating that a fully conjugated system had developed. FT-IR spectroscopy revealed the characteristic vibration frequencies of MPE-PPV (Figure 1b). The vibrationat 965 cm^{-1} originates from the *trans*-vinylene double bonds of the conjugated polymer and is applied as a standard criterion for the development of the conjugated PPV system. After work-up of the elimination reaction, the final polymer was isolated via precipitation in cold methanol. Molecular weights were determined by size exclusion chromatography (SEC). The obtained MPE-PPV had a M_w of 123 $\times 10^3$ g/mol and a PD of 2.5.

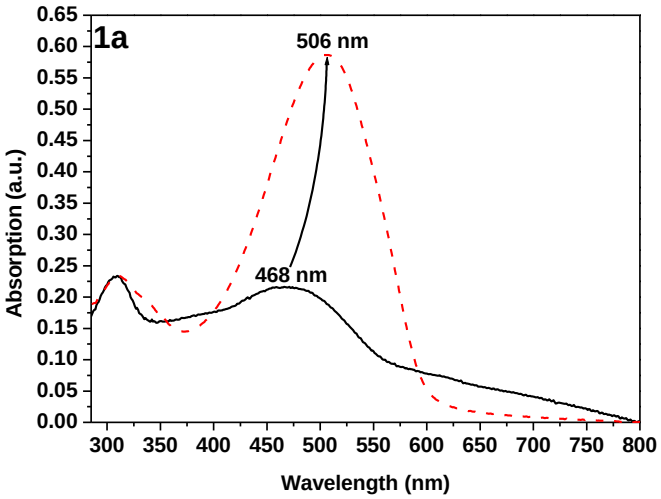

Figure 1a. Thin film UV-vis spectra before (full line) and after (dashed red line) thermal elimination of MPE-PPV.

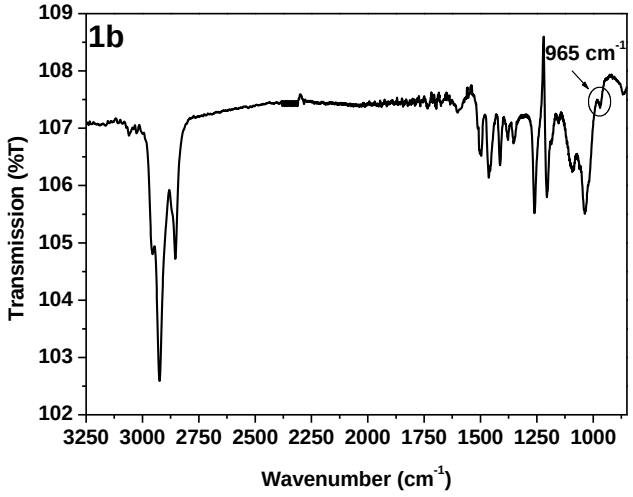

Figure 1b. FT-IR spectrum (b) of MPE-PPV.

3.2. Thermal Analysis

The thermal properties and phase behavior of MPE-PPV:[60]PCBM blends were investigated by means of MTDSC and RHC, which is a useful tool to investigate the glass transition of semi-crystalline samples due to its extremely high scan rate (about 2000 K min^{-1}). Both techniques were used to investigate crystallization, melting, and glass transition of the PPV:fullerene blends, with an emphasis on the different component miscibilities and possible phase separation. Differences in extent of phase separation can account for possible deviating performances of the corresponding polymer solar cells made from these blends.

In general, the initial morphology of deposited blend films is the result of a kinetically frozen phase separation or crystallization. Consequently, both thermodynamic and kinetic parameters are responsible for the morphology obtained.[28–30] The phase behavior of such blends with a well-defined thermal history is important to understand and (ultimately) control morphology development, long-term stability of the film morphology, and the photovoltaic performance of the corresponding solar cells.[31,32.]

Figure 2a shows MTDSC apparent specific heat capacity (c_p^{app}) curves of MPE-PPV:[60]PCBM blends over the full composition range. From these curves, the

crystallization and melting behavior of these blends can be seen. The pure MPE-PPV sample is amorphous, thus neither crystallization nor melting can be seen. Pure [60]PCBM samples are semi-crystalline, as reported before.[33] Therefore, both the crystallization and melting in the blends can be attributed to the fullerene component rather than the MPE-PPV polymer. All samples were quenched at about 100 K min^{-1} to reduce the crystallinity and enhance the visibility of the glass transition. Although the crystallinity only decreased slightly due to the high crystallization rate of [60]PCBM, clear glass transitions could be seen for all the blends and pure components.

To study if phase separation occurred in MPE-PPV:[60]PCBM blends, RHC was used.[34,35] Figure 2b shows the RHC heat flow (HF) curves for the blends. It can clearly be seen that only RHC can completely avoid crystallization of the PPV:[60]PCBM blends due to its considerably enhanced cooling rate (about 2000 K min^{-1}) compared to regular DSC (about 100 K min^{-1} without the use of liquid nitrogen). No melting peaks can be distinguished for the MPE-PPV:[60]PCBM blends, not even with high weight fractions of [60]PCBM ($f_w^{[60]PCBM}$).

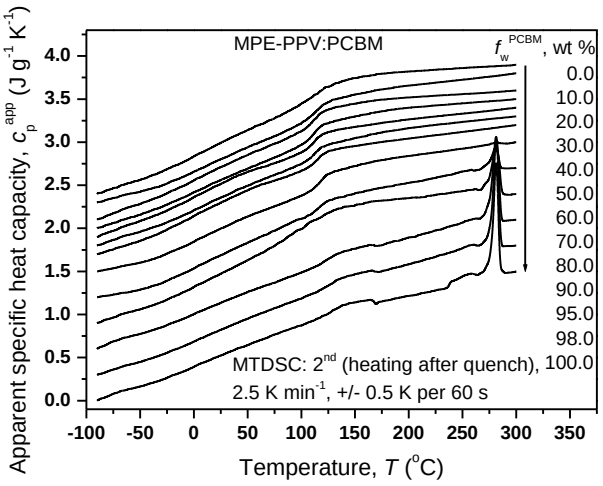

Figure 2a. MTDSC thermograms showing c_p^{app} during heating after quenching for MPE-PPV:[60]PCBM blends with various $f_w^{[60]PCBM}$. All curves are shifted vertically for clarity.

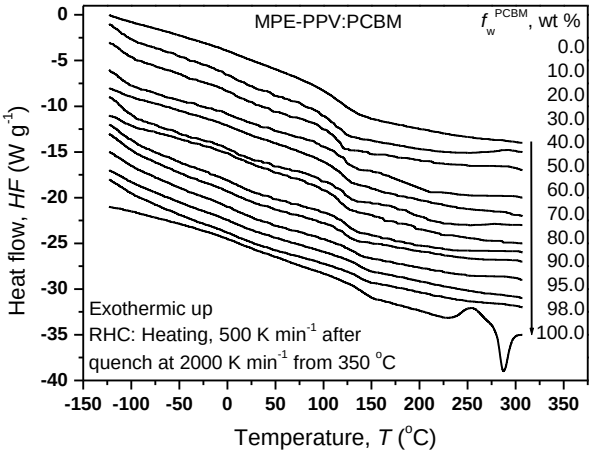

Figure 2b. RHC thermograms showing *HF* during heating after quenching for MPE-PPV:[60]PCBM blends with various $f_w^{[60]PCBM}$. All curves are shifted vertically for clarity.

Figure 3 summarizes all the characteristic temperatures of crystallization and melting: melt crystallization temperature (T_{mc}), cold crystallization temperature (T_{cc}), melting temperature (T_m) and glass transition temperature (T_g). It can clearly be observes that the T_{mc} increases with increasing $f_w^{[60]PCBM}$. The T_{cc} decreases slightly with increasing $f_w^{[60]PCBM}$. For the T_m, the peak area always increases with increasing $f_w^{[60]PCBM}$. Figure 3 shows the evolution of T_g with increasing $f_w^{[60]PCBM}$ for the blends. Pure [60]PCBM has a high T_g (about 131.2 °C), whereas neat MPE-PPV also shows a rather high T_g of about 111.2 °C. All the blends have a T_g in between those of the pure components.

In previous studies, it was demonstrated that MDMO-PPV:[60]PCBM blends show a clear double T_g, which is an obvious indication of phase separation in the molten state.[19,29,36] For the MPE-PPV:[60]PCBM blends, it was also supposed that phase separation occurs in the molten state due to the similar molecular structures. However, no clear double T_g was observed in our experiments, probably due to the very close T_g's of MPE-PPV and[60]PCBM. The gap of only ~20.0 °C is too small to see two separate glass transition steps since one T_g interval can be as wide as 50 °C.

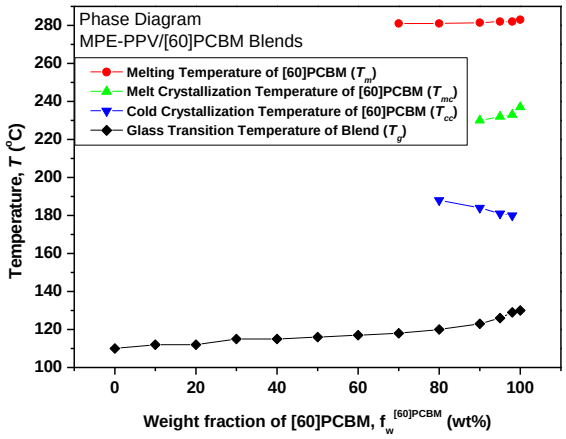

Figure 3. Dependence of the characteristic temperatures T_{mc}, T_{cc}, T_m, and T_g, measured by (MT)DSC, on the $f_w^{[60]PCBM}$ for MPE-PPV:[60]PCBM blends.

3.3. Device Characterization

Non-optimized bulk heterojunction solar cells, combining one out of two different conjugated polymers, MDMO-PPV or MPE-PPV with [60]PCBM (1:4 ratio), were made, with a general ITO/PEDOT-PSS/polymer:[60]PCBM/Ca/Al structure. Table 1 shows the initial values of short circuit current, fill factor, open circuit voltage and the efficiency of the solar cells. The initial IV-curves are depicted in Figure 4. The initial efficiencies were in the range of 1.3% for both PPV polymers. These first devices were, however, not optimized for maximum performance.

Table 1. Values of short circuit current (I_{sc}), open circuit voltage (V_{oc}), fill factor (FF) and power conversion efficiency (η) for MPE-PPV:[60]PCBM and MDMO-PPV:[60]PCBM (1:4) solar cells , spincoated from chlorobenzene (initial values and values after thermal annealing).

Polymer:[60]PCBM (1:4)	Annealing	I_{sc} (mA/cm^2)	V_{oc} (V)	FF	η (%)
MPE-PPV:[60]PCBM	0 h (25 °C)	4.14	0.783	0.40	1.30
	100 h at 90 °C	3.38	0.692	0.39	0.91
	100 h at 130 °C	2.92	0.713	0.37	0.76
MDMO-PPV:[60]PCBM	0 h (25 °C)	2.87	0.785	0.60	1.3
	100 h at 90 °C	1.70	0.710	0.43	0.52
	100 h at 130 °C	2.18	0.605	0.37	0.49

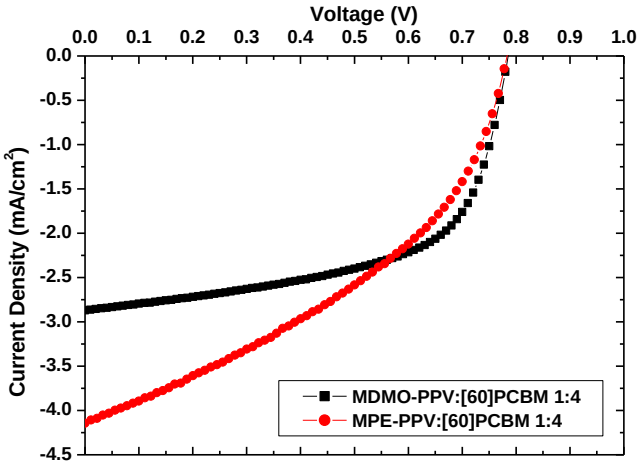

Figure 4. Current-voltage characteristics obtained for MPE-PPV:[60]PCBM and MDMO-PPV:[60]PCBM (1:4) solar cells under AM 1.5 illumination.

When these solar cells are to be used outdoors in full sunlight, the devices must be able to withstand the high temperatures (possibly up to 75 °C) reached in such case. Previous studies already demonstrated that the poor thermal stability of MDMO-PPV:[60]PCBM solar cells resulted in a gradual decrease of the efficiency upon heating.[22,23] To this end, our aim was to

investigate if the use of high T_g MPE-PPV as a donor material would result in a better thermal stability of the device. It is expected that, although the initial efficiency values are about the same for both devices, the MPE-PPV:[60]PCBM solar cells will have a better resistance towards high temperatures than MDMO-PPV:[60]PCBM based solar cells.

To verify this hypothesis, the devices were annealed at 2 different temperatures, either 90 °C or 130 °C, in a dark nitrogen atmosphere for 100 h. During the annealing treatment, the IV characteristics were monitored at specific time intervals. Figure 5 shows the relative decay of the photovoltaic parameters of both solar cells for the two annealing temperatures. There are clear differences to be noticed. As can be inferred from Figure 5, in most cases the open circuit voltage (V_{oc}) is barely sensitive to the thermal treatment performed over a long period of time. Only thermal annealing of MDMO-PPV:[60]PCBM solar cells at 130 °C resulted in a substantial decrease (23%) of V_{oc} (Figure 5 and Table 1) A relatively small decrease in V_{oc} of about 10% is observed in all other cases. This is consistent with the fact that the V_{oc} mainly depends on material properties, i.e. the ionization potential of the donor polymer and the electron affinity of the acceptor fullerene molecule. After 100 h of annealing at either 90 °C or 130 °C, the short circuit current of the MPE-PPV solar cells showed a decrease of 18% and 29%, respectively. The MDMO-PPV based solar cells suffered more substantially from the annealing process. Annealing at 90 °C resulted in a decrease of 41% of the initial short circuit current after 100 h. Remarkably, annealing at 130 °C resulted in a decrease of only 24% after 100 h. It was also observed that the short circuit current in the time interval between 2 and 10 h started to increase substantially, before the normal decreasing process took over again. A possible hypothesis for this observation is that, due to annealing at 130 °C, the electrical contact between the active layer and PEDOT-PSS was enhanced, thereby reducing the amount of recombination losses. Such an observation was already observed previously for MDMO-PPV:PCNEPV active layers.[37] This could explain the increase in I_{sc} during some time interval and the higher than expected I_{sc} value at the end of the measurement. After 100

h of annealing at either 90 °C or 130 °C, the fill factor of the MPE-PPV solar cells showed a decrease of only 2% and 7%, respectively. The fill factor of MDMO-PPV solar cells decreased 28% when annealed for 100 h at 90 °C, and 38% when annealed at 130 °C for 100 h. Finally, the overall efficiency, being proportional to the short-circuit current and the fill factor, is much more stable for MPE-PPV based solar cells (a decrease of 30% after 100 h of annealing at 90 °C and a decrease of 42% after 100 h of annealing at 130 °C) as compared to MDMO-PPV based solar cells (a decrease of 61% after 100 h of annealing at 90 °C and a decrease of 64% after 100 h of annealing at 130 °C). These results are consistent with earlier reported observations on a commercial high *Tg* PPV.[22,23]

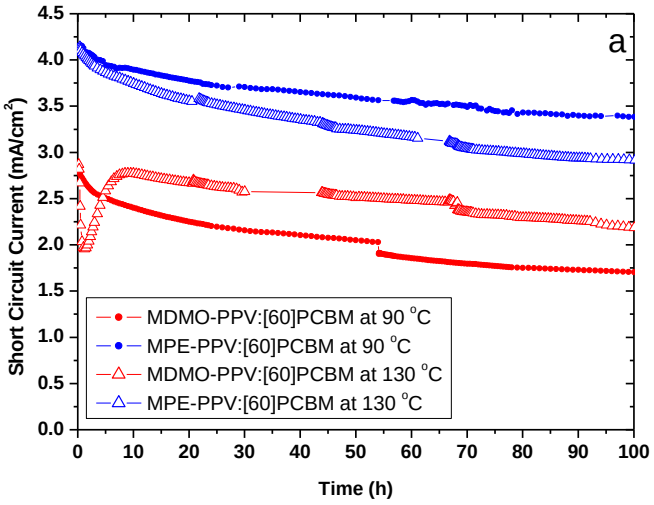

Figure 5a. Relative decay of short circuit current I_{sc} for MDMO-PPV:[60]PCBM (1:4) solar cells (red) and MPE-PPV:[60]PCBM (1:4) solar cells (blue), during annealing at 90 °C (circles) and 130 °C (triangles).

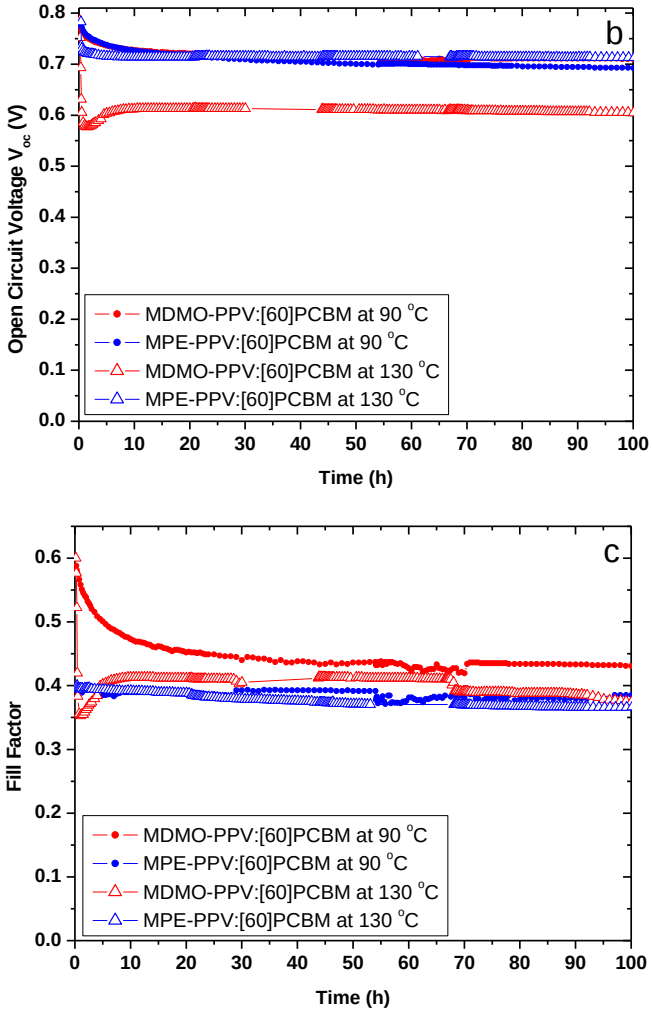

Figures 5c and 5d. Relative decay of open circuit voltage V_{oc} (b) and fill factor (c) for MDMO-PPV:[60]PCBM (1:4) solar cells (red) and MPE-PPV:[60]PCBM (1:4) solar cells (blue), during annealing at 90 °C (circles) and 130 °C (triangles).

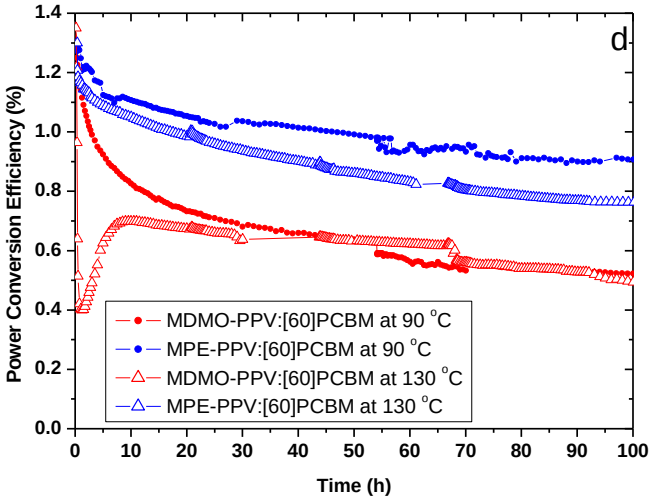

Figure 5d. Relative decay of power conversion efficiency (d) for MDMO-PPV:[60]PCBM (1:4) solar cells (red) and MPE-PPV:[60]PCBM (1:4) solar cells (blue), during annealing at 90 °C (circles) and 130 °C (triangles).

The higher thermal stability of the MPE-PPV solar cells is not only revealed in the photovoltaic parameters, but also in the bulk morphology of the active layer. The blend morphology of both types of solar cells was studied with TEM (Figure 6). For the MDMO-PPV:[60]PCBM blend, large [60]PCBM-clusters (dark areas) formed very rapidly upon annealing at 130 °C.[19] The selected area electron diffraction (SAED) patterns (insets in Figure 6) indicated that the clusters were groups of single [60]PCBM crystals. After only 0.5 h of annealing at 130 °C the homogeneous MDMO-PPV:[60]PCBM matrix disappeared. All the [60]PCBM has diffused out of the blend and assembled in the [60]PCBM-clusters. The same process occurred upon annealing at 90 °C, only slower (see Supporting Information). After 20 h of annealing at 90 °C, [60]PCBM crystals were formed. Due to the smaller interfacial area between donor and acceptor material the photocurrent output decreased, as was demonstrated above. The TEM images of the active layer of the MPE-PPV solar cells (Figure 6') show a much more stable morphology. The film had to be annealed for 20 h before a [60]PCBM-cluster was detected. It is assumed that, due to the considerably lower T_g (45 °C) of MDMO-PPV, the [60]PCBM is able to

crystallize at a higher rate in MDMO-PPV:[60]PCBM active layers than in high T_g MPE-PPV:[60]PCBM active layers. When the solar cell is subjected to temperatures below the T_g of the applied polymer, the matrix will remain rather stiff and the fullerene molecules are restricted to move freely. Thermal treatments near or above T_g cause the matrix to become soft, rendering it much easier for the fullerene molecules to move and cluster.

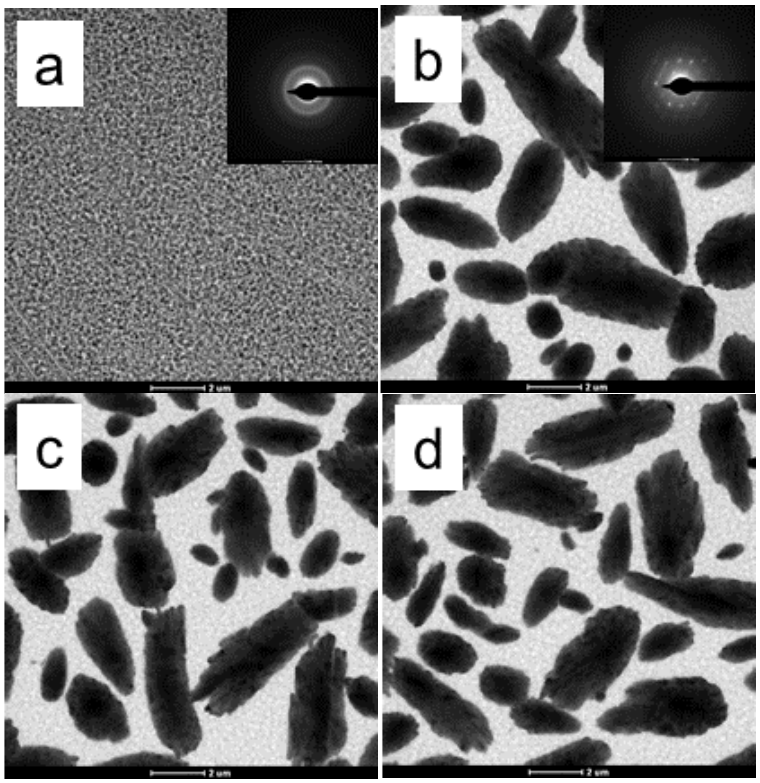

Figure 6. Bright-Field TEM images of the active layer of MDMO-PPV:[60]PCBM (1:4) solar cells, spincoated from chlorobenzene, after annealing at 130 °C for 0 h (a), 0.5 h (b), 4 h (c) and 20 h (d) (scale bar: 2 μm). Insets: SAED patterns of matrix (a) and [60]PCBM clusters (b).

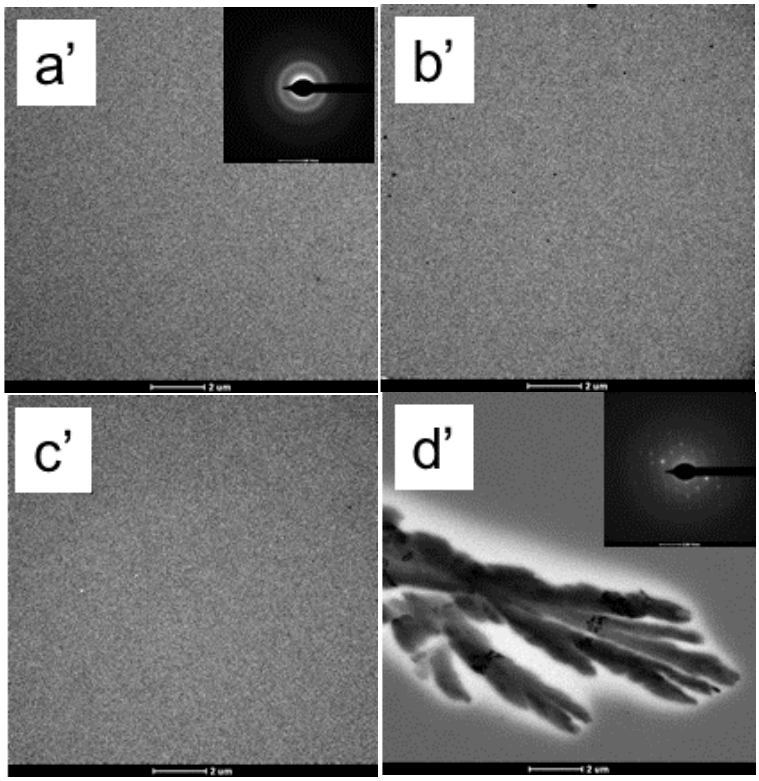

Figure 6'. Bright-Field TEM images of the active layer of MPE-PPV:[60]PCBM (1:4) solar cells, spincoated from chlorobenzene, after annealing at 130 °C for 0 h (a'), 0.5 h (b'), 4 h (c') and 20 h (d') (scale bar: 2 μm). Insets: SAED patterns of matrix (a') and [60]PCBM clusters (d').

As can be observed from the TEM images, the MPE-PPV:[60]PCBM solar cells do not exhibit an initial fine nanoscale phase separation, as compared to MDMO-PPV:[60]PCBM solar cells. This correlates also with the quite low fill factor of the obtained MPE-PPV based devices (FF = 0.40) compared to MDMO-PPV based solar cells (FF = 0.60). In order to improve this initial morphology, an optimization study was performed whereby the active layers were spincoated from either chloroform, chlorobenzene or toluene. Because of the varying solubility characteristics of both the polymer and fullerene materials in the different solvents, the initial morphology of the active layer will be influenced to a large extent. In addition, not only [60]PCBM was used as an

electron acceptor, but also the [70]PCBM derivative, which in some solvents can crystallize more easily than [60]PCBM. The results are shown in Table 2 and Figure 7.

Table 2. Values of short circuit current (I_{sc}), open circuit voltage (V_{oc}), fill factor (FF) and power conversion efficiency (η) for different MPE-PPV:fullerene (1:4) solar cells and a reference MDMO-PPV:[70]PCBM (1:4) solar cell, spincoated from different solvents, at room temperature. The currents reported are corrected for spectral mismatch.[8]

Polymer:Fullerene (1:4)	Processing Solvent	I_{sc} (mA/cm^2)	V_{oc} (V)	FF	η (%)
MPE-PPV:[60]PCBM	chloroform	3.31	0.84	0.45	1.25
MPE-PPV:[60]PCBM	chlorobenzene	2.87	0.83	0.42	1.00
MPE-PPV:[60]PCBM	toluene	3.14	0.78	0.42	1.03
MPE-PPV:[70]PCBM	chloroform	5.66	0.85	0.48	2.31
MPE-PPV:[70]PCBM	chlorobenzene	5.36	0.85	0.48	2.19
MPE-PPV:[70]PCBM	toluene	4.87	0.80	0.47	1.83
MDMO-PPV:[70]PCBM	1,2-dichlorobenzene	6.52	0.80	0.57	2.97

From the IV data, it can be derived that the use of [70]PCBM as the acceptor resulted in a substantial improvement of the device performance, mainly due to an improved light absorption of [70]PCBM, compared to [60]PCBM.[38] Consequently, higher current densities in the corresponding photovoltaic cells are observed. This was already demonstrated previously for MDMO-PPV:[70]PCBM solar cells, for which 1,2-dichlorobenzene proved to be the best processing solvent.[39] The IV characteristics have been added to Table 2 for comparison. Furthermore, the fill factor of MPE-PPV:[70]PCBM solar cells could be increased to 0.47, indicating an improved initial nanoscale phase separated morphology. Chloroform was found to be the best processing solvent for MPE-PPV:fullerene solar cells, and the most efficient device displayed an efficiency of 2.3%, after correction for spectral mismatch.[8] Whether this optimized MPE-PPV:[70]PCBM solar cell exhibits a comparable thermal stability as measured for the initial MPE-PPV:[60]PCBM devices, will be the subject of a follow-up study.

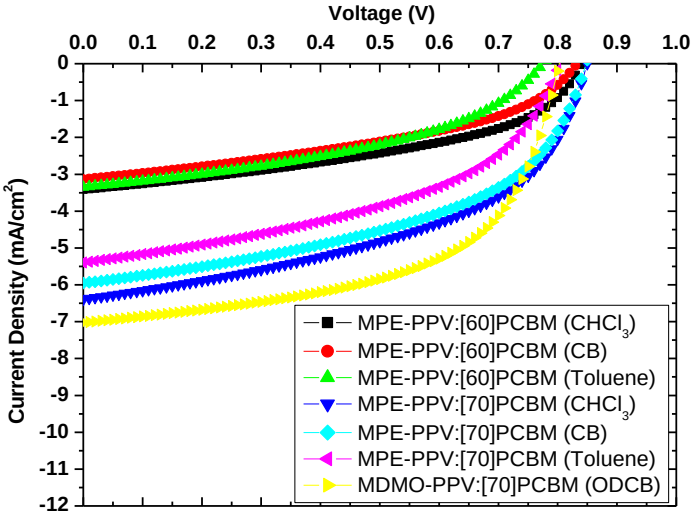

Figure 7. Current-voltage characteristics obtained for different MPE-PPV:fullerene (1:4) solar cells and a reference MDMO-PPV:[70]PCBM (1:4) solar cell under AM 1.5 illumination (not corrected for spectral mismatch).

4. Conclusions

A novel high *T*g PPV polymer, poly[2-methoxy-5-(2'-phenylethoxy)-1,4-phenylene vinylene] (MPE-PPV), has been synthesized by an efficient three-step Gilch protocol, and has been explored as a donor material in bulk heterojunction solar cells. We have compared the thermal stability of the nanomorphology of MDMO-PPV:fullerene and MPE-PPV:fullerene blends and analyzed the solar cell efficiencies of devices made from these blends. It can be concluded that devices based on high T_g MPE-PPV clearly outperform the MDMO-PPV:[60]PCBM based solar cells in terms of a (thermally) more stable bulk (nano)morphology and a longer life-time. For the MPE-PPV:[60]PCBM active layer, the stiffer polymer matrix reduces the movement of the fullerene molecules, thereby slowing down the detrimental phase separation process and maintaining a large interfacial area between donor and acceptor. It has hence been shown that the use of a high T_g polymer is an effective way towards the development of more stable and efficient organic photovoltaic devices. Using [70]PCBM instead of [60]PCBM as acceptor resulted in a 70%

increase in current density and device efficiency, with an optimized MPE-PPV:[70]PCBM device efficiency of 2.3%.

5. Acknowledgments

The authors gratefully acknowledge the Fund for Scientific Research-Flanders (FWO) and the Belgian Science Policy (BELSPO) in the frame of network IAP P6/27, initiated by the Belgian State Prime Minister's Office, for their financial support. We also want to thank the Institute for the Promotion of Innovation by Science and Technology in Flanders (IWT) for the financial support via the IWT-SBO project 060843 "Polyspec".

6. Supporting Information

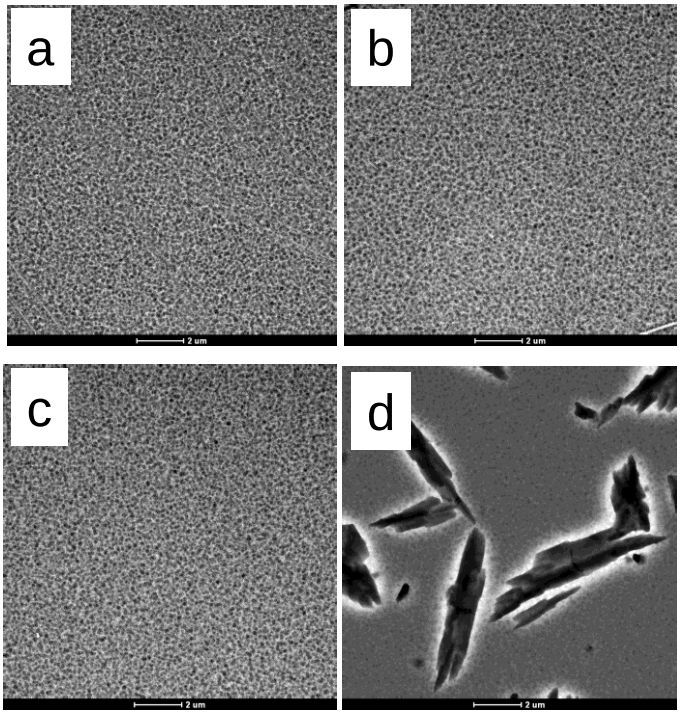

Figure 8. Bright-Field TEM images of the active layer of MDMO-PPV:[60]PCBM 1:4 solar cells, spincoated from chlorobenzene, after annealing at 90 °C for 0 h (a), 0.5 h (b), 4 h (c) and 20 h (d). (scale bar: 2 μm).

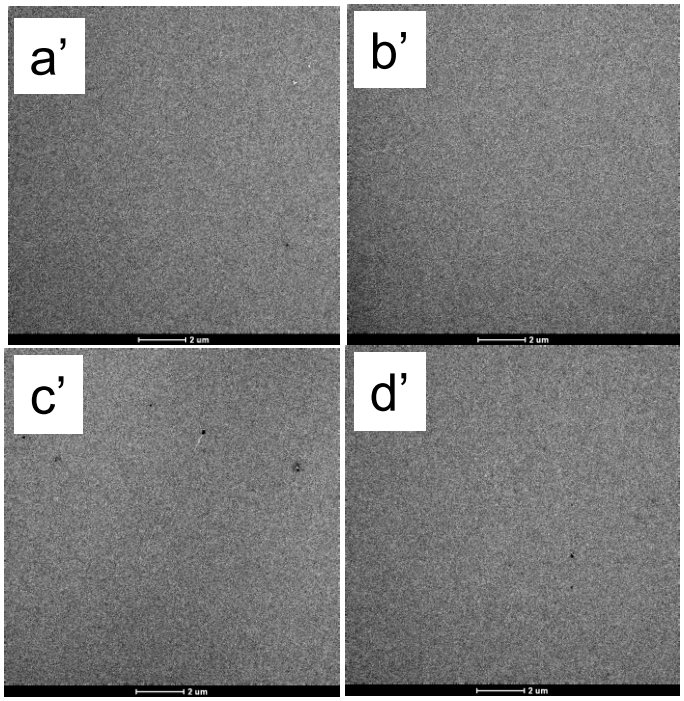

Figure 8'. Bright-Field TEM images of the active layer of MPE-PPV:[60]PCBM 1:4 solar cells, spincoated from chlorobenzene, after annealing at 90 °C for 0 h (a'), 0.5 h (b'), 4 h (c') and 20 h (d'). (scale bar: 2 μm).

7. References and Notes

(1) Yu, G.; Gao, J.; Hummelen, J. C.; Wudl, F.; Heeger, A. J. *Science* **1995**, *270*, 1789–1791.

(2) Roman, L. S.; Andersson, M. R.; Yohannes, T.; Inganas, O. *Adv. Mater.* **1997**, *9*, 1164–1168.

(3) Shaheen, S. E.;Brabec, C. J.; Sariciftci, N. S.; Padinger, F.; Fromherz, T.; Hummelen, J. C. *Appl. Phys. Lett.* **2001**, *78*, 841–843.

(4) Munters, T.; Martens, T.; Goris, L.; Vrindts, V.; Manca, J.; Lutsen, L.; De Ceuninck, W.; Vanderzande, D.; De Schepper, L.; Gelan, J.; Sariciftci, N. S.; Brabec, C. J. *Thin Solid Films* **2002**, *403-404*, 247–251.

(5) Ma, W.; Yang, C.; Gong, X.; Lee, K.; Heeger, A. J. *Adv. Funct. Mater.* **2005**, *15*, 1617–1622.

(6) Padinger, F.; Fromherz, T.; Denk, P.; Brabec, C. J.; Zettner, J.; Hierl, T.; Sariciftci, N. S. *Synthetic Met.* **2001**, *121*, 1605–1606.

(7) Neugebauer, H.; Brabec, C. J.; Hummelen, J. C.; Janssen, R. A. J.; Sariciftci, N. S. *Synthetic Met.* **1999**, *102*, 1002–1003.

(8) Kroon, J. M.; Wienk, M. M.; Verhees, W. J. H.; Hummelen, J. C. *Thin Solid Films* **2002**, *403-404*, 223–228.

(9) Krebs, F. C.; Carlé, J. E.; Cruys-Bagger, N.; Andersen, M.; Lilliedal, M. R.; Hammond, M. A.; Hvidt, S. *Sol. Energ. Mat. Sol. C.* **2005**, *86*, 499–516.

(10) Schuller, S.; Schilinsky, P.; Hauch, J.; Brabec, C. J. *Appl. Phys. A. Mater.* **2004**, *79*, 37–40.

(11) Neugebauer, H.; Brabec, C.; Hummelen, J. C.; Sariciftci, N. S. *Sol. Energ. Mat. Sol. C.* **2000**, *61*, 35–42.

(12) Camaioni, N.; Ridolfi, G.; Casalbore-Miceli, G.; Possamai, G.; Garlaschelli, L.; Maggini, M. *Sol. Energ. Mat. Sol. C.* **2003**, *76*, 107–113.

(13) Hoppe, H.; Sariciftci, N. S. *J. Mater. Res.* **2004**, 19, 1924–1945.

(14) Zhu, Z.; Hadjikyriacou, S.; Waller, D.; Gaudiana, R. *J. Macromol. Sci. Pure.* **2004**, *41*, 1467–1487.

(15) Krebs, F. C.; Spanggaard, H. *Chem. Mater.* **2005**, *17*, 5235–5237.

(16) Krebs, F. C.; Norrman, K. *Prog. Photovoltaics* **2007**, *15*, 697–712.

(17) Conings, B.; Bertho, S.; Vandewal, K.; Senes, A.; D'Haen, J.; Manca, J.; Janssen, R. A. J. *Appl. Phys. Lett.* **2010**, *96*, 163301.

(18) Yang, X.; van Duren, J. K. J.; Rispens, M. R.; Hummelen, J. C.; Janssen, R. A. J.; Michels, M. A. J.; Loos, J. *Adv. Mater.* **2004**, *16*, 802–806.

(19) Yang, X.; van Duren, J. K. J.; Janssen, R. A. J.; Michels, M. A. J.; Loos, J. *Macromolecules* **2004**, *37*, 2151–2158.

(20) Yang, X.; Loos, J.; Veenstra, S. C.; Verhees, W. J. H.; Wienk, M.; Kroon, J. M.; Michels, M. A. J.; Janssen, R. A. J. *Nano Lett.* **2005**, *5*, 579–583.

(21) Campo, B.; Oosterbaan, W.; Gilot, J.; Cleij, T.; Lutsen, L.; Janssen, R. A. J.; Vanderzande, D. *Proc. SPIE* **2009**, *7416*, 74161G.

(22) Bertho, S.; Haeldermans, I.; Swinnen, A.; Moons, W.; Martens, T.; Lutsen, L.; Vanderzande, D.; Manca, J.; Senes, A.; Bonfiglio, A. *Sol. Energ. Mat. Sol. C.* **2007**, *91*, 385–389.

(23) Bertho, S.; Janssen, G.; Cleij, T. J.; Conings, B.; Moons, W.; Gadisa, A.; D'Haen, J.; Goovaerts, E.; Lutsen, L.; Manca, J.; Vanderzande, D. *Sol. Energ. Mat. Sol. C.* **2008**, *92*, 753–760.

(24) Deimede, V.; Kallitsis, J. K.; Pakula, T. *J. Polym. Sci. Part A: Polym. Chem.* **2001**, *39*, 3168–3179.

(25) Strukelj, M.; Papadimitrakopoulos, F.; Miller, T. M.; Rothberg, L. J. *Science* **1995**, *267*, 1969–1972.

(26) Johansson, D. M.; Srdanov, G.; Yu, G.; Theander, M.; Inganas, O., Andersson, R. M. *Macromolecules* **2000**, *33*, 2525–2529.

(27) Gilch, H. G.; Wheelwright, W. L. *J. Polym. Sci.* **1966**, *4*, 1337–1349.

(28) Thompson, B. C.; Fréchet, J. M. J. *Angew. Chem. Int. Ed.* **2008**, *47*, 58–77.

(29) Yang, X.; Loos, J. *Macromolecules* **2007**, *40*, 1353–1362.

(30) Moulé, A. J.; Meerholz, K. *Adv. Mater.* **2008**, *20*, 240–245.

(31) Mueller, C.; Ferenczi, T. A. M.; Campoy-Quiles, M.; Frost, J. M.; Bradley, D. D. C.; Smith, P.; Stingelin-Stutzmann, N.; Nelson, J. *Adv. Mater.* **2008**, *20*, 3510–3515.

(32) Kim, J. Y.; Frisbie, C. D. *J. Phys. Chem. C* **2008**, *112*, 17726–17736.

(33) Zhao, J.; Swinnen, A.; Van Assche, G.; Manca, J.; Vanderzande, D.; Van Mele, B. *J. Phys. Chem. B* **2009**, *113*, 1587–1591.

(34) Danley, R. L.; Caulfield, P. A.; Aubuchon, S. R. *Am. Lab.* **2008**, *40*, 9–11.

(35) Miltner, H. E.; Grossiord, N.; Lu, K.; Loos, J.; Koning, C. E.; Van Mele, B. *Macromolecules* **2008**, *41*, 5753–5762.

(36) Zhao, J.; Bertho, S.; Vandenbergh, J.; Van Assche, G.; Manca, J.; Vanderzande, D.; Cleij, T.; Lutsen, L.; Van Mele, B. *Phys. Chem. Chem. Phys.* **2011**, accepted.

(37) Veenstra, S. C.; Verhees, W. J. H.; Kroon, J. M.; Koetse, M. M.; Sweelssen, J.; Bastiaansen, J. J. A. M.; Schoo, H. F. M.; Yang, X.; Alexeev, A.; Loos, J.; Schubert, U. S.; Wienk, M. M. *Chem. Mater.* **2004**, *16*, 2503–2508.

(38) Arbogast, J. W.; Foote, C. S. *J. Am. Chem. Soc.* **1991**, *113*, 8886–8889.

(39) Wienk, M. M.; Kroon, J. M.; Verhees, W. J. H.; Knol, J.; Hummelen, J. C.; van Hal, P. A.; Janssen, R. A. J. *Angew. Chem. Int. Ed.* **2003**, *42*, 3371–3375.

Chapter 7

A Quest for Controlling Molecular Weight

ABSTRACT: Since precursor routes based on a radical polymerization usually yield high molecular weight materials, the resulting PPV derivatives sometimes exhibit solubility problems. This may cause the failure of post-polymerization reactions, and any further functionalization of the PPV derivatives becomes troublesome. Therefore, a protocol needs to be developed to effectively control the molecular weight of PPV's, synthesized via precursor routes. This study describes some first attempts to gain insights into the reaction mechanism and polymerization kinetics of both the dithiocarbamate and sulfinyl precursor routes. As a first step, the influence of altering the reaction parameters such as temperature and concentration and the resulting effects on conversion and molecular weight are studied. Lowering the reaction temperature and diluting the premonomer concentration both lead to lower molecular weights but also decrease the conversion towards polymer. It is shown that the polymerization reaction of the sulfinyl route exhibits very fast reaction kinetics. Since the formation of the *p*-quinodimethane system is an important step of the polymerization reaction, a kinetic UV-vis study is carried out for both precursor routes, to reveal the formation and subsequent polymerization of the *p*-quinodimethane monomers. Out of these results, rate coefficients can be calculated via kinetic modeling of the polymerization reaction. In a first attempt to slow down the reaction kinetics of the sulfinyl route and to control the molecular weight, chain transfer reagents have been added to the reaction mixture and the effects on molecular weight, conversion and reaction time have been monitored. Finally, the reaction mixtures have been studied with ESI-MS to reveal the nature of the present molecules and gain more insight into the reaction mechanism.

1. Introduction

Globally, a lot of research is currently devoted to conjugated polymers, among which poly(*p*-phenylene vinylene)s (PPV's) have gained a lot of interest due to their luminescence behaviour.[1–22] PPV's are usually synthesised using precursor routes yielding precursor polymers that are subsequently converted into conjugated structures in an additional step.[23–34] The precursor polymer is formed through polymerization of a *p*-quinodimethane system that is produced through a base induced treatment of a *p*-xylene derivative. Within our research group, the sulfinyl and dithiocarbamate precursor routes towards PPV's were developed, which both lead to excellent conjugated materials with high molecular weights and low defect levels.[35,36]

Recently, our research unit published some first results on the post-polymerization functionalization of a novel copolymer of poly(2-methoxy-5-(3,7-dimethyloctyloxy)-1,4-phenylene vinylene) (MDMO-PPV) and poly(1,4-(2-(5-carboxypentyloxy)-5-methoxy)-phenylene vinylene) (CPM-PPV) (Figure 1).[37] The MDMO-CPM-PPV copolymer was synthesized via the sulfinyl precursor route. For the copolymer with MDMO/CPM ratio 9/1, the post-polymerization functionalization of the acid-groups was successful. A broad variety of functional groups could be built in via this procedure. However, only the 9/1 MDMO-CPM-PPV copolymer showed sufficient solubility in common organic solvents such as THF, $CHCl_3$ and chlorobenzene. A higher ratio of CPM monomers resulted in reduced solubility and as a consequence hampered further functionalization reactions via post-polymerization.

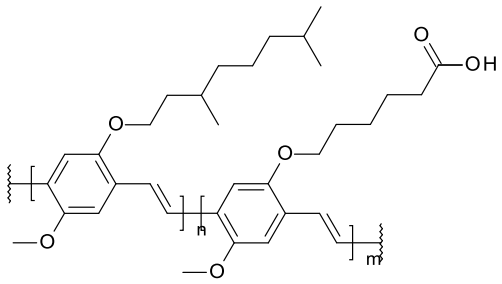

Figure 1. Molecular structure of the MDMO-CPM-PPV copolymer with n/m=9/1.

The proposed hypothesis for these solubility problems states that the molecular weight of the PPV copolymers probably is too high. Therefore, a procedure to control the molecular weight of the PPV derivative needs to be developed. To this end, the polymerization mechanism and reaction kinetics need to be extensively studied before any attempts to control the precursor routes can be induced.

In this study, both the sulfinyl and dithiocarbamate precursor routes are investigated. Firstly, the effect of changing the reaction conditions is described. Furthermore, a kinetic UV-vis study is executed to gain insights in the rate coefficient of the *p*-quinodimethane formation. Subsequently, the effect of adding chain transfer reactions to the sulfinyl polymerization mixture, is described. Finally, the dithiocarbamate and sulfinyl reaction mixtures are investigated with electron spray ionization – mass spectrometry (ESI-MS) to observe which molecules are present and to obtain more information about the reaction mechanism.

2. Experimental Section

2.1. General Data

Unless otherwise stated, all reagents and chemicals were obtained from commercial sources (Acros and Aldrich) and used without further purification. Tetrahydrofuran (THF) was dried by distillation from sodium/benzophenone. NMR spectra were recorded with a Varian Inova 300 spectrometer at 300 MHz

for ^{1}H NMR and at 75 MHz for ^{13}C NMR using a 5 mm probe. Analytical size exclusion chromatography (SEC) was performed using a Spectra series P100 (Spectra Physics) pump equipped with two mixed-B columns (10 µm, 0.75 cm x 30 cm, Polymer Laboratories) and a refractive index detector (Shodex) at 40°C. THF was used as the eluent at a flow rate of 1.0 mL/min. Molecular weight distributions are given relative to polystyrene standards. FT-IR spectra were collected with a Perkin-Elmer Spectrum One FT-IR spectrometer (nominal resolution 4 cm-1, summation of 16 scans).

The UV-vis measurements on the *p*-quinodimethane formation were performed on a Cary 500 UV-vis-NIR spectrophotometer equipped with a stop-flow module allowing very fast measurements. A 10^{-4} M solution of the sulfinyl premonomer in 2-butanol and $5*10^{-3}$ M solution of the dithiocarbamate premonomer in THF were prepared. The Na*t*BuO and LHMDS solutions in 2-BuOH and THF, respectively, were prepared with different concentrations from stock solutions. Both monomer and base solutions were degassed by nitrogen flushing. For each precursor route, both monomer and base solutions were injected simultaneously whereupon the monitoring of the signals of interest was started.

The ESI-MS Spectra were recorded on an LCQ mass spectrometer (Finigian MAT) equipped with an atmospheric pressure ionization source operating in the nebulizer assisted electro spray mode. The instrument was calibrated in the m/z range 220-2000 using a standard containing caffeine, MRFA and Ultramark 1621. A constant spray voltage of 4.5 kV was used and nitrogen at a dimensionless auxiliary gas flow-rate of 10 and a dimensionless sheath gas flow-rate of 60 were applied. The capillary voltage, the tube lens offset voltage and the capillary temperature were set to 34 V, 10 V and 270 °C respectively. A 250 µL aliquot of a polymer solution with concentration of 1 mg mL^{-1} was injected. A mixture of dichloromethane and methanol (DCM:MeOH = 1:3), all HPLC grade, were used as solvent.

2.2. Synthesis

Synthesis of premonomers *p-Xylylene bis(N,N-diethyldithiocarbamate) (**1**)*, *1-(Chloromethyl)-4-[(n-octylsulfinyl)methyl]benzene (**2**)*, *2,5-Bis(N,N-diethyl dithiocarbamate-methyl)-1-(3,7-dimethyloctyloxy)-4-methoxybenzene (**3**)* and the mixture of two isomers *2-[(n-Octylsulfinyl)methyl]-5-(chloromethyl)-1-(3,7-dimethyloctyloxy)-4-methoxybenzene (**4a**)* and *2-[(n-Octylsulfinyl) methyl]-5-(chloromethyl)-4-(3,7-dimethyloctyloxy)-1-methoxybenzene (**4b**)* was reported elsewhere (Figure 2).[32,35,38,39] All properties were in agreement with the previously reported materials.

RAFT agent *S-benzyl dithiobenzoate* (**5**) was synthesized according to a literature procedure.[40]

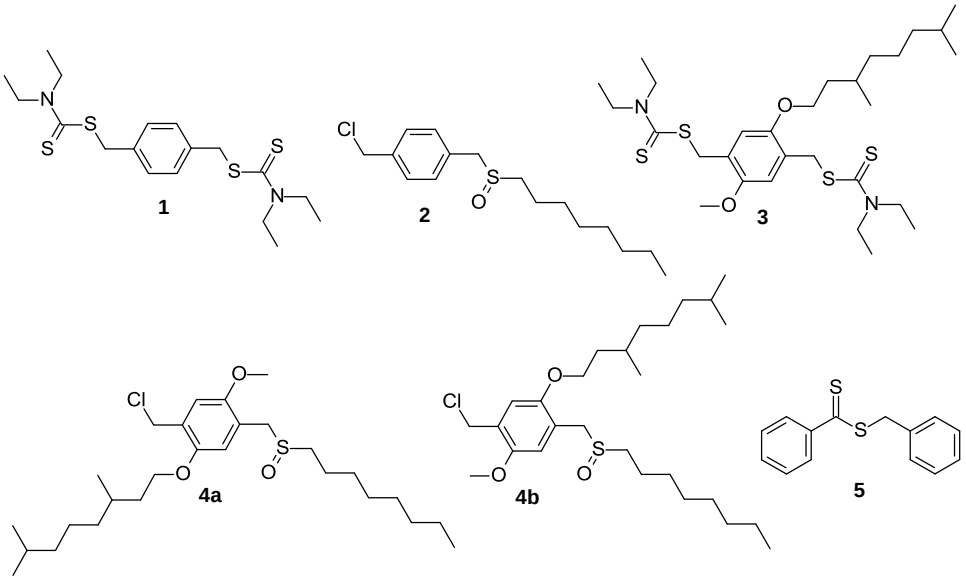

Figure 2. Molecular structures of plain dithiocarbamate and sulfinyl premonomers **1** and **2**, the alkoxy substituted dithiocarbamate and sulfinyl premonomers **3** and **4** (2 isomers), and RAFT agent S-Benzyldithiobenzoate **5**.

*Synthesis of MDMO Dithiocarbamate Precursor PPV (**6**)*. Bisdithiocarbamate MDMO premonomer **3** (500 mg, 0.851 mmol) was dissolved in dry THF (4.26 mL, 0.2 M or 42.6 mL, 0.02 M). The mixture was stirred at 0 °C or at 35 °C under a continuous flow of nitrogen. 1.5 equiv of a LHMDS solution (1 M in

THF) was added in one go to the stirred monomer solution. After different reaction times (see Figure 3 and Table 1) at 0 °C or at 35 °C under a nitrogen atmosphere, the mixture was subsequently quenched in ice water (100 mL). The excess of base was neutralized with HCl (1 M). The aqueous phase was extracted with $CHCl_3$ (3 x 40 mL). After combination of the organic phases and evaporation of the solvent, the obtained crude polymer was again dissolved in $CHCl_3$ (2 mL) and precipitated in stirred cold methanol (100 mL). The mixture was filtered and the polymer was collected and dried *in vacuo*. The residual fractions mostly contained monomers and cyclic oligomers. Yields: 8%–67%; ^{1}H NMR ($CDCl_3$): 6.97–6.45 (br m, 2H), 5.87–5.50 (br s, 1H), 4.23–3.05 (br m, 11H), 1.02–1.95 (br m, 16H), 1.02–0.74 (m, 9H); ^{13}C NMR ($CDCl_3$): 195.76, 150.85, 127.68, 114.11, 113.09, 67.10, 56.39, 51.98, 49.08, 46.38, 39.27, 37.54, 36.60, 34.45, 29.91, 27.92, 24.67, 22.69, 22.58, 19.66, 12.47, 11.55; IR (NaCl, cm^{-1}): 2953, 2929, 1504, 1484, 1462, 1413, 1267, 1210, 1140, 1041.

*Thermal Elimination of Dithiocarbamate Precursor Polymer **6** to Conjugated MDMO-PPV (**8**)*. From a solution of **6** (160 mg) in 1,2-dichlorobenzene (80 mL) oxygen was removed by purging for 1 h with nitrogen. Subsequently, the solution was heated to 180 °C and stirred for 3 h. After cooling to room temperature, the resulting 1,2-dichlorobenzene was evaporated and the crude polymer mixture was dissolved in chloroform (2 mL). The solution was precipitated drop wise in cold methanol (100 mL). The polymer was filtered off, washed with cold methanol and dried at room temperature under reduced pressure. The conjugated MDMO-PPV **8** was obtained as a red polymer. The elimination procedure was performed a second time to ensure complete elimination. Yields were quantitative; ^{1}H NMR ($C_2D_2Cl_4$): 7.5 (br, 2H) 7.2 (br, 2H) 4.6–3.2 (br m, 5H) 2.1–0.6 (br m; 19H); ^{13}C NMR ($CDCl_3$): 151.4; 127.0; 123.3; 110.5; 108.8; 67.9; 56.4; 39.2; 37.4; 36.6; 30.2; 27.9; 24.6; 22.6; 19.8; IR (KBr, cm^{-1}): 2957, 2925, 2860, 1510, 1469, 1395, 1217, 1028, 872.

*Synthesis of MDMO Sulfinyl precursor PPV (**7**)*. A solution of MDMO sulfinyl premonomer **4** (250 mg, 0.51 mmol) in 2-butanol (3.7 mL) and a solution of

Na*t*BuO (64 mg, 0.67 mmol) in 2-butanol (4.2 mL) were degassed for 1 h at 0 °C or at 30 °C by passing through a continuous stream of nitrogen. The base solution was added in one portion to the stirred monomer solution. After different reaction times (see Figure 4 and Table 2), the reaction mixture was quenched in ice water (100 mL). The excess of base was neutralized with HCl (1 M). The aqueous phase was extracted with $CHCl_3$ (3 x 40 mL). After combination of the organic phases and evaporation of the solvent, the obtained crude polymer was again dissolved in $CHCl_3$ (2 mL) and precipitated in stirred cold methanol (100 mL). The mixture was filtered and the polymer was collected and dried *in vacuo*. The residual fractions mostly contained monomers, solvent-substituted product and cyclic oligomers. Yields: 26%–77%; ^{1}H NMR ($CDCl_3$): 6.90–6.20 (br m, 2H), 4.90/4.60 (br t, 1H), 4.00–2.90 (br m, 7H), 2.70–2.10 (br t, 2H), 1.90–1.10 (br m, 22H), 1.00–0.80 (br m, 12 H); ^{13}C NMR ($CDCl_3$): 151.40, 127.0, 110.50, 67.90, 59.10–55.10, 56.40, 49.70, 39.20, 37.40, 36.60, 32.10–29.10, 30.20, 27.90, 24.60, 22.60, 21.9, 19.80, 13.50.

*Thermal Elimination of Sulfinyl Precursor Polymer **7** to Conjugated MDMO-PPV (**8**).* From a solution of **7** (160 mg) in toluene (20 mL) oxygen was removed by purging for 1 h with nitrogen. Subsequently, the solution was heated to 110 °C and stirred for 3 h. After cooling to room temperature, the resulting orange-red solution was precipitated drop wise in cold methanol (100 mL). The polymer was filtered off, washed with cold methanol and dried at room temperature under reduced pressure. The conjugated MDMO-PPV **8** was obtained as a red polymer. The elimination procedure was performed a second time to ensure complete elimination. Yields were quantitative.

Scheme 1. Synthesis of MDMO-PPV via the Dithiocarbamate and Sulfinyl Precursor Routes

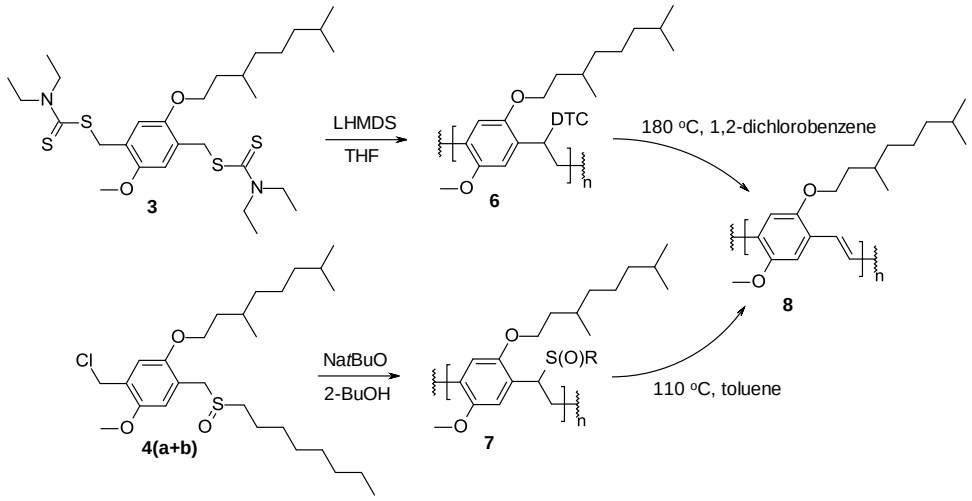

3. Results and Discussion

3.1. Effect of Reaction Parameters

To gain insights in the polymerization kinetics, either the premonomer concentration or the reaction temperature was changed to study the effects on the polymer conversion in function of the reaction time. This way, the optimal reaction time for maximal conversion could be determined. Furthermore, the molecular weight of the obtained MDMO-PPV was compared for the different reaction conditions used.

3.1.1. Dithiocarbamate Route

For the following experiments, the bisdithiocarbamate MDMO premonomer was dissolved in THF. 1.5 Equiv of a solution of LHMDS (1M in THF) were added (Scheme 1). After specific time intervals, samples of the same volume were taken out of the reaction mixture and quenched in ice water. The samples were neutralized, the organic phase was extracted and the solvent was evaporated. The samples containing the crude precursor polymer were dissolved in 1,2-dichlorobenzene and converted into the conjugated MDMO-

PPV via thermal elimination. The resulting MDMO-PPV was precipitated in cold methanol and collected on a filter. The material was dried under vacuum. At this stage, the polymer yield was calculated and the molecular weight was determined.

The standard conditions to execute the polymerization of MDMO-PPV via the dithiocarbamate precursor route are set at a reaction temperature of 35 °C and a premonomer concentration of 0.2 M.[36] Under these conditions, a polymer yield of 67% is achieved after a reaction time of 150 min. When the molecular weight (M_w) of the resulting conjugated MDMO-PPV is plotted in function of the reaction time, it is observed that high M_w material is already formed at the very early stages of polymerization (Figure 3b). This is in full agreement with the proposed chain-growth radical mechanism.[23,27,41–45] Prolonged reaction times lead to higher conversions but no further increase in M_w. Even a somewhat lower M_w is observed after longer reaction times. This can be explained by the increase of the oligomeric fraction and as a result a higher polydispersity.[46]

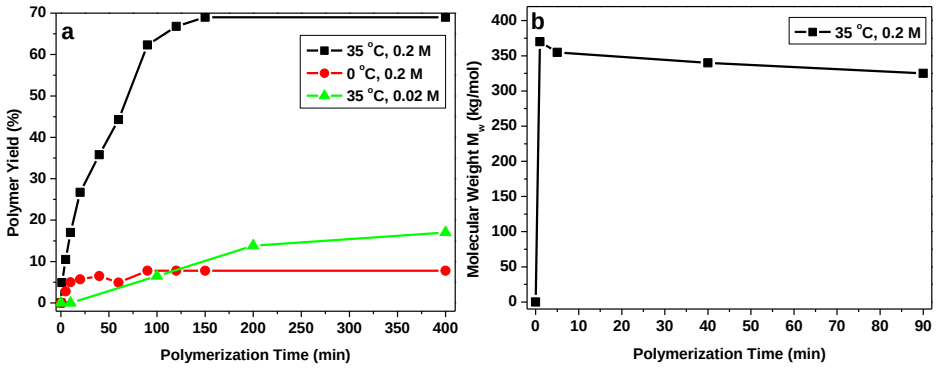

Figure 3. (a) MDMO-PPV polymerization yield in function of reaction time for the dithiocarbamate precursor route, using LHMDS as base. Results are displayed for different premonomer concentrations and reaction temperatures. (b) Molecular weight in function of reaction time.

Secondly, the polymerization reaction was carried out at 0 °C. Lowering the reaction temperature substantially decreased the M_w of the resulting MDMO-

PPV (see Table 1). The optimal reaction time to obtain maximal polymer conversion was found to be 90 min. However, the polymer yield was much lower than under normal polymerization conditions, only 8% was achieved (Figure 3a). Longer reaction times did not further increase this low yield.
Finally, the polymerization was executed using a lower premonomer concentration of 0.02 M, ten times lower than the standard concentration. Again, a lower M_w was obtained under these conditions. Furthermore, the reaction time to reach maximal conversion increased to 400 min, indicating slower reaction kinetics. The polymer yield obtained was only 17%.

Tabel 1. Polymerization Results for the Dithiocarbamate Precursor Route towards MDMO-PPV

Conditions	Reaction Time (min)	Yield (%)	M_w (g/mol)	M_n (g/mol)	PD
35 °C, 0.2 M	150	67	340000	94000	3.6
0 °C, 0.2 M	90	8	75000	29000	2.6
35 °C, 0.02 M	400	17	23000	7000	3.3

3.1.2. Sulfinyl Route

For the experiments on the sulfinyl route, the MDMO sulfinyl premonomer was dissolved in 2-BuOH giving an initial concentration $[M_i]$ (Scheme 1). 1.3 Equiv Na*t*BuO were dissolved in 2-BuOH with an initial concentration $[B_i]$. Although $[M_i]$ and $[B_i]$ varied along the different polymerizations, the same $[M_i]/[B_i]$ ratio was used for all experiments. After addition of the base solution, samples of the same volume were taken out of the reaction mixture after specific time intervals and quenched in ice water. The samples were neutralized, the organic phase was extracted and the solvent was evaporated. The samples containing the crude precursor polymer were dissolved in toluene and converted into the conjugated MDMO-PPV via thermal elimination. The resulting MDMO-PPV was precipitated in cold methanol and collected on a filter. The material was dried under vacuum. At this stage, the polymer yield was calculated and the molecular weight was determined.

The standard conditions to execute the polymerization of MDMO-PPV via the sulfinyl precursor route are set at a reaction temperature of 30 °C and a final premonomer concentration of 0.065 M. Under these conditions, a polymer yield of 77% is achieved already after a reaction time of less than 1 minute! This result clearly demonstrates that the sulfinyl precursor route is marked by very fast reaction kinetics. Plotting M_w versus reaction time again shows the formation of high M_w material at the very early stages of polymerization (Figure 4b).

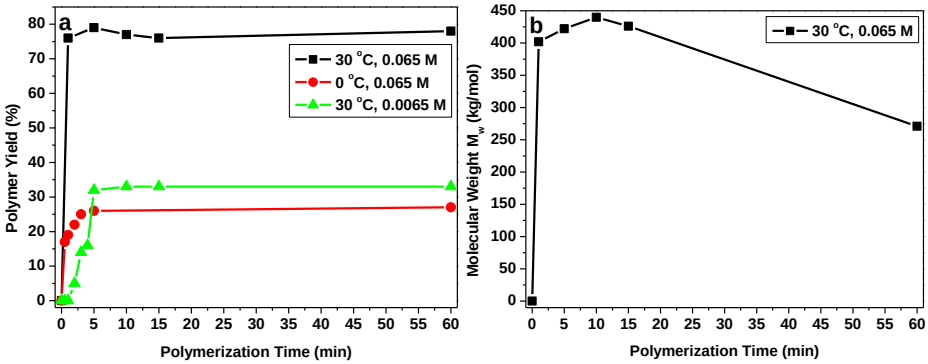

Figure 4. (a) MDMO-PPV polymerization yield in function of reaction time for the sulfinyl precursor route, using Na*t*BuO as base. Results are displayed for different premonomer concentrations and reaction temperatures. (b) Molecular weight in function of reaction time.

In an attempt to lower the reaction kinetics of the sulfinyl route, the polymerization reaction was carried out at 0 °C. Lowering the reaction temperature decreased the M_w of the resulting MDMO-PPV (see Table 2). Here, the reaction time to obtain maximal polymer conversion was found to be 5 min, so it was possible to decrease the reaction rate to some extent (Figure 4a). However, again the polymer yield was substantially lower than under normal polymerization conditions, only 26% was achieved.

When using a final premonomer concentration of 0.0065 M, ten times lower than the standard concentration, the reaction time to reach maximal

conversion also increased to 5 min and a polymer yield of 33% was obtained. Again, a lower M_w was obtained under these conditions.

Because the sulfinyl precursor route exhibits such fast reaction kinetics, there is a need to gather more information about the different rate coefficients of the polymerization reaction. In a first study, the formation of the real monomer, the *p*-quinodimethane system, is investigated by means of *in situ* UV-vis spectroscopy.

Tabel 2. Polymerization Results for the Sulfinyl Precursor Route towards MDMO-PPV

Conditions	Reaction Time (min)	Yield (%)	M_w (g/mol)	M_n (g/mol)	PD
30 °C, 0.065 M	≤1	77	402000	91000	4.5
0 °C, 0.065 M	5	26	253000	59000	4.3
30 °C, 0.0065 M	5	33	138000	56000	2.5

3.2. Kinetic UV-vis Study

To study the *p*-quinodimethane formation, a kinetic UV-vis study was carried out for both precursor routes. *p*-Quinodimethane systems show a typical absorption band around 310-350 nm and their formation can be investigated through constant monitoring of this signal.[41] Since alkoxy side chains would also show absorption in this area, we performed *in situ* UV-vis spectroscopy measurements on unsubstituted (plain) dithiocarbamate (**1**) and sulfinyl (**2**) monomers.

In order to measure very fast and accurate, the UV-vis spectrophotometer is equipped with a so-called stop flow accessory (Figure 5). Syringe 1 contains a monomer solution while syringe 2 contains a base solution. When these syringes are driven forward, equal amounts of the two solutions meet in the mixing chamber 3. The homogeneous solution is then transferred into the sample cell 4. At the same time, syringe 5 is driven out which will hit an electric switch 6. At this moment, the recording of the measurement will start. In this way UV-vis detection starts within a few milliseconds.

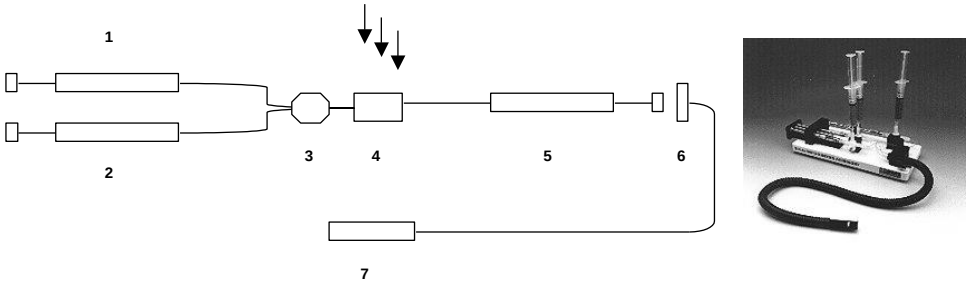

Figure 5. Schematic representation and picture of the UV-vis stop flow accessory.

3.2.1. Dithiocarbamate Route

In order to obtain a maximum amount of *p*-quinodimethane systems and to avoid any polymerization of these real monomers, the premonomer concentration used for the UV-vis experiments has to be much lower than in a typical polymerization experiment (0.2 M). Furthermore, a large excess of base has to be used to shift the equilibrium as much as possible towards *p*-quinodimethane formation. Via experiments in cuvette, we determined that a premonomer concentration of at least $5*10^{-3}$ M and a base concentration of $5*10^{-2}$ M was necessary to achieve substantial *p*-quinodimethane formation, visible in UV-vis. For the dithiocarbamate route, the *p*-quinodimethane system showed an absorption band around 352 nm (Figure 6a). The absorption increases immediately after base addition, reaches a maximum value, and subsequently decreases again (Figure 6b). This behavior corresponds with the formation and depletion of the real monomers, which is typical for reactive intermediates. However, after the experiment, a residual absorption is observed in the region 310−370 nm. This can be explained by the formation of some oligomers which apparently cannot be avoided under these conditions. The experiment was repeated for a base concentration of 10^{-1} M. For the increased base concentration, the maximum in the *p*-quinodimethane absorption was reached earlier.

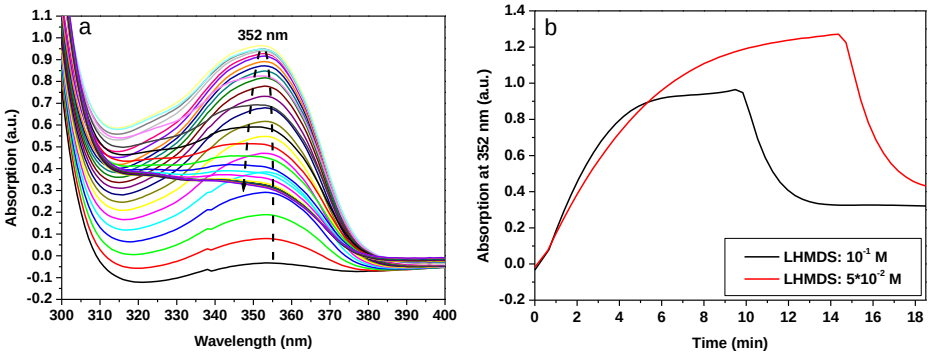

Figure 6. (a) UV-vis spectra of *p*-quinodimethane formation for plain dithiocarbamate premonomer in THF ($5*10^{-3}$ M), using LHMDS ($5*10^{-2}$ M). (b) UV-vis absorbance profiles at 352 nm vs. time for different base concentrations.

3.2.2. Sulfinyl Route

For the sulfinyl route, a premonomer concentration of 10^{-4} M and a base concentration of 10^{-3} M was sufficient to observe the *p*-quinodimethane formation with UV-vis spectroscopy using the stop flow module. The sulfinyl *p*-quinodimethane system showed an absorption band around 313 nm (Figure 7a). Again an increase in absorption is followed by a decrease (Figure 7b). After the experiment, a residual absorption is observed in the region 280−340 nm, probably originating from oligomer formation. The experiment was repeated for a range of increasing base concentrations up till 10^{-1} M, giving different reaction times to reach maximum absorption.

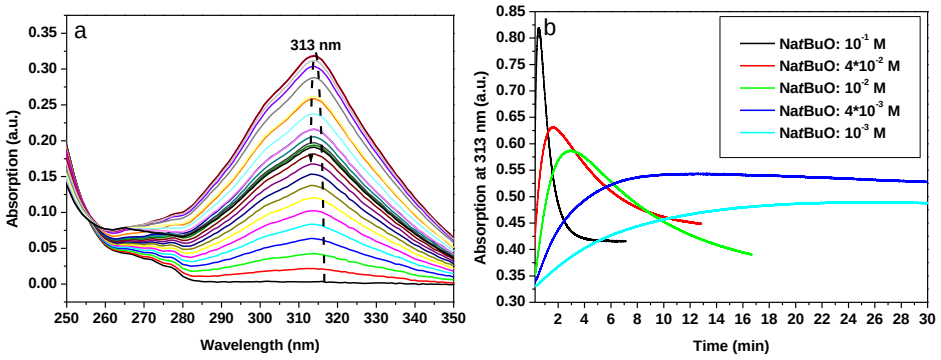

Figure 7. (a) UV-vis spectra of *p*-quinodimethane formation for plain sulfinyl premonomer in 2-BuOH (10^{-4} M), using Na*t*BuO (10^{-3} M). (b) UV-vis absorbance profiles at 313 nm vs. time for different base concentrations.

Previous studies on the formation of the *p*-quinodimethane system in the sulfinyl route revealed that electron donating substituents on the benzenering decreased the acidity of the benzylic protons hence resulting in a lower *p*-quinodimethane formation rate.[47] From these data it was concluded that proton abstraction is the rate-determining step in the *p*-quinodimethane formation and that the 1,6-elimination reaction to form the real monomer can be catalogued as an irreversible E1cb mechanism.[47] However, a recent mechanistic study on the *p*-quinodimethane formation using density functional theory calculations revealed the kinetic data also to be consistent with an E2 elimination mechanism.[48] Therefore, the detailed nature of the elimination mechanism stays undetermined.

3.2.3. Kinetic Modeling

Out of the above UV-vis results, a kinetic modeling study is performed at the moment to calculate the rate coefficient of the real monomer formation for both the dithiocarbamate and sulfinyl precursor routes. This study is currently performed by ir. P. Van Steenberge from the Laboratory of Chemical Technology at the University of Ghent. Once the rate coefficients are calculated, they can then be used to determine how fast *p*-

quinodimethane formation will take place in a typical polymerization reaction under standard conditions.

3.3. Effect of Chain Transfer Reagents on the Sulfinyl Route

As mentioned earlier, the sulfinyl route follows a free radical polymerization mechanism. The initiating moiety is a diradical (Scheme 2, step 1), which can at both sides propagate independently via reaction with *p*-quinodimethane intermediates (Scheme 2, step 2). For the termination reaction (Scheme 2, step 3), it is proposed that carbonyl formation by traces of oxygen can take place.

Scheme 2. Radical Precursor Polymerization Mechanism for MDMO-PPV[a]

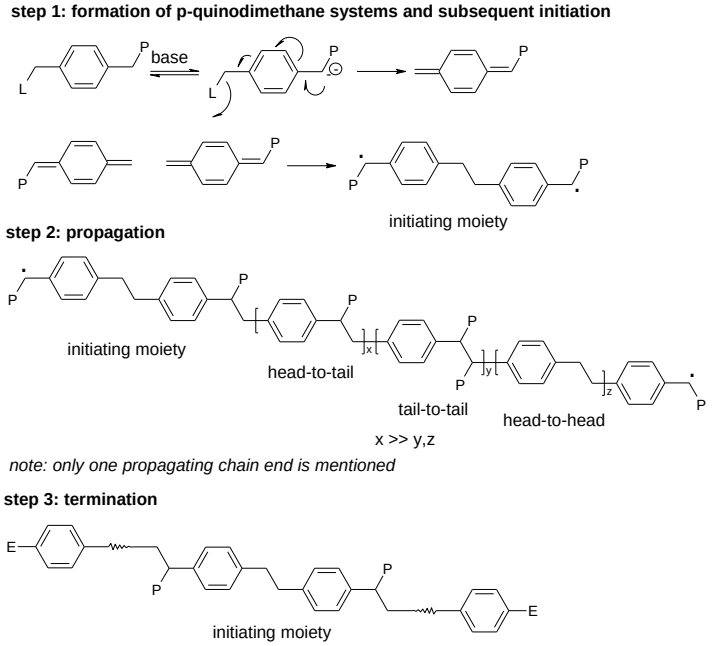

[a] L= Cl, P= S(O)R, and E= C(O)H or C(O)OH.

As a first attempt to lower the polymerization kinetics of the sulfinyl route and achieve control over the molecular weight, experiments using the chain transfer reagent CBr_4 have been executed. In a chain transfer reaction the reactivity of a growing polymer chain is transferred to another molecule, in

this case to the chain transfer reagent CBr_4 (Scheme 3).[49] This process will terminate the growing polymer chain but at the same time generates a new radical. This radical can either terminate another growing radical chain or can initiate the growing of a new polymer chain via reaction with monomer. Therefore, the use of chain transfer reagents will result in lower molecular weight products.

Scheme 3. Chain Transfer Reactions for CBr_4

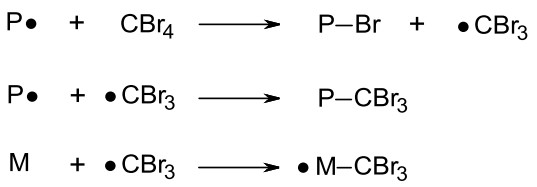

When 0.5 equiv of CBr_4 are added to a standard sulfinyl polymerization of MDMO-PPV, the obtained molecular weights (M_w) are almost 4 times lower than under standard conditions (Table 3). Furthermore, the polymerization kinetics are slowed down (Figure 8). The maximum polymer yield is reached after 10–15 min. Another advantage of using CBr_4 lies in the fact that the conversion to polymer is almost unchanged (66%), compared to the conversion under standard conditions (77%). This way, the polymerization reaction is as efficient as under normal conditions and almost no yield is lost.

Table 3. Polymerization Results for the Sulfinyl Precursor Route towards MDMO-PPV, with and without CBr_4

Conditions	Additive	Reaction Time (min)	Yield (%)	M_w (g/mol)	M_n (g/mol)	PD
30 °C, 0.065 M	/	≤1	77	402000	91000	4.5
30 °C, 0.065 M	CBr_4	10–15	66	143000	70000	2.0

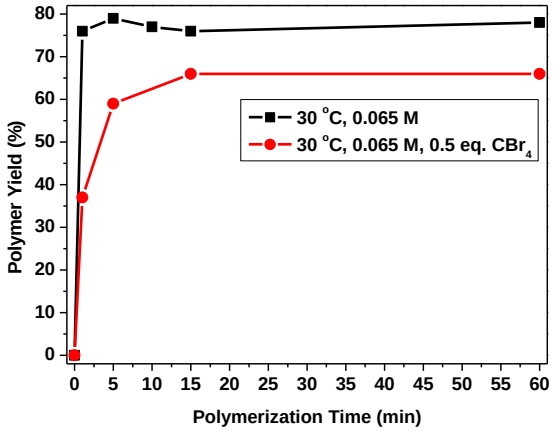

Figure 8. MDMO-PPV polymerization yield in function of reaction time for the sulfinyl precursor route, comparing standard polymerization conditions with polymerization under influence of CBr_4.

For the experiments with CBr_4, it is obvious that once a growing polymer chain is terminated, it can never be made active again. However, via some clever modifications it is possible to create a free radical polymerization in which chain transfer and chain terminations are absent. In this case, the radical chain ends remain active when all monomer is used up. When more monomers are added, the chains start to grow further, thereby increasing the M_w or generating block copolymers, when another monomer then the starting monomer is used. This process is called "living" free radical polymerization (LFRP). During the last decades, several living free radical processes have been developed, such as reversible addition-fragmentation chain transfer (RAFT),[50] atom transfer radical polymerization (ATRP),[51,52] nitroxide-mediated polymerization (NMP)[53,54] and metal-catalyzed radical polymerization (e.g. single-electron transfer LRP).[55] In our study to obtain control over the M_w and over the kinetics of the sulfinyl polymerization, we investigated if the polymerization reaction could be made living via use of the RAFT process, the most versatile and tolerant LFRP.

The mechanism of RAFT begins with a standard initiation step yielding a reactive free radical (Scheme 4). This free radical then reacts with a monomer to form an active center. In a sequential fashion additional

monomers are added to produce a growing polymer chain (Pm●). The propagating chain adds to the C=S bond of the RAFT agent to yield a radical intermediate. This stabilized radical intermediate does not undergo termination reactions, but instead reforms its C=S bond and fragments to give rise to either the original polymer chain (Pm●) or to a new radical (R●), which itself can reinitiate polymerization by reaction with monomers. This way, a new propagating chain (Pn●) is formed. The cycle of addition to the C=S bond, followed by fragmentation of a radical, continues until all monomer or intitiator is consumed. Ultimately, chain equilibration occurs in which there is a rapid equilibrium between the actively growing radical polymer chains and the dormant polymer chains. Because of this, all chains grow at the same rate and the molecular weight of the polymer increases linearly with conversion. Furthermore, low polydispersities are obtained. Termination is limited in this system by the low concentration of active radicals and any termination that does occur is negligible. To summarize, the RAFT process relies on a degenerative chain transfer process instead of using a persistent radical effect such as in most other controlled living radical polymerization processes.

Scheme 4. Mechanism of RAFT Polymerization[56]

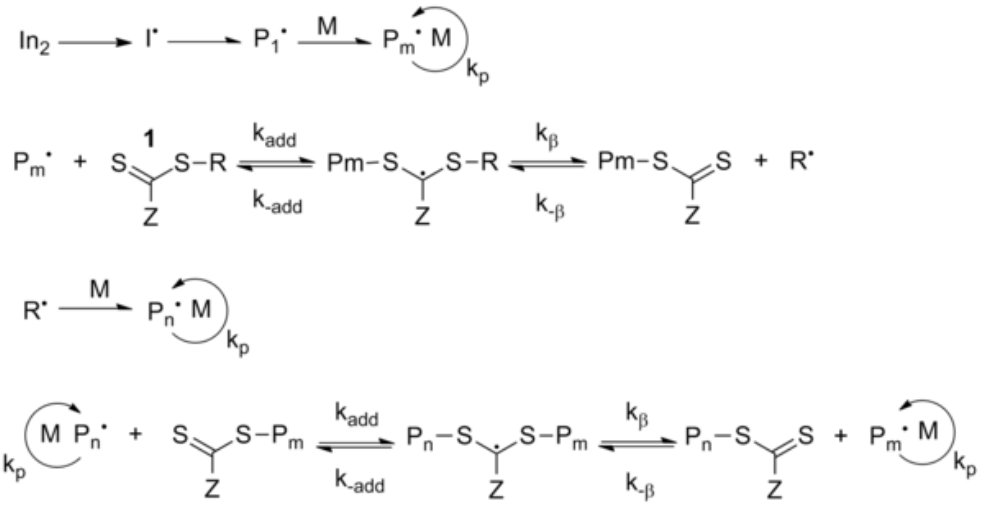

In this study, a specific RAFT agent, S-benzyl dithiobenzoate **5**, was used. Various increasing amounts of **5** were added to a standard sulfinyl polymerization and the effects on polymer yield and M_w were monitored (Figure 9). Both yield and M_w decreased exponentially upon increasing amounts of added RAFT agent. This possibly indicates that an initial chain transfer reaction of the growing polymer chain to the RAFT agent is taking place. However, in order to prove if a living radical polymerization (LRP) mechanism is occurring, the change in M_w needs to be studied in function of conversion. This way, there can be researched if M_w is linearly increasing with conversion, a necessary prerequisite for a RAFT process. Furthermore, to study if the polymerization kinetics are slowed down, the polymer yield will have to be plotted against reaction time or conversion, for each different equivalent of added RAFT agent. Finally, an experiment has to be carried out to investigate if the addition of extra monomer would lead to a further increase of M_w. Only then it is justified to state that a LRP mechanism is taking place. This will be subject of further studies.

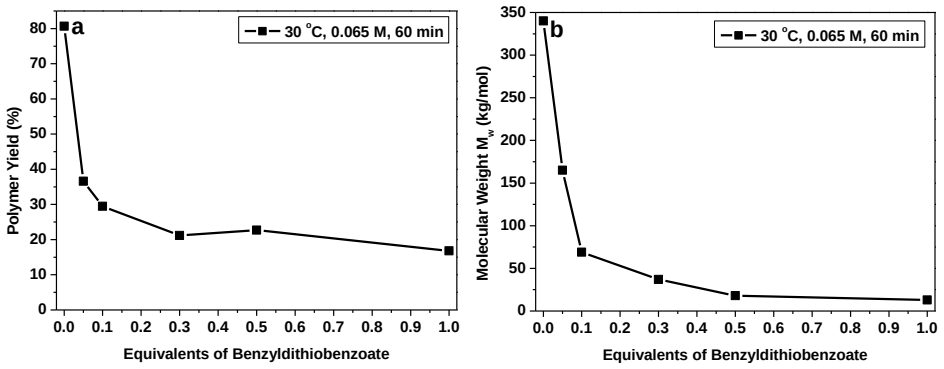

Figure 9. MDMO-PPV polymerization yield (a) and molecular weight (b) in function of number of equivalents of RAFT agent S-benzyl dithiobenzoate.

3.4. ESI-MS Analysis

As a last step to study the polymerization mechanisms and molecules present in the dithiocarbamate and sulfinyl precursor routes, electron spray ionization – mass spectrometry (ESI-MS) analyses have been carried out on

typical reaction mixtures, isolated right after the polymerization reaction took place. No further treatments were performed on the samples in order to decrease the possibility that secondary, not initially present molecules are generated during work-up or purification. Prior to the ESI-MS measurements, the samples were stored under inert atmosphere and in the dark to avoid any oxidation or other degradation processes.

3.4.1. Dithiocarbamate Route

The ESI-MS spectrum for a typical polymerization mixture of MDMO precursor PPV, synthesized via the dithiocarbamate route, is depicted in Figure 10. The m/z values of the abundant peaks are highlighted. The masses corresponding to identified molecules are highlighted in blue. The masses of the undefined molecules are highlighted in red.

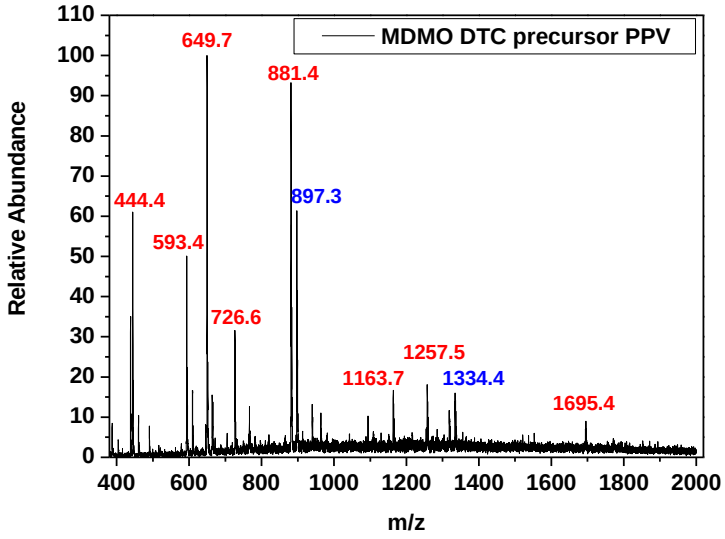

Figure 10. ESI-MS spectrum of MDMO dithiocarbamate precursor PPV.

For the dithiocarbamate route, ESI-MS analysis revealed the presence of two cyclic products: the ring-closured initiating dimer as well as a cyclic trimer, consisting of the initiating dimer and one monomer unit (Figure 11). These findings support the hypothesis that the polymerization takes place via a self-

initiating radical mechanism. This mechanistic assumption was also reported earlier for the Gilch route, in which the presence of similar cyclic [2,2]paracyclophanes was revealed by NMR spectroscopy.[44] However, in the ESI-MS spectrum a considerable number of undefined masses still need to be assigned to certain other molecules. To this end, also possible other initiating, propagating, termination or chain transfer mechanisms have to be considered. In order to gain more information about the undefined products present in the ESI-MS samples, extended MS/MS analyses of the different m/z values have to be carried out. This is subject of further research.

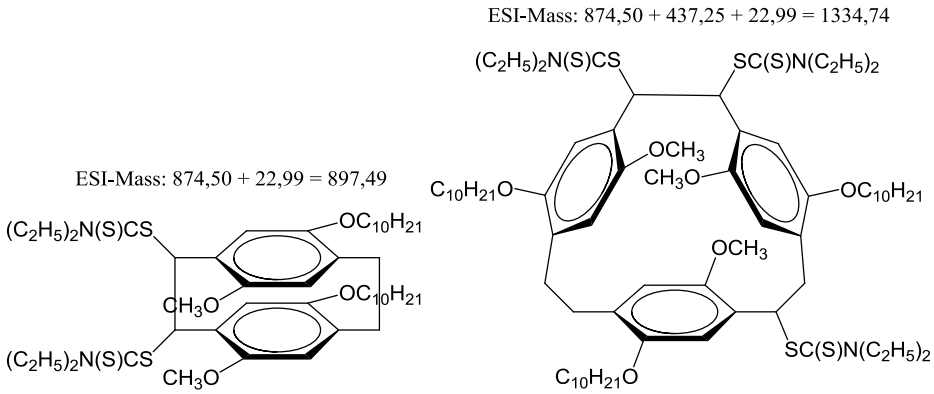

Figure 11. Structures and ESI masses for cyclic dimer and trimer molecules, formed as byproducts in the dithiocarbamate polymerization reaction of MDMO precursor PPV.

3.4.2. Sulfinyl Route

The ESI-MS spectrum for MDMO precursor PPV, synthesized via the sulfinyl route, is depicted in Figure 12. The m/z values corresponding to the identified molecules are again highlighted in blue and the masses of the undefined molecules are highlighted in red.

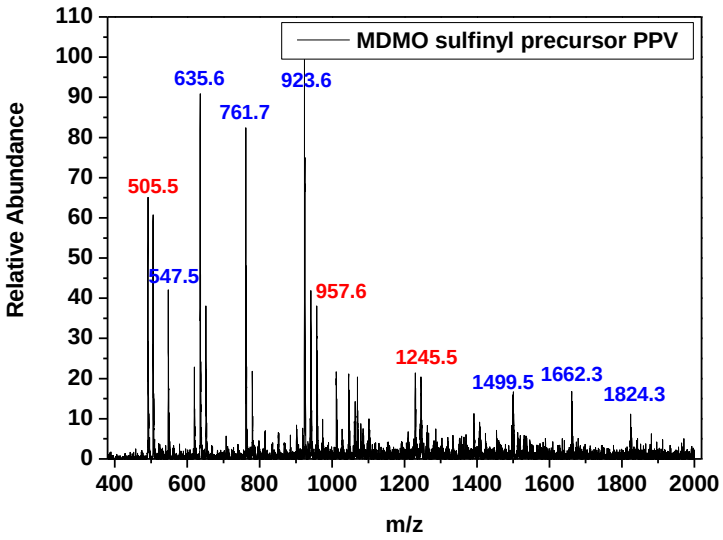

Figure 12. ESI-MS spectrum of MDMO dithiocarbamate precursor PPV.

For the sulfinyl route, ESI-MS analysis revealed the presence of the following molecules: a symmetrically disubstituted sulfinyl impurity, already present prior to polymerization. The solvent substituted product, which is the well-known byproduct of the sulfinyl route, when performed in 2-BuOH. Furthermore, the cyclic initiating dimer is observed, as well as the corresponding cyclodimerized molecules whereby one sulfinyl side chain is eliminated. Apparently, also cyclic products are formed whereby two initiating molecules are ring-closured, generating cyclic tetramers. These cyclic tetramers can also lose one or two sulfinyl side chains via elimination. All these structures are listed in Figure 13. Surprisingly, in the case of the sulfinyl route, no trimers are found. At this stage, it is not clear whether the absence of these molecules is a reproducible result. Furthermore, some other undefined masses still need to be assigned. To this end, further studies will have to be executed.

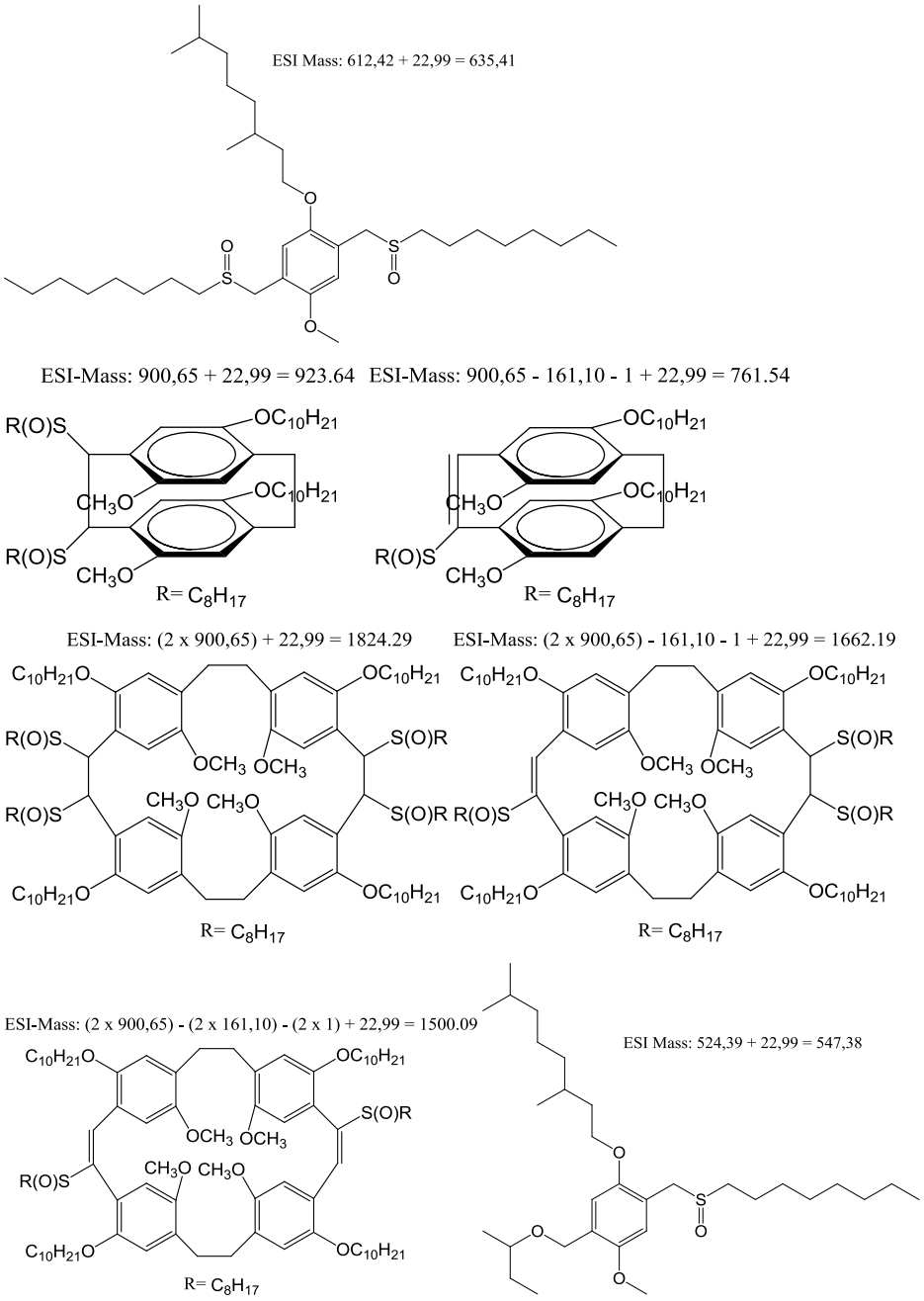

Figure 13. Structures and ESI masses for the di-sulfinyl impurity, and for the cyclic dimer and tetramer molecules and solvent substituted product, formed as byproducts in the sulfinyl polymerization reaction of MDMO precursor PPV.

4. Conclusions

In this work, the polymerization kinetics of the sulfinyl and dithiocarbamate precursor routes have been studied in order to gain control over the molecular weight of the PPV. Polymerization of MDMO precursor PPV via the sulfinyl route is completed after less than 1 min under standard conditions. Via the dithiocarbamate route, it takes about 150 min to obtain maximum conversion. Changing reaction conditions such as lowering the temperature and diluting the premonomer concentration resulted in lower M_w but also decreased conversion. For both precursor routes, it was possible to observe the formation and subsequent consumption/depletion of the *p*-quinodimethane system with *in situ* UV-Vis. The *p*-quinodimethane systems are much faster formed in the sulfinyl route than in the dithiocarbamate route. From these data, rate coefficients for the *p*-quinodimethane formation in both precursor routes will be calculated in a follow-up kinetic modeling study. In an attempt to control M_w, experiments with the chain transfer reagent CBr_4 as well as with the RAFT agent S-benzyl dithiobenzoate have been executed on a standard sulfinyl polymerization. Addition of CBr_4 resulted in lower M_w while the amount of conversion was almost unaffected, and the kinetics are slowed down. The addition of RAFT agent lowered both M_w and polymer conversion. However, to prove if the polymerization reaction is changed into a living radical polymerization, further experiments have to be executed. Finally, ESI-MS analyses of polymerization mixtures of both precursor routes reveal the presence of cyclic dimers, trimers and tetramers, supporting the hypothesis of a self-initiating radical polymerization mechanism.

5. Acknowledgments

The authors thank M. H. Grote for the ESI-MS measurements. The authors gratefully acknowledge The Fund for Scientific Research-Flanders (FWO) and The Institute for the Promotion of Innovation through Science and Technology in Flanders (IWT Vlaanderen) for financial support. The research was

performed in the framework of the IAP/IUAP/PAI P6/27 project "Functional Supramolecular Systems", funded by the Belgian Government.

6. References

(1) Friend, R. H.; Gymer, R. W.; Holmes, A. B.; Burroughes, J. H.; Marks, R. N.; Taliani, C.; Bradley, D. D. C.; Dos Santos, D. A.; Brédas, J. L.; Lögdlund, M.; Salaneck, W. R. *Nature* **1999**, *397*, 121–128.

(2) Rostalski, J.; Meissner D. *Sol. Energ. Mat. Sol. C.* **2000**, *61*, 87–95.

(3) Brabec, J. C.; Sariciftci, N. S.; Hummelen, J. C. *Adv. Funct. Mater.* **2001**, *11*, 15–26.

(4) Hoppe, H.; Sariciftci, N. S. *J. Mater. Res.* **2004**, *19*, 1924–1945.

(5) Hoppe, H.; Niggeman, M.; Winder C.; Kraut, J.; Heisgen, R.; Hinsch, A.; Meissner, D.; Sariciftci, N. S. *Adv. Funct. Mater.* **2004**, *14*, 1005–1011.

(6) Braun, D.; Heeger, A. J. *Appl. Phys. Lett.* **1991**, *58*, 1982–1984.

(7) Burn, P. L.; Holmes, A. B.; Kraft, A.; Bradley, D. D. C.; Brown, A. R.; Friend, R. H.; Gymer, R. W. *Nature*, **1992**, *356*, 47–49.

(8) Bradley, D. D. C. *Synthetic. Met.* **1993**, *54*, 401–415.

(9) May, P. *Phys. World* **1995**, *8*, 52–57.

(10) Salbeck, J. *Ber. Bunsen. Phys. Chem.* **1996**, *100*, 1667–1677.

(11) Kraft, A.; Grimsdale, A. C.; Holmes, A. B. *Angew. Chem. Int. Ed.* **1998**, *37*, 402–428.

(12) Roth, S. *One-dimensional metals*, Weinheim VCH, **1995**, 209–231.

(13) Sirringhaus, H.; Tessler, N.; Friend, R. H. *Science* **1998**, *280*, 1741–1744.

(14) Horowitz, G. *Adv. Mater.* **1998**, *10*, 365–377.

(15) Bao, Z. *Adv. Mater.* **2000**, *12*, 227–230.

(16) Dimitrakopoulos, C. D.; Malenfant, R. L. *Adv. Mater.* **2002**, *14*, 99–117.

(17) Scheinert, S.; Paasch, G. *Phys. Status Solidi A* **2004**, *201*, 1263–1301.

(18) MacDiarmid, A. G.; Zhang, W. J.; Huang, Z.; Wang, P.-C.; Huang, F.; Xie, S. *Polym. Prepr.* **1997**, *11*, 333–334.

(19) Heeger, P. S.; Heeger, A. J. *Proc. Natl. Acad. Sci.* **1999**, *96*, 12219–12221.

(20) Chen, L.; McBranch, W.; Wang, H.; Helgeson, R.; Wudl, F.; Whitten, D. G. *Proc. Natl. Acad. Sci.* **1999**, *96*, 12287–12297.

(21) McQuade, D. T.; Pullen, A. E.; Swager, T. M. *Chem. Rev.* **2000**, *100*, 2537–2574.

(22) Gerard, M.; Chaubey, A.; Malhotra, B. D. *Biosens. Bioelectron.* **2002**, *17*, 345–359.

(23) Gilch, H. G.; Wheelwright, W. L. *J. Polym. Sci.* **1966**, *4*, 1337–1349.

(24) Harper, K.; West, W. J. W. *Eur. Pat. Appl. No. 182548*, **1985**.

(25) Jen, K. Y.; Jow, R.; Eckhardt, H.; Elsenbaumer, R. L. *Polym. Mater. Sci. Eng.* **1987**, *56*, 49–53.

(26) Jen, K. Y.; Maxfield, M.; Shacklette, L. W.; Elsenbaumer, R. L. *J. Chem. Soc. Chem. Comm.* **1987**, 309–311.

(27) Wessling, R. A. *J. Polym. Sci. Pol. Sym.* **1985**, *72*, 55–66.

(28) Son, S.; Dodabalapur, A.; Lovinger, A. J.; Galvin, M. E. *Science* **1995**, *269*, 376–378.

(29) Kesters, E.; Gillissen, S.; Motmans, F.; Lutsen, L.; Vanderzande D. *Macromolecules* **2002**, *35*, 7902–7910.

(30) Mitchell, W. J.; Pena, C.; Burn, P. L. *J. Mater. Chem.* **2002**, *12*, 200–205.

(31) Henckens, A.; Lutsen, L.; Vanderzande, D.; Knipper, M.; Manca, J.; Aernouts, T.; Poortmans, J. *SPIE Proc.* **2004**, 52–59.

(32) Henckens, A.; Duyssens, I.; Lutsen, L.; Vanderzande, D.; Cleij, T. J. *Polymer* **2006**, *47*, 123–131.

(33) van Breemen, A. J. J. M.; Issaris, A. C. J.; de Kok, M. M.; Van Der Borght, M. J. A. N.; Adriaensens, P. J.; Gelan, J. M. J. V.; Vanderzande, D. J. M. *Macromolecules* **1999**, *32*, 5728–5735.

(34) Henckens, A.; Knipper, M.; Polec, I.; Manca, J.; Lutsen, L.; Vanderzande, D. *Thin solid films* **2004**, *451–452*, 572–579.

(35) Roex, H.; Adriaensens, P.; Vanderzande, D.; Gelan, J. *Macromolecules* **2003**, *36*, 5613–5622.

(36) Vandenbergh, J.; Wouters, J.; Adriaensens, P. J.; Mens, R.; Cleij, T. J.; Lutsen, L.; Vanderzande, D. *Macromolecules* **2009**, *42*, 3661–3668.

(37) Duchateau, J.; Lutsen, L.; Guedens, W.; Cleij, T. J.; Vanderzande, D. *Polym. Chem.* **2010**, *1*, 1313–1322.

(38) van Breemen, A. J. J. M.; Vanderzande, D. J. M.; Adriaensens, P. J.; Gelan, J. M. J. V. *J. Org. Chem.* **1999**, *64*, 3106–3112.

(39) Becker, H.; Spreitzer, H.; Ibrom, K.; Kreuder, W. *Macromolecules* **1999**, *32*, 4925–4932.

(40) Chernikova, E.; Terpugova, P.; Bui, C.; Charleux, B. *Polymer* **2003**, *44*, 4101–4107.

(41) Denton, F. R.; Lathi, P. M.; Karasz, F. E. *J. Polym. Sci., Part A: Polym. Chem.* **1992**, *30*, 2223–2231.

(42) Issaris, A.; Vanderzande, D.; Gelan, J. *Polymer* **1997**, *38*, 2571–2574.

(43) Hontis, L.; Vrindts, V.; Lutsen, L.; Vanderzande, D.; Gelan, J. *Polymer* **2001**, *42*, 5793–5796.

(44) Wiesecke, J.; Rehahn, M. *Angew. Chem., Int. Ed.* **2003**, *42*, 567–570.

(45) Schwalm, T.; Wiesecke, J.; Immel, S.; Rehahn, M. *Macromolecules* **2007**, *40*, 8842–8854.

(46) Hontis, L. *Ph.D. Dissertation*, **2002**, Limburgs Universitair Centrum, Diepenbeek, Belgium, 76–79.

(47) Motmans, F. *Ph.D. Dissertation*, **2004**, Limburgs Universitair Centrum, Diepenbeek, Belgium, 153–155.

(48) Hermosilla, L.; Catak, S.; Van Speybroeck, V.; Waroquir, M.; Vandenbergh, J.; Motmans, F.; Adriaensens, P.; Lutsen, L.; Cleij, T.; Vanderzande, D. *Macromolecules* **2010**, *43*, 7424–7433.

(49) Bandrup, J.; Immergut, E. H.; McDowell, W. *Polymer Handbook*, 2nd ed., Wiley-Interscience, New York, **1975**, pp. II–57ff.

(50) Chiefari, J.; Chong, Y. K.; Ercole, F.; Krstina, J.; Jeffery, J.; Le, T. P. T.; Mayadunne, R. T. A.; Meijs, G. F.; Moad, C. L.; Moad, G.; Rizzardo, E.; Thang, S. H. *Macromolecules* **1998**, *31*, 5559–5562.

(51) Kato, M.; Kamigaito, M.; Sawamoto, M.; Higashimura, T. *Macromolecules* **1995**, *28*, 1721−1723.

(52) Wang, J.; Matyjaszewski, K. *J. Am. Chem. Soc.* **1995**, *117*, 5614−5615.

(53) Georges, M. K.; Veregin, R. P. N.; Kazmaier, P. M.; Hamer, G. K. *Macromolecules* **1993**, *26*, 2987−2988.

(54) Hawker, C. J.; Bosman, A. W.; Harth, E. *Chem. Rev.* **2001**, *101*, 3661−3688.

(55) Kamigaito, M.; Ando, T.; Sawamoto, M. *Chem. Rev.* **2001**, *101*, 3689−3746.

(56) Barner-Kollowik, C. *Handbook of RAFT Polymerization*, Wiley-VCH, Weinheim, **2008**, 190.

Summary

Chapter 1 displayed a general introduction on conjugated polymers, which combine the mechanical properties and processing advantages of polymers with the electrical and optical properties of metals and semiconductors. In order to be semiconducting, these conjugated polymers need to have a backbone consisting of alternating single and double bonds. Furthermore charge carriers need to be injected into the polymer, to induce conductivity. The optical properties of these polymers, such as electroluminescence and photoluminescence, have been explained. Various optoelectronic devices which make use of conjugated polymers, e.g. light emitting diodes and photovoltaic cells, have been described. The thesis mainly focused on one class of semiconducting polymers, the poly(*p*-phenylene vinylene) (PPV) derivatives. They can be synthesized via direct routes, or via *p*-quinodimethane based precursor routes. The aim of the thesis was the synthesis and characterization of novel functionalized PPV derivatives for optoelectronic applications. To this end, usually the dithiocarbamate precursor route was used, unless otherwise stated.

The synthesis of high quality MDMO-PPV via the dithiocarbamate precursor route was presented in **Chapter 2**. This precursor route combines the easy monomer synthesis of the Gilch route with the superior polymer quality of the more complex sulfinyl route. The bisdithiocarbamate MDMO-monomer has been polymerized using either LHMDS or K*t*BuO, which resulted in polymers with high molecular weight, low PD, and sufficient high λ_{max} values after thermal conversion. Contrary to LDA-based dithiocarbamate polymerizations, no bimodal molecular weight distributions were obtained. Via experiments with a radical inhibitor (TEMPO), it was shown that the polymerization mechanism followed a radical pathway. A ^{13}C NMR study on ^{13}C labelled MDMO-PPV revealed that the dithiocarbamate polymerization mainly proceeded via head-to-tail additions and only very small amounts of defects were present in the resulting microstructure. Furthermore, MDMO-PPV

synthesized with LHMDS showed a 29.3% regioregularity excess, as revealed by ^{1}H NMR. By using even more sterically hindered bases, there is potential to synthesize PPV's with even higher degrees of regioregularity.

In **Chapter 3**, the thermal conversion process for dithiocarbamate PPV and PTV precursor polymers was compared to a new acid induced conversion method. Two different acids, benzenesulfonic acid and trifluoroacetic acid, have been used. While the thermal conversion process had to be executed at 180 °C, the acid induced conversion allowed to lower the conversion temperature to 70 °C. This way, degradation of the polymer chromophore could be avoided. The process was studied with UV-vis and FTIR and the results revealed that when trifluoroacetic acid was used, a more defect free polymer structure was obtained then when benzenesulfonic acid was applied. The latter resulted in degradation phenomena when too long reaction times were used. It was demonstrated that the use of an acid resulted in the formation of an intermediate carbenium ion, which is part of the rate limiting step. Furthermore, when the conversion was performed at room temperature a competition between the elimination reaction and a substitution reaction took place. By tuning the reaction conditions, the reaction mechanism could be controlled in favor of the elimination reaction. When less than one equivalent of acid was used, the conjugated system did not fully develop. This demonstrated that the acid does not act as a catalyst, but is effectively consumed during the reaction. Finally, it was shown that the acid induced conversion method was only displayed for the dithiocarbamate route and did not work for other precursor routes.

One objective of the thesis was to develop PPV derivatives which could be processed from environmentally friendly solvents. To this end, two highly polar PPV derivatives, BTEMP-PPV and MTEMP-PPV, have been synthesized via the dithiocarbamate precursor route and were presented in **Chapter 4**. After conversion, the solubility of the polar conjugated PPV's was tested and studied with UV-vis. Both polymers were soluble in a variety of solvents, including alcohols and even water (BTEMP-PPV). The relative permittivity (ε_r) and the hole-mobility (μ_h) of the polymers were investigated with impedance

spectroscopy and space charge limited current (SCLC) measurements, respectively. Due to the roughness and heterogeneity of the obtained thin films, a reduced hole mobility was found, compared to the reference polymer, MDMO-PPV. However, MTEMP-PPV showed a higher relative permittivity then MDMO-PPV. Therefore, this material was used to fabricate a proof-of-concept "green" solar cell device, processed from aceton. A low efficiency was achieved (0.04%) due to bad film formation. However, with some optimization these materials clearly show potential in the development of sustainable optoelectronic devices.

The synthesis and full characterization of the first two soluble tetra-alkoxy substituted PPV derivatives, TH-PPV and TEH-PPV, was reported in **Chapter 5**. Due to steric hindrance of the side chains, the well-known Gilch route had to be used. The resulting polymers were soluble in a large range of solvents and showed excellent thermal stability up to 200 °C. The regioregular polymers were studied with polarized optical microscopy and DSC. TEH-PPV was disordered because of the large steric hindrance of the branched side chains. However, TH-PPV exhibited thermally induced order which resulted in a liquid crystalline mesophase. Therefore, TH-PPV was used to prepare a solution processed electroluminescent device, which functioned well. The enhanced order in TH-PPV will benefit the usage of this new class of polymers in optoelectronic applications, in which improved charge carrier mobility is desirable.

Chapter 6 described the development of a new PPV derivative with a high glass transition temperature (*Tg*) of 110 °C. The proposed approach was to use a "high *Tg*" polymer to create a more thermally stable polymer:fullerene blend, used in bulk heterojuntion (BHJ) solar cells. The new polymer, MPE-PPV, was synthesized via the dehydrohalogenation (Gilch) route. After characterization, the phase behavior of donor:acceptor blends of MPE-PPV and [60]PCBM was investigated by means of MTDSC and RHC. Furthermore, the thermal stability of BHJ solar cells of MPE-PPV:[60]PCBM and MDMO-PPV:[60]PCBM blends have been compared. The use of "high *Tg*" MPE-PPV instead of MDMO-PPV (*Tg*= 45 °C) resulted in a significant improvement of the

thermal stability of the solar cell and a TEM study of the active layer demonstrated a more stable morphology. For the MPE-PPV:[60]PCBM active layer, the free movement of the fullerene molecules was hampered due to a stiffer matrix. It could be stated that the use of a "high *Tg*" material was a promising route for further developments towards high efficiency, high stability organic solar cells. Furthermore, the polymer:fullerene devices could be optimized by using [70]PCBM instead of [60]PCBM as fullerene acceptor, which resulted in a 70% increase in current density and device efficiency.

A kinetic study of the dithiocarbamate and sulfinyl precursor routes, has been described in **Chapter 7**. PPV derivatives synthesized via precursor routes can show solubility problems due to their high molecular weight. Functionalization of PPV derivatives via post-polymerization reactions will fail due to the insolubility of the polymer. In order to be able to control the molecular weight, the polymerization kinetics needed to be clarified as well as the reaction mechanism. Polymerization of MDMO precursor PPV via the sulfinyl route was completed after less than 1 min under standard conditions. Via the dithiocarbamate route, it took about 150 min to obtain maximum conversion. Lowering the temperature and diluting the premonomer concentration resulted in lower M_w but also decreased conversion. Via *in situ* UV-vis spectroscopy, the formation and subsequent consumption/depletion of the *p*-quinodimethane systems was observed. The *p*-quinodimethane systems were much faster formed in the sulfinyl route than in the dithiocarbamate route. The UV-vis data are currently used to calculate rate coefficients for the *p*-quinodimethane formation in a follow-up kinetic modeling study. In an attempt to control M_w, chain transfer reagent CBr_4 as well as a RAFT agent S-benzyl dithiobenzoate were added to standard sulfinyl polymerizations. Addition of CBr_4 yielded lower M_w polymers and did almost not affect the polymer conversion. Furthermore, the reaction rate was slowed down. The addition of RAFT agent lowered both M_w and polymer conversion. However, further experiments have to be performed to prove if the polymerization reaction under these conditions is a living radical polymerization. Finally, ESI-

MS analyses of polymerization mixtures of both precursor routes revealed the presence of cyclic dimers, trimers and tetramers, supporting the hypothesis of a self-initiating radical polymerization mechanism.

Samenvatting

Hoofdstuk 1 geeft een algemene inleiding over geconjugeerde polymeren. Deze materialen combineren de mechanische eigenschappen en gemakkelijke verwerkbaarheid van polymeren met de elektrische en optische eigenschappen van metalen en halfgeleiders. Om halfgeleidende eigenschappen te bezitten, moet de hoofdketen van het polymeer opgebouwd zijn uit afwisselend enkelvoudig en tweevoudige bindingen. Bovendien moeten er ladingsdragers, dus positieve of negatieve ladingen, in het polymeer geïnjecteerd worden, opdat het materiaal zou gaan geleiden. De optische eigenschappen zoals elektroluminescentie en photoluminescentie worden uitgelegd. Vervolgens worden de vele toepassingen, waarvoor deze geconjugeerde polymeren gebruikt kunnen worden, beschreven. Enkele belangrijke voorbeelden omvatten de lichtgevende diodes (LED 's) en de organische zonnecellen.

Eén klasse van geleidende polymeren wordt uitvoerig beschreven, namelijk de poly(*para*-phenylenevinylene) derivaten, oftewel PPV 's. Deze polymeren kunnen via verscheidene synthese routes verkregen worden. In deze thesis wordt enkel gebruik gemaakt van bepaalde precursor routes, die gebaseerd zijn op de reactiviteit van een *p*-quinodimethaan systeem. Deze precursor routes zijn gemakkelijk te controleren en laten toe om zeer diverse PPV derivaten te synthetiseren met voldoende hoge moleculaire gewichten.

Het doel van deze thesis omvat de synthese en het karakteriseren van nieuwe PPV derivaten. Via het inbouwen van bepaalde zijketens kunnen de eigenschappen van deze polymeren aangepast worden voor verscheidene doeleindes. Voor de synthese werd hoofdzakelijk de dithiocarbamaat precursor route gebruikt, tenzij anders vermeld.

Hoofdstuk 2 beschrijft de dithiocarbamaat precursor route als een zeer geschikte syntheseroute voor MDMO-PPV. Deze precursor route combineert immers een eenvoudige monomeersynthese met resulterende polymeren van hoge kwaliteit, zoals ze ook verkregen worden bij de meer complexe sulfinyl

precursor route. Het dithiocarbamaat premonomeer werd gepolymeriseerd onder invloed van een base. Zowel LHMDS als K*t*BuO werden hiervoor gebruikt. Er werden polymeren verkregen met hoge moleculaire gewichten en een lage polydispersiteit. Er werden geen bimodale moleculaire gewichtsverdelingen waargenomen. Via experimenten met een radicaal inhibitor (TEMPO) werd aangetoond dat de polymerisatie verliep via een radicaal mechanisme. Na omzetting van de precursor polymeren tot het geconjugeerde MDMO-PPV, werd het polymeer bestudeerd met UV-vis en FTIR. Een ^{13}C NMR studie op ^{13}C gelabeld MDMO-PPV toonde aan dat de polymerisatie hoofdzakelijk verloopt via kop-staart additions die resulteren in een polymeer-microstructuur met slechts zeer weinig defecten. Eveneens werd aangetoond dat het MDMO-PPV, gesynthetiseerd met het sterisch gehinderde LHMDS als base, een regioregulariteit van 29% vertoonde. Mogelijkerwijs kunnen nog hogere graden van regioregulariteit verkregen worden, indien men gebruik zou maken van nog meer sterisch gehinderde bases.

In **Hoofdstuk 3** werd de standaard thermische conversie van PPV en PTV precursor derivaten vergeleken met een nieuwe zuur geïnduceerde conversiemethode. Hiervoor werd gebruikt gemaakt van twee verschillende zuren, namelijk benzeensulfonzuur en trifluoroazijnzuur. Terwijl de thermische conversie methode uitgevoerd werd bij 180 °C, kon de conversie onder invloed van zuur al bij 70 °C of zelfs lagere temperaturen plaatsvinden. Op deze manier kon de thermische degradatie van het polymeer vermeden of uitgesteld worden. Het proces werd bestudeerd met UV-vis en FTIR en de resultaten toonden aan dat de meest defect-vrije polymeerstructuur verkregen werd bij gebruik van trifluoroazijnzuur. Conversie onder invloed van benzeensulfonzuur leidde echter tot polymeerdegradatie bij te lange reactietijden. Een plausibel reactiemechanisme werd voorgesteld waarbij de vorming van een intermediair carbenium-ion deel uitmaakte van de snelheidsbepalende stap. Het mechanisme veronderstelde eveneens een competitie tussen de eliminatiereactie en een substitutiereactie. Het is bekend dat hogere

reactietemperaturen de eliminatiereactie bevorderen terwijl lagere reactietemperaturen vooral leiden tot substitutie. Onder de juiste reactieomstandigheden kon de eliminatiereactie selectief optreden ter vorming van het geconjugeerd PPV of PTV derivaat. Bovendien werd waargenomen dat het zuur geen katalytische werking had, maar effectief verbruikt werd gedurende de reactie. Tot slot stelde men vast dat de zuur geïnduceerde eliminatiereactie enkel toegepast kon worden bij de dithiocarbamaat precursor route en niet bij de andere precursor routes.

Tijdens deze doctoraatsstudie werd ook getracht PPV derivaten te ontwikkelen die verwerkt konden worden vanuit milieuvriendelijke solventen. Daarom werden twee polaire PPV derivaten, MTEMP-PPV en BTEMP-PPV, ontwikkeld. Dit staat beschreven in **Hoofdstuk 4**. De polaire precursor PPV 's werden gesynthetiseerd via de dithiocarbamaat precursor route. Na conversie tot de geconjugeerde structuren, werd de oplosbaarheid van de materialen getest in een groot aantal oplosmiddelen. De absorptiespectra werden bestudeerd met UV-vis spectroscopie. De polaire PPV 's bleken op te lossen in tal van solventen, waaronder ook alcoholen en zelfs water. Vervolgens werden de elektrische parameters, zoals de diëlektrische constante en de ladingsmobiliteit gemeten met impedantiespectroscopie en SCLC metingen. Helaas werden voor beide materialen zeer heterogene dunne filmen verkregen waardoor voor BTEMP-PPV geen waardes konden gemeten. MTEMP-PPV had wegens heterogene filmvorming een lagere mobiliteit dan MDMO-PPV, het referentiemateriaal. MTEMP-PPV had echter een hoge diëlektrische constante, waardoor dit materiaal zeer geschikt was om te gebruiken in zonnecellen. Een eerste "groene" zonnecel werd gefabriceerd met als donormateriaal MTEMP-PPV, gespincoat vanuit aceton. Het device haalde maar een laag rendement maar toonde toch aan dat, mits enige optimalisatie, deze materialen geschikte kandidaten zijn voor de ontwikkeling van milieuvriendelijke opto-elektronische toepassingen.

Hoofdstuk 5 beschreef de synthese en karakterisering van twee tetra-alkoxy gesubstitueerde PPV derivaten, TH-PPV en TEH-PPV. Wegens sterische hinder kon de dithiocarbamaat precursor route niet gebruikt worden en werd de

Gilch route gebruikt voor de polymeersynthese. De resulterende polymeren waren oplosbaar in een groot aantal oplosmiddelen en waren thermisch stabiel tot 200 °C. De tetragesubstitueerde PPV derivaten zijn inherent regioregulair. Daarom werden dunne filmen van beide polymeren bestudeerd met Optische Microscopie en DSC. Wegens aanzienlijke sterische hinder van de vertakte zijketens vormde TEH-PPV ongeordende filmen. TH-PPV daarentegen vertoonde een thermisch geïnduceerde vloeibaar kristallijne mesofase en dus een meer gestructureerde filmmorfologie. Wegens dit gedrag, werd TH-PPV gebruikt voor de fabricage van een eenvoudig elektroluminescent device. Het device werkte naar behoren en toonde aan dat deze klasse van tetragesubstitueerde PPV 's geschikte materialen zijn om te worden gebruikt in opto-elektronische toepassingen waarvoor een hoge ladingsmobiliteit vereist is.

Een ander onderwerp binnen het doctoraatsonderzoek omvatte de synthese van PPV derivaten met hoge glastransitietemperaturen (*Tg*). In **Hoofdstuk 6** werd de synthese en karakterisering van MPE-PPV via de dehydrohalogeneringsroute (Gilch route) beschreven. Dit materiaal bleek een glastransitietemperatuur te hebben van 110 °C. Het idee was om dit materiaal te gebruiken als donormateriaal in polymer:fullerene bulk heterojunctie zonnecellen. Aangenomen werd dat de hogere *Tg* van het donorpolymeer zou leiden tot een meer thermisch stabielere morfologie resulterend in zonnecellen met een langere levensduur. Als eerste stap werd het fasegedrag van MPE-PPV:[60]PCBM mengsels met verschillende composities bestudeerd via MTDSC en RHC. Vervolgens werden de thermische stabiliteit van MPE-PPV:[60PCBM en MDMO-PPV:[60]PCBM zonnecellen vergeleken. Het gebruik van MPE-PPV in plaats van MDMO-PPV (*Tg*= 45°C) resulteerde in een significante toename van de thermische stabiliteit en dus levensduur van de zonnecellen. Een TEM studie van de actieve laag leidde tot dezelfde conclusies. De hoge *Tg* van MPE-PPV zorgde voor een stijvere polymeermatrix waardoor thermisch geïnduceerde fasescheiding of ontmenging van het PPV en [60]PCBM werd tegengehouden en aldus een stabielere morfologie verkregen werd. Er kon geconcludeerd worden dat,

naast enkele andere methodes, het gebruik van "hoge *Tg*" materialen een goede optie is voor de ontwikkeling van thermisch stabiele organische zonnecellen. Bovendien kon de zonnecelefficiency van de devices nog met 70% verbeterd worden door [70]PCBM te gebruiken als acceptor materiaal in plaats van [60]PCBM.

Hoofdstuk 7 omvatte de eerste resultaten van een kinetische en mechanistische studie van de dithiocarbamaat en sulfinyl precursor routes. PPV 's gesynthetiseerd via precursor routes hebben vaak te hoge moleculaire gewichten wat vervolgens kan leiden tot oplosbaarheidsproblemen. Het inbouwen van specifieke functionele groepen in de PPV zijketens via post-polymerisatiereacties wordt aldus bemoeilijkt wanneer het polymeer niet voldoende oplost in een bepaald solvent. Om het molecuulgewicht M_w van een PPV derivaat gericht te kunnen controleren, dient het reactiemechanisme alsook de kinetiek van de polymerisatie grondig onder de loep genomen te worden. Als eerste stap werd voor beide precursorroutes bestudeerd hoe snel de polymerisatie van MDMO precursor PPV onder standaard condities verliep. De sulfinyl polymerisatie leidde al na minder dan 1 minuut tot een maximale conversie. Bij gebruik van de dithiocarbamaat route duurde het 150 minuten alvorens het maximale rendement bereikt werd. Dit toont aan dat vooral de sulfinyl polymerisatie gekenmerkt wordt door een zeer snelle reactiekinetiek. Het veranderen van de reactiecondities zoals temperatuurverlaging of concentratieverdunning leidde voor beide precursorroutes tot lagere M_w maar zorgde ook voor een lager rendement. Vervolgens werd via *in situ* UV-vis spectroscopie de snelheid van ontstaan en verdwijnen van de *p*-quinodimethaansystemen bestudeerd voor beide precursorroutes. Wederom werden de *p*-quinodimethaansystemen veel sneller gevormd bij de sulfinyl route dan bij de dithiocarbamaat route. De behaalde UV-vis data worden op dit moment gebruikt in een kinetische modelstudie teneinde de snelheidscoëfficienten voor de *p*-quinodimethaanvorming te berekenen. Als een eerste poging om het M_w bij de sulfinylroute te controleren, werden testen uitgevoerd met het ketentransferreagens CBr_4 en met een RAFT reagens S-benzylditiobenzoaat. Additie van CBr_4 leidde tot een

aanzienlijke verlaging van het M_w, zonder het rendement van de polymerisatie aan te tasten. Ook het toevoegen van RAFT reagens leidde tot een verlaging in M_w, maar hier werd tevens een nefaste verlaging van het rendement waargenomen. Om aan te tonen of de additie van het RAFT reagens een levende radicalaire polymerisatie tot gevolg heeft, dienen verdere testen uitgevoerd te worden in de nabije toekomst. Tenslotte werden met ESI-MS analyses cyclische di-, tri- en tetra-meren aangetroffen in de polymerisatiemengsels. Deze resultaten ondersteunen de hypothese van een zelf-initiërend radicalair polymerisatiemechanisme.

Publications & Conferences
Personal Contributions

Publications

"Kinetic modeling of the formation and (co)polymerization of *p*-quinodimethane systems": Vansteenberge, P.; Vandenbergh, J.; Adriaensens, P.; Vanderzande, D.; Reyniers, M-F.; Marin, G.B. in preparation. (50 %)

- Kinetic (UV-Vis) experiments on the sulfinyl and dithiocarbamate route

*"Thermal stability of poly[(2-methoxy-5-(2'-phenylethoxy))-1,4-phenylene vinylene] (MPE-PPV):fullerene bulk heterojunction solar cells": Vandenbergh, J.; Conings, B.; Bertho, S.; Kesters, J.; Spoltore, D.; Piersimoni, F.; Esiner, S.; D'Haen, J.; Zhao, J.; Van Assche, G.; Wienk, M. M.; Maes, W.; Cleij, T. J.; Lutsen, L.; Van Mele, B.; Janssen, R. A. J.; Manca, J.; Vanderzande, D. J. M. in preparation. (60 %)

- Writing article
- Synthesis and characterization of MPE-PPV
- Preparation of MPE-PPV:PCBM blends

"Opto-Electrical and Morphological Characterization of Water Soluble Conjugated Polymers for Eco-Friendly Hybrid Solar Cells": Gopala Krishna, T. V. V.; Bolsée, J-C.; Gadisa, A.; Parchine, M.; Boonen, T.; D'Haen, J.; Boyukbayram, A. E.; Vandenbergh, J.; Cleij, T. J.; Lutsen, L.; Vanderzande, D.; Manca, J. V. *Sol. Energ. Mat. Sol. C.*, **2011**, submitted. (5 %)

- Writing article paragraph on water soluble conjugated polymers

*"Synthesis and Characterization of Water-Soluble PPV Derivatives via the Dithiocarbamate Precursor Route": Vandenbergh, J.; Dergent, J.; Conings,

B.; Gopala Krishna T. V. V.; Maes, W.; Cleij, T. J.; Lutsen, L.; Manca, J.; Vanderzande, D. J. M. *European Polymer Journal*, **2011**, submitted. (60 %)

- Writing article
- Synthesis and characterization of MTEMP-PPV and BTEMP-PPV

"Phase Behaviors of PCBM Blends with Different Conjugated Polymers": Zhao, J.; Bertho, S.; Vandenbergh, J.; Van Assche, G.; Manca, J.; vanderzande, D.; Cleij, T. J.; Lutsen, L.; Van Mele, B. *Phys. Chem. Chem. Phys.* **2011**, accepted. (20%)

- Preparation of MPE-PPV:PCBM blends

*"An Efficient Acid induced Conversion of Dithiocarbamate precursor polymers into Conjugated Materials": Diliën, H.; Vandenbergh, J.; Banishoeb, F.; Adriaensens, P.; Cleij, T. J.; Lutsen, L.; Vanderzande, D. J. M. *Macromolecules* **2011**, *44*, 711–718. (40 %)

- Article co-writing
- Synthesis, characterization and results analysis of PPV derivatives

*"Tetra-alkoxy substituted PPV derivatives: A new class of highly soluble liquid crystalline conjugated polymers": Vandenbergh, J.; Van Severen, I.; Lutsen, L.; Adriaensens, P.; Bolink, H. J.; Cleij, T. J.; Vanderzande, D. *Polymer Chemistry*, **2011**, *2*, DOI:10.1039/C1PY00027F. (40 %)

- Article co-writing
- Synthesis and characterization of TEH-PPV

"Kinetic and mechanistic study on the *p*-quinodimethane formation in the sulfinyl precursor route for the polymerization of poly(*p*-phenylene vinylene) (PPV)": Hermosilla, L.; Catak, S.; Van Speybroeck, V.; Waroquir, M.; Vandenbergh, J.; Motmans, F.; Adriaensens, P.; Lutsen, L.; Cleij, T.; Vanderzande, D. *Macromolecules* **2010**, *43*, 7424–7433. (10 %)

- Correcting kinetic UV-Vis data

"Hysteresis-free electron currents in poly(*p*-phenylene vinylene) derivatives": Craciun, N. I.; Zhang, Y.; Palmaerts, A.; Nicolai, H. T.; Kuik, M.; Kist, R.; Wetzelaer, G. A. H.; Wildeman, J.; Vandenbergh, J.; Lutsen, L.; Vanderzande, D.; Blom, P. W. M. *J. Appl. Phys.* **2010**, *107*, 124504, 1−5. (5 %)

- Purifying MEH-PPV
- Writing article paragraph on synthesis and purification of MEH-PPV

*"Exploring the Dithiocarbamate Precursor Route: Observation of a Base Induced Regioregularity Excess in Poly[(2-methoxy-5-(3′,7′,-dimethyloctyloxy))-1,4-phenylenevinylene] (MDMO-PPV)": Vandenbergh, J.; Wouters, J.; Adriaensens, P. J.; Mens, R.; Cleij, T. J.; Lutsen, L.; Vanderzande, D. J. M. *Macromolecules* **2009**, *42*, 3661−3668. (60 %)

- Article writing
- Synthesis and characterization of MDMO-PPV

Articles with a * are presented in thesis chapters.

Conferences

Oral presentations

"Exploring the dithiocarbamate precursor route: observation of a base induced regioregularity in PPV derivatives": Vandenbergh, J.; Wouters, J.; Adriaensens, P. J.; Mens, R.; Cleij, T. J.; Lutsen, L.; Vanderzande, D. J. M., Annual Meeting of the Belgian Polymer Group, May 25−26, 2010, Blankenberge, Belgium.

Poster presentations

"Mechanistic study on the *p*-quinodimethane formation in the synthesis of PPV through the sulfinyl and dithiocarbamate precursor routes": Vandenbergh, J.; Penxten, H.; Adriaensens, P. J.; Lutsen, L.; Cleij, T. J.; Vanderzande, D. J. M., MACRO 2010 World Polymer Congres, July 11−16, 2010, Glasgow, United Kingdom.

"Tetra-alkoxy substituted PPV derivatives: a new class of highly soluble liquid-crystalline conjugated polymers": Vandenbergh, J.; Van Severen, I.; Lutsen, L.; Adriaensens, P. J.; Bolink, H. J.; Cleij, T. J.; Vanderzande, D. J. M., Frontiers of Chemistry Symposium, May 21, 2010, Paris, France.

"Construction of phase diagrams of polymer/PCBM blends by means of DSC and MTDSC and the implication for the stability of morphology": Vandenbergh, J.; Zhao, J.; Bertho, S.; Van Assche, G.; Lutsen, L.; Cleij, T. J.; Vanderzande, D. J. M.; Manca, J.; Van Mele, B., E-MRS Spring Meeting, June 8−12, 2009, Strasbourg, France.

"Synthesis and study of 3,4-diphenyl substituted PPV derivatives: Exploring the dithiocarbamate precursor route", Vandenbergh, J.; Wouters, J.; Cleij, T. J.; Lutsen, L.; Vanderzande, D. J. M., Annual Meeting of the Belgian Polymer Group, May 22−23, 2008, De Haan, Belgium.

Abbreviations & Symbols

^{13}C NMR	Carbon 13 nuclear magnetic resonance spectroscopy
^{1}H NMR	Hydrogen 1 nuclear magnetic resonance spectroscopy
Ag	Silver
Al	Alumina
ATRP	Atom transfer radical polymerization
Au	Gold
Ba	Barium
BELSPO	Belgian Federal Science Policy Office
BTEMP-PPV	Poly(2,5-bis(1,3-bis(triethoxymethoxy)propan-2-yloxy)-1,4-phenylene vinylene)
CBr_4	Carbontetrabromide
$CDCl_3$	Deuterated chloroform
CCl_4	Tetrachloromethane
CF_3COOH	Trifluoro acetic acid
CH_2Cl_2	Dichloromethane
$CHCl_3$	Chloroform
CH_3CN	Acetonitrile
CPM-PPV	poly(1,4-(2-(5'-carboxypentyloxy)-5-methoxy)-phenylene vinylene)
DMF	Dimethylformamide
DSC	Differential scanning calorimetry
DTC	Dithiocarbamate
EI	Electron impact
Eg	Energy gap/ band gap
Equiv	Equivalents
ESI-MS	Electron spray ionization mass spectrometry
ESF	European Science Foundation
Et_2O	Diethyl ether
EtOAc	Ethyl acetate

EtOH	Ethanol
eV	electron volt
FET	Field effect transistor
FF	Fill factor
FT-IR	Fourier transform-infrared
FWO	Fonds Wetenschappelijk Onderzoek
GC/MS	Gas chromatography-mass spectrometry
GPC	Gel permeation chromatography
H_2O	Water
H_2SO_4	Sulfuric acid
HCl	Hydrochloric acid
HOMO	Highest Occupied Molecular Orbital
I_{sc}	Short circuit current
IAP	Interuniversity Attraction Poles
IR	Infrared
ITO	Indium Tin Oxide
IWT	Agentschap voor Innovatie door Wetenschap en Technologie
K*t*BuO	Potassium tert-butoxide
λ	Wavelength
LDA	Lithium diisopropylamide
LED	Light-emitting diode
LHMDS	Lithium hexamethyldisilazane
LFRP	Living free radical polymerization
LUMO	Lowest Unoccupied Molecular Orbital
M	Molar
M_n	Number-average molecular weight
M_w	Weight-average molecular weight
M^+	Molecular ion
MDMO-PPV	poly[2-methoxy-5-(3′,7′-dimethyloctyloxy)-1,4-phenylene vinylene]
MHz	MegaHertz

MeOH	Methanol
$MgSO_4$	Magnesium sulphate
MPE-PPV	Poly[2-methoxy-5-(2'phenylethoxy)-1,4-phenylene vinylene]
MS	Mass spectrometry
MTDSC	Modulated temperature DSC
MTEMP-PPV	Poly(2-methoxy-5-(1,3-bis(triethoxymethoxy)propan-2-yloxy)-1,4-phenylene vinylene)
Na	Sodium
NaCl	Sodium chloride
NaOH	Sodium hydroxide
$NaSC(S)NEt_2.H_2O$	Sodium diethyldithiocarbamate trihydrate
Na*t*BuO	Sodium tert-butoxide
NMP	nitroxide-mediated polymerization
NMR	Nuclear magnetic resonance
N_2	Nitrogen
OCH_3	Methoxy
$OC_{10}H_{21}$	Dimethyloctyloxy
OLED	Organic light-emitting diode
O-PTV	Octyl-PTV
OPV	Organic photovoltaics
p-	para
[60]PCBM	[6,6]-phenyl-C_{61}-butyric acid methyl ester
[70]PCBM	[6,6]-phenyl-C_{71}-butyric acid methyl ester
PCE	Power Conversion Efficiency
PD	Polydispersity
PEDOT	Poly(3,4-ethylenedioxythiophene)
pK_a	Acid dissociation constant
ppm	Parts per million
PLM	Polarized light microscopy
PPV	Poly(*p*-phenylene vinylene)
PSS	Poly(styrenesulfonate)

PTV	Poly(thienylene vinylene)
RAFT	Reversible addition fragmentation chain transfer
RHC	Rapid heating-cooling calorimetry
RT	Room temperature
SCLC	Space charge limited current
SEC	Size exclusion chromatography
$SOCl_2$	Thionyl chloride
T1	Relaxation decay time
TBB	Tolane-bisbenzyl
TEH-PPV	poly[2,3,5,6-tetra(2'-ethyl-hexyloxy)-1,4-phenylene vinylene]
TEM	Transmission electron microscopy
TEMPO	2,2,6,6-tetramethylpiperidinoxyl
TFA	Trifluoroacetic acid
THF	Tetrahydrofuran
TH-PPV	poly(2,3,5,6-tetrahexyloxy-1,4-phenylene vinylene)
TLC	Thin Layer Chromatography
TMS	Tetramethylsilane
UV-vis	Ultra Violet visible
V_{oc}	Open circuit voltage
WSCP	Water-soluble conjugated polymer
ε_r	Relative Permittivity
λ_{max}	Wavelength at maximum absorbance
μ_h	Hole mobility
T_g	Glass transition temperature
ΔT	Elevated temperature

The meeting of two personalities is like the contact of two chemical substances: if there is any reaction, both are transformed.

Carl Jung

Dankwoord

Zo, het zit er bijna op. Ik had nooit gedacht dat de tijd zo snel voorbij kon vliegen. Dit kan alleen maar betekenen dat mijn doctoraatsjaren een zeer leuke en leerrijke periode uit mijn leven waren. Het schrijven van de doctoraatsthesis was een vrij eentonige bezigheid, maar ik ben zeer blij met en trots op het uiteindelijke resultaat. Tijdens het schrijven heb ik vaak gedacht aan de vele mensen die mij op één of andere manier gebracht hebben tot waar ik nu sta. Zonder hen zou ik dit doctoraat niet hebben kunnen aanvatten of het tot een goed einde hebben kunnen brengen. Daarom verdienen al deze personen mijn oprechte dank.

Als eerste zou ik mijn promotor, prof. dr. Dirk Vanderzande, willen bedanken voor de kans die hij me gegeven heeft om te doctoreren. Bedankt voor het grote vertrouwen dat je van bij het begin in me had. De vele korte en lange gesprekken die we de voorbije jaren gevoerd hebben, waren altijd nuttig en gaven me steeds nieuwe inzichten om verder te doen. Als prof stond je toch dicht bij de studenten, wat ik altijd heel erg apprecieerde. Ook je aparte en zeer uitgelaten dansstijl tijdens de beruchte BPG fuiven zullen me altijd bijblijven.

Mijn copromotoren dr. Laurence Lutsen en prof. dr. Thomas Cleij wil ik erkennen voor de vele momenten waarop ze mij met raad en/of daad hebben bijgestaan tijdens Ph. D. meetings en andere bijeenkomsten. Thomas, het was zeer aangenaam om samen met jou in het labo te werken met de beruchte waterstofgasopstelling. Het artikel rond de tetragesubstitueerde PPV derivaten is er grotendeels gekomen dankzij jou, waarvoor mijn dank. Ook wil ik je nog bedanken voor de vele gezellige barbecue- en andere eetfestijnen bij je thuis, waar we steeds zeer gastvrij onthaald werden. Het was telkens overheerlijk en superleuk!

Prof. dr. Peter Adriaensens wil ik bedanken voor de grote hulp bij het opnemen en analyseren van NMR spectra en voor het zeer nauwgezet verbeteren van enkele van mijn artikels. Prof. dr. Wouter Maes en prof. dr.

Thomas Junkers verdienen een pluim voor hun enthousiasme waarmee ze onze onderzoeksgroep bijstaan. Goede begeleiding is een must voor nieuwe doctoraatsstudenten en Wouter, jij doet dit met volle overgave. Thomas, ik wil je bedanken voor de goede samenwerking gedurende het laatste half jaar van mijn doctoraat. Ik ben heel blij dat er ook eindelijk een professor is die de organisatie van de labmeetings in handen genomen heeft.

Voor de financiering van mijn doctoraat bedank ik graag de Universiteit Hasselt voor de overbruggingsbeurs en het FWO Vlaanderen voor het aspirant mandaat.

En dan kom ik nu tot de woorden van dank voor de vele mededoctoraat-studenten die samen met mij in hetzelfde schuitje zaten of zitten en waarmee ik ontelbare uren op de bureau of in het labo heb doorgebracht. Hanne, reeds van bij het begin hebben we net naast elkaar in het labo gestaan en ons doorheen de jaren samen geamuseerd op vele congressen. Ondertussen moet ik je aanspreken met dr. Hanne en ik wens je heel veel succes in je verdere carrière. Hetzelfde wens ik toe aan Frederik, gij gaat u ongetwijfeld goed amuseren als MIP-postdoc en tijdens de middag het grote woord kunnen voeren aan tafel ;-). Sarah, de overstap van het onderwijs naar een doctoraat is ongetwijfeld een goede keuze geweest. Ik bewonder je voor je harde werk en voor de vele uren die je in het labo en op bureau doorbrengt. Je bent een voorbeeld voor velen. In één adem wil ik ook alle andere, meer recent tot onze groep toegetreden doctoraatstudenten vermelden: Ans (Ansiepansie), Inge, Lidia (my skiing partner in crime), Matthias (my climbing partner in crime), Toon, Suleyman, Tom, Pieter en Jurgen.

Gunter, Erik en David (the biochemical connection): jullie zaten helaas niet bij ons op de bureau, maar ik vergeet jullie niet.

Wibren, jou wil ik bedanken voor de vele raad en tips die je als postdoc steeds kon geven wanneer ik ergens vragen over had. Ook op de skitrips naar Frankrijk en Oostenrijk was je van de partij. Wat was het toch leuk om van de zwarte piste af te skiën bij hevige mist hé!

Ook de oudere garde collegae die onze groep reeds verlaten hebben dienen genoemd te worden: Lien, Sofie, Wouter, Juliette, Raoul, Fateme, Zarina, Brecht, Steven, Burak en Elif. Daarenboven verdienen enkele individuen een aparte vermelding. Arne, Kristof, Bert en Jan, met jullie vieren hebben ik me goed geamuseerd tijdens de vele kooklessen bij de Syntra. Ook de wedstrijdjes zaalvoetbal waren zeer intensief en ontspannend tegelijkertijd. Sylvain, ik vond het een fantastische uitdaging om samen met jou op een hoogte van 70 meter ergens aan een rots te bengelen in de Ardennen! Heel sjiek! Hopelijk komen we elkaar ooit nog eens tegen. Jimmy, het was aangenaam om je als bureau-gebuur te hebben tijdens de eerste 2 jaar van men doctoraat. Ik hoop dat je toch nog ergens de tijd zult vinden om je eigen doctoraat te verdedigen…

Tijdens mijn doctoraatsjaren heb ik ook de kans gekregen om enkele bachelor-studenten te begeleiden. Jeroen, Frank en Arno, jullie hebben alle drie een mooie thesis afgeleverd en zeker bijgedragen aan mijn onderzoek. Bedankt voor jullie hulp.

De mensen van het vast personeel mag ik zeker niet vergeten. Iris en Veerle, bedankt voor de ontelbare GPC metingen, Huguette voor de vruchtvolle samenwerking rond de kinetische UV-vis studie en Jan de massaman voor het uitvoeren van GC/MS. Koen wil ik bedanken voor het opnemen van de NMR spectra en vergeet niet: Chiro Rules! Merci ook aan Jos en Tim van de glasblazerij en Christel voor de bestellingen van chemicaliën en ander materiaal. De leden van het didactische team Hilde, Gène en Rita wil ik bedanken voor het steeds mooi klaarzetten van alle materiaal bij de studentenpractica en de hulp tijdens de labozittingen.

Wanneer ik mijn polymeren wilde testen in devices, kon ik steeds rekenen op de hulp van enkele doctoraatstudenten van IMO fysica. Mijn dank gaat uit naar Koen Vandewal, Bert Conings en Gopala Krishna voor de hulp bij het maken en meten van organische zonnecellen, Fortunato Piersimoni en Donato Spoltore voor de verouderingsstudies, Sabine Bertho en Tine Boonen voor de TEM metingen en Linny Baeten van “Anorganische” voor het aanleveren van de ZnO nanorod-substraten.

Naast het werk in ons onderzoekslabo, kon ik voor bijkomende studies terecht bij enkele onderzoeksgroepen van andere universiteiten. In het bijzonder zou ik de volgende personen willen bedanken: prof. dr. ir. Bruno Van Mele, prof. dr. ir. Guy Van Assche en dr. Jun Zhao van de Vrije Universiteit Brussel voor het uitvoeren van de MTDSC en RHC metingen. Prof. dr. ir. Paul Blom en ir. Martijn Kuik van de Rijksuniversiteit Groningen voor het elektronisch karakteriseren van MDMO-PPV. Dr. Henk Bolink van de Universiteit van Valencia voor de opto-elektrische metingen op de tetragesubstitueerde PPV derivaten. De groep van prof. dr. ir. Veronique Van Speybroeck en prof. dr. Michel Waroquier van de Universiteit Gent voor het modelleren van de sulfinyl route. Prof. dr. ir. Guy Marin, prof. dr. ir. Marie-Françoise Reyniers en ir. Paul Van Steenberge van de Universiteit Gent voor de kinetische modellering van de sulfinyl en dithiocarbamaat routes. En tot slot prof. dr. ir. René Janssen, dr. ir. Martijn Wienk en Serkan Esiner van de Technische Universiteit Eindhoven voor het maken en meten van organische zonnecellen. Mijn vroegere collega en goede vriend Alessandro en zijn vrouw Michelle bedank ik van harte voor hun gastvrijheid tijdens mijn korte recentelijk verblijf in Eindhoven.

Nu ik bijna aan het einde van dit dankwoord gekomen ben, zou ik graag de mensen willen bedanken die het belangrijkste zijn in mijn leven, mijn vrienden en familie. Mama en papa, bedankt om me steeds alle kansen te geven in het leven, dankzij jullie kon ik gaan studeren en men eigen weg gaan. Maai, je bent mijn enige zus en jij weet ook dat we twee handen op één buik zijn. Wij zullen er altijd voor elkaar zijn. Ik hoop ook dat onze vrijdagavonden, waarbij we ons steevast goed amuseren met dE MEESER en andere tooghangers en kaarters uit het Sweert, nog lang mogen blijven plaatsvinden. Het is de ideale ontspanning om het weekend te beginnen. Liesbeth, mijn wekelijks bezoek aan jou en je gezin doen me altijd veel plezier. Ik denk dat Noor en Yasmine net zo een grote bengeltjes gaan worden als jij vroeger ;-). En als allerlaatste, maar zeker niet als allerminste,

bedank ik jou, Didier, om er altijd voor mij te zijn en me te steunen in alles wat ik doe. Je hart zit op de goede plaats.

Bedankt allemaal!

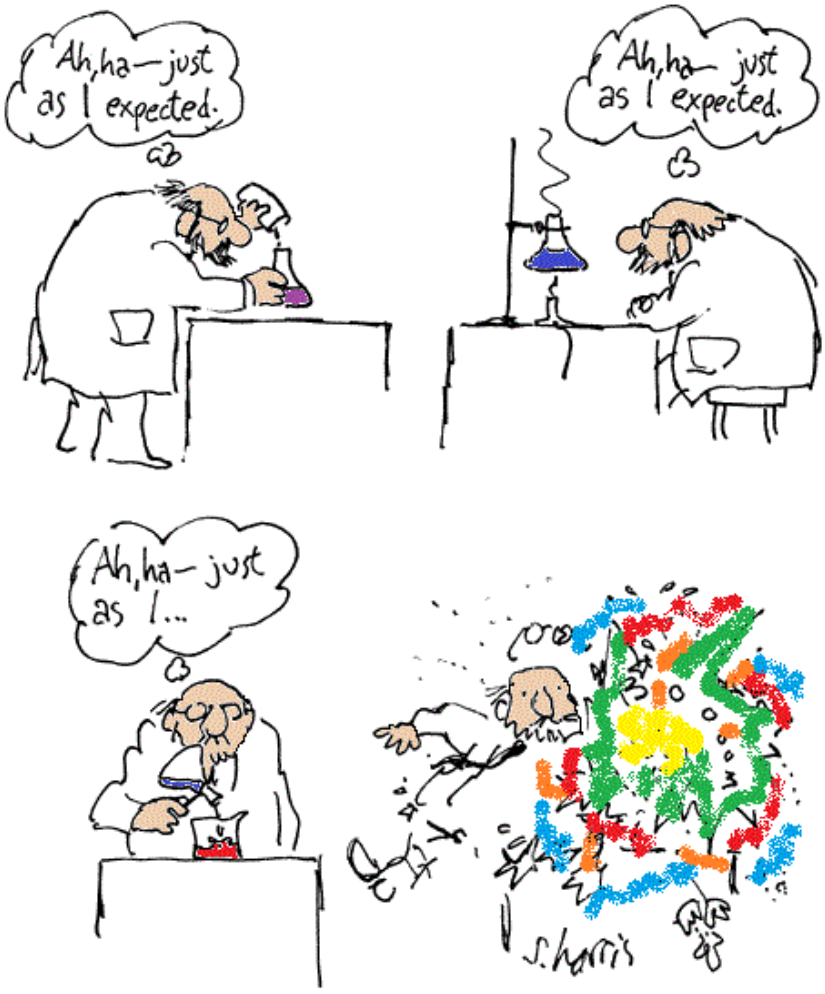

Only two things are infinite, the universe and human stupidity, and I'm not sure about the former.

Albert Einstein